Fall 1983

DIGITAL ANALYSIS OF PULSE CODE MODULATED SIGNALS IN TELECOMMUNICATIONS CHANNELS

EDMUND LITTLEFIELD CHASE
University of New Hampshire, Durham

INFORMATION TO USERS

This reproduction was made from a copy of a document sent to us for microfilming. While the most advanced technology has been used to photograph and reproduce this document, the quality of the reproduction is heavily dependent upon the quality of the material submitted.

The following explanation of techniques is provided to help clarify markings or notations which may appear on this reproduction.

1. The sign or "target" for pages apparently lacking from the document photographed is "Missing Page(s)". If it was possible to obtain the missing page(s) or section, they are spliced into the film along with adjacent pages. This may have necessitated cutting through an image and duplicating adjacent pages to assure complete continuity.

2. When an image on the film is obliterated with a round black mark, it is an indication of either blurred copy because of movement during exposure, duplicate copy, or copyrighted materials that should not have been filmed. For blurred pages, a good image of the page can be found in the adjacent frame. If copyrighted materials were deleted, a target note will appear listing the pages in the adjacent frame.

3. When a map, drawing or chart, etc., is part of the material being photographed, a definite method of "sectioning" the material has been followed. It is customary to begin filming at the upper left hand corner of a large sheet and to continue from left to right in equal sections with small overlaps. If necessary, sectioning is continued again—beginning below the first row and continuing on until complete.

4. For illustrations that cannot be satisfactorily reproduced by xerographic means, photographic prints can be purchased at additional cost and inserted into your xerographic copy. These prints are available upon request from the Dissertations Customer Services Department.

5. Some pages in any document may have indistinct print. In all cases the best available copy has been filmed.

University Microfilms International
300 N. Zeeb Road
Ann Arbor, MI 48106

Chase, Edmund Littlefield

DIGITAL ANALYSIS OF PULSE CODE MODULATED SIGNALS IN TELECOMMUNICATIONS CHANNELS

University of New Hampshire PH.D. 1983

PLEASE NOTE:

In all cases this material has been filmed in the best possible way from the available copy. Problems encountered with this document have been identified here with a check mark __√__.

1. Glossy photographs or pages _____
2. Colored illustrations, paper or print _____
3. Photographs with dark background ✓
4. Illustrations are poor copy _____
5. Pages with black marks, not original copy _____
6. Print shows through as there is text on both sides of page _____
7. Indistinct, broken or small print on several pages ✓
8. Print exceeds margin requirements _____
9. Tightly bound copy with print lost in spine _____
10. Computer printout pages with indistinct print _____
11. Page(s) _____ lacking when material received, and not available from school or author.
12. Page(s) _____ seem to be missing in numbering only as text follows.
13. Two pages numbered _____. Text follows.
14. Curling and wrinkled pages _____
15. Other _____

DIGITAL ANALYSIS OF PULSE CODE MODULATED SIGNALS IN TELECOMMUNICATIONS CHANNELS

BY

Edmund Littlefield Chase
B.S., University of Maine, 1972
M.S., University of Lowell, 1978

DISSERTATION

Submitted to the University of New Hampshire
in Partial Fulfillment of
the Requirements for the Degree of

Doctor of Philosophy
in
Engineering

September, 1983

This dissertation has been examined and approved.

L Gordon Kraft

Dissertation director, Gordon Kraft
Associate Professor of Electrical
and Computer Engineering

Ronald R. Clark

Ronald Clark, Professor and Chairman
of Electrical and Computer Engineering

John L Pokoski

John Pokoski, Professor of Electrical
and Computer Engineering

David E. Limbert

David Limbert, Professor of
Mechanical Engineering

Filson Glanz

Filson Glanz, Associate Professor of
Electrical and Computer Engineering

7/26/83

Date

ACKNOWLEDGEMENTS

I would like to express my gratitude to Western Electric for providing their support through the Western Electric Engineering and Science Fellowship Program. In particular, I would like to thank my previous Department Chief, Neil Dickerson, for his efforts in obtaining the fellowship for me. Also, my current Department Chief, Oliver Niemi, deserves many thanks for his continued support.

My appreciation is extended to my dissertation director, L. Gordon Kraft, for the considerable assistance and direction which he provided throughout this project and to the remaining members of my committee for their inputs toward the preparation of this manuscript.

Finally, I would like to express my most sincere thanks to my wife, Brenda, for her loving support and patience during this period.

TABLE OF CONTENTS

LIST OF TABLES

LIST OF FIGURES

ABSTRACT

DIGITAL ANALYSIS OF PULSE CODE MODULATED SIGNALS IN TELECOMMUNICATIONS CHANNELS

by

EDMUND LITTLEFIELD CHASE

University of New Hampshire, September 1983

In this dissertation the techniques required to test pulse code modulated telecommunications channels are developed using the fast Fourier transform. The techniques are then applied through the design and assembly of the corresponding hardware. Windowing of data to improve spectral estimation is discussed as well as the conditions where special test signals may be synthesized to preclude the need for windowing. Conjugate-periodic functions encountered in prime radix transforms are defined and their fast transform techniques are developed.

CHAPTER 1

INTRODUCTION

Techniques for digitally processing signals to estimate their frequency spectra have been in use for about eighty years. The improvements made over the past fifteen years in both the algorithms and the machines used to perform them have greatly extended their applications. Advances in general seem to be made in small but deliberate steps as a new application of a mathematical 'trick' is found here or an algorithm is improved there. Various authors have talked about either digitally generating analog signals or digitally analyzing analog signals. In this thesis these two operations are examined and then coupled together to show how special advantages may be gained by phase locking the signal generator and the sampler used to analyze an analog channel. The results presented here are intended for, but not limited to, the specific application of testing digital telecommunications channels. At the current time, virtually all of the testing of these channels is done using very specialized and expensive low distortion sine wave generators and low noise detectors with specialized notch filters and noise weighting filters. The work done here provides the specific ingredients needed to replace most of this specialized equipment with low cost, off-the-shelf computer equipment.

Some of the specific areas of this thesis where advances have been made are the following. It is demonstrated here both mathematically and experimentally how

special signals may be generated digitally, transmitted through a channel, sampled synchronously and analyzed digitally to produce accurate spectral estimates without the need for using data windows. A series of new data windows has been developed for use in spectral estimation when an independent signal source must be used. Interface hardware has been designed, built and tested for the direct connection of a computer to a digital telecommunications channel. New algorithms are developed which may be used in calculating the discrete Fourier transform of conjugate-periodic functions.

Chapter 2 is a survey of the literature. The main sources of reference material used in this dissertation are cited here. Included also are some references which provide good background material by defining basic digital processing techniques used in this field.

Chapter 3 defines the telecommunications equipment used in this work and describes the parameters which are to be measured. The computer interface which was designed and built is also explained here.

Chapter 4 provides the theoretical developments in the area of the fast Fourier transform. This includes more information about how various techniques may be applied than was available in the literature. The conditions under which the discrete Fourier transform will produce the same results as a continuous transform are reviewed. Also included is a precise derivation for the number of complex multiplications required to perform transforms on any number of data points.

Chapter 5 describes the signal synthesizer which has been designed and constructed. This synthesizer generates the special signal characteristics which will provide

precise results from the discrete Fourier transform.

Chapter 6 describes the transform techniques used in evaluating the telecommunications hardware. A new set of data windows are developed here for use in spectral estimation.

Chapter 7 describes the procedures used to make the various measurements on the telecommunications equipment. Examples are given of actual measurements and some comparisons are made to measurements made with conventional analog equipment.

Chapter 8 contains the conclusions summarizing the work which has been done here and suggestions of areas for future investigation.

CHAPTER 2

LITERATURE SURVEY

The first two references are intended to provide an introduction and review of digital signal processing techniques with which the reader of this paper is assumed to be familiar. In reference [1] Rabiner et al provide a general introduction to digital signal processing and define most of the commonly used terms. This reference also includes a mathematical definition of discrete systems, the comparison of discrete and continuous signals, the theory and design of digital filters, the effects of quantization, the discrete and fast Fourier transforms, and convolution and spectral estimation. Cooley et al in reference [2] put the contributions of various investigators into historical perspective and provide a comparison of the early prime factor algorithm of L. H. Thomas to the more recent Cooley-Tukey algorithm. It is interesting to note that, even though J.W.Cooley and J.W.Tukey [20] were credited with the general form of the complex fast Fourier transform in 1965, much work of a similar nature was accomplished many years before. In the period of 1903 to 1905 C.Runge published papers [22,23] on a doubling technique which took advantage of the symmetries of the sine and cosine functions to combine the transforms of two N point series to form the transform of 2N points. This method was used by G.C.Danielson and C.Lanczos [24] in 1942 when they published a method of calculating the transform of a number of points equal to a power of two. In 1948 L.H.Thomas was working on a method, base on work by K.Stumpff [25] in 1939, which

performed a Fourier transform on a composite number of points where the factors had to be mutually prime. All of these early developments occurred prior to the "computer age". After 1960, as computers were becoming generally available to many researchers, new interest was sparked in these techniques. As a result, in 1963 Thomas published an algorithm [26] based on his prior work. Cooley and Tukey followed in 1965 with their generalized algorithm. P.Rudnick responded in 1966 with a paper [27] describing work which he had been doing based on the doubling technique of Runge. This was equivalent to the special case of the Cooley-Tukey algorithm when the number of points is a power of two. Since the Cooley-Tukey algorithm is the most general they are credited with the present Fast Fourier Transform (FFT).

A method for estimating the power spectrum of a signal using the Fast Fourier Transform (FFT) is discussed by P.D.Welch in [3] including an analysis of two different data windows. An improvement in the auto correlation techniques used in spectral estimation is presented by C.M.Rader in [4]. Computation of the spectrum at unequally spaced frequencies is discussed in [5] by Oppenheim, Johnson and Steiglitz. The windows discussed in these papers are reviewed in this dissertation. One of the contributions of this dissertation is the development of a new series of data windows which produce improved spectral estimates. Although these windows are used here in a specific application they should have general applicability to any spectral estimation problem.

An algorithm presented by R.C.Singleton in [6] gives a means of performing a mixed radix FFT on any set of points whose factors are no greater than five. Also discussed are

the permutation techniques and the efficient calculation of the complex rotation factors. In reference [7] Rader develops the method for reducing the DFT of a prime number of points to a circular correlation which may be performed using FFT techniques. These methods are combined, extended and generalized in this dissertation to show how an FFT may be efficiently performed on any number of points. Also an additional short-cut is provided here for use in the prime FFT.

A statistical method is used by C.J.Weinstein in [8] to predict the signal-to-noise ratio which results from the computation of an FFT using floating point arithmetic.

In reference [9] Tierney, Rader and Gold discuss a means of digitally synthesizing sinusoids using two table look-ups and a complex multiplication to generate digital samples of the complex exponential. The synthesizer developed in this dissertation extends these ideas by using a table of prime length. The prime length table insures that all generated frequencies will contain the same amount of quantization error.

The next two references define the pulse code modulation techniques used in telecommunications channels. The "Orange Book" [10] is an exhaustive description of all the standard telecommunications design specifications developed by both the Bell System and the Consultative Committee on International Telegraph and Telephone (CCITT). The test requirements used here are taken from this reference. The requirements and objectives published by A.T.&T. for digital telecommunications equipment are referenced in [11].

CHAPTER 3

DIGITAL TRANSMISSION SYSTEMS

III-A System Configuration

III-A.1 Time Multiplexed Pulse Code Modulation

Modulation is the encoding of information into a form which for various reasons may be better suited for transmission through a given medium. Pulse code modulation is a method in which samples are taken of an analog signal and the amplitudes of the samples are coded into binary words. These binary words may then be serially transmitted, one bit at a time, over a pair of wires. Inherent in this coding process is a certain amount of inaccuracy called quantization noise. This results from the discrete nature of the coded word which permits only a finite number of discrete analog levels to be exactly represented. The infinite number of continuous levels which exist between any two of these discrete levels are approximated by rounding them off to the nearest discrete level. The amount by which they must be rounded determines the magnitude of the quantization noise. Increasing the number of bits used to encode the samples or decreasing the largest signal which may be exactly represented are both methods of reducing the quantization error. Both of these methods have their drawbacks. Increasing the number of bits will either require more time for the transmission of each sample, resulting in a smaller signal bandwidth, or will require the bits to be transmitted faster, increasing the bandwidth requirement of

the transmission channel. On the other hand, decreasing the maximum representable signal decreases the dynamic range of the transmitted signal. The quantity of most importance is not the magnitude of the quantization noise directly, but instead, the ratio of the magnitude of the signal to that of the noise. Since decreasing the dynamic range will not improve the overall signal to noise ratio, this is not a viable solution to the quantization problem. Notice, however, that with a given number of bits in the code word, the signal to noise ratio gets progressively worse for lower level signals when the quantization levels are spread linearly over the dynamic range. For this reason coding schemes have been developed which space the quantization levels closer together at lower levels and further apart at higher levels.

When more bandwidth is available in the transmission medium than is required to transmit a given pulse code modulated signal with acceptable bandwidth and signal to noise ratio, a method known as time multiplexing may be applied to transmit a number of separate signals over the same transmission medium. This is done by transmitting the code words at a higher bit rate, thus using up more of the bandwidth. With the sampling rate held constant, this would leave dead time between the transmission of one sample and the next. This dead time would be used to transmit the code words for other signals one at a time; hence the term time multiplexing.

III-A.2 The Digital Channel Bank

One of the standard digital transmission systems used in telephone communications multiplexes twenty-four voice

channels into one digital pulse stream to be transmitted over a single twisted pair of wires [10]. The multiplexing and demultiplexing equipment is normally supplied in pairs to provide two-way communications. This transmitting and receiving equipment at either end of the digital line is called a D-type channel bank. The operating mode where twenty-four channels are multiplexed into one digital signal is called DS-1. The transmission medium for the DS-1 signal is called a T1 digital line. Although other modes such as DS-1C with fourty eight channels, DS-2 with ninety-six channels, etc., are in common use, the sampling rates and coding schemes remain the same. Therefore, it will suffice to restrict any discussion herein to the DS-1 mode of operation.

The transmitting portion of a D-type channel bank is shown in Figure III-1. Here twenty-four individual voice channels enter from the left. Each channel is low pass filtered to remove any frequency components above 4000 Hz. An analog switch samples each channel in sequence and passes the sample to an analog to digital converter which converts it to an eight bit serial data word for transmission. The analog switch samples each channel 8000 times per second, resulting in a Nyquist frequency of 4000 Hz [1]. One complete cycle through the 24 channels produces a bit stream of 192 bits, called a frame, to which is added an extra framing bit used to synchronize the receiver to the transmitter. These 193 bits per frame at 8000 frames per second result in a data rate of 1,544,000 bits per second on the T1 line. The low pass filters are an important part of the transmitter, since any frequency components above the 4000 Hz Nyquist frequency will be aliased by the sampling

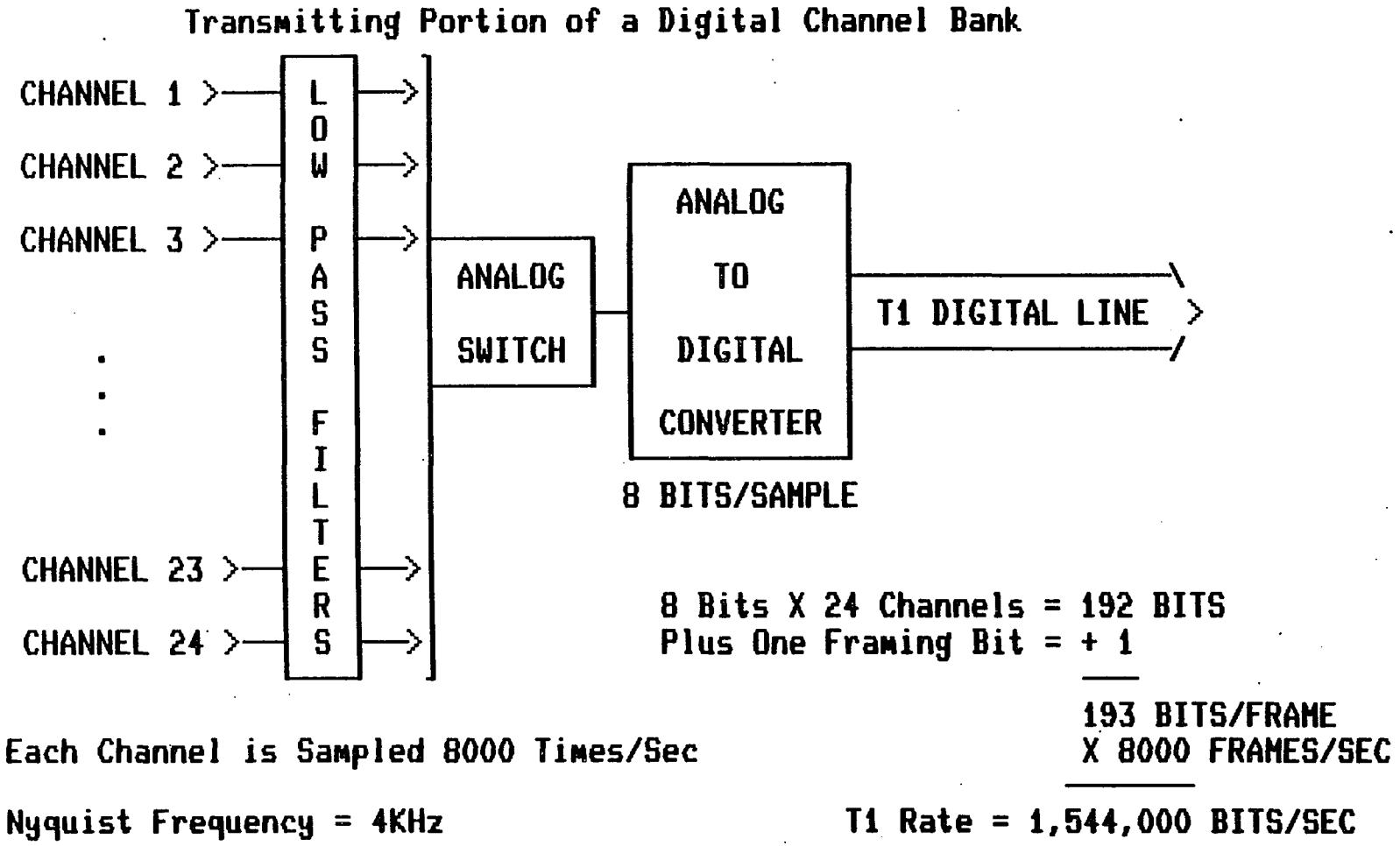
Transmitting Portion of a Digital Channel Bank
CHANNEL 1
CHANNEL 2
CHANNEL 3
CHANNEL 23
CHANNEL 24
LOW PASS FILTERS
ANALOG SWITCH
ANALOG TO DIGITAL CONVERTER
T1 DIGITAL LINE
8 BITS/SAMPLE
8 Bits X 24 Channels = 192 BITS
Plus One Framing Bit = + 1
193 BITS/FRAME
X 8000 FRAMES/SEC
Each Channel is Sampled 8000 Times/Sec
Nyquist Frequency = 4KHz
T1 Rate = 1,544,000 BITS/SEC

Figure III-1

operation and appear as noise in the range of 0 to 4000 Hz.

The receiving portion of the digital channel bank is shown in Figure III-2. The bit serial information is compiled by a digital to analog converter into an 8 bit word and then into an amplitude modulated pulse which is directed to the proper channel filter by the analog switch. These compilation and switching operations are synchronized to the bit stream by the framing pulse which appears prior to each frame of information. The low pass filters remove the modulation products between the voice signals and the 8000 Hz sampling frequency by removing any frequency components above 4000 Hz.

The framing bit is not always a 'one' bit, but instead cycles through a known pattern of 12 bits (100011011100) which is unlikely to occur anywhere else in the data stream. Signalling information such as idle vs. busy and dial pulses are also transmitted as part of each channel's data. This signalling data toggles at a relatively slow rate so that transmitting it at the same 8000 Hz rate is not necessary. Therefore, the least significant bit in each channel's 8 bit data word is stolen every sixth frame to create two signalling paths. Table III-1 shows how the framing signal is used to indicate the presence of the signalling information [10].

III-B Data Encoding Format

III-B.1 Compression Law

The coding used by the D-type channel banks to digitally represent the analog sample is approximately logarithmic. This produces quantization levels which are closer together for the lower values and farther apart for

Receiving Portion of a Digital Channel Bank

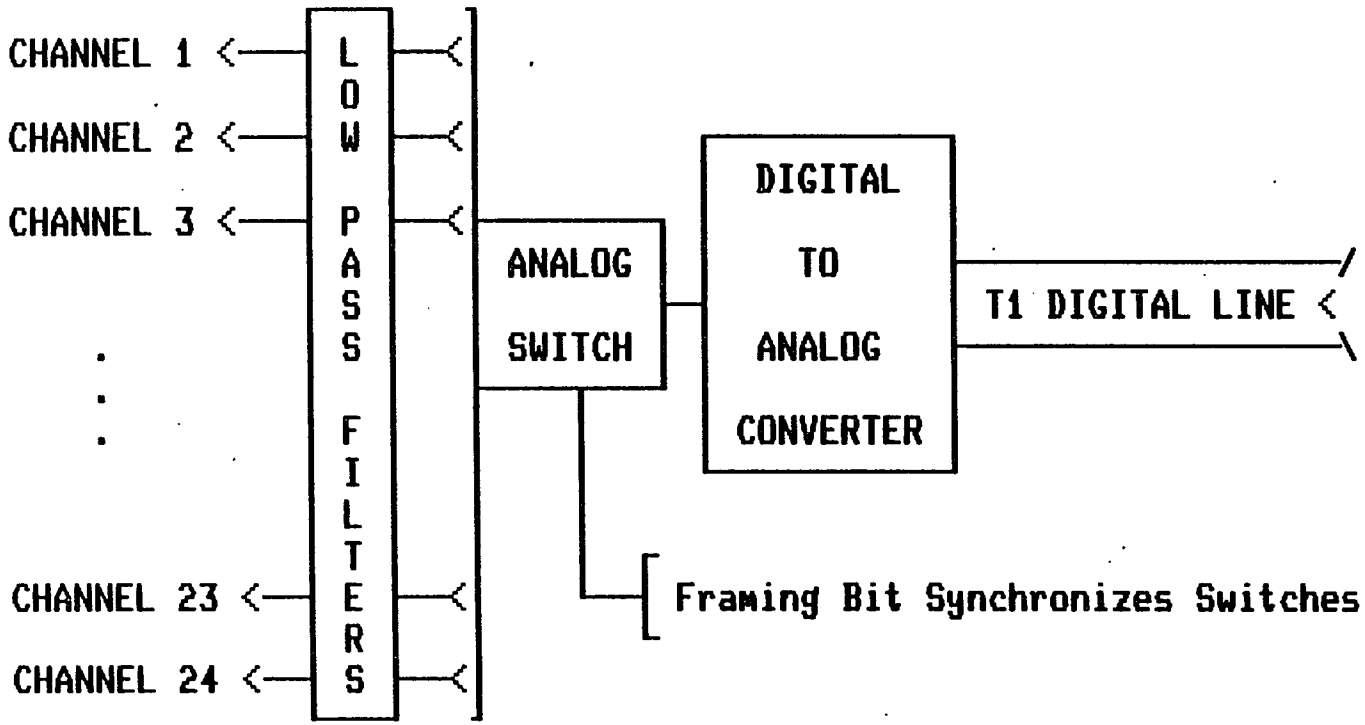

Figure III-2

Table III-1

DS-1 Mode Framing Pattern

FRAME NUMBER	FRAMING PATTERN	CODE LENGTH	SIGNALLING PATH
1	1	8	
2	0	8	
3	0	8	
4	0	8	
5	1	8	
6	1	7	A
7	0	8	
8	1	8	
9	1	8	
10	1	8	
11	0	8	
12	0	7	B

the higher ones. The actual coding used is a piece-wise linear approximation to a mu=255 law compression which is defined by:

$$|y| = \frac{\ln(1+mu|x|)}{\ln(1+mu)} , \quad mu = 255$$

where x and y are the compressor input and output respectively, normalized to unity.

III-B.2 Coder and Decoder Characteristics

As previously mentioned, the analog to digital converter codes the signal sample into 8 bits for all of the information frames and into 7 bits for the signalling frames. Thus, to minimize the quantization error incurred, different transfer characteristics are used in each of these two cases.

The information is always coded in sign-magnitude and ones complement form regardless of whether 8 or 7 bits are available. This leaves 7 and 6 bits respectively for the magnitude portion. Ones complement form is used so that low level signals, which are more likely to occur, will generate a higher concentration of pulses on the digital line. The pulse regenerators which are used on the T1 line and the receiver circuits in the digital bank have internal oscillators which are synchronized to the oscillator in the transmitter by the data pulses on the digital line. In order to maintain this synchronization no more than 15 zeroes (missing pulses) are allowed in a row. Any number of ones are allowed because the data is transmitted with bypolar pulses, i.e., every other pulse is inverted. This provides better synchronization, eliminates any d.c. component and

reduces the bandwidth requirements of the pulse stream. To guarantee meeting the maximum zeroes requirement, whenever an all zeroes signal is encoded, the seventh (next to last) bit is changed to a one. The next to last bit is used rather than the last bit so that the signalling paths will not be affected. Note that this all zeroes condition will only occur when the maximum amplitude is reached in the negative direction. This should occur very seldom in normal voice data; otherwise, clipping of both positive and negative peaks will occur, producing large amounts of distortion.

Figure III-3 shows a portion of the actual transfer characteristic of the compression used to produce the 8 bit code word. The end points of each horizontal line segment represent the decision levels used to determine the range in amplitudes of the analog input signal which will be coded into a given quantization level. Note that there are 128 quantization level numbers shown on the vertical axis, representing the values which are coded in ones complement form into the 7 magnitude bits of the 8 bit code word. The analog input signal is considered normalized to 8159 (the peak value of a 3.17 dBm0 sine wave) so that all of the decision levels may be represented as integers. Table III-2 shows the formulas which may be used to determine the exact values of the decision levels X(N) which correspond to each quantization level N. The output Y(N) of the decoder is always half way between the decision levels.

$$Y(0) = X(0) = 0$$

$$Y(N) = \frac{X(N) + X(N+1)}{2}, \quad N = 1, 2, \ldots 127$$

This minimizes the average amount of quantization error.

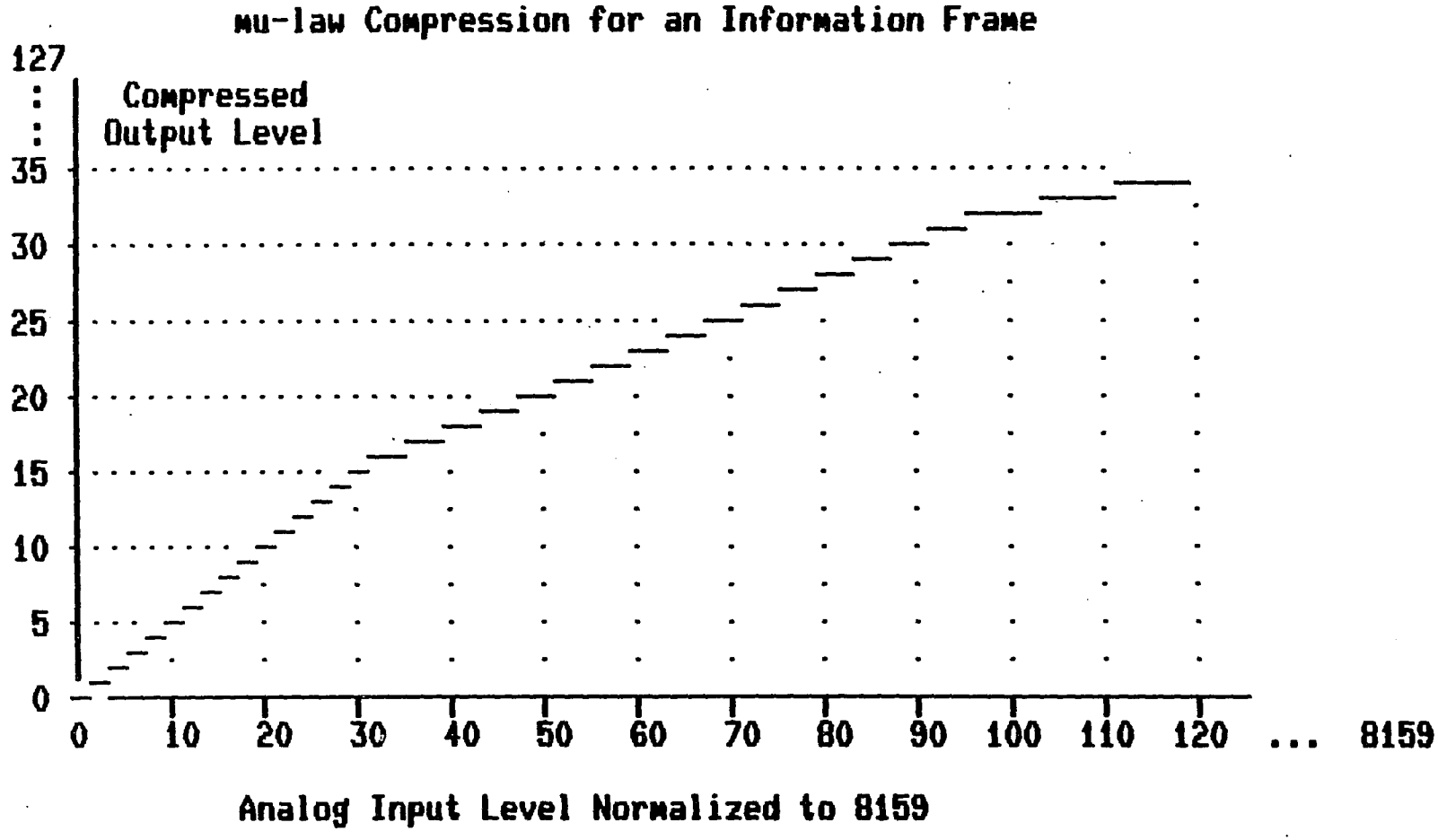
mu-law Compression for an Information Frame
127
:
:
Compressed
Output Level
35
30
25
20
15
10
5
0
0
10
20
30
40
50
60
70
80
90
100
110
120
...
8159
Analog Input Level Normalized to 8159

Figure III-3

Table III-2
Code Decision Levels

LEVEL NUMBER, N	LEVEL MAGNITUDE, |X(N)|
0	0
$1 \leq N \leq 16$	2(N+16)-33
$17 \leq N \leq 32$	4(N- 0)-33
$33 \leq N \leq 48$	8(N-16)-33
$49 \leq N \leq 64$	16(N-32)-33
$65 \leq N \leq 80$	32(N-48)-33
$81 \leq N \leq 96$	64(N-64)-33
$97 \leq N \leq 112$	128(N-80)-33
$113 \leq N \leq 128$	256(N-96)-33

The magnitude, |X(N)|, is normalized to lie in the range of 0 to 8159, where 8159 is the peak value of a 3.17 dBm0 sine wave.

Figure III-4 shows the transfer characteristic for the signalling frame where only 6 bits are available to represent the magnitude information. Note that there are only half as many quantization levels here. Each level covers twice the range of the previous case and uses only the even numbered decision levels. Again, the decoder output Z(N) will be midway between the decision levels.

$$Z(N) = \frac{X(2N) + X(2N+2)}{2} = X(2N+1) \quad , \quad N = 0, 1, \ldots 63$$

Figure III-5 demonstrates another way of interpreting the 8 bit code format. It is observed that the sign and ones complement magnitude form may be separated into three parts, including a sign bit, a three bit exponent and a four bit mantissa, very similar to the floating point representation used in many computers. Also given is a formula for calculating the normalized output value of the decoder. Figure III-6 shows the same data only for a signalling frame.

Rather than carrying out the computations in these formulas each time a mu-law expansion is necessary, the data shown in Table III-3 is stored into a ROM and the conversion then becomes a very fast table look-up.

III-C Digital Reference Levels

The basic reference level used in alignment and testing of all digital channel banks is the digital milliwatt. Figure III-7 gives the definition of the 0 dBm0, 1000 Hz sine wave reference signal which is used to align the receiving equipment in digital channel banks. This signal involves the repetition of eight samples consisting of only

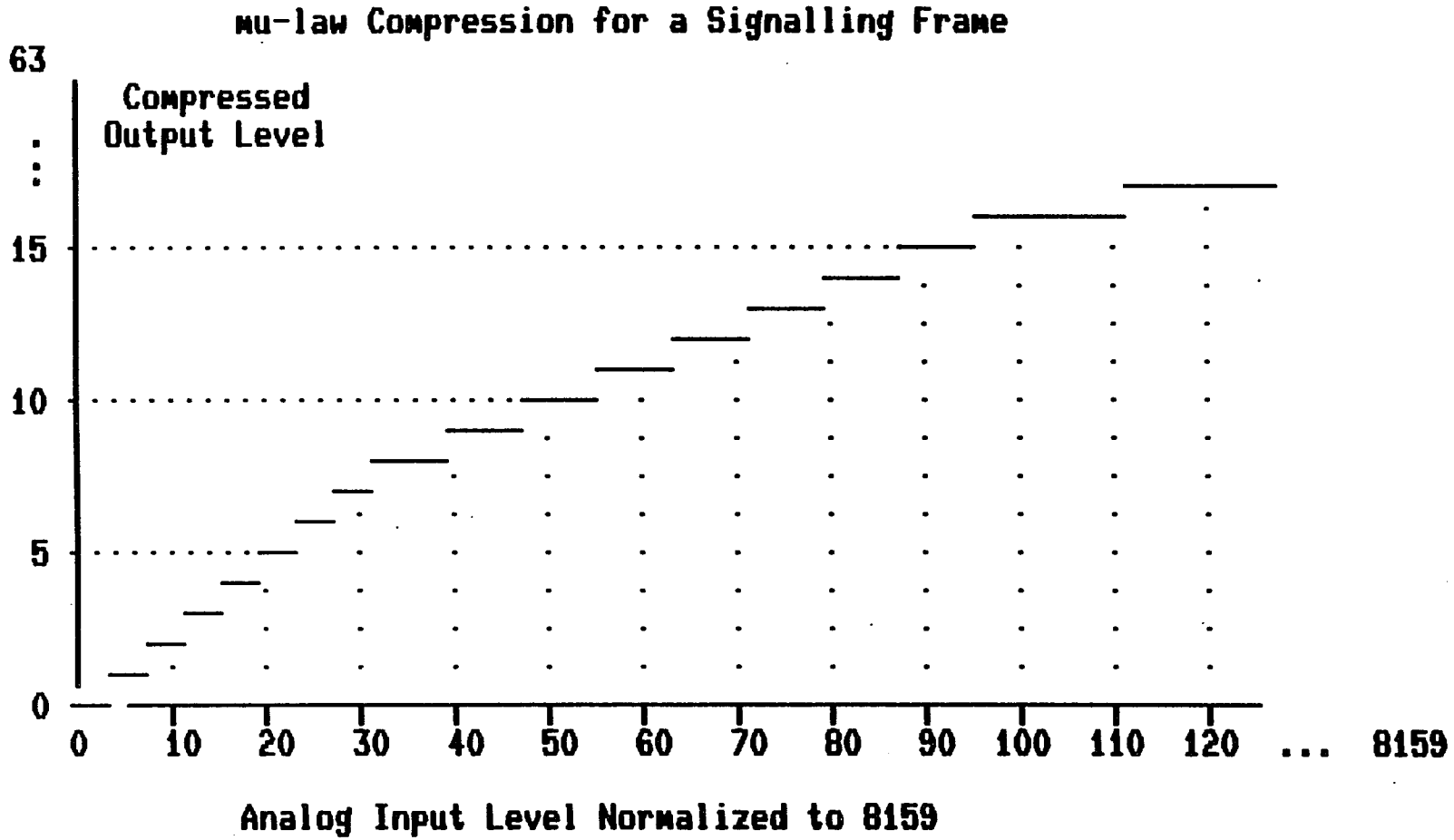
mu-law Compression for a Signalling Frame
63
Compressed
Output Level
15
10
5
0
0
10
20
30
40
50
60
70
80
90
100
110
120
...
8159
Analog Input Level Normalized to 8159

Figure III-4

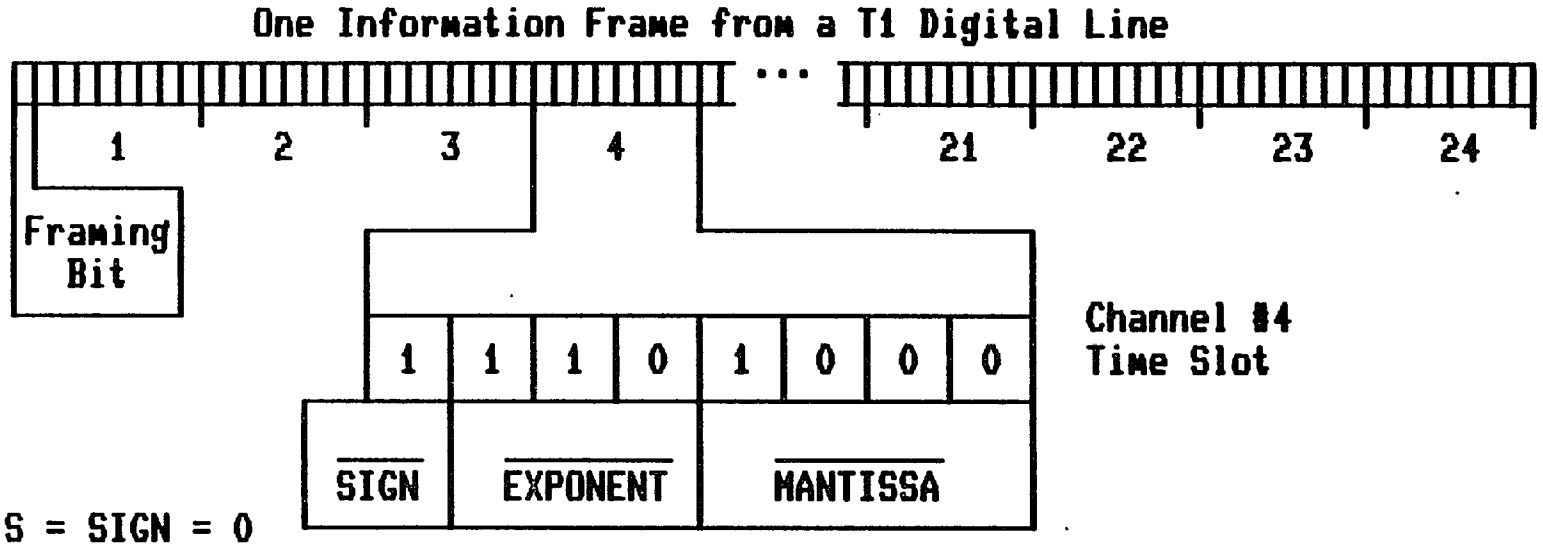

S = SIGN = 0

E = EXPONENT = 1

M = MANTISSA = 7

$$Y(N) = Y(16 \cdot E + M) = (-1)^{S} \cdot \left[2^{E} \cdot (2M + 33) - 33 \right]$$

mu-law Expansion: $$Y(16 \cdot 1 + 7) = Y(23) = (-1)^{0} \cdot \left[2^{1} \cdot (2 \cdot 7 + 33) - 33 \right] = 61$$

Extraction of a Sample Value from Time Slot #4 During an Information Frame.

The Result is Normalized to 8159, the Peak Value of a 3.17 dBm0 Sine Wave.

Figure III-5

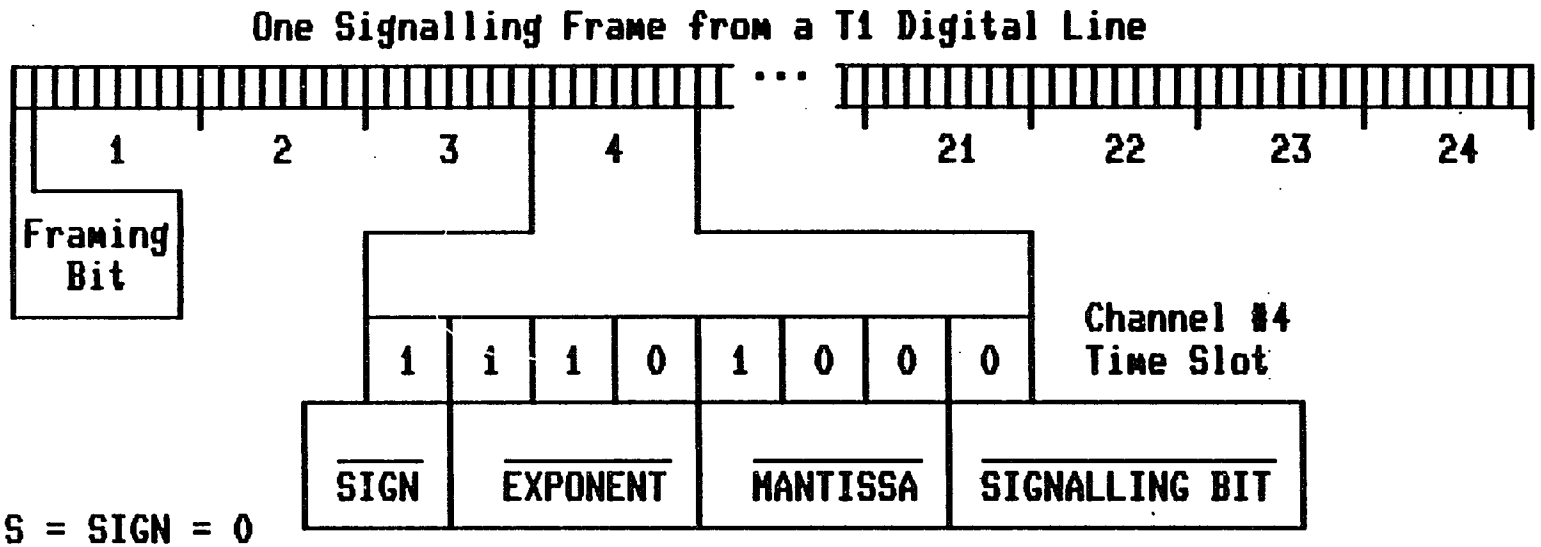

S = SIGN = 0

E = EXPONENT = 1

M = MANTISSA = 3

$$Z(N) = Z(8 \cdot E + M) = (-1)^{S} \cdot \left[2^{E} \cdot (4M + 34) - 33 \right]$$

mu-law Expansion:

$$Z(8 \cdot 1 + 3) = Z(11) = (-1)^{0} \cdot \left[2^{1} \cdot (4 \cdot 3 + 34) - 33 \right] = 59$$

Extraction of a Sample Value from Time Slot #4 During a Signalling Frame.

The Result is Normalized to 8159, the Peak Value of a 3.17 dBm0 Sine Wave.

Figure III-6

Table III-3 Conversion of mu-law compressed data to linear form.

INPUT		OUTPUT		INPUT		OUTPUT		INPUT		OUTPUT	
CODED DATA		DECODED		CODED DATA		DECODED		CODED DATA		DECODED	
LEVEL #	BINARY CODE	INFO FRM	SIG FRM	LEVEL #	BINARY CODE	INFO FRM	SIG FRM	LEVEL #	BINARY CODE	INFO FRM	SIG FRM
0000	11111111	0000	0001	0015	11110000	0030	0029	0030	11100001	0089	0091
0001	11111110	0002	0001	0016	11101111	0033	0035	0031	11100000	0093	0091
0002	11111101	0004	0005	0017	11101110	0037	0035	0032	11011111	0099	0103
0003	11111100	0006	0005	0018	11101101	0041	0043	0033	11011110	0107	0103
0004	11111011	0008	0009	0019	11101100	0045	0043	0034	11011101	0115	0119
0005	11111010	0010	0009	0020	11101011	0049	0051	0035	11011100	0123	0119
0006	11111001	0012	0013	0021	11101010	0053	0051	0036	11011011	0131	0135
0007	11111000	0014	0013	0022	11101001	0057	0059	0037	11011010	0139	0135
0008	11110111	0016	0017	0023	11101000	0061	0059	0038	11011001	0147	0151
0009	11110110	0018	0017	0024	11100111	0065	0067	0039	11011000	0155	0151
0010	11110101	0020	0021	0025	11100110	0069	0067	0040	11010111	0163	0167
0011	11110100	0022	0021	0026	11100101	0073	0075	0041	11010110	0171	0167
0012	11110011	0024	0025	0027	11100100	0077	0075	0042	11010101	0179	0183
0013	11110010	0026	0025	0028	11100011	0081	0083	0043	11010100	0187	0183
0014	11110001	0028	0029	0029	11100010	0085	0083	0044	11010011	0195	0199

Table III-3 (cont.) Conversion of mu-law compressed data to linear form.

INPUT		OUTPUT		INPUT		OUTPUT		INPUT		OUTPUT	
CODED DATA		DECODED		CODED DATA		DECODED		CODED DATA		DECODED	
LEVEL #	BINARY CODE	INFO FRM	SIG FRM	LEVEL #	BINARY CODE	INFO FRM	SIG FRM	LEVEL #	BINARY CODE	INFO FRM	SIG FRM
0045	11010010	0203	0199	0060	11000011	0423	0431	0075	10110100	0847	0831
0046	11010001	0211	0215	0061	11000010	0439	0431	0076	10110011	0879	0895
0047	11010000	0219	0215	0062	11000001	0455	0463	0077	10110010	0911	0895
0048	11001111	0231	0239	0063	11000000	0471	0463	0078	10110001	0943	0959
0049	11001110	0247	0239	0064	10111111	0495	0511	0079	10110000	0975	0959
0050	11001101	0263	0271	0065	10111110	0527	0511	0080	10101111	1023	1055
0051	11001100	0279	0271	0066	10111101	0559	0575	0081	10101110	1087	1055
0052	11001011	0295	0303	0067	10111100	0591	0575	0082	10101101	1151	1183
0053	11001010	0311	0303	0068	10111011	0623	0639	0083	10101100	1215	1183
0054	11001001	0327	0335	0069	10111010	0655	0639	0084	10101011	1279	1311
0055	11001000	0343	0335	0070	10111001	0687	0703	0085	10101010	1343	1311
0056	11000111	0359	0367	0071	10111000	0719	0703	0086	10101001	1407	1439
0057	11000110	0375	0367	0072	10110111	0751	0767	0087	10101000	1471	1439
0058	11000101	0391	0399	0073	10110110	0783	0767	0088	10100111	1535	1567
0059	11000100	0407	0399	0074	10110101	0815	0831	0089	10100110	1599	1567

Table III-3 (cont.) Conversion of mu-law compressed data to linear form.

INPUT		OUTPUT		INPUT		OUTPUT		INPUT		OUTPUT	
CODED DATA		DECODED		CODED DATA		DECODED		CODED DATA		DECODED	
LEVEL #	BINARY CODE	INFO FRM	SIG FRM	LEVEL #	BINARY CODE	INFO FRM	SIG FRM	LEVEL #	BINARY CODE	INFO FRM	SIG FRM
0090	10100101	1663	1695	0105	10010110	3231	3167	0120	10000111	6239	6367
0091	10100100	1727	1695	0106	10010101	3359	3423	0121	10000110	6495	6367
0092	10100011	1791	1823	0107	10010100	3487	3423	0122	10000101	6751	6879
0093	10100010	1855	1823	0108	10010011	3615	3679	0123	10000100	7007	6879
0094	10100001	1919	1951	0109	10010010	3743	3679	0124	10000011	7263	7391
0095	10100000	1983	1951	0110	10010001	3871	3935	0125	10000010	7519	7391
0096	10011111	2079	2143	0111	10010000	3999	3935	0126	10000001	7775	7903
0097	10011110	2207	2143	0112	10001111	4191	4319	0127	10000000	8031	7903
0098	10011101	2335	2399	0113	10001110	4447	4319				
0099	10011100	2463	2399	0114	10001101	4703	4831				
0100	10011011	2591	2655	0115	10001100	4959	4831				
0101	10011010	2719	2655	0116	10001011	5215	5343				
0102	10011001	2847	2911	0117	10001010	5471	5343				
0103	10011000	2975	2911	0118	10001001	5727	5855				
0104	10010111	3103	3167	0119	10001000	5983	5855				

T1-Line Code	8159 Normalization	Graphic Representation
10001011	+5215	
10011110	+2207	
00011110	-2207	
00001011	-5215	

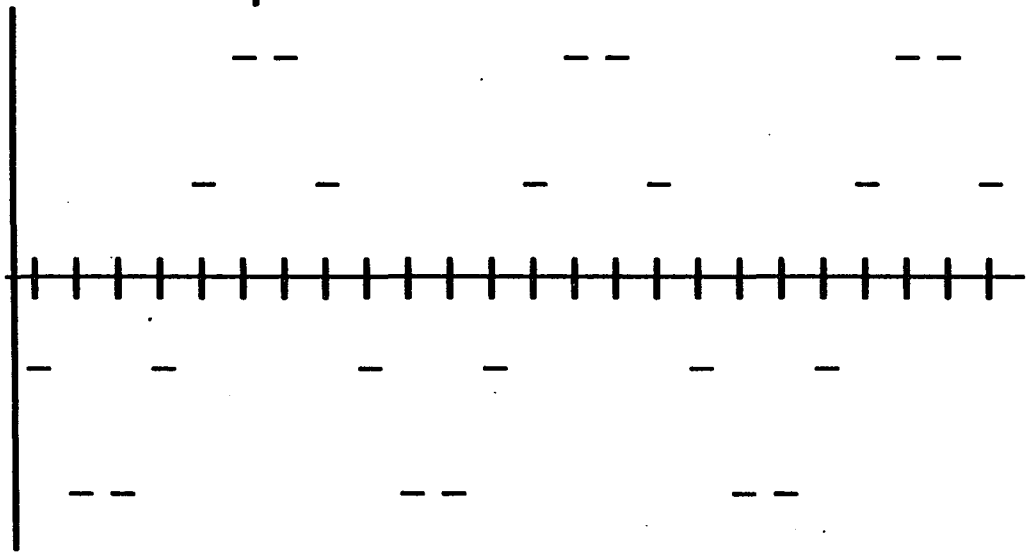

$$\left[\frac{5215^2 + 2207^2}{2}\right]^{1/2} = 4004 \text{ RMS Value} \longrightarrow 5663 \text{ Peak Value}$$

Definition of the Digital Milliwatt: 1000 HZ Sine Wave at 0 dBm

Figure III-7

four unique levels and only two unique magnitudes. Therefore, in order to establish the relationship between the normalized values and the signal power which they represent, the RMS value of this reference signal is calculated as shown in the figure. The value of 4004 equates to a peak value of 5663 for a 0dBm0 sine wave. Therefore, a sine wave at any desired frequency may be generated by calculating the values of the sine function at the appropriate angles and multiplying by 5663.

III-D Digital Channel Bank Test Requirements

III-D.1 Minimum Set of Tests

The following set of test requirements are intended as a minimum to certify with reasonable certainty that a given transmission channel is operating within acceptable limits. Not all of the published specifications are tested here.

Frequency Response - The frequency response should be measured with test stimuli at 0 dBm0. Figure III-8 shows the permissible range for the frequency distortion over the entire 4000 Hz channel bandwidth [10]. Rather than trying to characterize this response for any given channel over the entire band, it is generally acceptable to measure the response at a few discrete points near the critical frequencies. Measurements at 182 Hz, 302 Hz and 3020 Hz are commonly used for this purpose. A reference frequency near 1020 Hz is also commonly used instead of 800 Hz.

Gain Tracking - The magnitude of the difference in the gain variation of a given channel for various input levels should not exceed the limits specified in Figure III-9, where the difference is measured relative to the gain with a

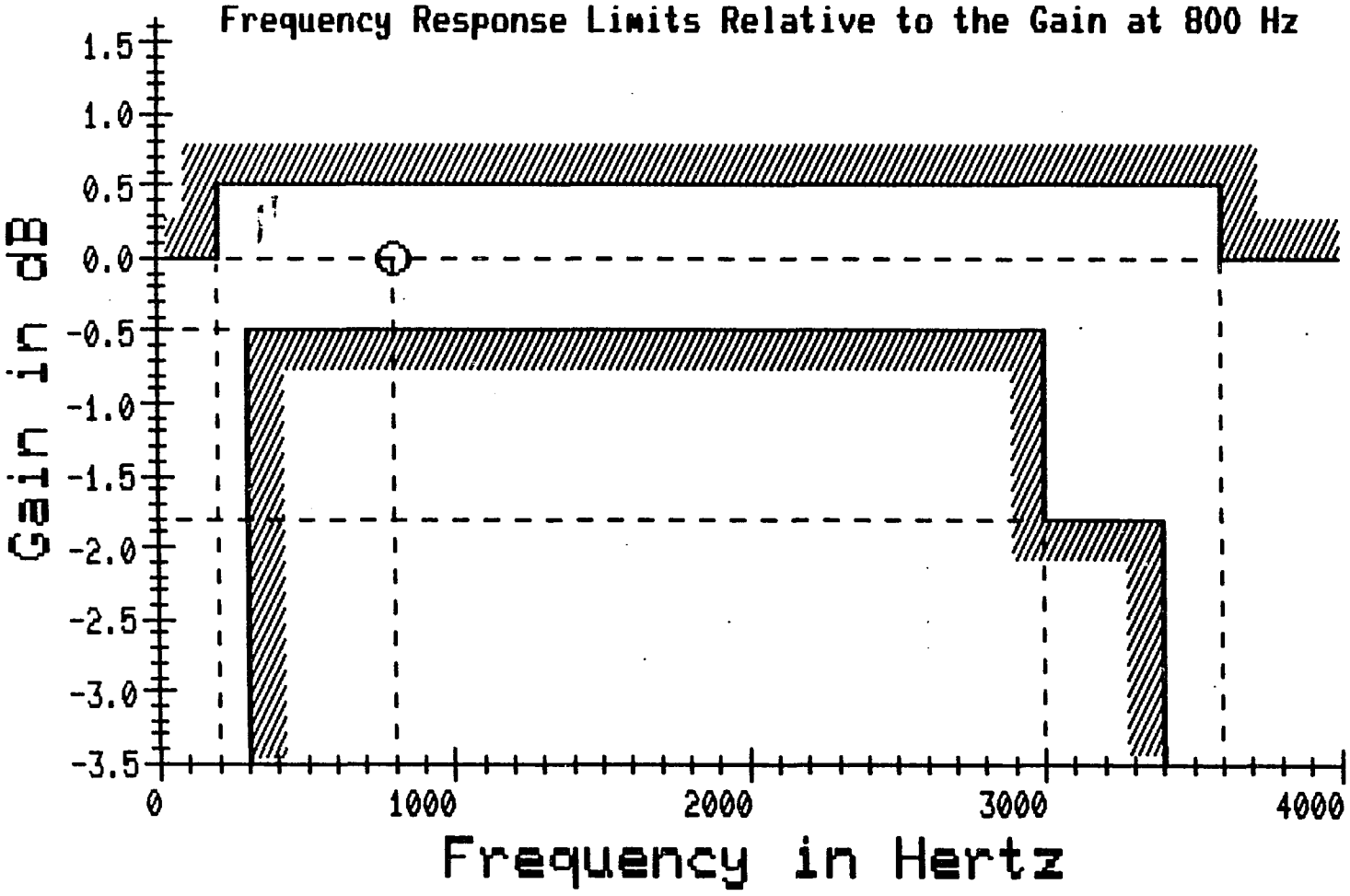
Frequency Response Limits Relative to the Gain at 800 Hz
Gain in dB
1.5
1.0
0.5
0.0
-0.5
-1.0
-1.5
-2.0
-2.5
-3.0
-3.5
0
1000
2000
3000
4000
Frequency in Hertz

Figure III-8

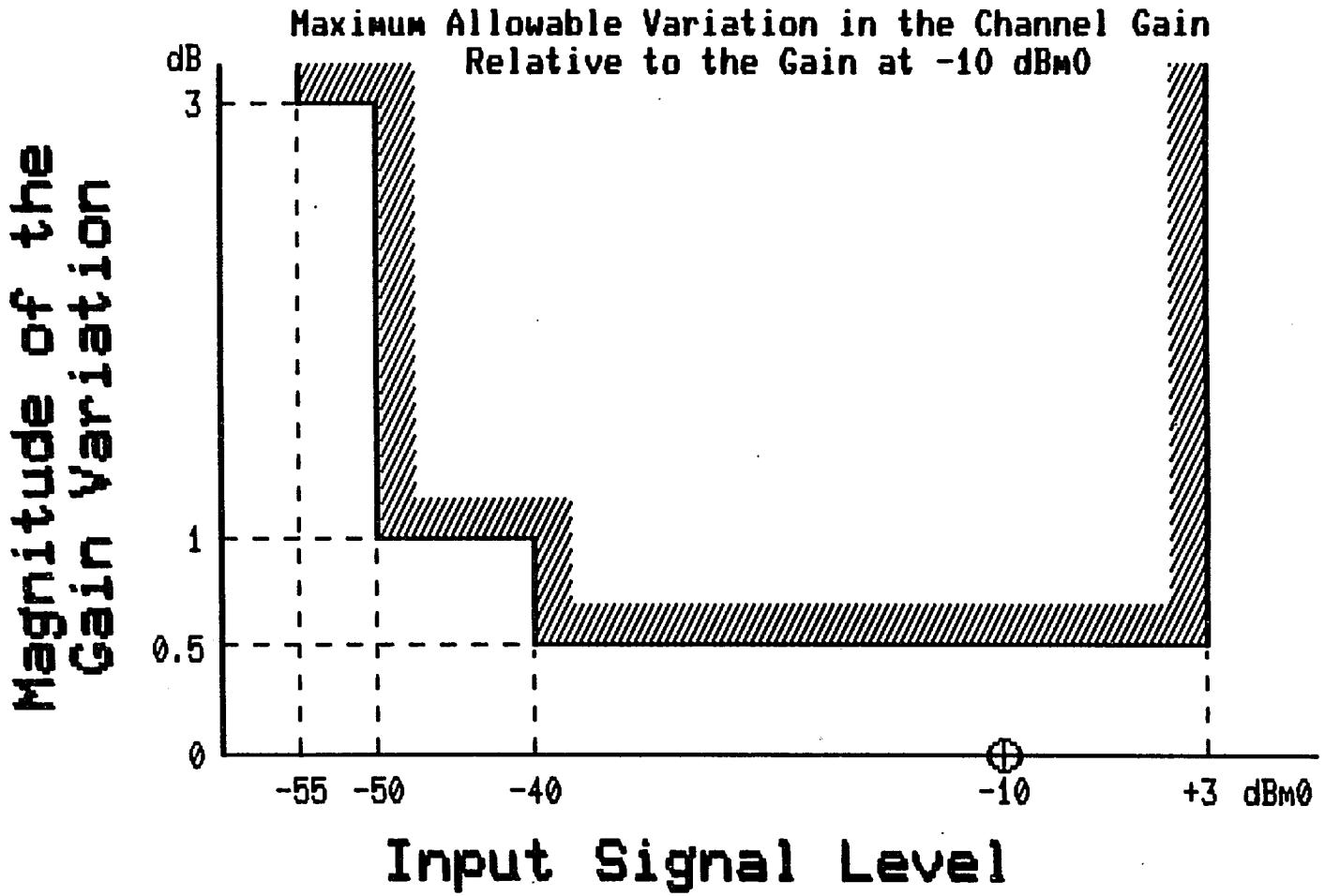
Maximum Allowable Variation in the Channel Gain
Relative to the Gain at -10 dBm0
dB
3
1
0.5
0
Magnitude of the
Gain Variation
-55
-50
-40
-10
+3 dBm0
Input Signal Level

Figure III-9

-10 dBm0 input signal [10]. It will suffice to measure this variation at a few points within the more commonly used range of levels. Measurements are often made with a 1020 Hz sinusoidal input signal at levels of 0 dBm0, -10 dBm0, -20 dBm0, -30 dBm0 and -40 dBm0.

Distortion - The quantization distortion greatly overshadows any noise which may be present in a channel when a signal of at least -45 dBm0 is being transmitted. Therefore, the signal to distortion ratio may be measured as the signal to noise ratio for any signal above this level. Figure III-10 gives the minimum acceptable signal to total distortion ratio as a function of the input level [10]. This measurement is normally made with the same test signals used for the gain tracking tests.

Noise - The idle circuit noise, which is measured with the input and output of the channel terminated with the proper impedances, should not exceed -65 dBm0p (psophometric weighting) [10]. Measurements are often made with C-message weighting, in which case the idle circuit noise should not exceed 23 dBrnc0 (relative to one nanowatt and with C-message weighting) [11]. A value of 0 dBrnc0 is equivalent to -90 dBm0 with C-message weighting. The C-message and psophometric weightings refer to the use of special bandpass filters which remove some of the high and low frequency noise.

Crosstalk - The crosstalk should be measured with a 0 dBm0 signal in the range of 700 Hz to 1100 Hz applied to one channel and all unused inputs and outputs terminated. The level measured in the adjacent channels should not exceed -65 dBm0 [10].

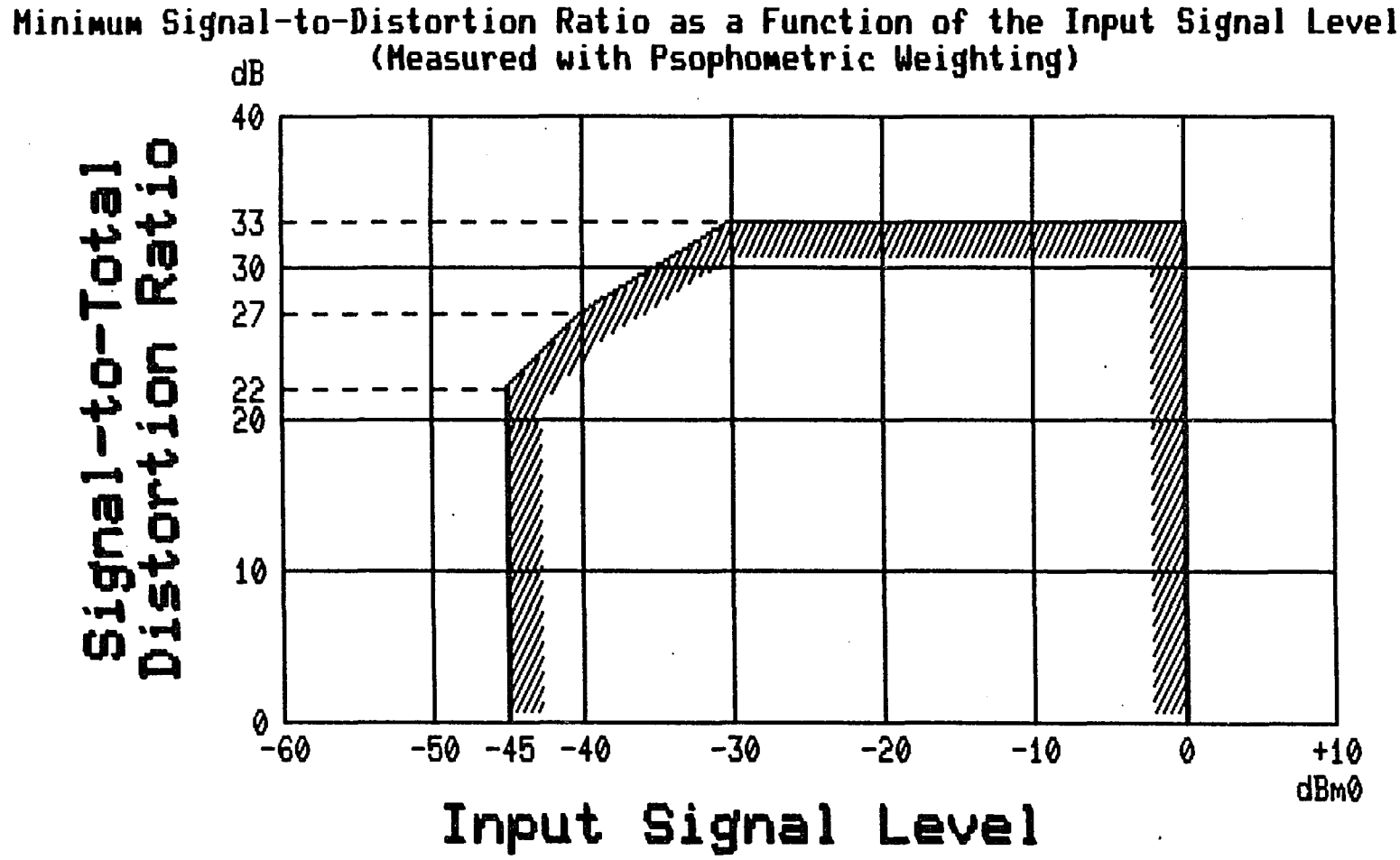

Figure III-10

III-D.2 Other Desirable Tests

In addition to the above tests, it would be desirable to measure some other parameters which are not considered necessary when making an installation or acceptance check of a channel bank.

Frequency Response - It would be desirable to make additional frequency measurements to more completely specify the response characteristic of the channels and compare them to the limits of Figure III-8. A frequency response measurement just below 4000 Hz should be at or below -28 dB indicating that the combined response of the transmitting and receiving low pass filters is sufficient to suppress out-of-band signals. A failure here would require the capability of measuring the individual responses of the transmit and receive units to determine which is at fault. If the phase portion of the frequency response is available, it may be compared to the mask of Figure III-11 to determine whether the requirements concerning intersymbol interference for voiceband data signals are met [11].

Intermodulation Distortion - With two sine wave signals of different frequencies in the range of 300 Hz to 3400 Hz and not harmonically related and with equal amplitudes in the range of -4 to -21 dBm0, no intermodulation products should be produced with levels greater than -35 dB below the input signals [10].

Crosstalk - The crosstalk requirement should include measurements between all channels in the bank, not just to adjacent channels.

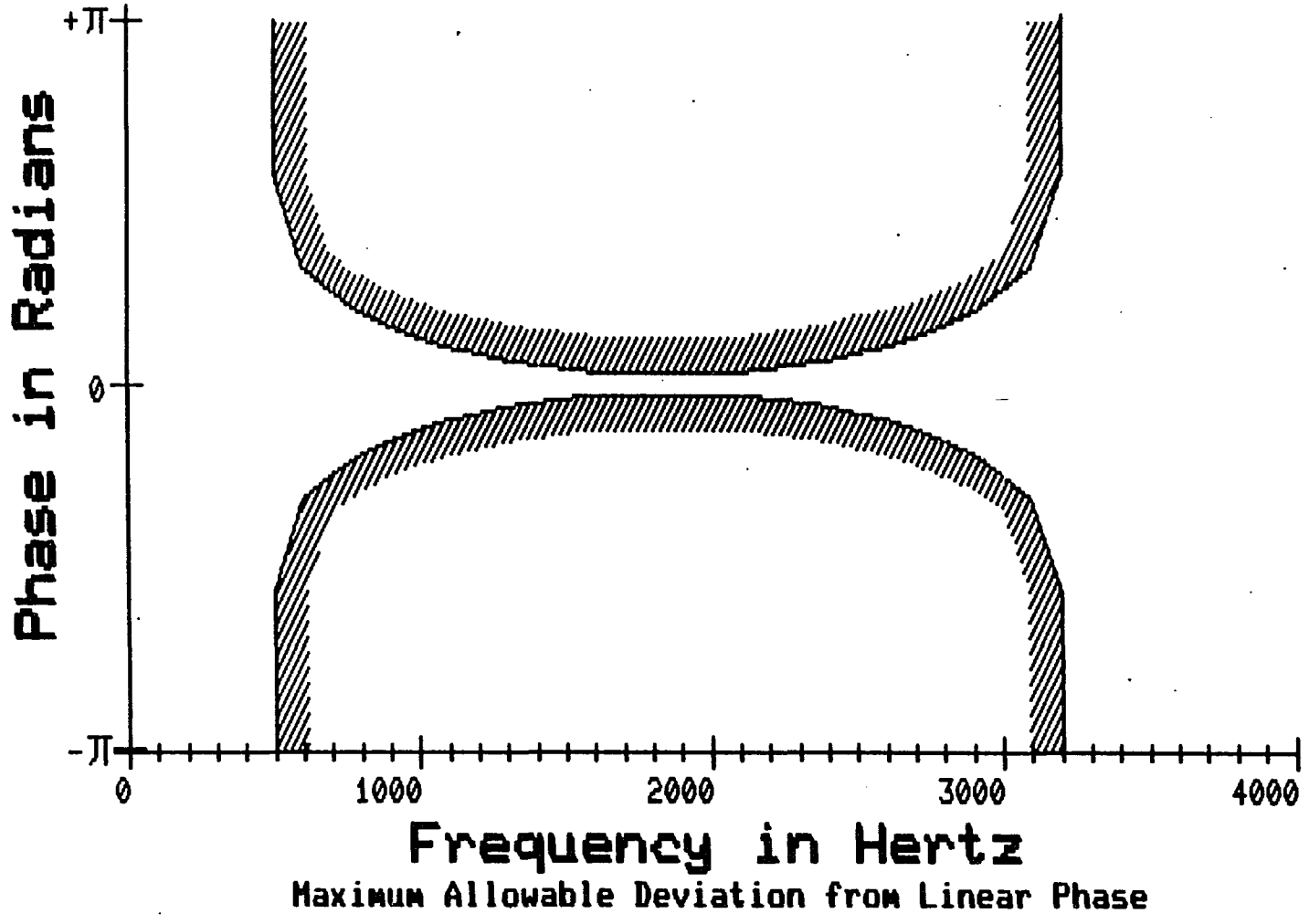

Figure III-11

III-E Testing Methods

The conventional way of testing a digital telephone channel is to connect a transmitter and receiver in the same fashion in which they will be connected in actual service and make the required measurements on the voice channel which is established. This method is acceptable and usually required in a telephone office environment. However, in the factory where all of the interconnections have not yet been made and where high volume testing is necessary, this method becomes cumbersome. This conventional test arrangement, as shown in Figure III-12, must be considerably modified if it is to support automatic testing. The digital channel bank, which is actually the unit being tested here, consists of not one, but effectively forty-eight individual voice channels (since the 24 channels are bidirectional). This number of channels may also be multiplied by the number of banks being tested at a given time. With the automation of a test system of this size comes the problem of switching the signal generators and detectors to all of the various channels. Also, whenever a failure is detected, manual intervention is usually required to determine which of the two series units, the transmitter or the receiver, is actually at fault.

It is suggested that this last problem may be solved by a test configuration as shown in Figure III-13. Here the transmitter and receiver are tested as two independent units, so that there is no ambiguity when a fault is detected. This test system must still include the modest switching matrices of the previous configuration in order to test large numbers of channels automatically.

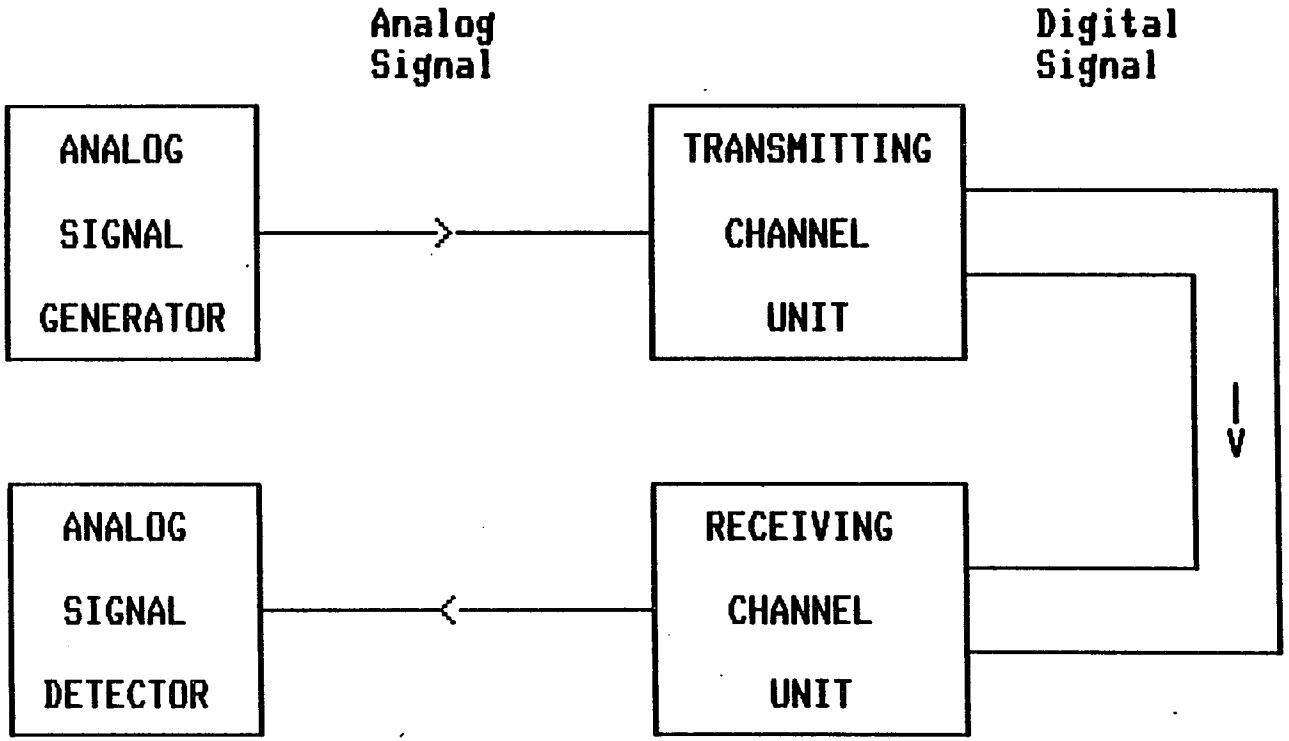

Usual Method of Testing a Telephone Voice Channel

Figure III-12

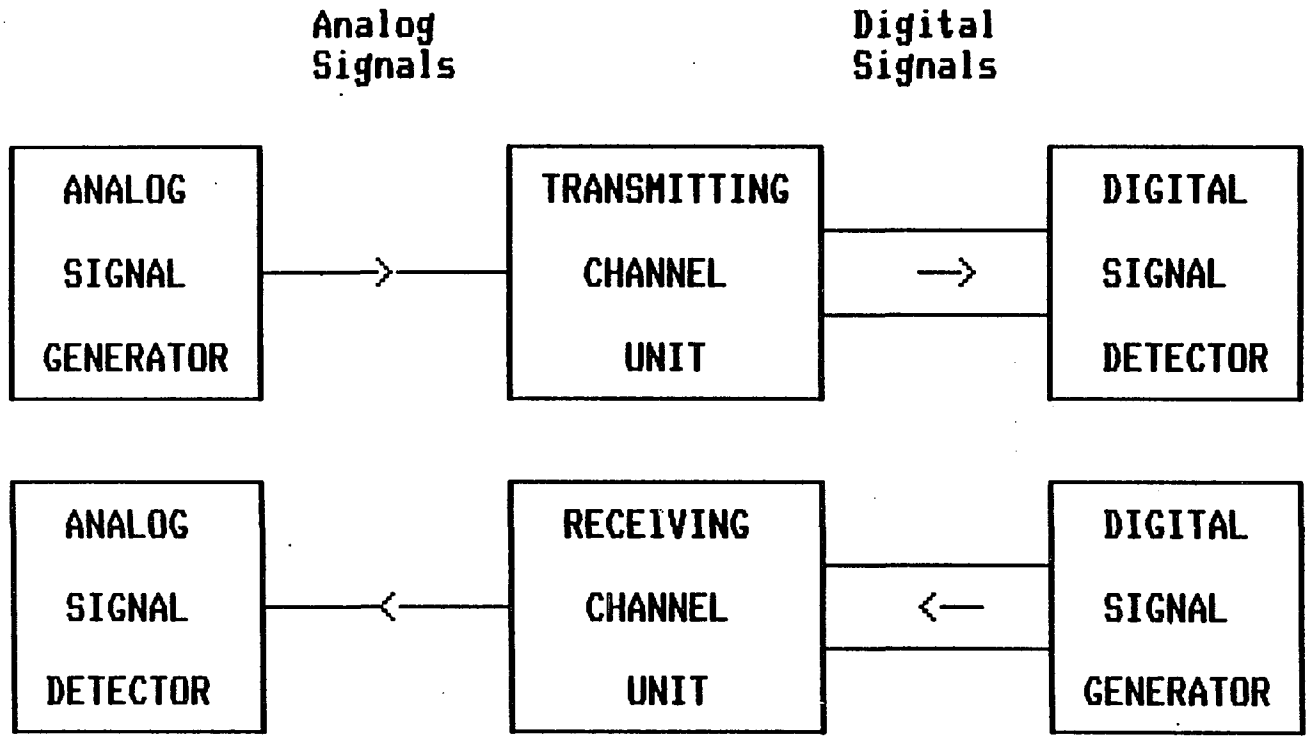

Inclusion of Digital Signal Processors
Allows Complete Isolation of Failures

Figure III-13

The final decision as to what test configuration is optimal in a given situation depends on many factors, all of which either directly or indirectly affect the final cost of the product. The quality or percent of the units tested which pass test has the greatest affect on the type of test system chosen. For example, a semi-automatic test configuration as suggested in Figure III-12 may be quite efficient when very few units are found defective. The test system could run virtually unattended for hours proving unit after unit of good quality. However, since defects require manual intervention, a large number of bad units would make such a test more labor intensive, causing the ultimate cost to rise. As an alternative, the test system of Figure III-13 is capable of further diagnostics without manual intervention. This system would, therefore, be more cost effective in an environment with a high defective rate. The trade-off is that this test system requires a greater initial capital expenditure in order to reduce steady state labor costs. In turn, this trade-off may not be cost effective in a low defect rate environment. Another consideration which must not be overlooked is the advantage gained by having a maximum amount of pertinent information available whenever a fault is detected, in order to expedite the correction of the problem and its cause in an attempt to prevent it from recurring, and ultimately improve the quality of the product. With this in mind, it is suggested that two test strategies be adopted. First, during a product's infancy when not all of the bugs have been ironed out of the production process, the test system should be more highly automated and be able to more completely test the units, providing maximum diagnostic aids. This system

would be used to fine tune the production process and at the same time determine which tests are most useful in detecting faulty product. As the production system matures, the quality of the product should increase until at some point it reaches a steady state where the faults occur due to random variables in the production process which may not be economically controlled. At this point, further feedback in an attempt to improve the process may actually be a waste of time and money. The set of tests which can most expeditiously detect defective product should be used in the majority of testing. Obviously, a more complete set of tests must still be made available for repair of the small number of fall outs if this repair is considered cost effective. The ideal situation would be where the comprehensive test system, which was used during the initial production runs, could be easily adapted either to aid in the repair of defective product or to be used in another new product line during its infancy. In a quality assurance environment, where the purpose of test is merely to estimate the quality of the product, the conversion to a repair facility is not considered. A valuable by-product of the quality assurance testing, especially during initial production, is to insure that the production shop's product screening equipment is capable of detecting any and all faults which may be detrimental to the in-service operation of the product. For this reason the initial testing should be more comprehensive and should attempt to simulate future, actual operating conditions as closely as possible. This latter point may prove to be an invaluable aid in cost avoidance by the early discovery of problems which may otherwise only surface after the customer has purchased and attempted to use the procuct.

As a result of this reasoning, two test configurations are suggested. The first is essentially that of Figure III-13 where the most complete set of diagnostics may be provided. The second, which is intended for testing mature product, is shown in Figure III-14. This latter test set avoids the need for a large switching matrix by connecting the multitude of voice frequency channels to each other and providing test access only from the digital side. Since the format of the digital line is standard, things such as the impedance of the voice frequency path and the various types of signalling used will not affect the hardware requirements of the test set. Various types of channel units may affect the types of tests performed, but this is controlled by software and is easily upgraded as different tests become necessary. The remainder of this thesis is dedicated to developing the signal processing techniques needed to realize the digital portion of the two test configurations shown in Figures III-13 and III-14.

III-F Data Input Hardware

The basic philosophy of the hardware design is to use as many of the readily available, standard production circuit packs as possible. This not only prevents an unnecessary replication of design effort but also provides a very cost efficient supply of spare parts. Since virtually all of the digital carrier systems are compatible with the standard digital line format, the D4 product line was selected to provide the necessary units to perform the required standard functions within the interface. The production process of the D4 digital channel banks is currently at the mature stage where an ample supply of high

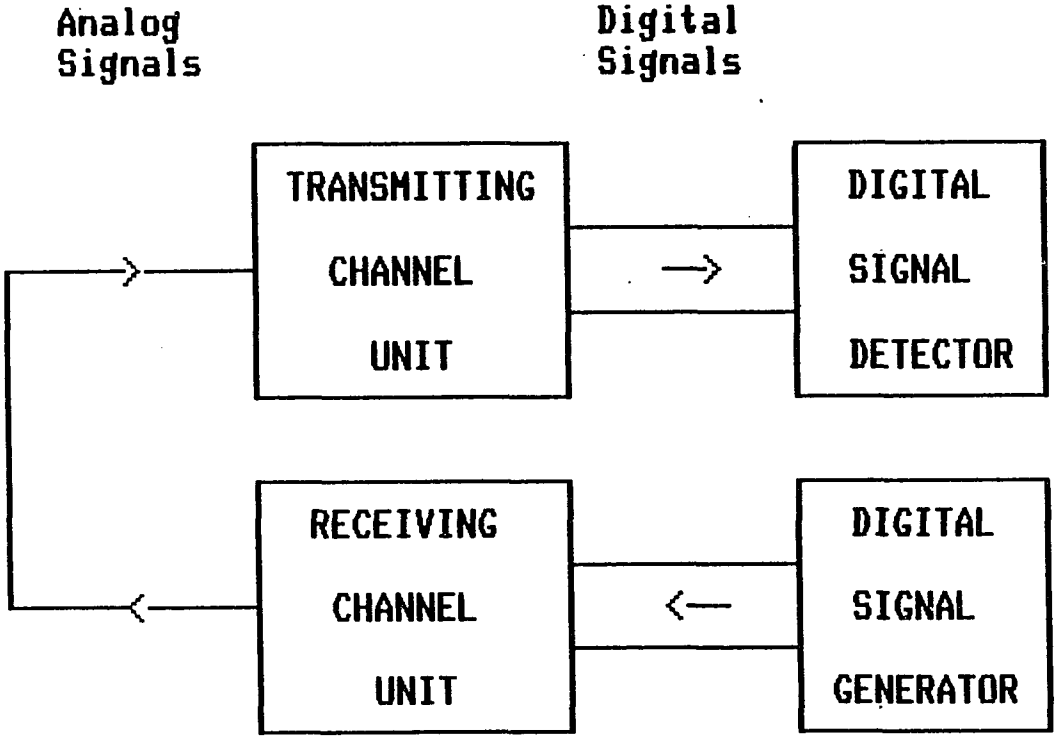

Looping of the Analog Lines Permits the Units to be Completely Tested with Digital Signal Processors

Figure III-14

quality circuit packs are available. This product also has built in the means for a channel unit circuit pack to digitally access the information on the T1 line for use in high speed data communications. For these reasons this product seems ideal for the intended application.

The task of the digital input hardware is to take a specified number of consecutive 8 bit data words from a given channel's time slot, as they are presented by the D4 hardware, and transfer them into the test computer's memory. Rather than require the computer to perform the mu-law expansions on every data word, it is more efficient to build a look-up table in the form of a read-only-memory into the input hardware. This expansion should be optional so that the actual 8 bit data from the digital line may be returned if desired. Three additional features were also implemented with a minimul of additional circuitry, making the interface more flexible. First, the states for the two signalling paths for the selected channel are stored within the interface and made continuously available to the computer. Second, provision is made for optionally reading the data for all channels on the T1 line instead of just a single one. Data retrieval is synchronized to begin one frame prior to an A-signalling frame so that data retrieved in the read-all-channels mode may be separated into the proper channels and the signalling information recovered. Finally, the provision has been made so that the computer may use the expansion look-up table to convert an 8 bit compressed word into its expanded value.

The read-all-channels mode requires that data be stored at 8000 times 24 or 196,000 words per second, thus requiring a Direct Memory Access (DMA) interface. The DRV11-B DMA

interface chosen for the task is capable of 250,000 transfers per second in the single cycle mode. Using the single cycle mode means that the processor may use the time between samples to continue with other tasks. Figure III-15 shows the bit assignments used for connecting to the DMA interface.

As previously mentioned, the common circuitry within a standard D4 channel bank, which is shared by all of the 24 channel units, is designed to provide all of the signals necessary for direct retrieval of the 8 bit data words from the T1 line. Figure III-16 lists these signals and gives a brief description of their usage. The AND-ing of the proper combination of RSQ and RSP signals produces a signal indicating the presence of a given channel's time slot. The RSA, RSB and RSAB signals may be used to derive the proper signalling states. RCLK provides a falling edge for each data bit when it is valid at the RNDATA output. The RWD signal is used to qualify the other signals as valid. Figure III-17 shows the control portion of the interface circuitry. The RSQ qnd RSP signals are consolidated into just five signals which may be used to uniquely define any channel. This is done so that only a five bit comparator is needed to determine the occurrence of a given channel's time slot. The five bit code which the computer passes through the DMA interface must be precoded by the software as shown in Table III-4. The portion of the circuit in the upper right corner qualifies the occurrence of the proper time slot with the RWD signal, and logically AND's this with either RFA or RFB to clock the signalling data RSAB into the proper signalling status flip-flop. An additional flip-flop stores the fact that either type of signalling frame has occurred for use in

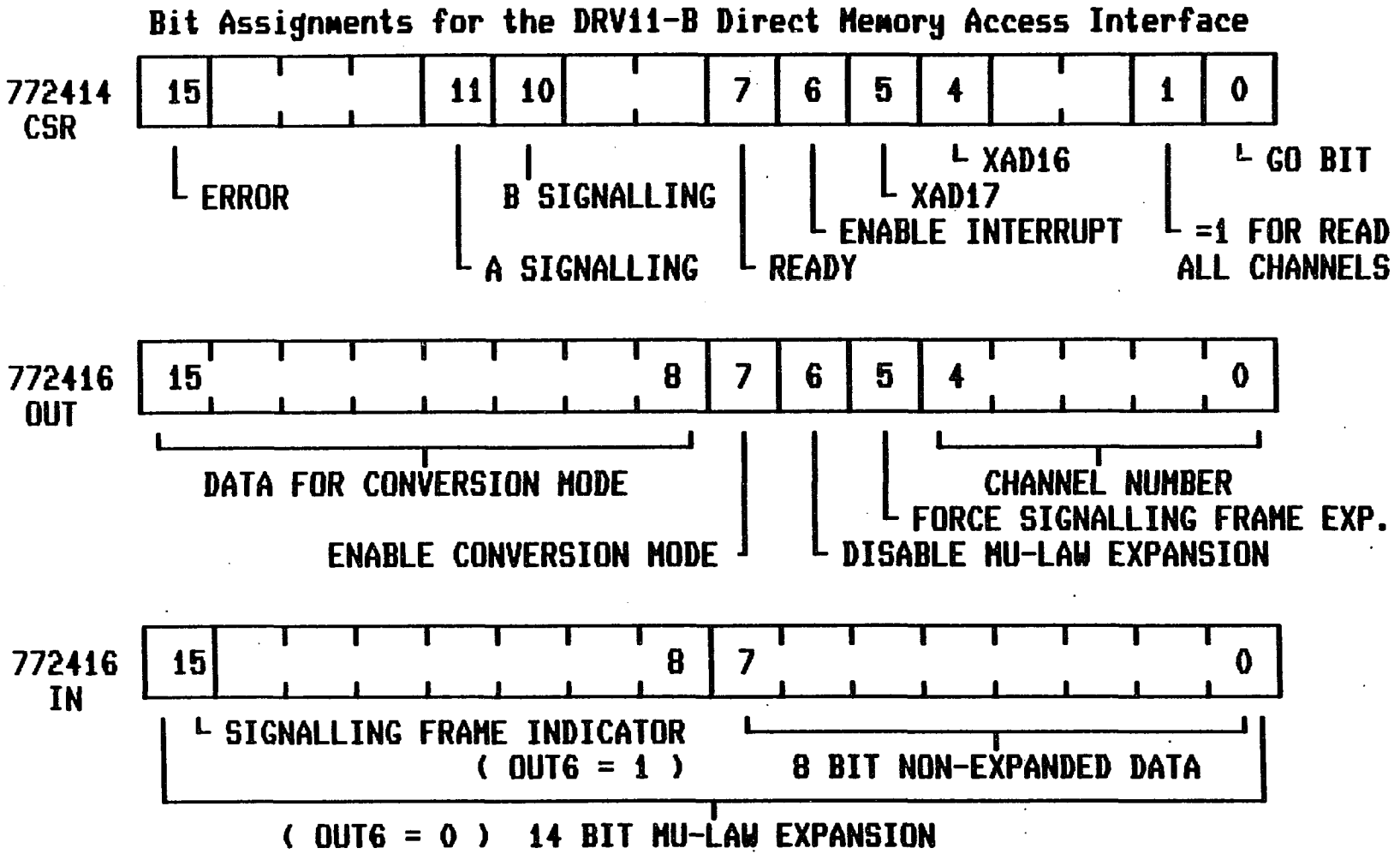

Figure III-15

Output Signals Provided from the D4 Common Units for Digital Data Retrieval

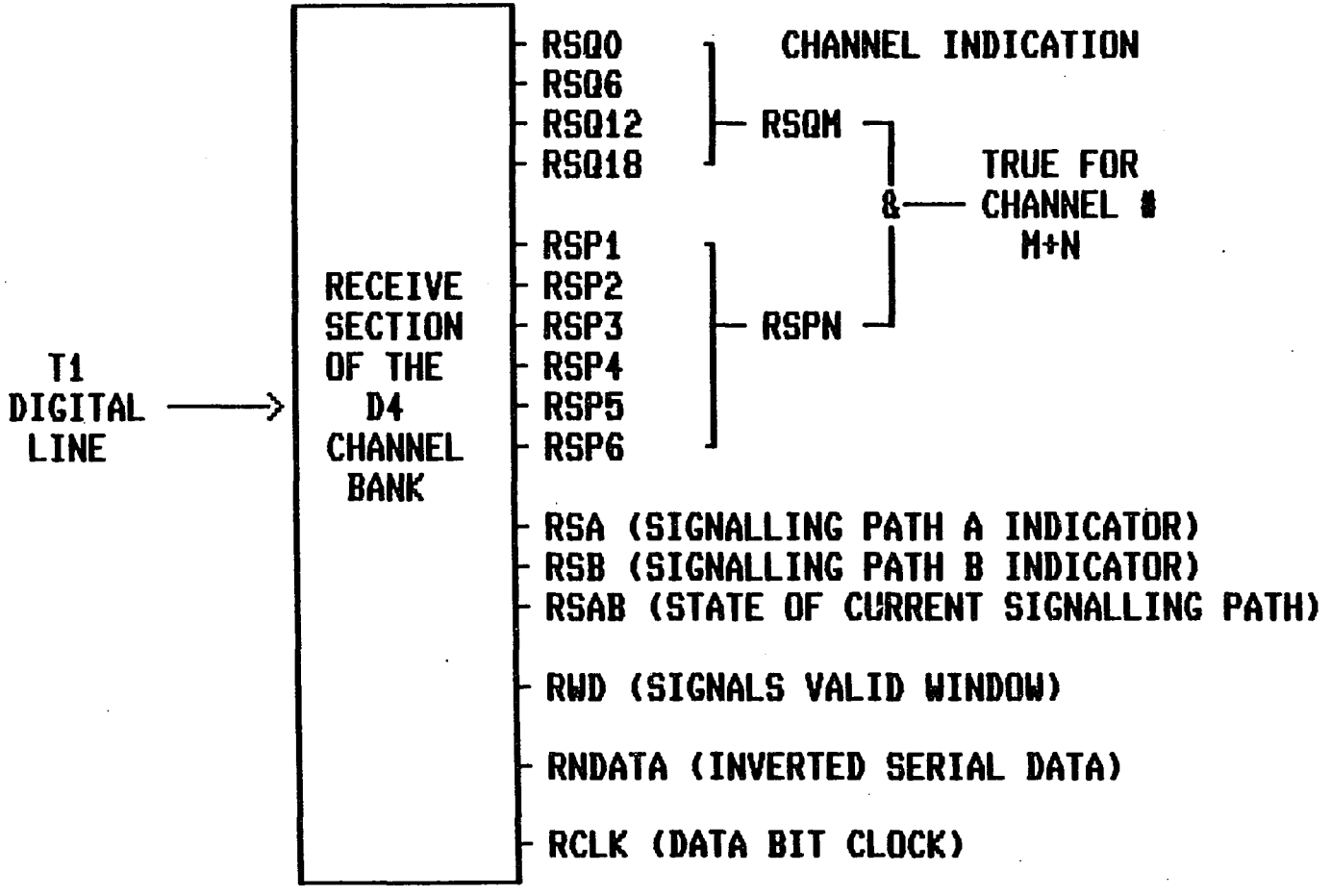

Figure III-16

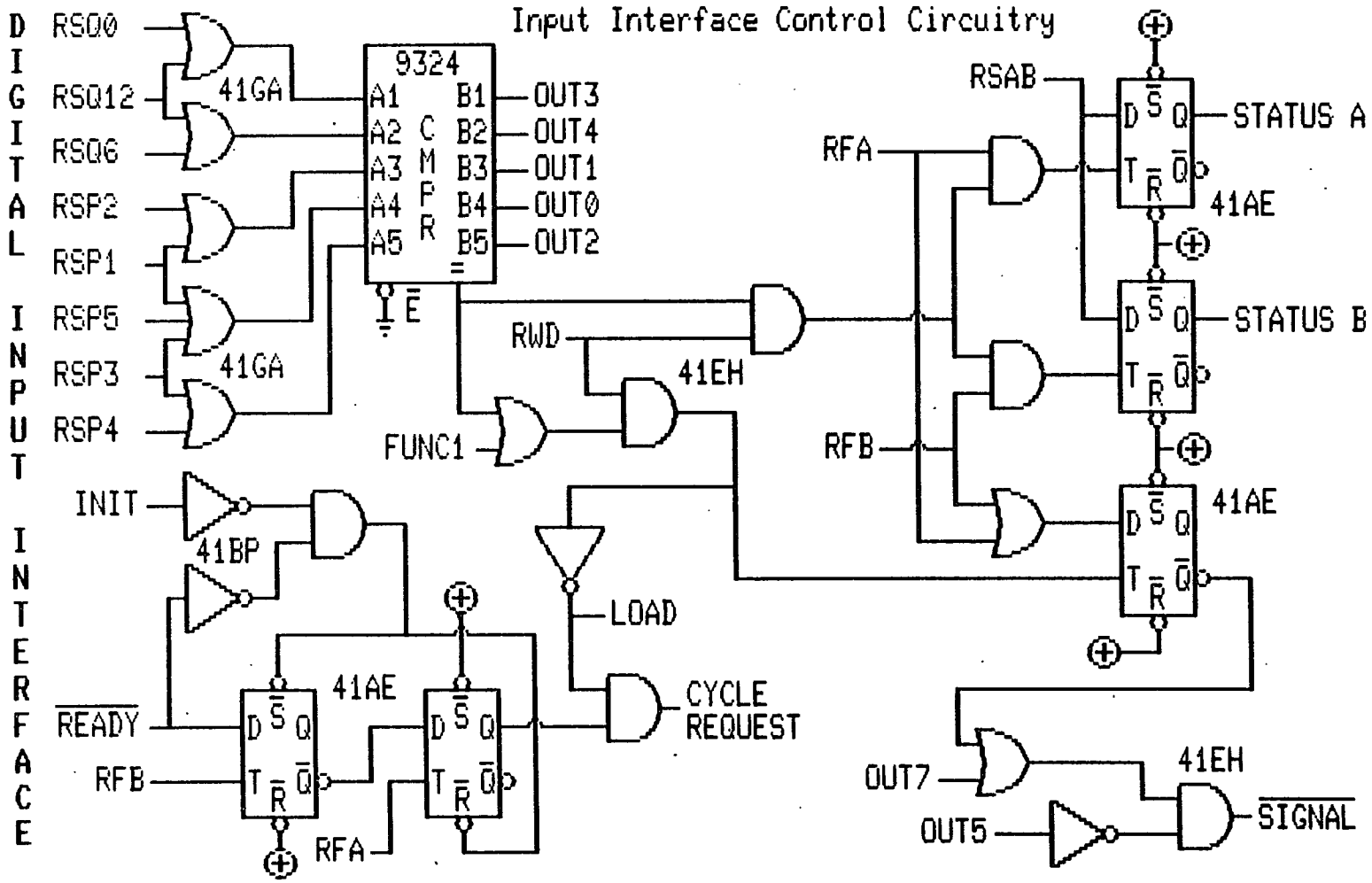

Figure III-17

Table III-4 Codes for selecting various channels with the DMA interface.

DECIMAL CHANNEL NUMBER	OCTAL CODE	DECIMAL CHANNEL NUMBER	OCTAL CODE	DECIMAL CHANNEL NUMBER	OCTAL CODE
1	13	9	25	17	31
2	12	10	24	18	30
3	15	11	21	19	03
4	14	12	20	20	02
5	11	13	33	21	05
6	10	14	32	22	04
7	23	15	35	23	01
8	22	16	34	24	00

modifying the mu-law expansion characteristic during a signalling frame. This modified expansion may be inhibited by OUT7 or forced by OUT5 when the computer is using the look-up table. The remaining circuitry, in the lower left corner, generates a DMA cycle request for each eight bit data word, which is to be stored in the computer memory, and synchronizes the first sample to begin just one frame prior to an A signalling frame.

Figure III-18 shows the data portion of the interface. The serial data is clocked into what is effectively an eight bit, serial in, parallel out, shift register by the RCLK signal. The LOAD signal from the control part of the circuit latches the eight bit word into a holding register from which it is presented to an eight bit wide, two input multiplexer. The multiplexer is used to select either this data during the input mode or data from the computer which is to be expanded. The 2716 EPROM's have the mu-law expansion look-up table stored in them for both the information and signalling frames and also include a table where the output data is the same as the input for use in the case where no expansion is to be done.

Programming of the interface is relatively straight forward. The computer outputs the desired channel code, sets the control bits to the desired states, gives the DMA interface a starting memory location and the number of samples to be taken, and then sets the GO bit. The sampling and subsequent storage of the sample data into the computer's memory then progresses without further action by the program. Once the requested number of samples has been taken, an interrupt notifies the computer that the process has been completed.

DIGITAL INPUT INTERFACE

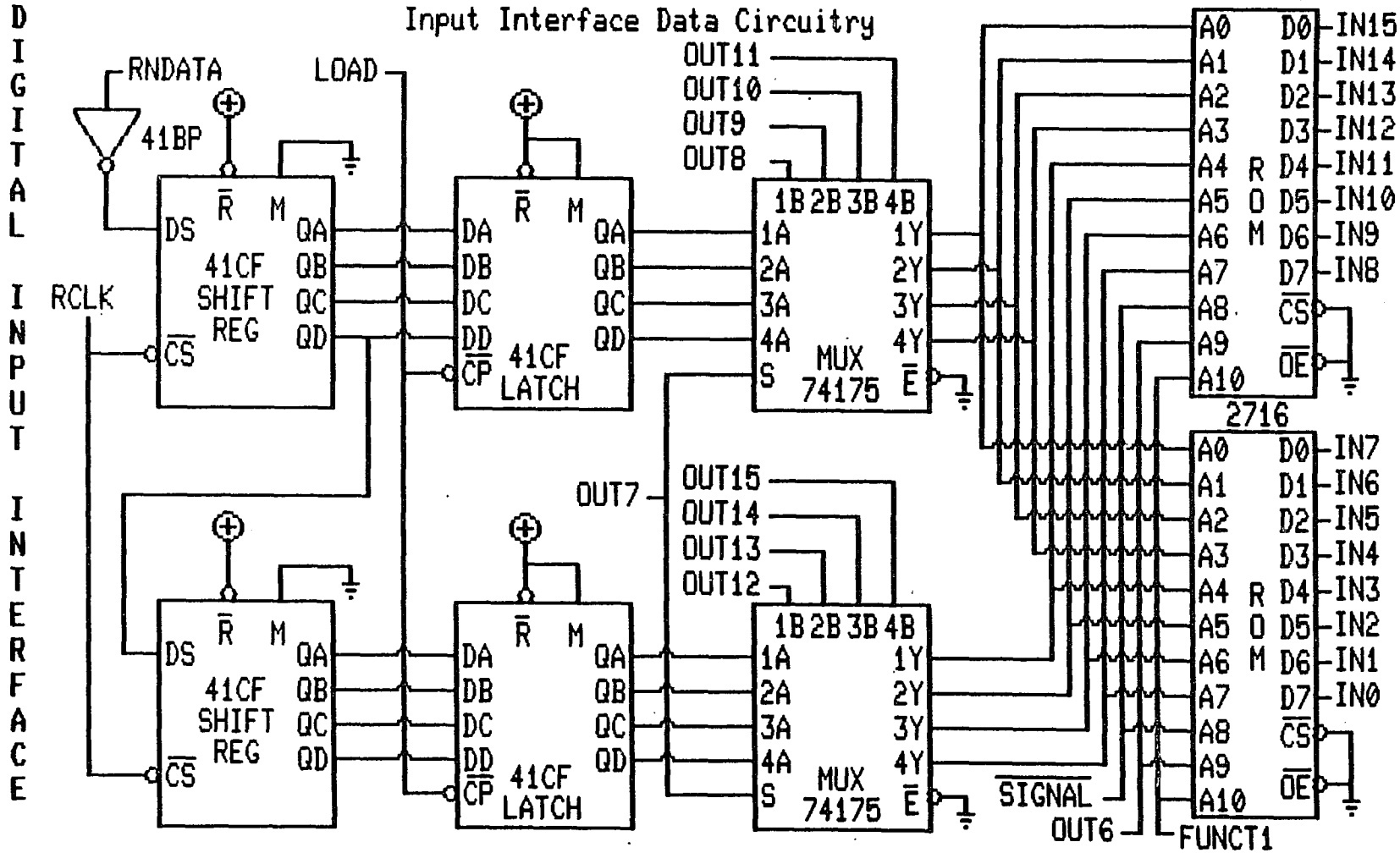

Figure III-18

CHAPTER 4

MIXED RADIX FAST FOURIER TRANSFORM TECHNIQUES

IV-A Introduction

Section IV-B of this chapter contains derivations for the exact number of complex multiplications required to perform the most efficient Fast Fourier Transform (FFT) on any number of points. As background leading into the derivations, the complex multiplication is examined, followed by some observations about and techniques for calculating the complex exponential rotation factors.

Section IV-C describes the data shuffling required in performing a mixed radix FFT using any number of data points.

Section IV-D discusses the effects of taking a time limited sample of a continuous signal to be used as input to a Discrete Fourier Transform (DFT) algorithm and how the results should be interpreted. Also discussed are the advantages of using stimuli with certain special characteristics and how this may simplify the analysis and improve the results.

IV-B Fast Fourier Transform Techniques

IV-B.1 Complex Multiplication Techniques

A complex multiplication is usually thought of as

$$(a + jb)\ (c + jd) = ac - bd + j(ad + bc)$$

requiring four real floating point multiplications.

However, if the operations are performed in a slightly different order, the same result may be obtained with only three multiplications. First form the combinations

$$x = c + d$$
$$y = a + b$$
$$z = a - b$$

Then form the three products

$$p = ax = a(c + d) = ac + ad$$
$$q = dy = d(a + b) = ad + bd$$
$$r = cz = c(a - b) = ac - bc$$

Now take the differences

$$s = p - q = ac + ad - ad - bd = ac - bd$$
$$t = p - r = ac + ad - ac + bc = ad + bc$$

and the result is that

$$s + jt = ac - bd + j(ad + bc)$$

which is the desired product of $(a + jb)$ and $(c + jd)$. This eliminated one of the relatively slow multiplications at the expense of including five additions or subtractions which can be performed very fast. As a result, one complex multiplication may be thought of as being equivalent in speed to three real multiplications.

IV-B.2 Calculating the Complex Rotation Factors

In performing Fourier transform operations, the rotation factor

$$W_N^k = e^{(-j2\pi/N)k} = \cos(-2\pi\, k/N) + j \sin(-2\pi\, k/N)$$

which represents a unit vector in the complex plane at an angle of (-2pi k/N) radians, is used extensively. Virtually all of the complex multiplications performed in a transform operation involve multiplication by one of these rotation factors. They are called rotation factors because when any number is multiplied by one of them it merely causes that number to be rotated in the complex plane by the angle (-2pi k/N) radians leaving its magnitude unchanged.

Certain of these rotations do not really require complex multiplications, but may be performed by simply moving numbers around and/or changing signs. These are

$$W_N^0 = W_N^{Nk} = 1 \qquad k = 0,1,2, \ldots$$

$$W_N^{N/2} = W_N^{N(k + 1/2)} = -1$$

$$W_N^{N/4} = W_N^{N(k + 1/4)} = -j$$

$$W_N^{3N/4} = W_N^{N(k + 3/4)} = j$$

Multiplying by the first one obviously does nothing. The second one merely changes the sign. The third and fourth, however, cause a pi/2 rotation, which may be performed by interchanging the real and imaginary parts of the complex number and changing signs as follows:

$$j(a + jb) = -b + ja$$

$$-j(a + jb) = b - ja$$

When speed is important the rotation factors may be precomputed and stored in tabular form prior to the computation of the transform. However, when time is of less concern than the large storage space which may be required for such a table, the rotation factors may be calculated as they are used. One way of doing this might be to use a library function which calculates exponentials to produce each individual factor. A more efficient way is to recognize that the rotation factors for a given N will be equally spaced around the unit circle in the complex plane and successive values may be calculated with just one complex multiplication as follows.

$$W_N^0 = 1$$

$$W_N^k = e^{(-j2pi/N)k} = e^{(-j2pi/N)} \times e^{(-j2pi/N)(k-1)}$$

$$= W_N^1 \times W_N^{(k-1)}$$

This method works fine for small values of N. But for larger values of N it begins to suffer from accumulated round-off error.

A better method is to use a difference equation, where, rather than multiplying the entire unit vector by an incremental rotation factor, a small difference vector is added to the unit vector to move the tip of it to the desired adjacent position on the unit circle [6].

$$W_N^{(k+1)} = W_N^K + z\,W_N^K$$

$$z = W_N^1 - 1 = \cos(-2pi/N) + j\,\sin(-2pi/N) - 1$$

$$= 1 - 2 \sin^2(-\pi/N) + j \sin(-2\pi/N) - 1$$

$$= -2 \sin^2(-\pi/N) + j \sin(-2\pi/N)$$

The value of z is calculated only once for a given value of N so one might use double precision arithmetic to improve its accuracy. Each successive value of the rotation vector still requires only one complex multiplication. The multiplier z decreases in magnitude with increasing N. This produces reasonably accurate results on computers with rounded floating-point arithmetic [12].

IV-B.3 Transforms for a Composite Number of Points

The following derivation is intended to demonstrate how the Fourier transform using a composite number of points N=PQ may be broken down into two steps, first doing P Q-way transforms then Q P-way transforms.

The discrete Fourier transform formula is given as follows [13].

$$X(k) = \sum_{n=0}^{N-1} x(n) W_N^{nk} \qquad W_N = e^{-j2\pi/N}$$

If N=P*Q then the points x(n) can be broken into P sets of Q points each as follows.

$$x_0(n) = x(Pn) \qquad n = 0, 1, \ldots, Q-1$$

$$x_1(n) = x(Pn+1)$$

$$\vdots$$

$$x_{P-1}(n) = x(Pn+P-1)$$

The transform may then be written in terms of these new

sets.

$$X(k) = \sum_{n=0}^{Q-1} x_0(n)\, W_N^{Pnk} + \sum_{n=0}^{Q-1} x_1(n)\, W_N^{(Pn+1)k} + \ldots + \sum_{n=0}^{Q-1} x_{P-1}(n)\, W_N^{(Pn+P-1)k}$$

This can be further simplified as follows.

$$W_N^P = e^{-j2\pi P/N} = e^{-j2\pi/Q} = W_Q$$

$$X(k) = \sum_{n=0}^{Q-1} x_0(n)\, W_Q^{nk} + W_N^k \sum_{n=0}^{Q-1} x_1(n)\, W_Q^{nk} + \ldots + W_N^{(P-1)k} \sum_{n=0}^{Q-1} x_{P-1}(n)\, W_Q^{nk}$$

A closer inspection of the summations in the above equation reveals that each one represents a Q-way transform.

$$X(k) = X_0(k) + W_N^k X_1(k) + \ldots + W_N^{(P-1)k} X_{P-1}(k)$$

However, each of these transforms is only Q points long so each must be replicated P times as k goes from 0 to N-1. That is

$$X_s(k) = X_s(k+Q) = X_s(k+2Q) = \ldots = X_s(k+tQ), \quad t=0 \text{ to } P-1$$

The transform X(k) may then be broken into P sections.

$$X(k) = X_0(k) + W_N^{k} X_1(k) + \ldots + W_N^{(P-1)k} X_{P-1}(k)$$

$$X(k+Q) = X_0(k) + W_N^{k+Q} X_1(k) + \ldots + W_N^{(P-1)(k+Q)} X_{P-1}(k)$$

$$\vdots$$

$$X(k+tQ) = X_0(k) + W_N^{k+tQ} X_1(k) + \ldots + W_N^{(P-1)(k+tQ)} X_{P-1}(k)$$

Now since $W_N^{Q} = W_P$ a further simplification may be made.

$$X(k) = X_0(k) + W_N^{k} X_1(k) + \ldots + W_N^{(P-1)k} X_{P-1}(k)$$

$$X(k+Q) = X_0(k) + W_P^{1} W_N^{k} X_1(k) + \ldots + W_P^{P-1} W_N^{(P-1)k} X_{P-1}(k)$$

$$\vdots$$

$$X(k+tQ) = X_0(k) + W_P^{t} W_N^{k} X_1(k) + \ldots + W_P^{t(P-1)} W_N^{(P-1)k} X_{P-1}(k)$$

$t = 0, 1, \ldots, P-1$

If k is held constant while P values of X(k+tQ) are calculated as t varies from 0 to P-1, then two new variables may be defined.

$$x'_k(t) = X(k+tQ)$$

$$x'_k(s) = W_N^{sk} X_s(k)$$

The equations may now be rewritten in terms of these new variables.

$$x'_k(t) = x'_k(0) + W_P^{t} x'_k(1) + \ldots + W_P^{t(P-1)} x'_k(P-1)$$

Expressing this as a summation yields the familiar form of a

Fourier transform.

$$X'_k(t) = \sum_{s=0}^{P-1} x'_k(s)\, W_P^{st}$$

Here it has been shown that the P-way joining of P Q-way transforms, to form the transform of a composite number of points, may be done by performing Q P-way transforms. This result is important because it shows that the P-way joining to form the composite transform may take advantage of any of the fast transform techniques developed to perform a P-way Fourier transform.

The number of complex multiplications required to do a P-way joining of P Q-way transforms is figured as follows. Assume that F(N) represents the number of complex multiplications to do an FFT on N points. The number P may be assumed prime, since if it were not, then it could be broken into its prime components and joining done for each of them. From above

$$x'_k(s) = W_N^{sk} X_s(k) \qquad \begin{matrix} s = 0,1,2, \ldots ,P-1 \\ k = 0,1,2, \ldots ,Q-1 \end{matrix}$$

The forming of these would requires PQ multiplications. An exception occurs when (sk mod N) = 0. The exponent is zero and the result is a multiplication by $W_N^0 = 1$, which should not be counted. Since the product sk never exceeds N, this will only happen when s = 0 or k = 0 which occurs P+Q-1 times. There are three other cases when W_N^{sk} produces values which do not require any multiplications.

$$W_N^{sk} = W_N^{N/2} = -1 \qquad sk = N/2$$

$$W_N^{sk} = W_N^{N/4} = -j \qquad sk = N/4$$

$$W_N^{sk} = W_N^{3N/4} = j \qquad sk = 3N/4$$

The first, sk = N/2, can only happen when the following conditions are met:

$$Q > P$$

$$P/2 < s < P$$

$$Q = 2 s z$$

Where N = PQ, P is prime and z is an integer. Remember that s = 0,1,2, ... ,P-1 and k = 0,1,2, ... ,Q-1. This says that Q must be greater than P so that k can be chosen with P as a factor.

$$k = N/2s = PQ/2s = 2Psz/2s = Pz$$

Now s must be greater than P/2 because

$$Pz = k < Q = 2sz$$

$$Pz < 2sz$$

$$P < 2s$$

$$P/2 < s.$$

Thus, if $M_{1/2}(P,Q)$ is defined as the number of combinations of sk found equal to N/2, then $M_{1/2}(P,Q)$ may be found by counting how many integers between P/2 and P are factors of Q/2.

In a similar fashion sk = N/4 may occur when

$$Q > P$$

$$P/4 < s < P$$

$$Q = 4\ s\ z$$

$$k = P\ z.$$

So every value of s between P/4 and P must be tested to see if it is a factor of Q/4 to determine how many times multiplication by -j will occur. Let the function $M_{1/4}(P,Q)$ be this number of times. The only exception to this is when P = 2 and Q is even as follows:

$$P = 2$$

$$s = 1$$

$$k = Q/2$$

$$sk = Q/2 = N/4$$

Therefore, $M_{1/4}(2,Q) = 1$ for even Q

$M_{1/4}(2,Q) = 0$ for odd Q

Finally, factors in which sk = 3N/4 may only occur if

$$Q > P$$

$$3P/4 < 3y < P$$

$$Q = 4\ y\ z$$

$$s = 3y$$

$$k = P\ z$$

where y and z are integers. Here every value of s between 3P/4 and P which is divisible by three must tested to see if s/3 is a factor of Q/4. Each time this occurs, multiplication by the rotation factor degenerates to just swapping the real and imaginary parts of the multiplicand and changing a sign, effecting a multiplication by j. Since

no complex multiplication has been required to do this operation, each should be deducted from the total number of complex multiplications. The function $M_{3/4}(P,Q)$ is defined to represent this value. Also define

$$M(P,Q) = M_{1/2}(P,Q) + M_{1/4}(P,Q) + M_{3/4}(P,Q).$$

A close examination of the above techniques for determining M(P,Q) shows that if P is chosen as the smallest factor of N then there will be no s which is a factor of Q that is less than P. Therefore, in order to maximize M(P,Q) and thus minimize the number of complex multiplications, any composite number of points should be broken down into its prime factors. Then these factors ordered from smallest to largest. The first transform step should be performed using the smallest factor as the number of points, followed by a number of P-way combinations for each of the remaining factors going from the smallest to the largest.

The total number of multiplications required to generate

$$x'_k(s) = W_N^{sk} X_s(k) \qquad \begin{matrix} s = 0,1,2, \ldots ,P-1 \\ k = 0,1,2, \ldots ,Q-1 \end{matrix}$$

is given as

$$PQ - P - Q + 1 - M(P,Q) = (P - 1)(Q - 1) - M(P,Q).$$

Now each FFT

$$X'_k(t) = \sum_{s=0}^{P-1} x'_k(s)\, W_P^{st}$$

will require an additional F(P) multiplications and k = 0,1, ... Q-1 so actually Q times F(P) will be required. The result is thus

$$(P-1)(Q-1) - M(P,Q) + Q\,F(P)$$

complex multiplications required to do the P-way combination. The complete transform of N = PQ points also requires doing P Q-way FFT's with an additional P times F(Q) multiplications. The final result is thus

$$F(N) = F(PQ) = (P-1)(Q-1) - M(P,Q) + Q\,F(P) + P\,F(Q)$$

complex multiplications required to transform a composite number of points. It should be understood that P is prime but Q may itself be composite and the Q-point transforms would have been done in a similar fashion.

For a radix 2 Fourier transform $N = 2^m$, P = 2 and $Q = 2^{m-1}$. There is no s between P/2 = 1 and P = 2 so

$$M_{1/2}(2,Q) = 0.$$

As stated above, since Q is even

$$M_{1/4}(2,2^{m-1}) = 1.$$

There is no s between 3P/4 = 3/2 and P = 2 so

$$M_{3/4}(2,Q) = 0.$$

The result is that

$$M(2,2^{m-1}) = 1.$$

From F(N) above

$$F(N) = F(PQ) = (P-1)(Q-1) - M(P,Q) + Q\,F(P) + P\,F(Q)$$

$$F(2^m) = 2^{m-1} - 1 - 1 + 0 + 2\,F(2^{m-1}) = 2\,F(2^{m-1}) + 2^{m-1} - 2$$

This formula could be used repeatedly starting with $F(2) = 0$ to calculate values of $F(2^m)$. A better formula may be developed, however, which can calculate $F(N)$ for radix 2 FFT's directly without recursion.

$$N = 2^m$$

$$m = \log_2 N$$

Take the general form for $F(N)$ and carry it out a few times to see what pattern develops.

$$\begin{aligned} F(N) = F(2^m) &= 2\,F(2^{m-1}) + N/2 - 2 \\ &= 2(\,2\,F(2^{m-2}) + N/4 - 2\,) + N/2 - 2 \\ &= 4\,F(2^{m-2}) + 2N/2 - 6 \\ &= 4(\,2\,F(2^{m-3}) + N/8 - 2\,) + 2N/2 - 6 \\ &= 8\,F(2^{m-3}) + 3N/2 - 14 \\ &= 8(\,2\,F(2^{m-4}) + N/16 - 2\,) + 3N/2 - 14 \\ &= 16\,F(2^{m-4}) + 4N/2 - 30 \end{aligned}$$

The pattern forming is

$$F(2^m) = 2^a\,F(2^{m-a}) + a\,N/2 - 2(\,2^a - 1\,)$$

Now letting $a = m - 1$ produces

$$F(2^m) = 2^{m-1}\,F(2) + (m - 1)\,N/2 - 2^m + 2$$

Since $F(2) = 0$, then

$$F(2^m) = (m - 1)\ N/2 - 2^m + 2$$

$$F(N) = (m - 1)\ N/2 - N + 2$$

$$= (m - 3)\ N/2 + 2$$

$$= (\log_2 N - 3)\ N/2 + 2$$

Thus, the exact number of complex multiplications required to do a radix-2 FFT is given by

$$F(N) = (\log_2 N - 3)\ N/2 + 2.$$

which does approach the familiar $N/2 \log_2 N$ as N gets large [13].

Fast Fourier transform (FFT) techniques for radix two transforms are well documented in the literature. However an intuitive feel for how and why these techniques actually work is useful when working on non-radix two FFT's. For this reason it is felt worth while to step through a simple four point FFT comparing the operations to those accomplished in a standard discrete Fourier transform (DFT).

The standard DFT is accomplished by the following series of summations.

$$X(k) = \sum_{n=0}^{N-1} x(n)\ e^{nk(-j2pi/N)} = \sum_{n=0}^{N-1} x(n)\ W_N^{nk}$$

where

$$W_N = e^{-j2pi/N}$$

For a four point DFT this becomes:

$$X(0) = x(0)\ W_4^0 + x(1)\ W_4^0 + x(2)\ W_4^0 + x(3)\ W_4^0$$

$$X(1) = x(0)\,W_4^{0} + x(1)\,W_4^{1} + x(2)\,W_4^{2} + x(3)\,W_4^{3}$$

$$X(2) = x(0)\,W_4^{0} + x(1)\,W_4^{2} + x(2)\,W_4^{4} + x(3)\,W_4^{6}$$

$$X(3) = x(0)\,W_4^{0} + x(1)\,W_4^{3} + x(2)\,W_4^{6} + x(3)\,W_4^{9}$$

The efficiencies of the FFT are accomplished by realizing that W_4^{n} is a unit vector in the complex plane and each factor W_4 represents a rotation of -pi/2 radians.

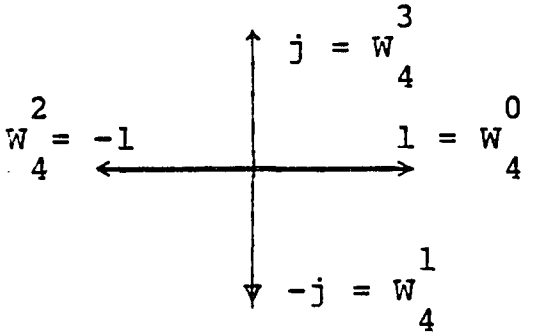

$$W_4^{n} = W_4^{(n \bmod 4)}$$

$$W_4^{4} = W_4^{0} = 1$$

$$W_4^{6} = W_4^{2} = -1$$

$$W_4^{9} = W_4^{1} = -j$$

Rewriting the four point DFT using these results yields the following.

$$X(0) = 1\,x(0) + 1\,x(1) + 1\,x(2) + 1\,x(3)$$

$$X(1) = 1\,x(0) - j\,x(1) - 1\,x(2) + j\,x(3)$$

$$X(2) = 1\,x(0) - 1\,x(1) + 1\,x(2) - 1\,x(3)$$

$$X(3) = 1\,x(0) + j\,x(1) - 1\,x(2) - j\,x(3)$$

A grouping of terms makes it evident that taking the difference x(1)-x(3) prior to multiplication by j will allow

the entire transform to accomplished with only one multiplication. Although multiplication by j may be accomplished by just swapping the real and imaginary parts and changing the sign on the new real part, its is useful to still consider this as a complex multiplication in this case just to demonstrate the technique used here to reduce four multiplications down to only one. In transforms with larger numbers of points these reduction techniques still work, but most of the multiplication steps will not degenerate to just moving data items and/or changing signs, but will actually require that the complex multiplications be carried out.

$$X(0) = 1\ \{x(0) + x(2)\} \quad +1\ \{x(1) + x(3)\}$$

$$X(1) = 1\ \{x(0) - x(2)\} \quad -j\ \{x(1) - x(3)\}$$

$$X(2) = 1\ \{x(0) + x(2)\} \quad -1\ \{x(1) + x(3)\}$$

$$X(3) = 1\ \{x(0) - x(2)\} \quad +j\ \{x(1) - x(3)\}$$

Notice the sum and difference of x(0) and x(2) in the first terms and likewize of x(1) and x(3) in the last terms. These are formed by the standard butterfly notation as follows.

$$\begin{array}{ll} x(0) \searrow\ \swarrow & \{x(0) + x(2)\} \\ x(2) \swarrow\ \searrow & \{x(0) - x(2)\} \end{array}$$

$$\begin{array}{ll} x(1) \searrow\ \swarrow & \{x(1) + x(3)\} \\ x(3) \swarrow\ \searrow & \{x(1) - x(3)\} \end{array}$$

These terms are then combined with additional butterflies and the -j weighting factor to form the complete four point FFT.

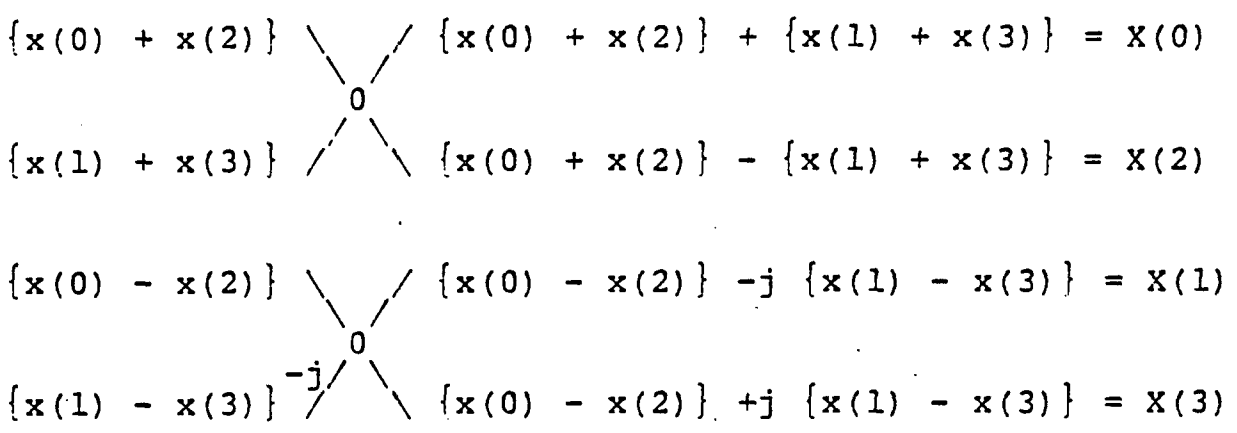

Combining these butterflies together produces the usual butterfly form.

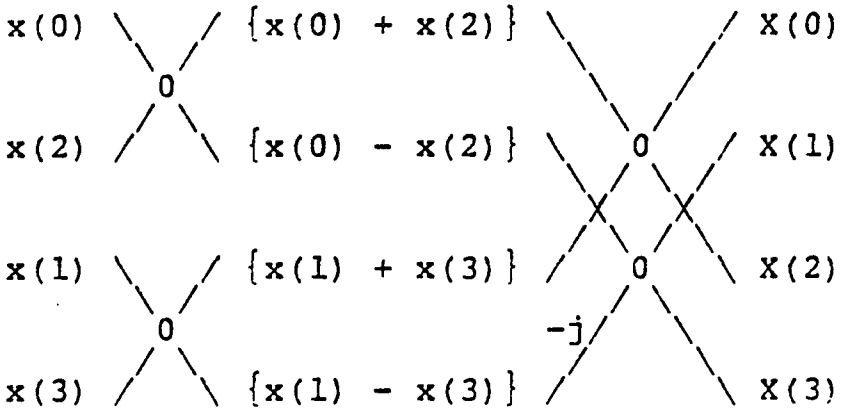

From this notation it is obvious as stated above that only one multiplication by -j is required to do a four point FFT. Also note the permutation of points x(1) and x(2) prior to the application of the first butterfly computations.

IV-B.4 The Prime Radix Fast Fourier Transform

Now, as an introduction to the techniques used in performing a Fourier transform on a prime number of points, it is instructive to look at a reasonably simple example using only three points. Proceeding as with the four point DFT above, the three point DFT begins as follows.

$$X(0) = x(0)\ W_3^0 + x(1)\ W_3^0 + x(2)\ W_3^0$$

$$X(1) = x(0)\ W_3^0 + x(1)\ W_3^1 + x(2)\ W_3^2$$

$$X(2) = x(0)\ W_3^0 + x(1)\ W_3^2 + x(2)\ W_3^4$$

Since $W_3^n = W_3^{(n \bmod 3)}$ each power of W_3 greater than two may be replace by a power between zero and two as follows.

$$X(0) = x(0)\ W_3^0 + x(1)\ W_3^0 + x(2)\ W_3^0$$

$$X(1) = x(0)\ W_3^0 + x(1)\ W_3^1 + x(2)\ W_3^2$$

$$X(2) = x(0)\ W_3^0 + x(1)\ W_3^2 + x(2)\ W_3^1$$

With the exception of X(0) which multiplies each point by W_3^0 = 1, each point in the transform result uses all powers of W_3 from 0 to N-1. This turns out to be the case for any prime number of points N. As a proof of this note that the terms comprising any given X(k) always begin with $x(0)\ W_N^0$ and the exponent on W_N increments by k, so that each term is given by $x(n)\ W_N^{nk}$ as n varies from 0 to N-1. The exponent nk may be reduced to (nk mod N) or (nk-pN) where p is the integer part of nk/N. Since N is prime and thus N and k are mutually prime, the exponent starts at 0 and does not cycle back to 0 until n = N and p = k. This however will not occur because n only varies from 0 to N-1. The exponents then will

cycle through all possible values between 0 and N-1 for each X(k).

If N is prime, none of the exponentials $W_N^{(nk \bmod N)}$ will be equal to or the negative of another as is true when N has 2 as a factor. The only relation between them is that the sum of all of them will be zero as follows:

$$\sum_{n=0}^{N-1} W_N^n = 0$$

From this there is the capability of saving a complex multiplication by calculating the last point as the negative of the sum of all the others.

$$-\sum_{n=0}^{N-2} W_N^n = W_N^{N-1}$$

Returning to the case where N = 3 above, the exponentials may be represented as vectors in the complex plane as follows:

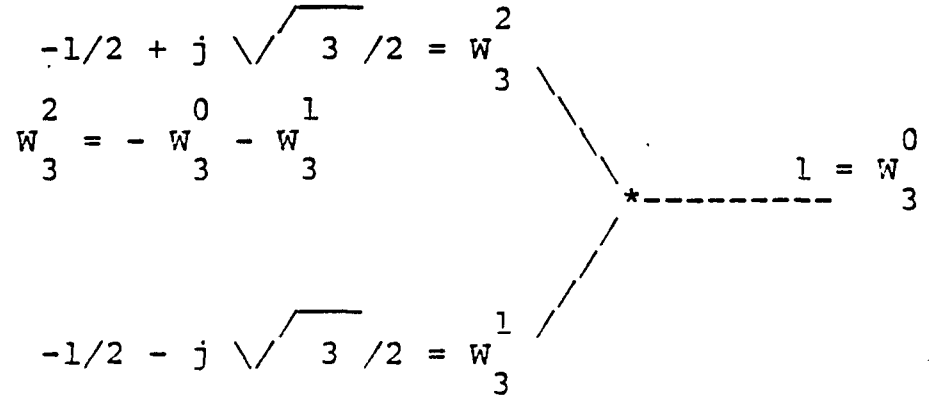

Now the three point DFT equations above may be rewritten as:

$$X(0) = x(0) + x(1) + x(2)$$

$$X(1) = x(0) + x(1)\ Z - x(2) - x(2)\ Z$$

$$X(2) = x(0) - x(1) - x(1)\ Z + x(2)\ Z$$

From this it is obvious that the three point transform may be performed with just two complex multiplications. However, using this technique the number of complex multiplications would be (N-1)(N-2) for each prime number of points. Thus, the number of multiplications would approach N^2 as N gets large.

An interesting phenomenon is observed, however. If only the exponents are written down in an array the symmetry becomes more obvious. The three point DFT results in:

0	0	0
0	1	2
0	2	1

As a further example, lets look at a five point DFT to see how the same symmetry results.

$$X(0) = x(0)\ W_5^0 + x(1)\ W_5^0 + x(2)\ W_5^0 + x(3)\ W_5^0 + x(4)\ W_5^0$$

$$X(1) = x(0)\ W_5^0 + x(1)\ W_5^1 + x(2)\ W_5^2 + x(3)\ W_5^3 + x(4)\ W_5^4$$

$$X(2) = x(0)\ W_5^0 + x(1)\ W_5^2 + x(2)\ W_5^4 + x(3)\ W_5^6 + x(4)\ W_5^8$$

$$X(3) = x(0)\ W_5^0 + x(1)\ W_5^3 + x(2)\ W_5^5 + x(3)\ W_5^9 + x(4)\ W_5^{12}$$

$$X(4) = x(0)\ W_5^0 + x(1)\ W_5^4 + x(2)\ W_5^8 + x(3)\ W_5^{12} + x(4)\ W_5^{16}$$

Since $W_5^n = W_5^{(n \bmod 5)}$ each power of W_5 greater than four may be replaced by a power between zero and four as follows:

$$X(0) = x(0)\,W_5^0 + x(1)\,W_5^0 + x(2)\,W_5^0 + x(3)\,W_5^0 + x(4)\,W_5^0$$

$$X(1) = x(0)\,W_5^0 + x(1)\,W_5^1 + x(2)\,W_5^2 + x(3)\,W_5^3 + x(4)\,W_5^4$$

$$X(2) = x(0)\,W_5^0 + x(1)\,W_5^2 + x(2)\,W_5^4 + x(3)\,W_5^1 + x(4)\,W_5^3$$

$$X(3) = x(0)\,W_5^0 + x(1)\,W_5^3 + x(2)\,W_5^1 + x(3)\,W_5^4 + x(4)\,W_5^2$$

$$X(4) = x(0)\,W_5^0 + x(1)\,W_5^4 + x(2)\,W_5^3 + x(3)\,W_5^2 + x(4)\,W_5^1$$

Now, writing down the array of exponents, the five point DFT produces:

0	0	0	0	0
0	1	2	3	4
0	2	4	1	3
0	3	1	4	2
0	4	3	2	1

Column k is identical to row k in all cases (due to the exponent being equal to nk) and with the exception of the first row and first column any given exponent appears once and only once in each row or column. This suggests the possibility that a circular convolution might work here if the points could be ordered properly. The circular convolution may be pictured as follows.

CIRCULAR CONVOLUTION OF 3,4,2,1 AND a,b,c,d

```
 1       2       4       3       1       2       4
 x       x       x       x
 a       b       c       d
---     ---     ---     ---
1a  +   2b  +   4c  +   3d  = Y(0)

 1       2       4       3       1       2       4
         x       x       x       x
         a       b       c       d
        ---     ---     ---     ---
        2a  +   4b  +   3c  +   1d  = Y(1)

 1       2       4       3       1       2       4
                 x       x       x       x
                 a       b       c       d
                ---     ---     ---     ---
                4a  +   3b  +   1c  +   2d  = Y(2)

 1       2       4       3       1       2       4
                         x       x       x       x
                         a       b       c       d
                        ---     ---     ---     ---
                        3a  +   1b  +   2c  +   4d  = Y(3)
```

Writing the result in matrix form:

$$\begin{bmatrix} Y(0) \\ Y(1) \\ Y(2) \\ Y(3) \end{bmatrix} = \begin{bmatrix} 1 & 2 & 4 & 3 \\ 2 & 4 & 3 & 1 \\ 4 & 3 & 1 & 2 \\ 3 & 1 & 2 & 4 \end{bmatrix} \begin{bmatrix} a \\ b \\ c \\ d \end{bmatrix}$$

Neglecting the first row and column of the array of exponents above (since they don't represent any complex multiplications) the following array results.

1	2	3	4
2	4	1	3
3	1	4	2
4	3	2	1

This may be put in the same form as the matrix in the

circular convolution by interchanging rows three and four and columns three and four. This is equivalent to interchanging X(3) and X(4) and also x(3) and x(4) in the original DFT. Now the five point DFT has been reduced to a four point circular convolution which may be done using radix 2 FFT techniques.

The above result was arrived at by somewhat different means by Charles M. Rader [7] who found an analytical method of determining the permutation of the points required to allow an N-1 point correlation to be used to produce an N point DFT when N is prime. He essentially said the following.

Let the notation [X] = X modulo N. If N is prime, then there exists some number g called a primitive root of N which provides a one-to-one mapping of the integers i=1,...N-1 to the integers j=1,...N-1 given by

$$j = [g^{i}].$$

The DFT represented by

$$X(k) = \sum_{n=0}^{N-1} x(n) \, W_N^{nk}$$

can be broken down into

$$X(0) = \sum_{n=0}^{N-1} x(n) \quad \text{and} \quad X(k) - x(0) = \sum_{n=1}^{N-1} x(n) \, W_N^{nk}$$

Now the order of the points in the second summation are permuted by the transformations

$$n \dashrightarrow [g^{n}] \qquad \text{and} \qquad k \dashrightarrow [g^{k}]$$

and the following results.

$$X([g^k]) - x(0) = \sum_{n=1}^{N-1} x([g^n])\, W_N^{[g^{(n+k)}]}$$

Note that $[g^{N-1}] = [g^0]$ which can be used to change the limits on the sum. Also since

$$W_N^n = W_N^{[n]} \qquad \text{then} \qquad W_N^{[g^{(n+k)}]} = W_N^{g^{(n+k)}}.$$

Now making the change of variables

$$G(n+k) = W_N^{g^{(n+k)}} \qquad \text{and} \qquad y(n) = x([g^n])$$

the summation becomes

$$X([g^k]) - x(0) = \sum_{n=0}^{N-2} y(n)\, G(n+k)$$

which is the form of a circular correlation of y(n) and G(n+k). This, however, is an N-1 point correlation and if N is prime it will at least have a factor of two and it could be highly composite allowing FFT techniques to be used to do the correlation. The operation would be as follows:

$$X([g^k]) = DFT^{-1}\{ DFT\{ x([g^{-n}]) \}\, DFT\{ W_N^{g^n} \} \} + x(0)$$

The DFT involving W could be precalculated so that only two DFT's would need to be performed (one is an inverse). If N-1 is highly composite the savings of the FFT algorithm will overcome the fact that two FFT's must be performed instead of one DFT on a prime number of points.

An interesting case where the savings will be maximized

is when N = 257 and N-1 = 256 = 2^8. Here the correlation will require 1284 complex multiplications instead of a DFT with 65536 multiplications. Obviously some prime FFT's will be more efficient than others depending on how composite the number N-1 is.

Apply this technique to the three point example as follows. The number g = 2 is a primitive root of 3 so the mapping becomes

n	1	2
$[g^n]$	2	1

But $[g^2] = [g^0] = 1$ so the mapping changes to

n	0	1
$[g^n]$	1	2

$$W_3^1 = -1/2 - j\sqrt{3}/2 \qquad W_3^2 = -1/2 + j\sqrt{3}/2$$

DFT of W^{g^n} :

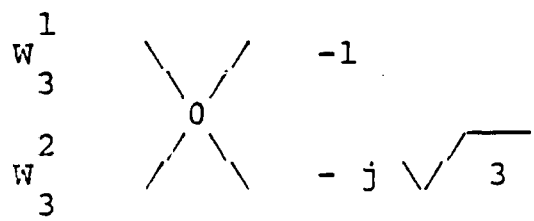

DFT of $x([g^{-n}])$:

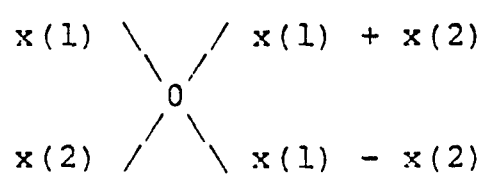

Note that X(0) can be easily formed by adding x(0) to the first term x(1) + x(2) above.

Multiply the two DFT's to do the correlation and inverse DFT :

$$-(x(1)+x(2)) \quad \overset{\text{IFT}}{\underset{0}{\diagdown\ \diagup}} \quad -(1/2+j\sqrt{3})x(1)-(1/2-j\sqrt{3})x(2)$$

$$-j\sqrt{3}\,(x(1)-x(2)) \quad \diagup\ \diagdown \quad -(1/2-j\sqrt{3})x(1)-(1/2+j\sqrt{3})x(2)$$

The division by 2 results form the inverse Fourier transform (IFT). This yields X(1) - x(0) and X(2) - x(0). The x(0) could easily be added back in by summing it with the -(x(1) + x(2)) term prior to the IFT operation, but after the division by two has been done. With these additions the three point FFT is performed as follows.

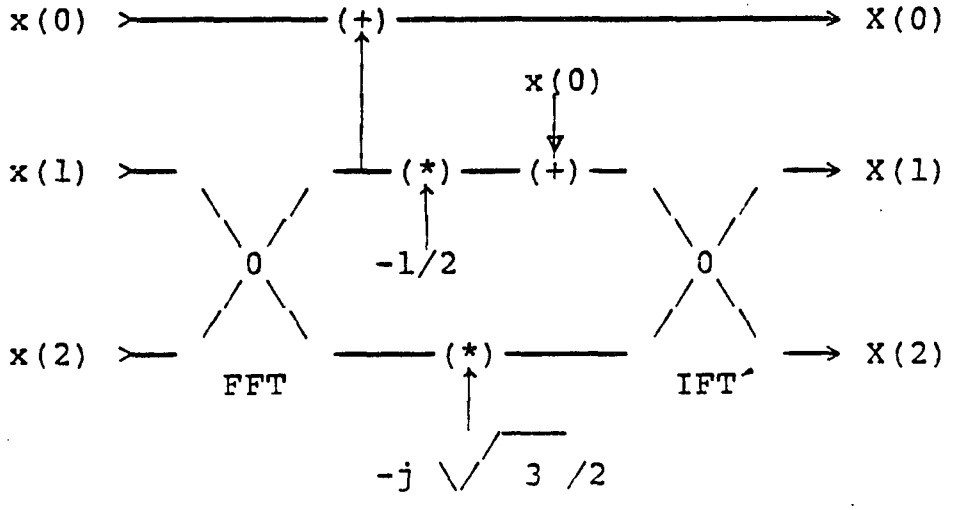

Note that only one complex multiplication was performed in the entire FFT process, resulting in an improvement over the previous method. Division by two is assumed to be trivial since it only requires subtracting one from the floating point exponent. The notation IFT' means the IFT operation excluding the division by N which has already been performed. Actually, only two real multiplications are

required here because of the $-j\sqrt{3}$ factor. This is equivalent to two-thirds of a regular complex multiply, so $F(3) = 2/3$.

This method may be adapted by inclusion of the proper rotation factors to perform a three-way combination as follows.

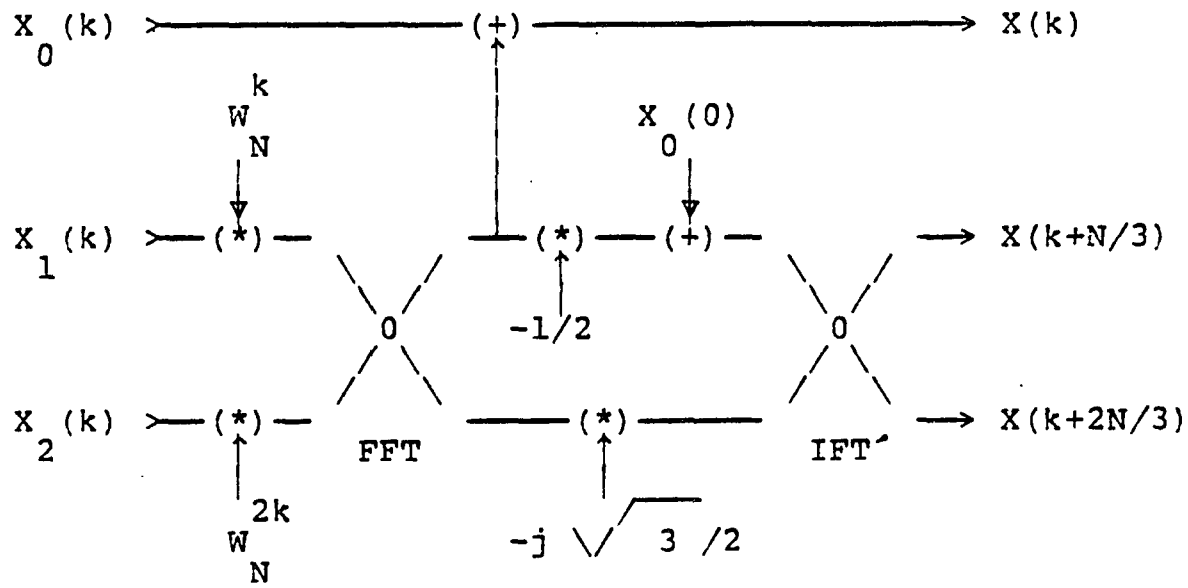

where $k = 0,1,2, \ldots ,(N/3 - 1)$.

As previously derived, the total number of complex multiplications required to do a P-way combination where $N = PQ$ is given by

$$(P-1)(Q-1) - M(P,Q) + Q\,F(P)$$

where $M(P,Q)$ is the number of trivial multiplications occurring when a multiplication by $-j$, -1 or j occurs, and $F(P)$ is the number required to do a transform with P points. In this case with $P = 3$, $F(3) = 2/3$ and $Q = N/3$ the result is

$$\begin{aligned}&(3 - 1)(Q - 1) - M(3,Q) + 2Q/3\\ &= 2(N/3 - 1) - M(3,Q) + 2N/9\\ &= 8N/9 - 2 - M(3,Q)\end{aligned}$$

complex multiplications required to do the 3-way combination. The number of trivial multiplications M(3,Q) will have a value of one if N is divisible by two, of two more if N is divisible by four and of yet two more if N is divisible by eight.

Using the information derived above the total number of complex multiplications required to perform an FFT on any number of points may be derived. The correlation method described above is assumed to be used on all prime factors. The following formula has been developed to give the number of complex multiplications required to do a composite transform where N is composite, P is a prime factor of N and Q = N/P may be either prime or composite.

$$F(N) = F(PQ) = (P-1)(Q-1) - M(P,Q) + Q\,F(P) + P\,F(Q)$$

Also developed was a formula for F(N) when N is a power of two.

$$F(2^m) = (m-3)\,2^{m-1} + 2$$

Now if Q is a composite number other than a power of two, then F(Q) may be found by factoring Q into P′ and Q′ and calcualting F(P′Q′) using the formula for F(PQ) above. What remains then is evaluating F(P) and also F(Q) when Q is a prime number.

The procedure given above, using fast correlation techniques to perform a DFT on a prime number of points, requires doing two N-1 point forward transforms, multiplying them together and doing an N-1 point inverse transform. It is assumed that the forward transform of the rotation factors could be precomputed and the division be N-1 required in the inverse transform could be included in these transformed rotation factors. This results in eliminating

the need for calculating one of the forward transforms and makes the inverse transform take the same number of multiplications F(N-1) as the forward transform. Now let N = P a prime number. Then the total number of complex multiplications required to do a Fourier transform on P points is

$$F(P) = 2F(P-1) + P - 1.$$

The number P-1 will at least have two as a factor and is therefore composite and F(P-1) may be calculated using the formula for F(PQ) above. Some trivial multiplications were found in the special case where N = 3 causing reductions in F(3) beyond what this formula indicates. Further investigation will show similar reductions in other prime transforms.

At least one and sometimes two of the terms in the precomputed transform of the rotation factors will be real numbers, resulting in a reduction in the multiplication effort. As mentioned earlier,

$$\sum_{n=0}^{N-1} W_N^n = 0.$$

Therefore

$$\sum_{n=1}^{N-1} W_N^n = -W_N^0 = -1.$$

When the N-1 point transform is taken of the permuted points, $W_N^{g^n}$, the first term in the DFT will result in the summation of all of the rotation factors except W_N^0 producing a -1 as shown above.

In the prime FFT derivation above it was noted that

$$[g^{N-1}] = [g^{0}] = 1$$

but also it can be seen that

$$[(N-1)^{2}] = [N^{2} - 2N + 1] = 1$$

so N-1 must be the square root of one in modulo N arithmetic. But since N-1 is even then

$$[g^{(N-1)/2}] = N - 1.$$

Since N-1 is even, when the N-1 point transform of the rotation factors is performed in at least two steps, (N-1)/2 two-way FFT's followed by two (N-1)-way combinations. In order to do the two-way FFT's the points must be paired such that point n gets paired with point n + (N-1)/2. This pairing results in point $[g^{n}]$ being paired with point

$$[g^{(n + (N-1)/2)}] = [g^{n} g^{(N-1)/2}]$$

$$= [(N-1)g^{n}] = [Ng^{n} - g^{n}]$$

$$= [-g^{n}] = - [g^{n}]$$

The actual points are

$$W_{N}^{[g^{n}]} \quad \text{and} \quad W_{N}^{-[g^{n}]}$$

which are complex conjugates of each other. Now, these are combined in the 2-way FFT as follows

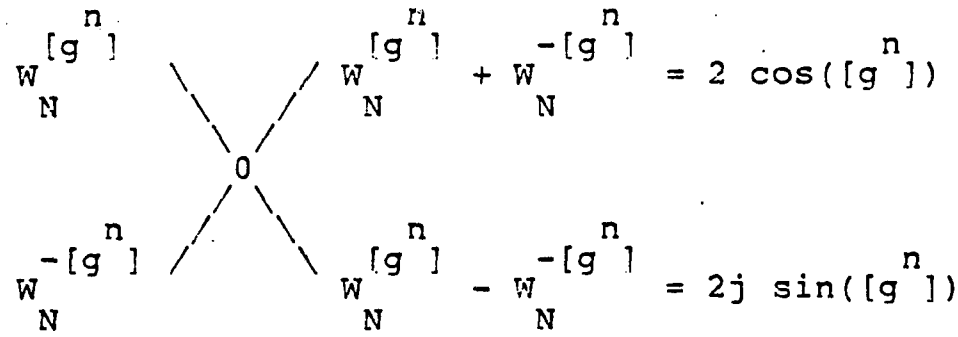

resulting in one real term and one pure imaginary term. When the two (N-1)-way combinations are performed, the first combination will be weighted sums of all these real parts while the second combination will be weighted sums of these pure imaginary parts. In the case of the 3-way transform no further combination was required resulting in one real and one pure imaginary transformed rotation factor.

From the derivation of the P-way combination

$$X'_k(t) = \sum_{s=0}^{P-1} x'_k(s)\, W_P^{st}$$

here

$$s = 0,1,2, \ldots ,P-1$$

$$t = 0,1,2, \ldots ,P-1$$

$$k = 0,1,2, \ldots ,Q-1$$

$$X'_k(t) = X(k+tQ)$$

$$x'_k(s) = W_N^{sk}\, X_s(k)$$

$$X_s(k) = \sum_{n=0}^{Q-1} x_s(n)\, W_Q^{nk}$$

$$x_s(n) = x(Pn+s)$$

In this case Q = 2 and P = (N-1)/2 so the 2-way transforms

$X_s(k)$ are $X_s(0)$ containing all the real parts from the 2-way transforms above and $X_s(1)$ containing all the pure imaginary parts from above. The P-way combination then becomes

$$X(k+2t) = X'_k(t) = \sum_{s=0}^{P-1} x'_k(s)\, W_P^{st} = \sum_{s=0}^{P-1} X_s(k)\, W_{2P}^{sk}\, W_P^{st}$$

$$s = 0,1,2, \ldots ,(N-1)/2 - 1$$

$$t = 0,1,2, \ldots ,(N-1)/2 - 1$$

$$k = 0,1$$

which can be broken into two parts.

$$X(2t) = \sum_{s=0}^{P-1} X_s(0)\, W_P^{st}$$

containing all the real parts of the 2-way transforms and

$$X(2t+1) = \sum_{s=0}^{P-1} X_s(1)\, W_{2P}^{s}\, W_P^{st}$$

containing all the pure imaginary parts. Every X(2t+1) will be complex since even for t=0 there is a complex rotation factor included. However, X(2t) will be real for t=0

$$X(0) = \sum_{s=0}^{(N-1)/2 - 1} X_s(0)$$

which is actually equal to -1 as previously shown and, if (N-1) is evenly divisible by four, then X(2t) will be real at

$$t = P/2 = (N-1)/4$$

$$X(P) = X((N-1)/2) = \sum_{s=0}^{(N-1)/2 - 1} X_s(0)\, W_P^{sP/2}$$

because

$$W_P^{sP/2} = W_2^s = \begin{cases} 1 & \text{for even } s \\ -1 & \text{for odd } s \end{cases}$$

These real transformed rotation factors will actually be considered as 2/3 of a complex multiplication, even though the first is always -1, because, as stated earlier, the 1/(N-1) factor, which is part of the inverse Fourier transform operation, will be included in these precomputed rotation factors. The only exception to this occurs when N-1 is a power of two, in which case dividing by N-1 is merely a subtraction of exponents.

To summarize these results, if P is a prime number other than two, then the total number of complex multiplications required to do a Fourier transform on P points is

$$F(P) = 2F(P-1) + P - 4/3$$

with additional cumulative reductions by 1/3 if N=3, by 1/3 if N-1 is evenly divisible by four and also by 2/3 if N-1 is a power of two. In the case of N=3 this results in F(3) = 2/3 which was previously shown.

IV-B.5 Two-at-a-Time Method

When an even number of real points are being transformed, additional savings in complex multiplications may be realized by using a two-at-a-time algorithm. Here, the points are broken into a set of odd numbered points and

a set of even numbered point. Start with

$$x(n) \quad \text{where } n=1,2,3, \ldots ,N-1 \text{ and } N \text{ is even.}$$

Let $x_0(n) = x(2n)$ and $x_1(n) = x(2n+1)$

where $n = 1,2,3, \ldots ,N/2 - 1.$

Now form $x'(n)$ such that

$$x'(n) = x_0(n) + j\, x_1(n)$$

The transform $X'(k)$ of $x'(n)$ is given by

$$X'(k) = \sum_{n=0}^{N/2-1} x'(n)\, W_{N/2}^{nk} = \sum_{n=0}^{N/2-1} \{ x_0(n) + j\, x_1(n) \}\, W_{N/2}^{nk}$$

$$= \sum_{n=0}^{N/2-1} x_0(n)\, W_{N/2}^{nk} + j \sum_{n=0}^{N/2-1} x_1(n)\, W_{N/2}^{nk}$$

$$= X_0(k) + j\, X_1(k)$$

The problem remaining is to be able to separate the sum of these two transforms into their individual components after the transform $X'(k)$ has been calculated. It is noted that

$$W_N^{-n} = W_N^{N-n} = \tilde{W}_N^{n}$$

where the notation $\tilde{W}$ means the complex conjugate of W. As a result of this, when the set of points x(n) is real the resulting transform X(k) will be conjugate even.

$$X(k) = \tilde{X}(-k) = \tilde{X}(N-k) \qquad \text{if } x(n) \text{ is real}$$

Also if x(n) is pure imaginary then the transform X(k) will be conjugate odd.

$$X(k) = - \tilde{X}(-k) = - \tilde{X}(N-k) \quad \text{if } x(n) \text{ is imaginary}$$

As a result of this, since $x_0(n)$ and $x_1(n)$ are both real then their transforms will be conjugate even.

$$X_0(k) = \tilde{X}_0(N-k)$$

$$X_1(k) = \tilde{X}_1(N-k)$$

Multiplication of $x_1(n)$ by j will result in multiplication of $X_1(k)$ by j also and the result is that $jX_1(k)$ will be conjugate odd.

$$j X_1(k) = - \tilde{}(j X_1(N-k))$$

Which leads to

$$\tilde{}(j X_1(N-k)) = - j X_1(k)$$

$$j X_1(N-k) = - \tilde{}(j X_1(k))$$

$$j X_1(N-k) = j \tilde{X}_1(k)$$

since

$$\tilde{}(j X_1(k)) = - j \tilde{X}_1(k)$$

as proven by

$$X_1(k) = a + jb$$

$$\tilde{}(j X_1(k)) = \tilde{}(j(a + jb))$$

$$= \tilde{}(-b + ja) = (-b - ja)$$

$$= - j(a - jb) = - j \tilde{X}_1(k)$$

Now the sum of these two will result in

$$X'(k) = X_0(k) + j X_1(k)$$

But also

$$X'(N-k) = X_0(N-k) + j\,X_1(N-k) = \tilde{X}_0(k) + j\,\tilde{X}_1(k)$$

and

$$\tilde{X}'(N-k) = X_0(k) - j\,X_1(k)$$

Now the sum and difference of $X'(k)$ and $\tilde{X}'(N-k)$ result in

$$X'(k) + \tilde{X}'(N-k) = X_0(k) + j\,X_1(k) + X_0(k) - j\,X_1(k)$$

$$= 2\,X_0(k)$$

$$X'(k) - \tilde{X}'(N-k) = X_0(k) + j\,X_1(k) - X_0(k) + j\,X_1(k)$$

$$= 2j\,X_1(k)$$

Therefore the individual transforms $X_0(k)$ and $X_1(k)$ may be extracted from $X'(k)$ by the formulas

$$X_0(k) = (X'(k) + \tilde{X}'(N-k))/2$$

$$X_1(k) = (X'(k) - \tilde{X}'(N-k))/2j$$

To use this algorithm, the even number of real points is rearranged to form $x'(n)$. Then an N/2 point FFT is performed on these points to obtain $X'(k)$. The resulting $X'(k)$ is then split up using the formulas given above for $X_0(k)$ and $X_1(k)$. These two transforms are then combined using a 2-way merge to form the desired N point transform $X(k)$. The alternative to doing this is to do two N/2 point transforms then a 2-way merge, so the savings here result from only having to do one N/2 point transform. Note that the forming of $x'(n)$ and the subsequent splitting up of $X'(k)$ may be done without any actual floating point multiplications.

As noted above, the transform for a set of real points

will be conjugate even. It stands to reason then, that an inverse transform on conjugate even data can be done by inverting this process, forming $X'(k)$ then inverse transforming it to get $x'(n)$ which may be simply converted to the real $x(n)$, with similar savings in multiplications. Likewise, conjugate even points may be forward transformed into real results with these same savings.

When an even number, $N = 2Q$, of real or conjugate even points is transformed using the two-at-a-time procedure the number of complex multiplications is reduced by $F(Q)$ to

$$F(2Q) = Q - 1 - M_{1/4}(2,Q) + F(Q)$$

where

$$M_{1/4}(2,Q) = 1 \quad \text{for even } Q$$

$$M_{1/4}(2,Q) = 0 \quad \text{for odd } Q$$

and in the special case where N is a power of two and the points are real or conjugate even

$$F(2^m) = (m - 3)\, 2^{m-1} + 2 - (m - 4)\, 2^{m-2} - 2$$

$$= (2m - 6 - m + 4)\, 2^{m-2}$$

$$= (m - 2)\, 2^{m-2}$$

$$= (\log_2 N - 2)\, N/4$$

$$F(2^m) = (N/4) \log_2 (N/4)$$

IV-B.6 The FFT of a Conjugate Periodic Function

The two-at-a-time algorithm may always be used in calculating the transform of the shuffled rotation factors for use in the multiplication step in the middle of the fast

correlation when performing a prime FFT. As proven before

$$[g^{(n + (N-1)/2)}] = - [g^{n}]$$

and thus

$$W_N^{[g^{(n + (N-1)/2)}]} = W_N^{-[g^{n}]}$$

But this is the complex conjugate of $W_N^{[g^{n}]}$. For simplicity of notation, define new variables such that

$$z(n) = W_N^{[g^{n}]} \quad \text{and} \quad N' = (N - 1)/2$$

Therefore,

$$z(n + N') = \tilde{z}(n)$$

and we will call this a conjugate periodic function. The Fourier transform of this conjugate periodic function is

$$Z(k) = \sum_{n=0}^{2N'-1} z(n)\, W_{2N'}^{nk} = \sum_{n=0}^{N'-1} z(n)\, W_{2N'}^{nk} + \sum_{n=N'}^{2N'-1} z(n)\, W_{2N'}^{nk}$$

$$Z(k) = \sum_{n=0}^{N'-1} z(n)\, W_{2N'}^{nk} + \sum_{n=0}^{N'-1} z(n + N')\, W_{2N'}^{(n+N')k}$$

$$Z(k) = \sum_{n=0}^{N'-1} \left(z(n) + z(n + N')\, W_{2N'}^{N'k} \right) W_{2N'}^{nk}$$

$$Z(k) = \sum_{n=0}^{N'-1} \left(z(n) + \tilde{z}(n)\, W_2^{k} \right) W_{N'}^{nk/2}$$

This may be broken into odd and even parts as follows.

$$Z(2k) = \sum_{n=0}^{N'-1} (z(n) + \tilde{z}(n))\, W_{N'}^{nk} = 2 \sum_{n=0}^{N'-1} Re[z(n)]\, W_{N'}^{nk}$$

$$Z(2k+1) = \sum_{n=0}^{N'-1} (z(n) - \tilde{z}(n))\, W_{2N'}^{n} W_{N'}^{nk}$$

$$= 2 \sum_{n=0}^{N'-1} Im[z(n)]\, W_{2N'}^{n} W_{N'}^{nk}$$

where the function Re[ ] means "the real part of" and Im[ ] means "the imaginary part of". It is now obvious that the even and odd values of Z(k) may be seperately calculated as transforms of $N' = (N-1)/2$ points each. The even part Z(2k), however, is a transform of real points and may make use of the two-at-a-time algorithm, either directly if N' is even or indirectly if N' is odd, by transforming the largest prime factor P of N' first and using the algorithm to transform the P-1 real points in the first part of the prime transform.

When a prime transform is being done on real data the two-at- a-time algorithm may be used in both the forward and inverse FFT portions as follows. Define the variables

$$y(n) = x([g^{n}]), \qquad Y(k) = X([g^{k}]) \quad \text{and} \quad N' = (N-1)/2.$$

Then the prime transform proceeds as follows.

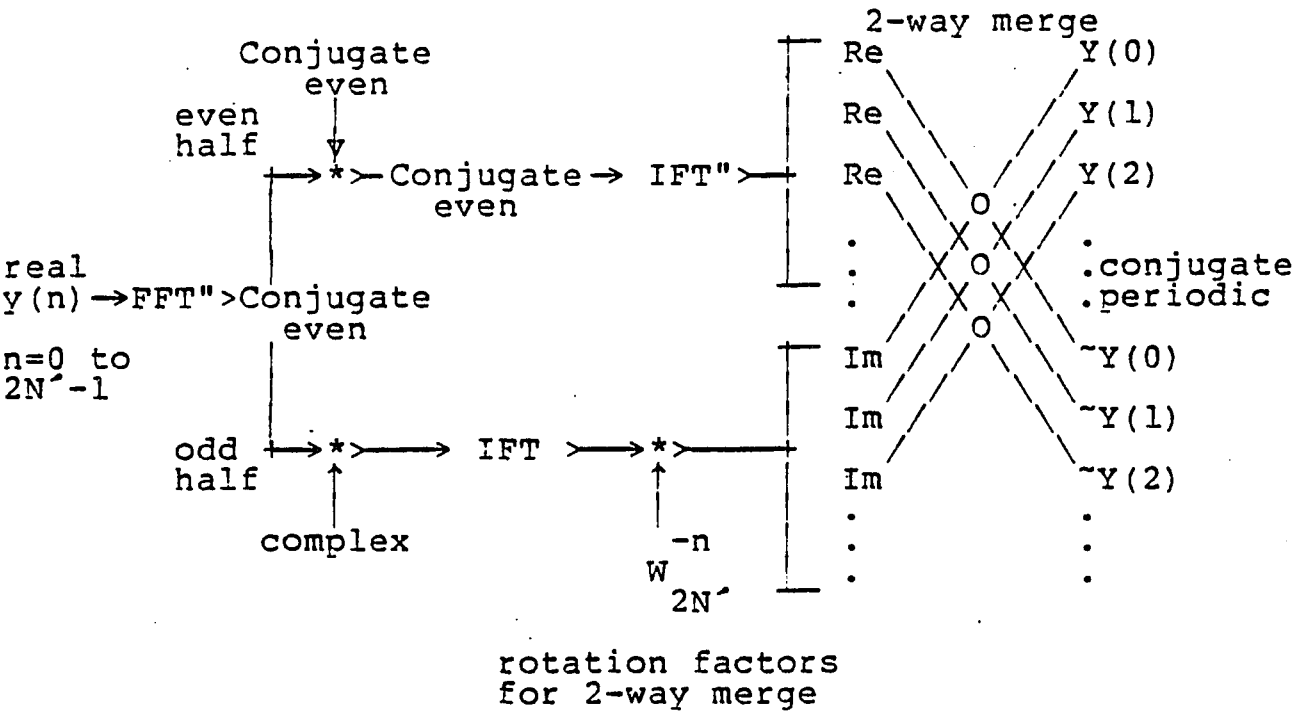

rotation factors
for 2-way merge

Where the notation FFT" and IFT" indicate which operations may take advantage of the two-at-a-time method.

IV-B.7 Total Number of Complex Multiplications Required

In summary, the number of complex multiplications required to perform an FFT on any number of points N may be found as follows. If N is even and the points are real or conjugate even use

$$F(N) = (N/4) \log_2 (N/4) \qquad \text{when } N = 2^m$$

or when N is not a power of two

$$F(N) = N/2 - 1 + F(N/2) - M$$

where

$$M = \begin{cases} 1 & \text{if N is divisible by 4} \\ 0 & \text{if N is not divisible by 4} \end{cases}$$

and F(N/2) is determined without using these two-at-a-time formulas. If N is not even or the points are not real or

conjugate even then

$$F(N) = (N/2) \log_2(N/8) + 2 \quad \text{for } N = 2^m$$

or when N is composite N = PQ and not a power of two then use

$$F(PQ) = (P-1)(Q-1) - M(P,Q) + Q\,F(P) + P\,F(Q)$$

where

$$M(P,Q) = M_{1/4}(P,Q) + M_{1/2}(P,Q) + M_{3/4}(P,Q)$$

is non-zero only if P<Q and its components are defined as:

$M_{1/4}(P,Q)$ is the number of integers between P/4 and P such that four times the integer evenly divides Q.

$M_{1/2}(P,Q)$ is the number of integers between P/2 and P such that twice the integer evenly divides Q.

$M_{3/4}(P,Q)$ is the number of integers between P/4 and P/3 such that four times the integer evenly divides Q.

When N is prime use

$$F(N) = 2F(N-1) + N - 4/3 - M$$

where

$$M = \begin{cases} 1/3 & \text{if } N = 3, \\ 2/3 & \text{if } N-1 = 2^m \\ 1/3 & \text{if } N-1 \text{ not} = 2^m \text{ but is divisible by 4} \\ 0 & \text{otherwise} \end{cases}$$

Using these formulas in a recursive manner will allow calculation of the number of complex multiplications

required to perform an FFT on any number of points. To minimize this number, if the number of points is even and they are real or conjugate even, the two-at-a-time algorithm should be used first. If the number of points is not even, but the points are still either real or conjugate even, then choose the largest prime factor P and use the two-at-a-time method to calculate the FFT's for P-1 points. Then the remaining transforms should be done using the smallest remaining factor first and progressing up to the largest. Figure IV-1 shows the result of using these formulas to calculate the number of floating point multiplications required to perform FFT's on any number of points up to and including 2048.

IV-C Data Shuffling in the Fast Fourier Transform

The bit reversal techniques used to determine the order into which data points must be shuffled prior to performing a radix two FFT are described throughout the literature. Although the theory of point shuffling for mixed radix transforms is described, the step from theory to practice is left somewhat obscure. For this reason it was decided to include here a more detailed explanation of how this step may be performed.

The number of points N to be transformed is assumed to be composite. That is, N may be factored into its prime factors as follows.

$$N = N_0 \times N_1 \times \ldots \times N_m$$

Singleton [6] gives the permutation of the data items as

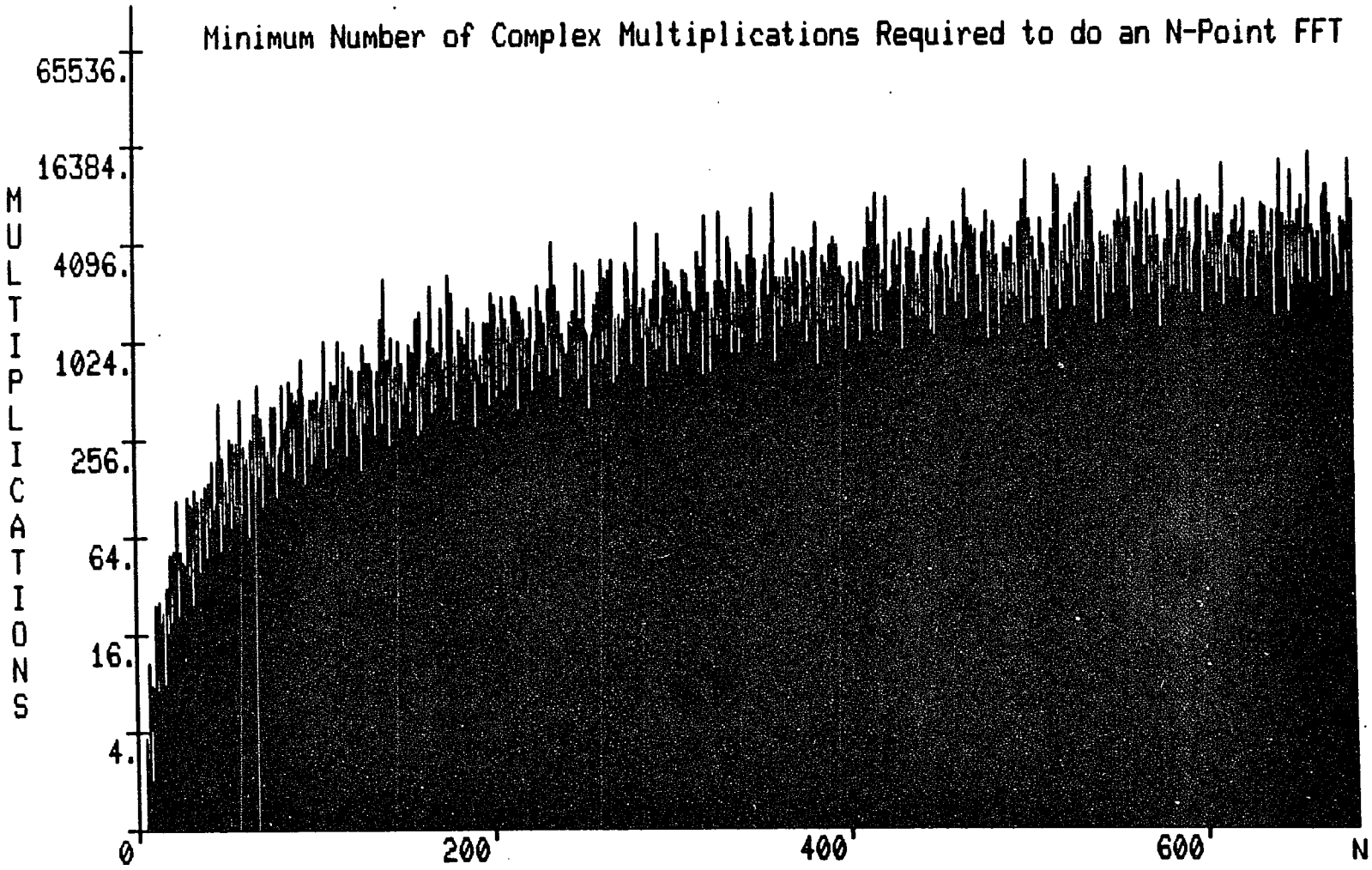
Minimum Number of Complex Multiplications Required to do an N-Point FFT
MULTIPLICATIONS
65536.
16384.
4096.
1024.
256.
64.
16.
4.
0
200
400
600
N

Figure IV-1

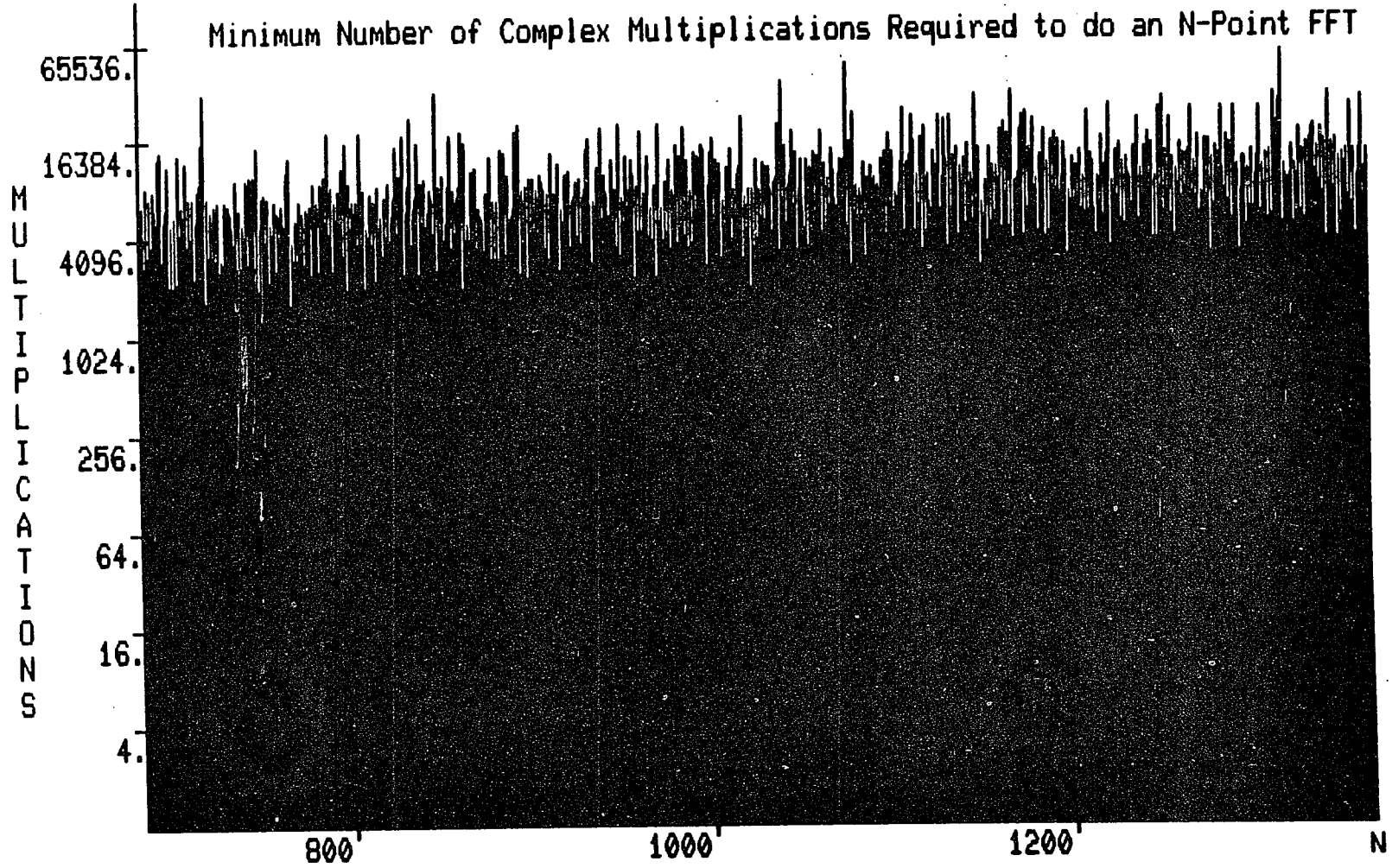

Figure IV-1 (continued)

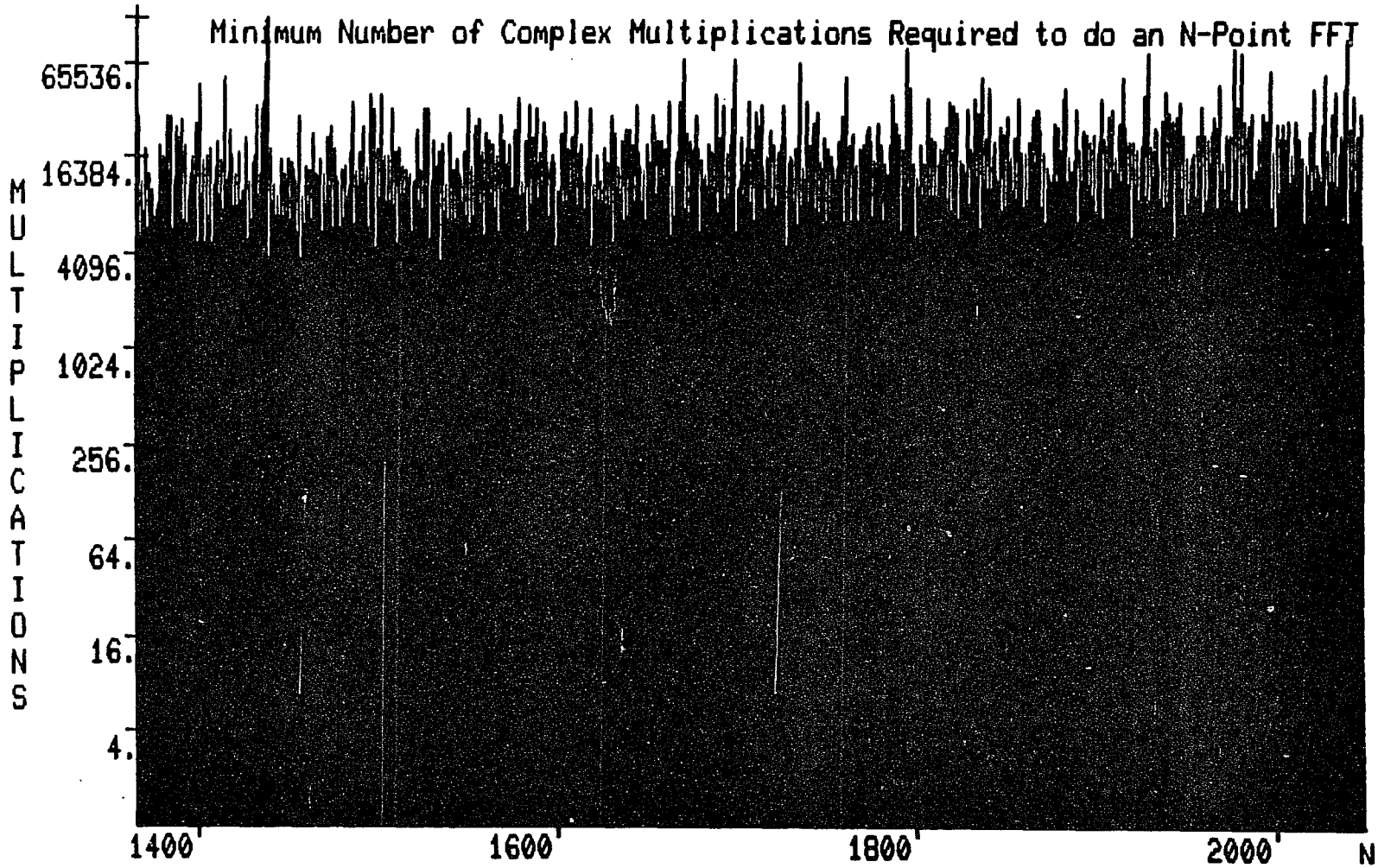

Figure IV-1 (continued)

$$k = k_m N_{m-1} N_{M-2} \ldots N_0 + \ldots + k_2 N_0 + k_1$$

$$k' = k_1 N_1 N_2 \ldots N_m + k_2 N_2 N_3 \ldots N_m + \ldots + k_m$$

where the item in position k should be moved to position k′ prior to the FFT operation for the results to be in the correct order. His algorithm, however, requires that N be symmetrically factored so that

$$N_0 = N_m$$

$$N_1 = N_{m-1}$$

$$\vdots$$

$$N_s = N_{m-s}$$

as far as possible and the remaining mutually prime factors left in the middle between N_s and N_{m-s}. This allows data items to undergo a one-for-one exchange initially, but if any mutually prime factors are left in the middle, a subsequent interchange of relatively short permutation cycles must be performed. This procedure is reasonably well suited for a general mixed radix FFT algorithm. However, in a given application where speed is important it is usually desirable to write a special FFT algorithm for that number of points thus allowing the maximum number of precomputations to be performed. Also, as prescribed earlier, it is generally more efficient to order the factors from smallest to largest rather than symmetrically. The permutation cycles required to shuffle the data may be precomputed and each item moved only once instead of twice as Singleton's method suggests.

The procedure involves counting in a mixed radix numbering system as follows. In any numbering system the right most digit is always the units and each successive position to the left of it has the weighting of the previous position times the radix. For example in a fixed radix system such as base ten each position to the left of the units position has a weighting which is the radix (ten) times that of the previous position.

digit	5	2	9	4
radix	10	10	10	10
weighting	1000	100	10	1
value	5000	200	90	4

In a mixed radix numbering system each position may have a different radix associated with it. For example lets assume that N is 60 which factors into 60 = (2)(2)(3)(5). The number 0123 in base 2,2,3,5 is

digit	0	1	2	3
radix	2	2	3	5
weighting	30	15	5	1
value	0	15	10	3

or 0 + 15 + 10 + 3 = 28 in base 10. The radix in each column is one greater than the largest digit permitted in that column. The weighting always starts with unity at the right and the weighting of a given column times the radix of that column gives the weighting for the next column. The product of the digit and its weighting is the value of each column. The sum of the values in all columns is the total value

which the number represents. Counting in this radix 2,2,3,5 system would progress as follows.

0,1,2,3,4,10,11, ... ,14,20, ... ,24,100, ... ,1124

where 1124 radix 2,2,3,5 is 30(1) + 15(1) + 5(2) + 1(4) = 59 in base ten is the largest number which can be represented in this system. Now to determine the order into which to shuffle the points to do an FFT on the N = 60 points, one merely counts in digit-reversed order by incrementing the leftmost digit first up to its maximum, then increment the next digit to the right and start again. This is just a mirror image of what is done in the normal counting scheme. The result is

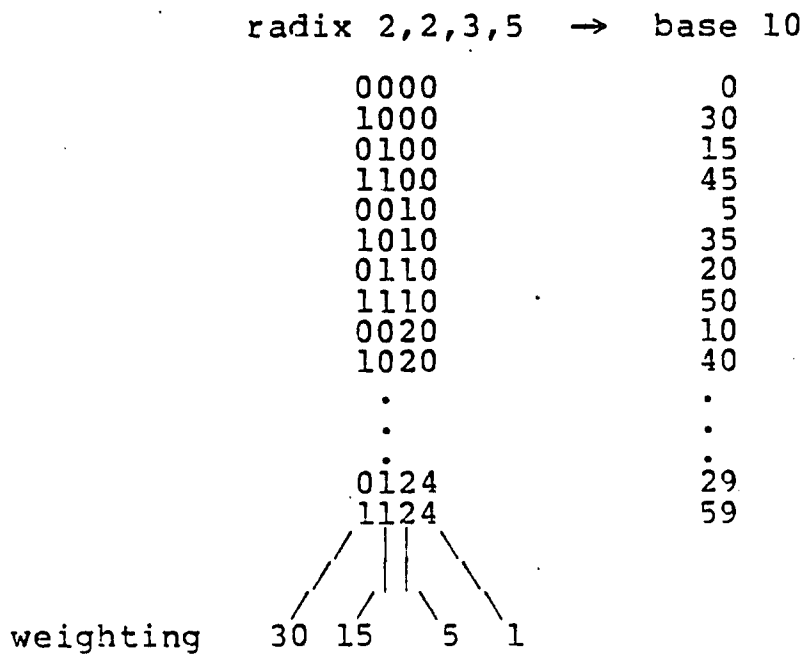

This is the order into which the data points must be shuffled. The FFT would then proceed by doing 30 radix-2 FFT's, then 30 2-way merges, followed by 20 3-way merges and finally 6 5-way merges. The 3- and 5-way merges would of course be done using the prime radix FFT techniques to minimize the number of complex multiplications required.

It would appear at first glance that the data points will have to be shuffled again each time a prime radix FFT is performed. After all, the prime radix transform algorithm calls for reordering the points using the primitive root technique, then the subsequent FFT and IFT should require additional shuffling and may even involve further prime radix transforms. This, fortunately, is not the case. Sure, the prime radix FFT requires a primitive root shuffle followed by an FFT on one less point. However, the following IFT would undo the FFT shuffle and then the primitive root shuffle must be undone to return the data to the order of the resulting prime FFT. As a result the temporary shuffling required in these steps is best done using a set of indirect pointers and leaving the actual data items in place. In addition, these indirect pointers may be precomputed to save time when actually performing the FFT.

A generalized mixed radix FFT algorithm using these techniques would only be feasible if written in a computer language which allows recursive subroutine calls such as PASCAL or APL. Programs for performing these FFT's on a given number of points may be efficiently written in FORTRAN. An interesting project would be to write an FFT compiler which would essentially write a FORTRAN program to perform an FFT on any fixed number of points. This could include performing any possible precomputations which would make the resulting FFT algorithm as fast as possible.

IV-D The Effects of Sampling on the Spectral Results

Although the following derivation is available in the literature [15], it is repeated here for completeness.

The operation of time limiting a signal may be

mathematically represented as multiplying the signal by a rectangular window starting at time t=0 and ending at time t=T. The rectangular window will be represented by

$$\Pi\left(\frac{t - T/2}{T}\right) = \begin{cases} 1 & \text{for } t = 0 \text{ and } 0 < t < T \\ 0 & \text{for } t < 0,\ t = T \text{ and } T < t \end{cases}$$

The continuous Fourier transform of this function is given in [15] as

$$x(t) \quad <----> \quad X(f)$$

$$\Pi\left(\frac{t - T/2}{T}\right) \quad <----> \quad T\ \mathrm{sinc}[\ fT\ ]\ e^{-j\ PI\ fT}$$

Multiplication of x(t) by the rectangular function in the time domain represents a convolution of their transforms in the frequency domain. Thus

$$x(t)\,\Pi\left(\frac{t - T/2}{T}\right) \quad <----> \quad X(f) * T\ \mathrm{sinc}[\ fT\ ]\ e^{-j\ PI\ fT}$$

Now this time limited signal is turned back into an infinite time signal by convolving it with an infinite series of impulses spaced at intervals of T.

$$\sum_{m\ =\ -inf}^{inf} d[\ t - mT\ ] \quad <----> \quad \frac{1}{T} \sum_{n\ =\ -inf}^{inf} d[\ f - n/T\ ]$$

where d[t - mT] is an inpulse at time mT and the summation represents an infinite train of these impulses. This convolution in the time domain represents multiplication in the frequency domain.

$$x(t) \sqcap\!\sqcap\!\sqcap \left| \frac{t - T/2}{T} \right| * \sum_{m=-\inf}^{\inf} d[\, t - mT]$$

$$\langle ----- \rangle$$

$$X(f) * \mathrm{sinc}[\, fT\,]\, e^{-j\,PI\,fT} \sum_{n=-\inf}^{\inf} d[\, f - n/T\,]$$

This result says that any function which is periodic with period T will only contain frequency components at discrete frequencies spaced by 1/T Hertz. Also, if the time function x(t) is periodic with period T, then the functions above reduce to just x(t) and X(f).

Now sample the above signal at intervals of T/N.

$$x(t) \sqcap\!\sqcap\!\sqcap \left| \frac{t - T/2}{T} \right| * \sum_{m=-\inf}^{\inf} d[t - mT] \sum_{n=-\inf}^{\inf} d[t - nT/N]$$

$$\langle ----- \rangle$$

$$X(f) * \mathrm{sinc}[\, fT\,]\, e^{-j\,PI\,fT} \sum_{n=-\inf}^{\inf} d[f - n/T] * \sum_{m=-\inf}^{\inf} d[f - mN/T]$$

Inspection of this spectrum shows that the sampling operation causes the spectrum to get shifted and superimposed on itself over and over again ad infinitum. As a result of this the spectrum becomes periodic with a period of N/T. Now, if the spectrum, prior to this last convolution, had an insignificant value at a distance N/T from a particular frequency of interest, then the resulting spectrum could still be used to approximate the value at this frequency. This, it turns out, is how the discrete Fourier transform may be used to approximate the continuous

transform. Also, if a digital signal generator repeats a sequence of points with period T, the resulting spectrum will be discrete and periodic.

Both the continuous Fourier transform and the discrete Fourier transform are linear, thus allowing superposition [13,15]. It will suffice then to show the relationship between the continuous and discrete transforms at one frequency and superposition will allow this to be extended to all frequencies.

Assume that x(t) is a sine wave at some discrete frequency F = q/T. Then it will have the following transform:

$$A \cos[\, Wt + p \,] \;\langle\text{-->}\; \frac{A}{2} \left| e^{jp} d[\, f - F \,] + e^{-jp} d[\, f + F \,] \right|$$

$$= \begin{cases} A/2\ e^{jp} & \text{at } f = F = q/T \\ A/2\ e^{-jp} & \text{at } f = -F = -q/T \\ 0 & \text{otherwise} \end{cases}$$

where W = 2PI F = 2PI q/T. Substituting this into the above formulas yield

$$A \cos[\, Wt + p \,] \sqcap\!\sqcap\!\sqcap \left| \frac{t - T/2}{T} \right| * \sum_{m=-\inf}^{\inf} d[t - mT] \sum_{n=-\inf}^{\inf} d[t - nT/N]$$

$$\langle\text{---->}$$

$$\frac{A}{2} \left| e^{jp} d[f-F] + e^{-jp} d[f+F] \right| * \operatorname{sinc}[fT]\, e^{-jPI\ fT} \sum_{n=-\inf}^{\inf} d[f-n/T] * \sum_{m=-\inf}^{\inf} d[f-mN/T]$$

Carrying out the first convolution results in

$$\frac{e^{j\{p-PI(f-F)T\}}\,\mathrm{sinc}[T(f-F)] + e^{-j\{p+PI(f+F)T\}}\,\mathrm{sinc}[T(f+F)]}{2/A} \sum_{n=-\inf}^{\inf} d[f-n/T] * \sum_{m=-\inf}^{\inf} d[f-mN/T]$$

This frequency domain representation prior to the last convolution represents two sinc functions centered at +F and -F and sampled by the delta function at intervals of 1/T. Notice that the first sinc functions will have the value one at f = F and zero values at f = F + s/T where s = ... ,-2,-1,1,2, ... and the second sinc function will be one at f = -F and be zero at f = -F + s/T. Now, since F is an integer multiple of 1/T, i.e. F = q/T, the zeroes of the sinc functions will occur at the sample points and the transform reduces to

$$A\cos[Wt + p]\sum_{n=-\inf}^{\inf} d[t - nT/N] \;\langle\!-\!-\!\rangle\; \begin{cases} e^{jp}\,A/2 & \text{at } f = F + mN/T \\ e^{-jp}\,A/2 & \text{at } f = -F + mN/T \\ 0 & \text{otherwise} \end{cases}$$

where m = ... ,-1,0,1, ...

Let f = k/T and F = q/T

$$A\cos[Wt + p]\sum_{n=-\inf}^{\inf} d[t - nT/N] \;\langle\!-\!-\!\rangle\; \begin{cases} e^{jp}\,A/2 & \text{at } k = q + mN \\ e^{-jp}\,A/2 & \text{at } k = -q + mN \\ 0 & \text{otherwise} \end{cases}$$

The discrete Fourier transform is seen to give a similar result.

$$X(k) = \sum_{n=0}^{N-1} A\cos[W'n + p]\; e^{-2pi\ nk/N}$$

$$= \begin{cases} N e^{jp} A/2 & \text{at } k = q + mN \\ N e^{-jp} A/2 & \text{at } k = -q + mN \\ 0 & \text{otherwise} \end{cases}$$

where W' = W T/N. The only difference is the factor N. Thus it can be seen that if x(t) is a sine wave at the frequency q/T, where q is an integer, then the discrete Fourier transform X(k) may be used to produce the continuous Fourier transform X(f). Due to superposition, this will also be true if x(t) is any function whose component frequencies are all integral multiples of 1/T. In the real world this may not happen very often. However, if a digital signal generator which is phase locked to the sampler is used, then the above conditions may be forced to occur and the DFT results will show the actual frequency components of the generated waveform.

Now let's investigate the case where F is not a multiple of 1/T to see what information about X(f) may be derived from X(k). Assume that x(t) is a sine wave and that F = (r/PI + q)/T where q is an integer and r is some fraction between zero and PI. The operation of sampling the function for a limited time prior to performing a DFT is synonymous to the continuous time operation performed above and the DFT is comparable to its continuous Fourier transform which is repeated here.

$$A \cos[\, Wt + p \,] \sqcap\!\sqcap\!\sqcap \left| \frac{t - T/2}{T} \right| * \sum_{m=-\inf}^{\inf} d[t - mT] \sum_{n=-\inf}^{\inf} d[t - nT/N]$$

<----->

$$\frac{e^{j\{p-PI(f-F)T\}} \operatorname{sinc}[T(f-F)] + e^{-j\{p+PI(f+F)T\}} \operatorname{sinc}[T(f+F)]}{2/A} \sum_{n=-\inf}^{\inf} d[f-n/T] * \sum_{m=-\inf}^{\inf} d[f-mN/T]$$

Take just a portion of this transform out, call it X'(f) and analyze it.

$$X'(f) = \frac{e^{j\{p-PI(f-F)T\}} \operatorname{sinc}[T(f-F)]}{2/A} \sum_{n=-\inf}^{\inf} d[f - n/T]$$

Substitute F = (r/PI + q)/T and f = k/T where q and k are integers.

$$X'(k) = A \frac{e^{j\{p+r-PI(k-q)\}} \operatorname{sinc}[-r/PI+k-q]}{2}$$

k = ... ,-1,0,1, ...

Replace the sinc[u] function with sin[PI u]/(PI u).

$$X'(k) = A \frac{e^{j\{p+r\}} e^{-jPI(k-q)} \sin[-r+PI(k-q)]}{2\{-r+PI(k-q)\}}$$

Since (k-q) is an integer

$$e^{-jPI(k-q)} = \cos[\, PI(k-q) \,] = (-1)^{(k-q)}$$

$$\sin[PI(k-q)] = 0$$

and

$$\sin[-r+PI(k-q)] = \sin[PI(k-q)]\cos[r] - \cos[PI(k-q)]\sin[r]$$

$$= -(-1)^{(k-q)}\sin[r]$$

then

$$X'(k) = A\frac{e^{j\{p+r\}}\sin[r]}{2\{r+PI(q-k)\}}, \text{ where } k = \ldots ,-2,-1,0,1,2, \ldots$$

From this, it is seen that the phase is constant except for a 180 degree shift as k increases beyond q. The magnitude of the numerator remains constant while the denominator varies linearly with k and its magnitude goes through a minimum near k = q. The resulting magnitude of X'(k) is maximum near k = q and rolls off reciprocally on either side. Note that this 'positive frequency' portion of X(f) actually extends infinitely in both the positive and negative directions. If the 'negative frequency' portion is added back in, the two will overlap throughout the entire frequency spectrum. The amount that one portion modifies the spectrum in the vicinity of the other depends upon the value of q or in other words the value of the sine wave frequency F relative to the time sample length T. The final step in the transform above convolves this spectrum with a summation of impulses causing this frequency spectrum to be repeatedly shifted by N/T in both directions and summed to produce the final spectrum, as previously stated. As a result of this, the spectrum of the sine wave at f = q/T will be overlapped the most by the negative frequency portion centered near f = -q/T or f = (2N - q)/T whichever is closer. By choosing N sufficiently large, the amount of overlap can be made arbitrarily small and the DFT results may be used to estimate the amplitude and frequency of the original sine wave. Note that the aliasing effects seen here are not

produced by a component of the original signal exceeding the Nyquist rate, but are instead produced by spurious frequencies generated in the sampling process as the sample is limited to a finite number of points.

For example, assume that we have a fixed sampling rate of 8000 samples per second and we wish to know what minimum number of samples can be taken to insure that the contribution by the negative frequency portion of the DFT of a 1020 Hertz sine wave is down at least 40dB near the peak of the positive frequency portion.

$$T = N/8000$$

$$F = 1020 \text{ Hz} = (r/PI + q)/T$$

$$q = F\ T = 1020\ N/8000 = 0.1275\ N$$

Since q is smaller than N-q = 0.8725 N, then q will be the determining factor. Let Vr represent the ratio of the negative to the positive portions at the point n = q.

$$-40 \text{ dB} = 20 \log_{10} Vr$$

$$Vr = 10^{(-40/20)} = 0.01$$

The ratio of the positive to negative portions is approximately given by

$$Vr \doteq \frac{1}{2PI\ q}\ .$$

Therefore

$$q \doteq \frac{1}{2PI\ Vr} = \frac{1}{2(3.14)(0.01)} = 15.9 \doteq 16$$

and

$$N = q/0.1275 \doteq 125.5 = 126$$

Thus if at least 126 samples are taken the peaks of this spectrum will not be significantly distorted.

An additional problem remains. How can we establish the true amplitude A and frequency F of the actual sine wave from this dispersed spectrum resulting from the DFT?

Here we assume that the frequency of the sine wave x(t) is not an integral multiple of 1/T, otherwise the solution would be trivial. The approximate spectrum in the vicinity of F was previously derived as

$$X'(k) = A \frac{e^{j\{p+r\}} \sin[r]}{2\{r+PI(q-k)\}} \qquad \text{where } k = \ldots, q, q+1, \ldots \text{ and } F=(r/PI + q)/T$$

assuming negligible contributions from the negative frequency portion. The two values of the DFT results at k = q and k = q+1 are easily located (even though q is not known) as the two adjacent points with the largest magnitudes. Also a 180 degree phase shift occurs between them. Take these two largest magnitudes, divide them each by N and call the results y and z respectively.

$$| X'(q) | = y = A \frac{\sin[r]}{2r}$$

$$| X'(q+1) | = z = A \frac{\sin[r]}{2\{PI-r\}}$$

Remember that 0 < r < PI. Now these two equations may be solved for A and r.

$$A = \frac{2\ r\ y}{\sin[r]}$$

$$z = \frac{2\ r\ y \sin[r]}{2\{PI-r\} \sin[r]} = \frac{r\ y}{PI - r}$$

$$(PI - r)\ z = r\ y$$

$$r = \frac{PI\ z}{y + z}$$

$$A = \frac{2\ r\ y}{\sin[r]} = \frac{2\ PI\ y\ z}{(y + z)\ \sin[PI\ z/(y + z)]}$$

$$F = (r/PI + q)/T = \frac{z + q(y + z)}{(y + z)T} = \frac{y(q) + z(q+1)}{(y + z)T}$$

With these formulas the amplitude and frequency of the input sine wave may be determined. As either y or z gets very large with respect to the other, the formula for the amplitude A may be simplified. The value of sin[PIu] approaches PIu as u approaches zero and it approaches PI(1-u) as u approaches one. Therefore, if the computations are done with an accuracy of seven decimal places, the following approximations may be made to simplify the computation.

$$A = \begin{cases} 2z & \text{if } |\ y/z\ | < 0.0002 \\ 2y & \text{if } |\ y/z\ | > .5000 \\ \dfrac{2PIyz}{(y + z)\ \sin[PI\ z/(y + z)]} & \text{otherwise} \end{cases} \qquad \text{(accurate to 7 places)}$$

In summary, it has been shown here that if a digital signal generator, which is synchronized to the sampler, is used to generate a signal, which is periodic with period T equal to the length of the time sample taken to do a DFT, then the result of the DFT will be an exact representation of the spectrum of the input signal. It also follows that this may be used as a test signal to be passed through any time-invariant system prior to sampling and the DFT will still yield a true measure of the spectrum of the signal at the output of this system. If a synchronized digital signal

generator is not used, then a sine wave signal of a frequency sufficiently below the Nyquist frequency may be used and the number of samples may be made sufficiently large to allow the signal's amplitude and frequency to be calculated to a desired accuracy. Note that submultiples of the sampling frequency should be avoided because the spurious frequencies, which would be generated by nonlinearities in the system, may appear superimposed on the test signal frequency due to aliasing.

CHAPTER V

SIGNAL SYNTHESIS FOR DIGITAL TRANSMISSION SYSTEMS

V-A Signal Requirements

As seen in the previous chapter, the main source of the inaccuracies encountered when trying to estimate the spectrum of a continuous signal, using discrete methods, stems from having to take a time limited sample of what is really a continuous signal. Even if the analog signal is periodic, the only way that the Discrete Fourier Transform (DFT) will yield results identical to the continuous transform is if the sample interval is an integral multiple of this signal period. For example, Figure V-1 shows a plot of 1542 samples taken at 1/8000 second intervals from a 2000.9808 Hz sine wave. From visual inspection it is obvious that this signal is not periodic in the sample interval of 1542/8000 = 0.19275 second. In fact, with the samples spaced at 1/8000 second, a sample size of 2039 points or some integral multiple thereof, would have to be taken in order for the image to be symmetrical and the analog signal to be periodic in the sample interval. If a Discrete Fourier Transform is performed on the 1542 points sampled, the spectrum of Figure V-2 results. This shows the spreading of the signal power from a single frequency sine wave over the entire spectrum with the sinc function's 1/x-shaped envelope, which was predicted in the previous chapter. Windowing techniques, which will be discussed at length later, may be used to reduce this spreading, as shown in

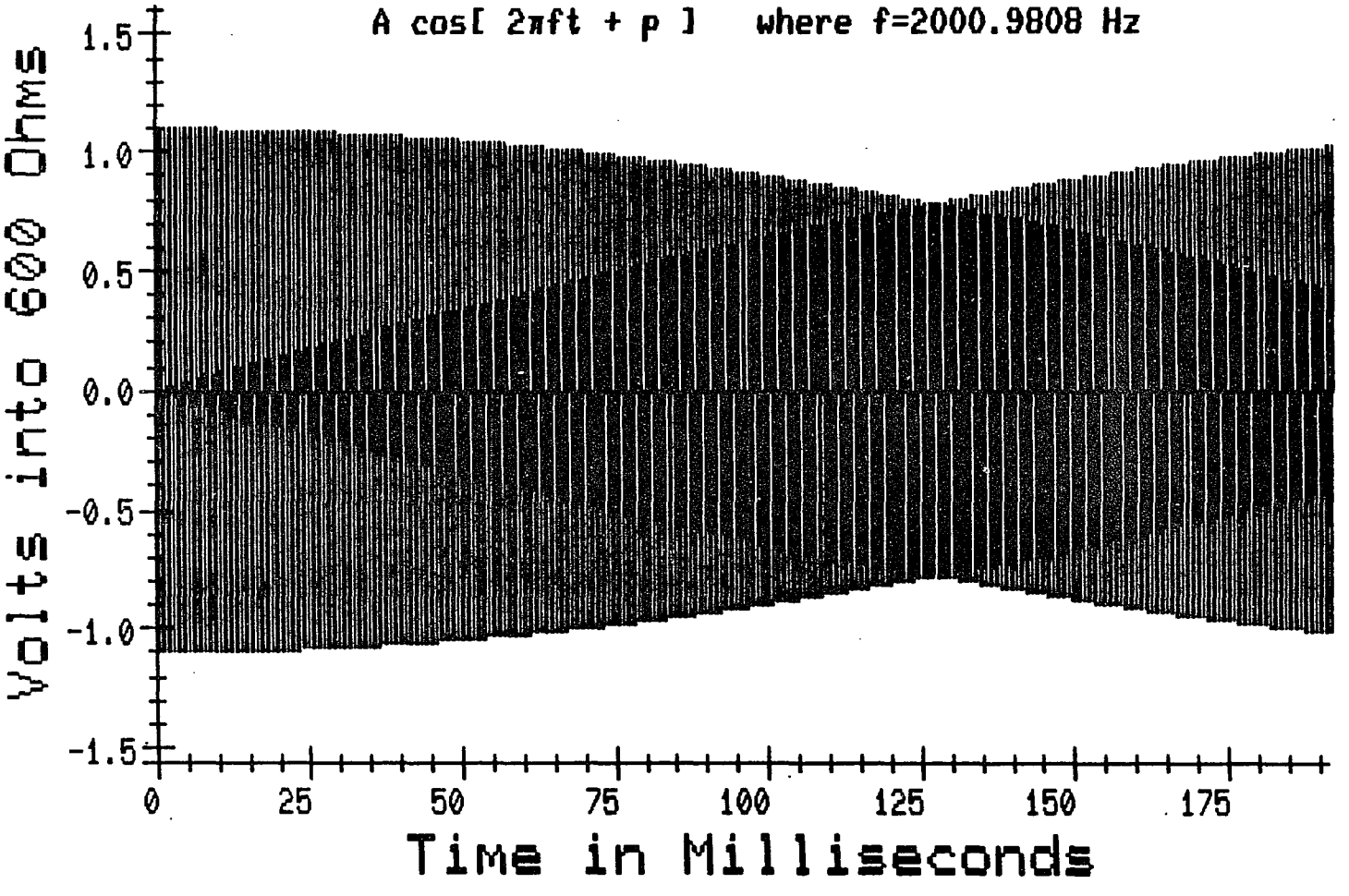
A cos[2πft + p] where f=2000.9808 Hz
Volts into 600 Ohms
1.5
1.0
0.5
0.0
-0.5
-1.0
-1.5
0
25
50
75
100
125
150
175
Time in Milliseconds

Figure V-1

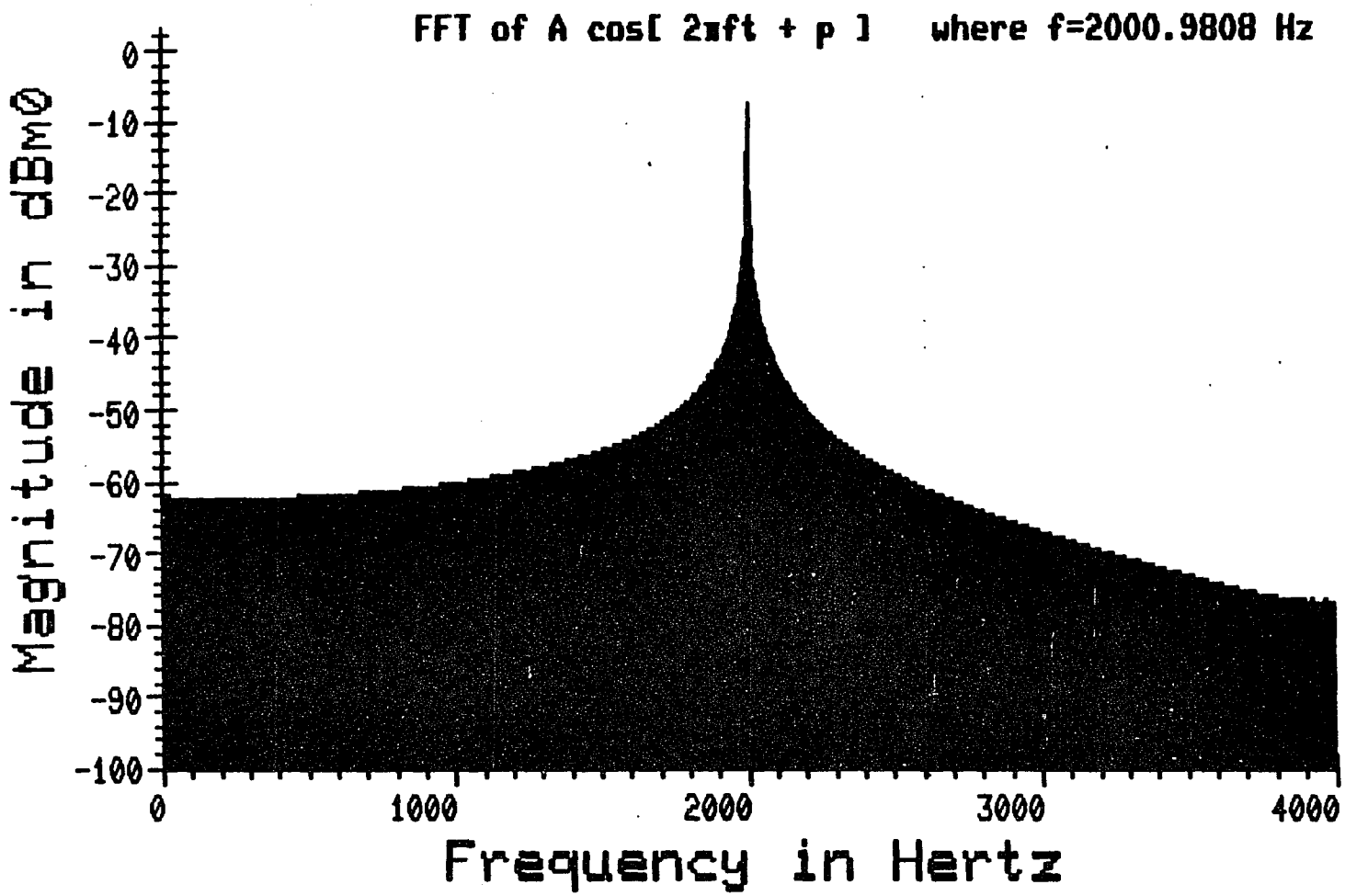
FFT of A cos[2πft + p] where f=2000.9808 Hz
Magnitude in dBm0
0
-10
-20
-30
-40
-50
-60
-70
-80
-90
-100
0
1000
2000
3000
4000
Frequency in Hertz

Figure V-2

Figure V-3; however, the 1 result is still just an estimate of the actual single line spectrum, which might have been expected. It also should be noted that the discrete spectrum, produced by the 1542 point DFT, has its frequency sample points spaced at 8000/1542 or about 5.19 Hz apart. This results in the true frequency of the analog signal of 2000.9808 Hz falling between the two sample frequencies of 1990.406 Hz and 2002.594 Hz. If the frequency of the analog signal is increased slightly to the sample frequency of 2002.594 Hz then the sampled signal of Figure V-4 results. It is evident from the symmetry of this plot that the signal is periodic in the sample interval. The DFT of this signal results in the pure line spectrum of Figure V-5 and, unlike the previous case, the discrete results are accurate.

The condition necessary to produce accurate results from the DFT process requires that any and all frequency components of the analog signal fall exactly on the frequency sample points produced by the transform as a result of time limiting the sample. This is equivalent to saying that the analog signal must be periodic in the sample interval. The only way to guarantee that this will happen is to have the signal source phase locked to the sampling clock so that no frequency drift will occur. It turns out that this is easily done in a digital channel bank because provisions have already been made to phase lock a given pair of transmitter and receiver.

Of the various methods available for digital signal synthesis, ranging from real-time calculation of each value to a simple table look-up, the latter is the simplest to implement. The tabular values are precomputed and may be calculated to any desired accuracy and may represent any

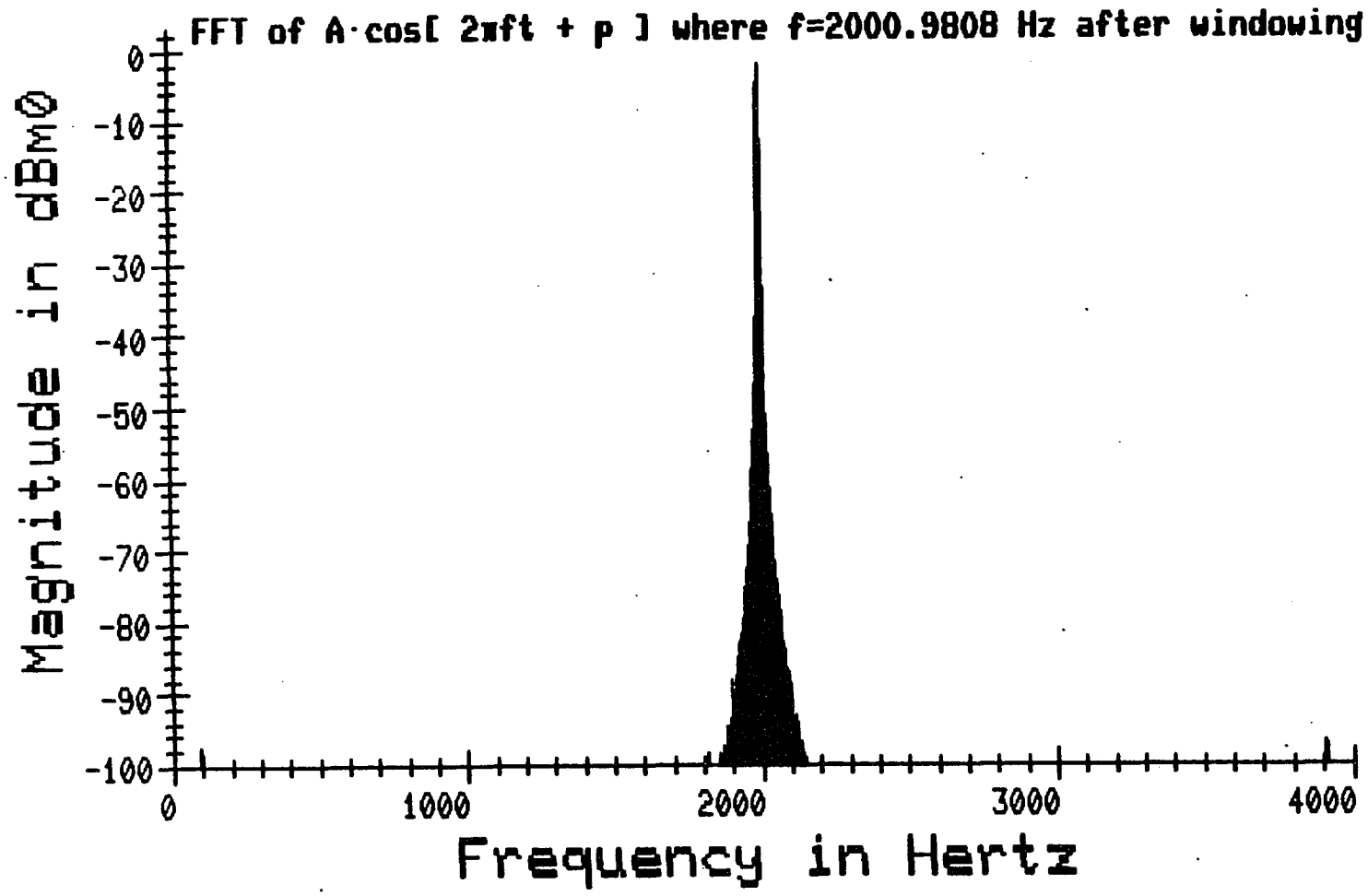
FFT of A·cos[2πft + p] where f=2000.9808 Hz after windowing
Magnitude in dBm0
0
-10
-20
-30
-40
-50
-60
-70
-80
-90
-100
0
1000
2000
3000
4000
Frequency in Hertz

Figure V-3

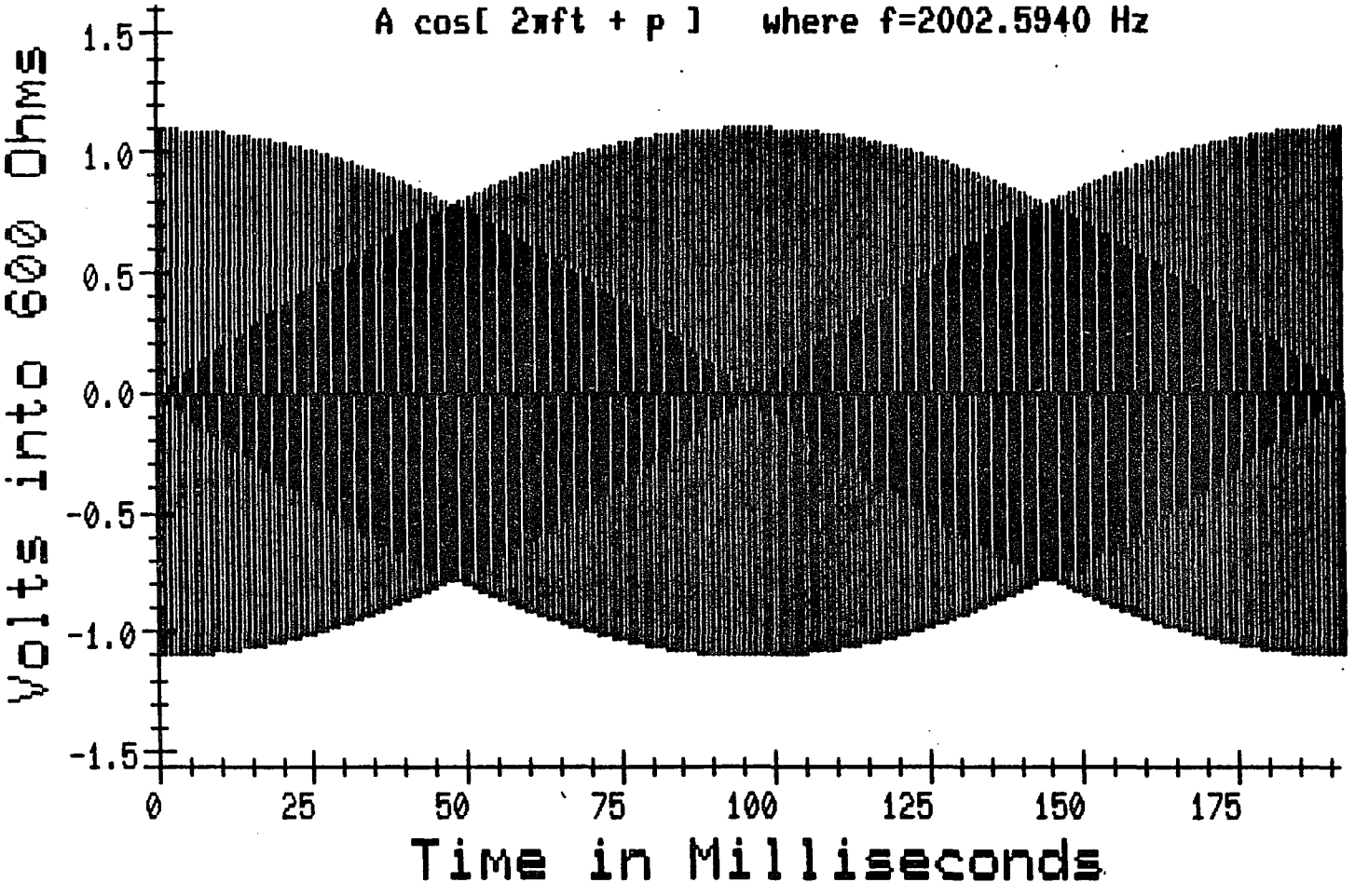
A cos[2πft + p] where f=2002.5940 Hz
Volts into 600 Ohms
1.5
1.0
0.5
0.0
-0.5
-1.0
-1.5
0
25
50
75
100
125
150
175
Time in Milliseconds

Figure V-4

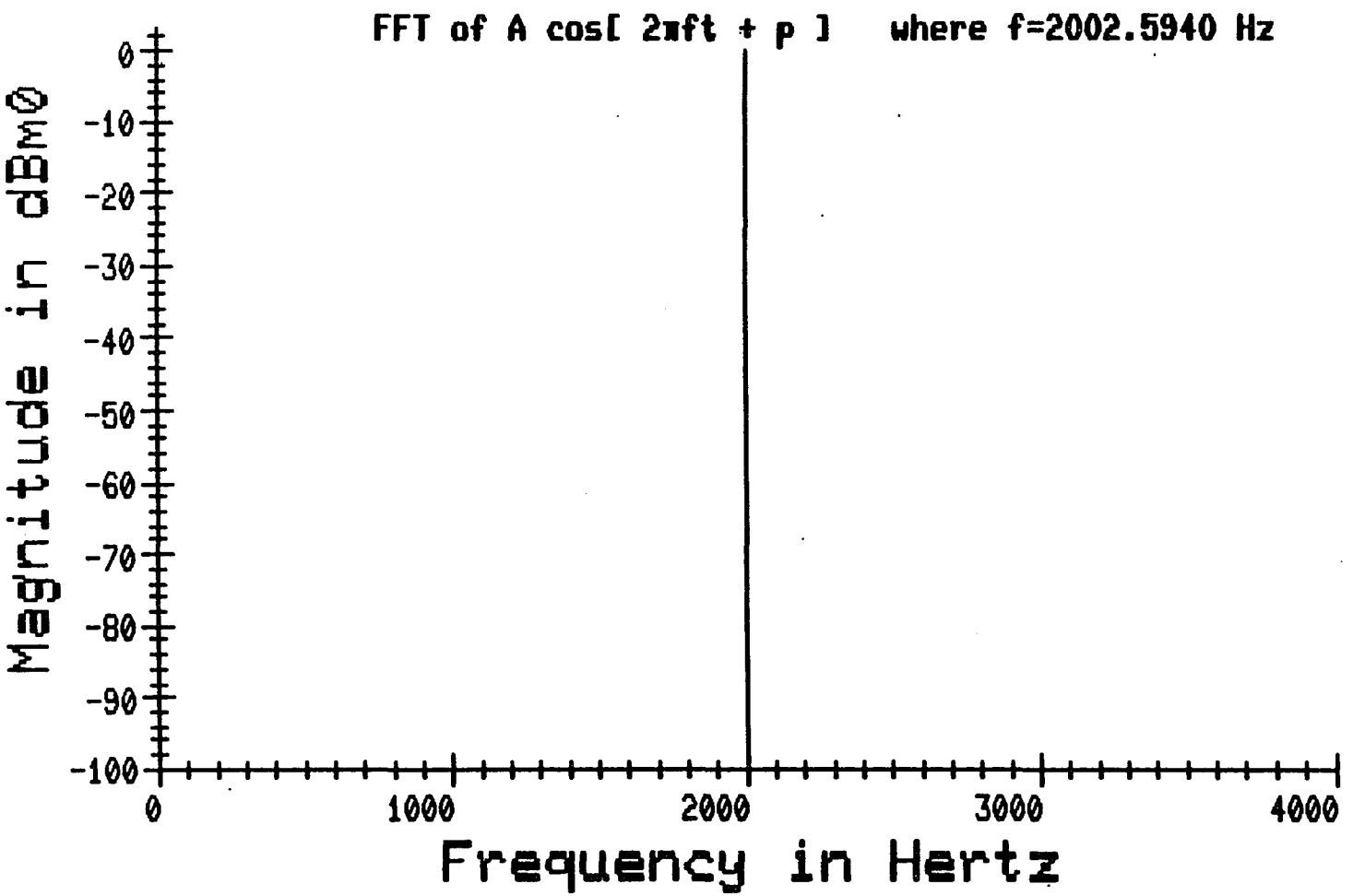
FFT of A cos[2πft + p] where f=2002.5940 Hz
Magnitude in dBm0
0
-10
-20
-30
-40
-50
-60
-70
-80
-90
-100
0
1000
2000
3000
4000
Frequency in Hertz

Figure V-5

desired function. The limitations involve the restricted repertoire of signals which may be derived from a given table and, of course, the size of the table which may be stored in a certain amount of memory. The technique for generating the signal involves cycling though the table over and over again, which guarantees that the signal will be periodic. The number of values extracted from the table in a given cycle must evenly divide the number of samples to be taken, in order to force the generated signal's frequency components to lie at the required discrete frequencies. Since a finite number of samples are to be taken, this will put a practical limit on the required length of the table.

A technique for increasing the utility of a given table follows. Say, for example, a table is generated which consists of only the eight values used to define a digital milliwatt back in Chapter 3. Repeatedly transmitting these eight values over and over again in a given time slot on a T1 digital line would produce a 1000 Hz sine wave at the output of the associated receiving channel unit with a level of precisely 0 dBm0 as shown in Figure V-6. If, rather than transmitting every stored value, only every other value is transmitted, the resulting signal will be at 2000 Hz and 0 dBm0 as indicated in Figure V-7. Again, if every third value is transmitted, a 3000 Hz, 0 dBm0 signal results as demonstrated by Figure V-8. Thus, with a given set of tabular values, more than one signal may be generated merely by skipping over various numbers of table values. Note that when the 2000 Hz signal was generated, half of the table values were never used; however, they were all used for the 3000 Hz signal. This results from the fact that eight values were stored and every second value was transmitted for the

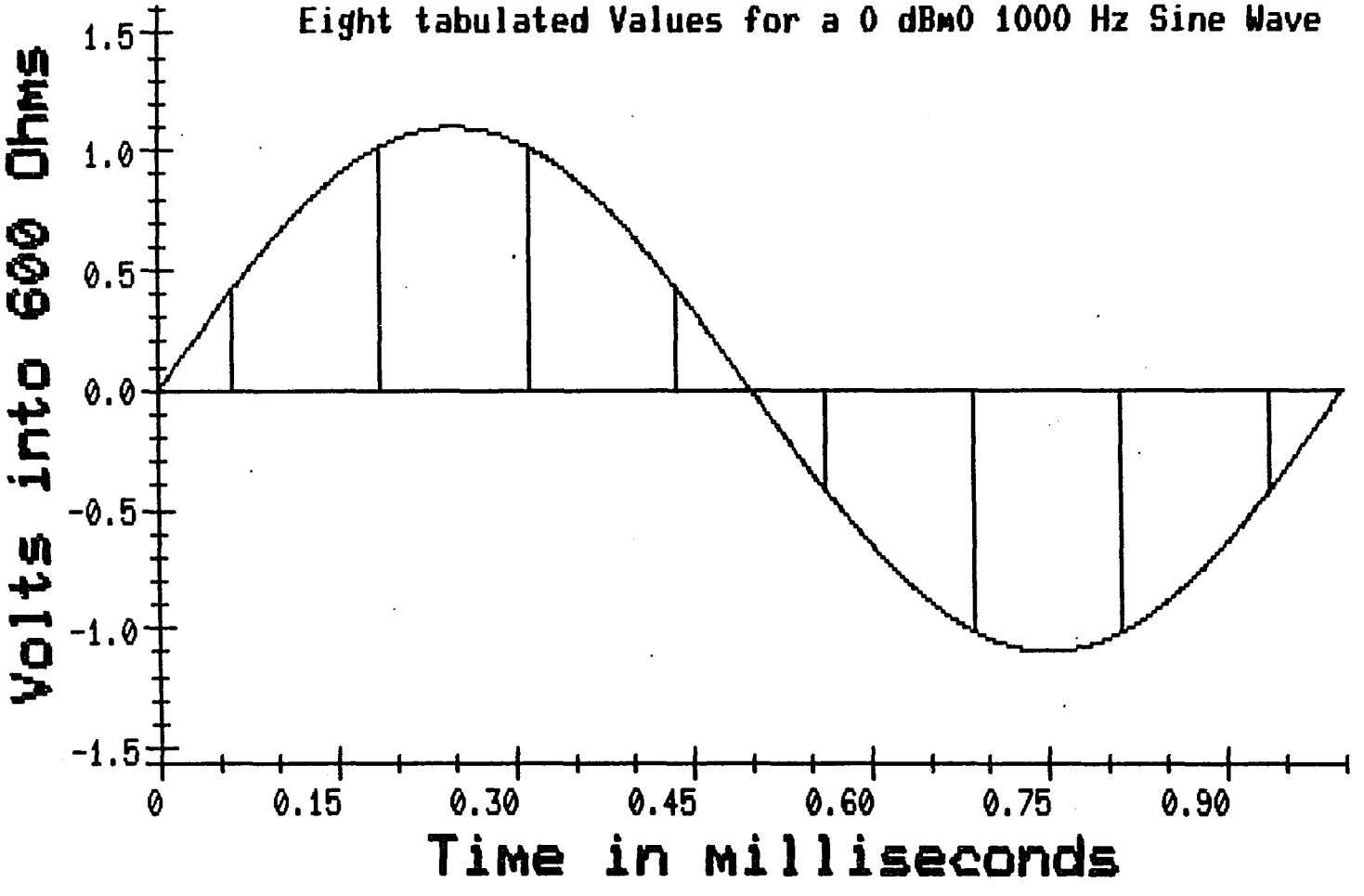
Eight tabulated Values for a 0 dBm0 1000 Hz Sine Wave
Volts into 600 Ohms
1.5
1.0
0.5
0.0
-0.5
-1.0
-1.5
0
0.15
0.30
0.45
0.60
0.75
0.90
Time in Milliseconds

Figure V-6

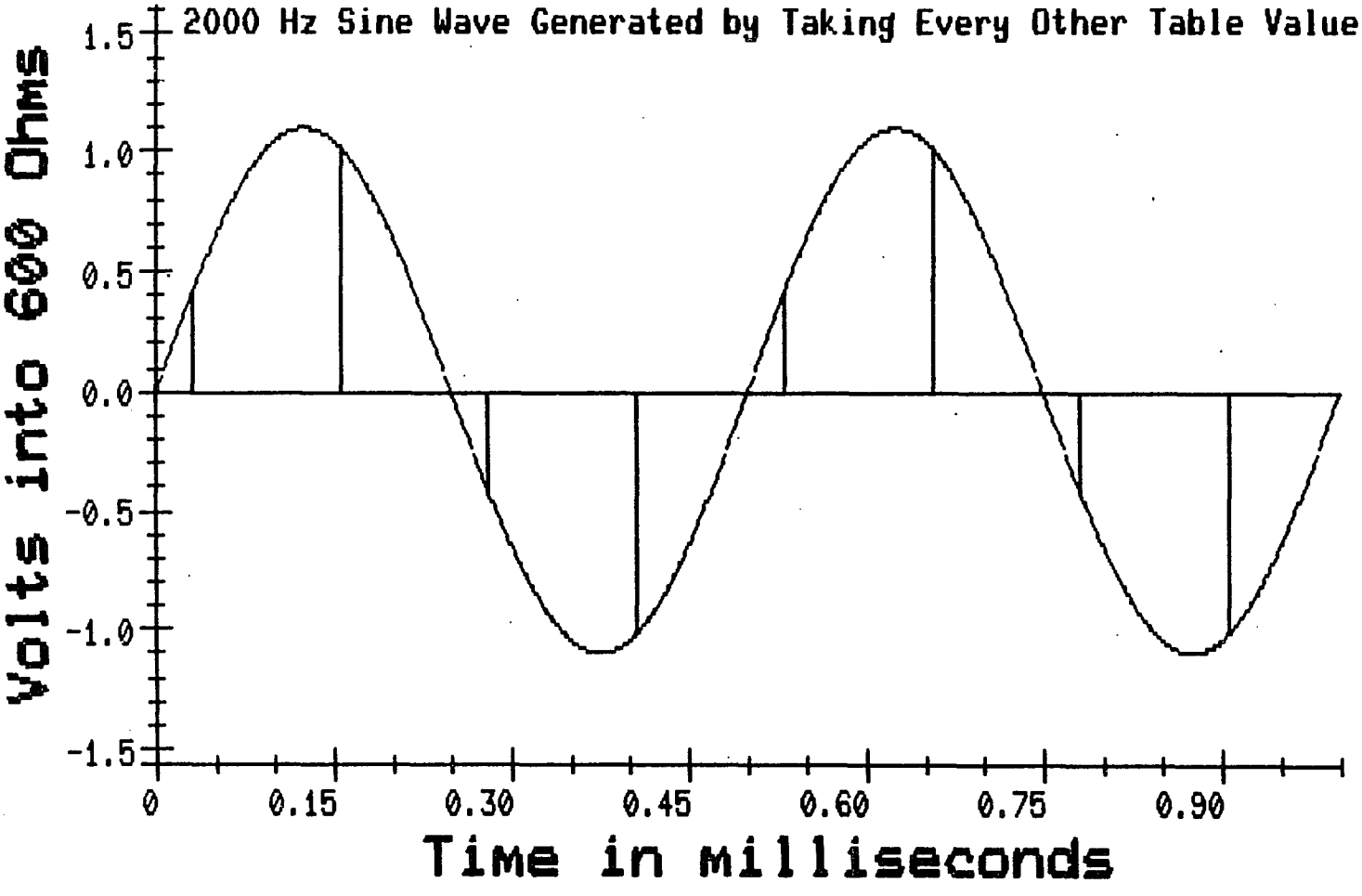
2000 Hz Sine Wave Generated by Taking Every Other Table Value
Volts into 600 Ohms
1.5
1.0
0.5
0.0
-0.5
-1.0
-1.5
0
0.15
0.30
0.45
0.60
0.75
0.90
Time in milliseconds

Figure V-7

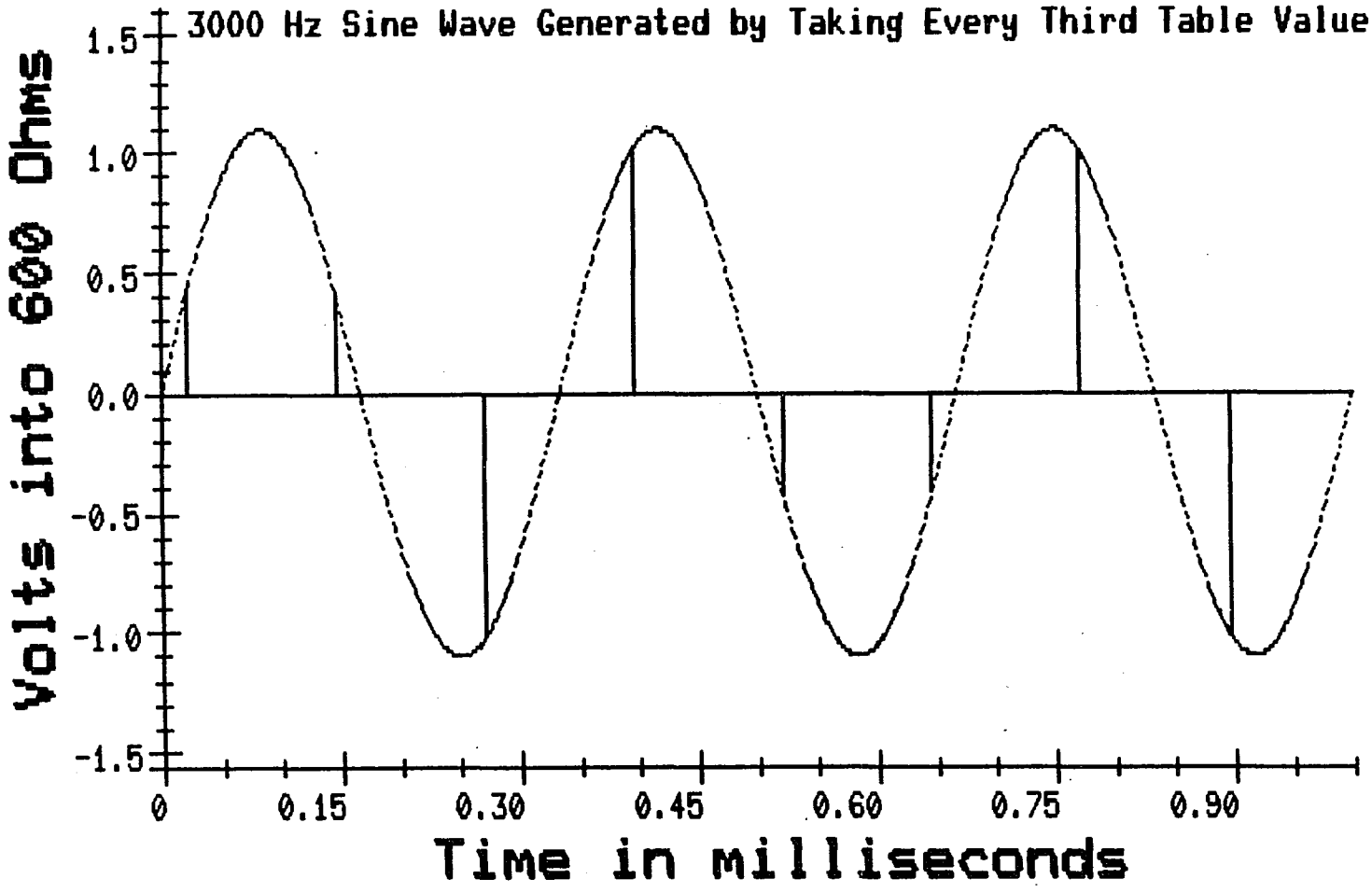
3000 Hz Sine Wave Generated by Taking Every Third Table Value
Volts into 600 Ohms
1.5
1.0
0.5
0.0
-0.5
-1.0
-1.5
0
0.15
0.30
0.45
0.60
0.75
0.90
Time in milliseconds

Figure V-8

2000 Hz signal. Eight and two are not mutually prime, but have two as a common factor. Thus, only one half of the tablular values were transmitted. On the other hand, three and eight are mutually prime, so all of the values are used. The eight points shown in any one of these last three figures when transformed by an eight point DFT result in individual line spectra. Figure V-9 shows the DFT of the 1000 Hz reference signal. The extra spectral line at 3000 Hz represents the noise added by the quantization of the sample values. An interesting phenomenon happens when the DFT is taken of the 2000 Hz signal. Here, as shown in Figure V-10, only the spectral line of fundamental frequency is present. This has occurred, not because of the absence of quantization noise, but because the third harmonic, where the noise should appear, is at 6000 Hz and, due to the aliasing effects of the DFT, this is folded over and appears as additional energy at 2000 Hz. In a similar manner, the quantization noise in the 3000 Hz signal, which should appear at 9000 Hz, gets aliased and becomes the component seen at 1000 Hz in Figure V-11. In each of these DFT's only eight points were used; however, since the eight tabular values are to be repeated over and over to generate a continuous signal, any DFT using a sample of some integral multiple of eight points will generate these same spectral results.

All of these signals investigated so far have ignored the presence of additional quantization noise, which will be added during every sixth sample by the digital channel bank due to the stealing of one bit for signalling purposes. Switching between these two different coding functions every sixth channel effectively multiplies or modulates the

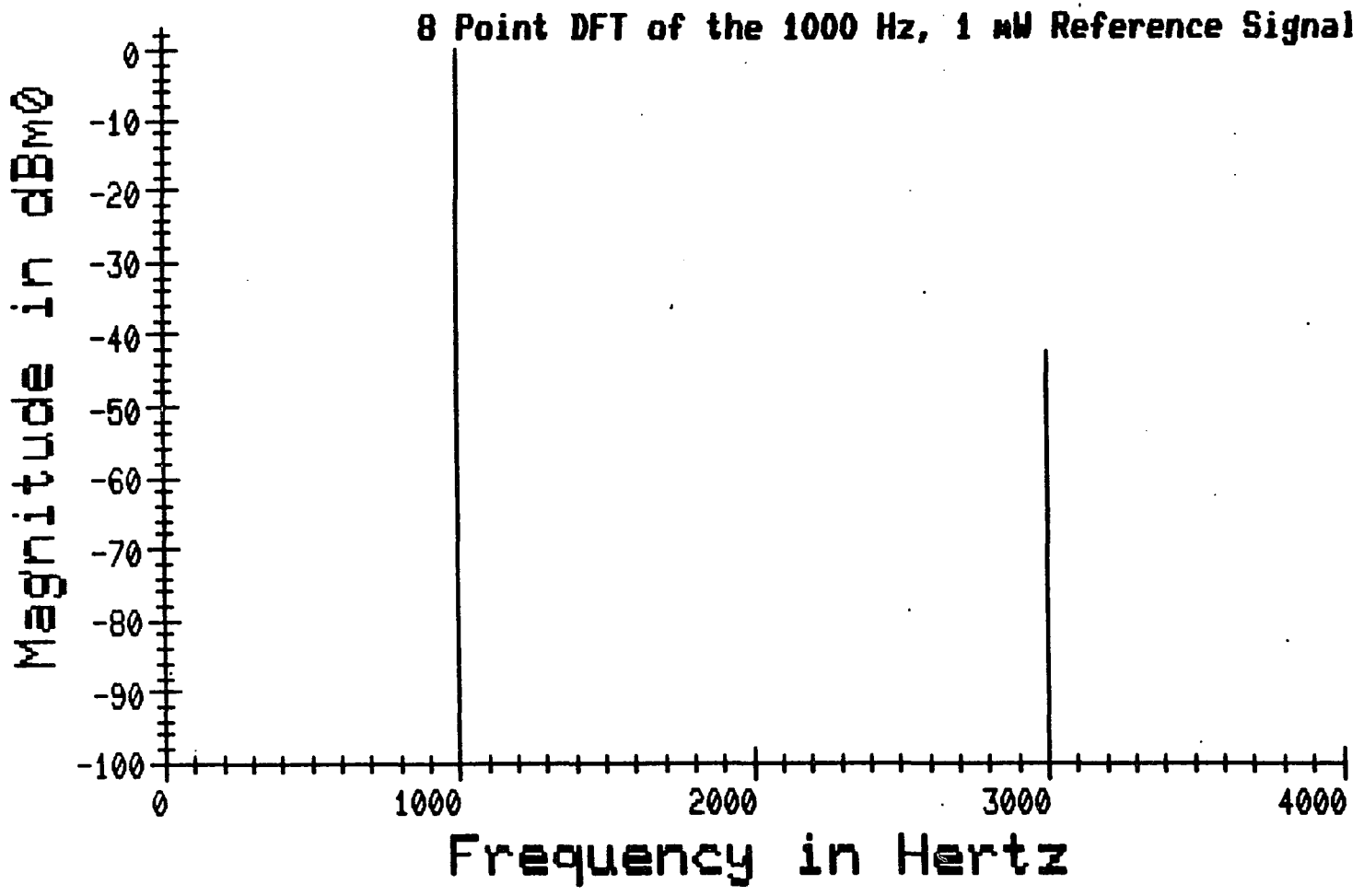
8 Point DFT of the 1000 Hz, 1 mW Reference Signal
Magnitude in dBm0
0
-10
-20
-30
-40
-50
-60
-70
-80
-90
-100
0
1000
2000
3000
4000
Frequency in Hertz

Figure V-9

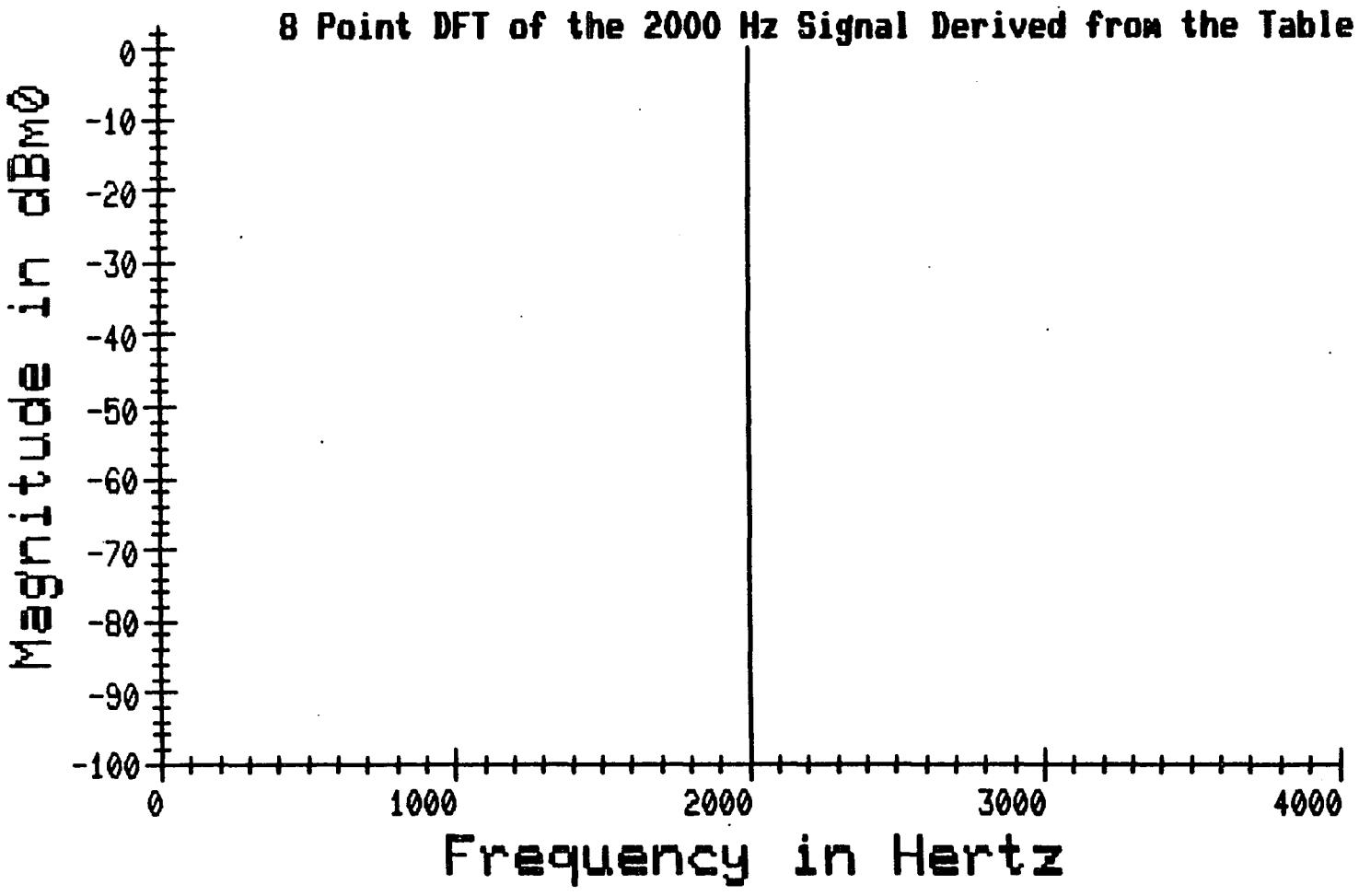
8 Point DFT of the 2000 Hz Signal Derived from the Table
Magnitude in dBm0
0
-10
-20
-30
-40
-50
-60
-70
-80
-90
-100
0
1000
2000
3000
4000
Frequency in Hertz

Figure V-10

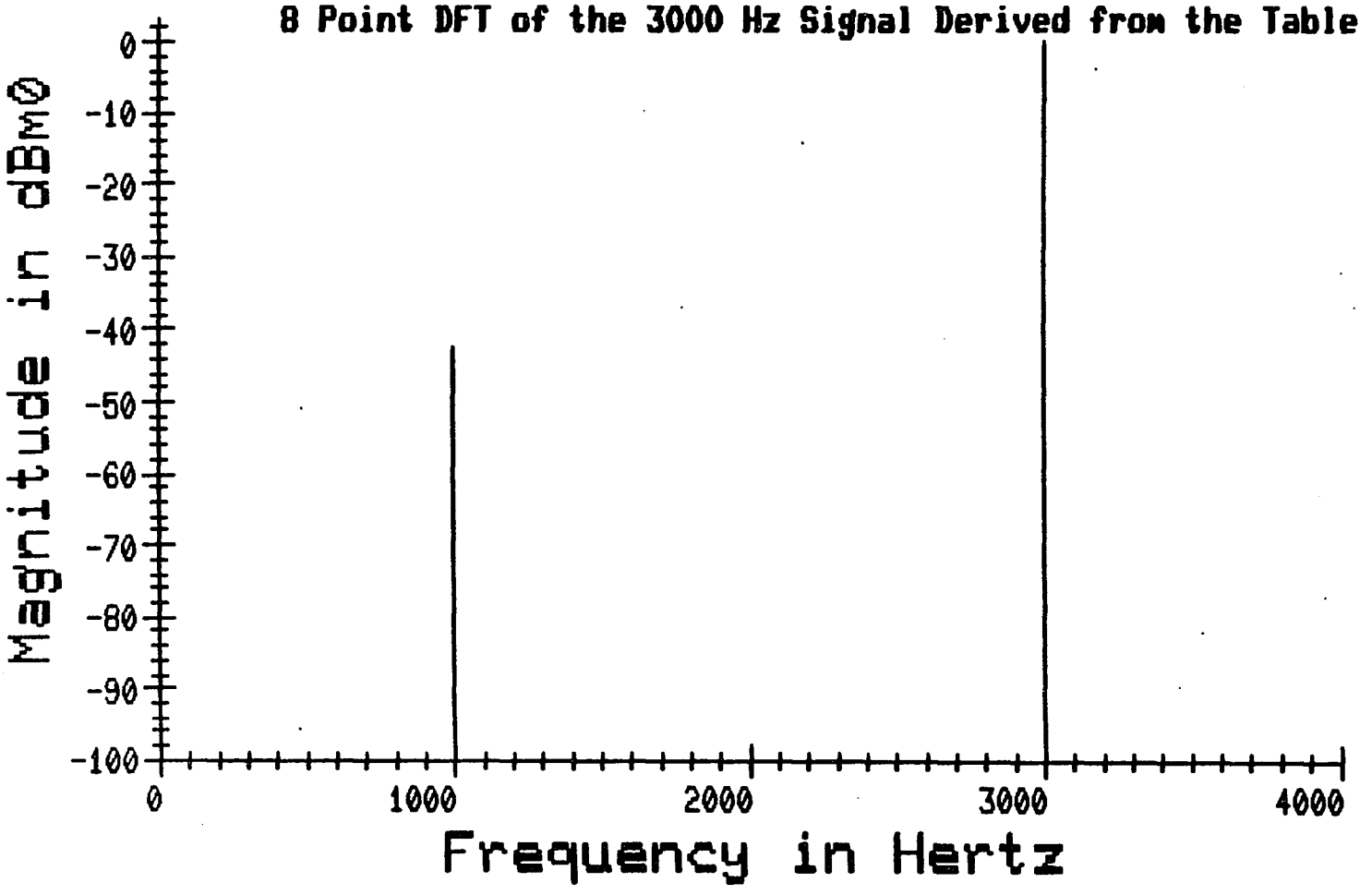
8 Point DFT of the 3000 Hz Signal Derived from the Table
Magnitude in dBm0
0
-10
-20
-30
-40
-50
-60
-70
-80
-90
-100
0
1000
2000
3000
4000
Frequency in Hertz

Figure V-11

transmitted signal by the harmonics of this switching rate of 8000/6 = 1333.333 Hz. Figure V-12 is the DFT of a 1024 point sample of this 1000 Hz reference signal with the inclusion of this signalling frame quantization noise. As noted before, the sinc-shaped spectrum is caused by the actual frequency components in the signal not coinciding with the frequency sample points of the DFT. As before, the application of a window to the data will improve this estimate of the spectrum as shown in Figure V-13. The DFT may be made exact by choosing a sample length which will cause the discrete frequency points in the resulting DFT to coincide with these modulation products. It turns out that the number of points must be chosen so that it is evenly divisible by both the table length and the signalling frame rate. In this case the table length is eight and the signalling frame rate is always six, so the number of points in the sample must be chosen as an integral multiple of 24. The result of transforming a 24 point sample is shown in Figure V-14 and the results obtained by sampling any multiple of 24 points will be identical to these. Note the presence of the fundamental 1000 Hz spike. Modulation products should appear at 1000 Hz plus and minus 1333 Hz, 2667 Hz and 4000 Hz. These generate directly the components at 333 Hz, 2333 Hz, 1667 Hz and 3000 Hz, and the aliasing of the 4333 Hz modulation product results in the 3667 Hz component. All higher order modulation products will be aliased to coincide with these same frequencies.

The quantization noise observed in this example is quite atypical. With a more random input, such as a voice signal, the quantization noise would generate many more frequency components. If the sampled values of the input

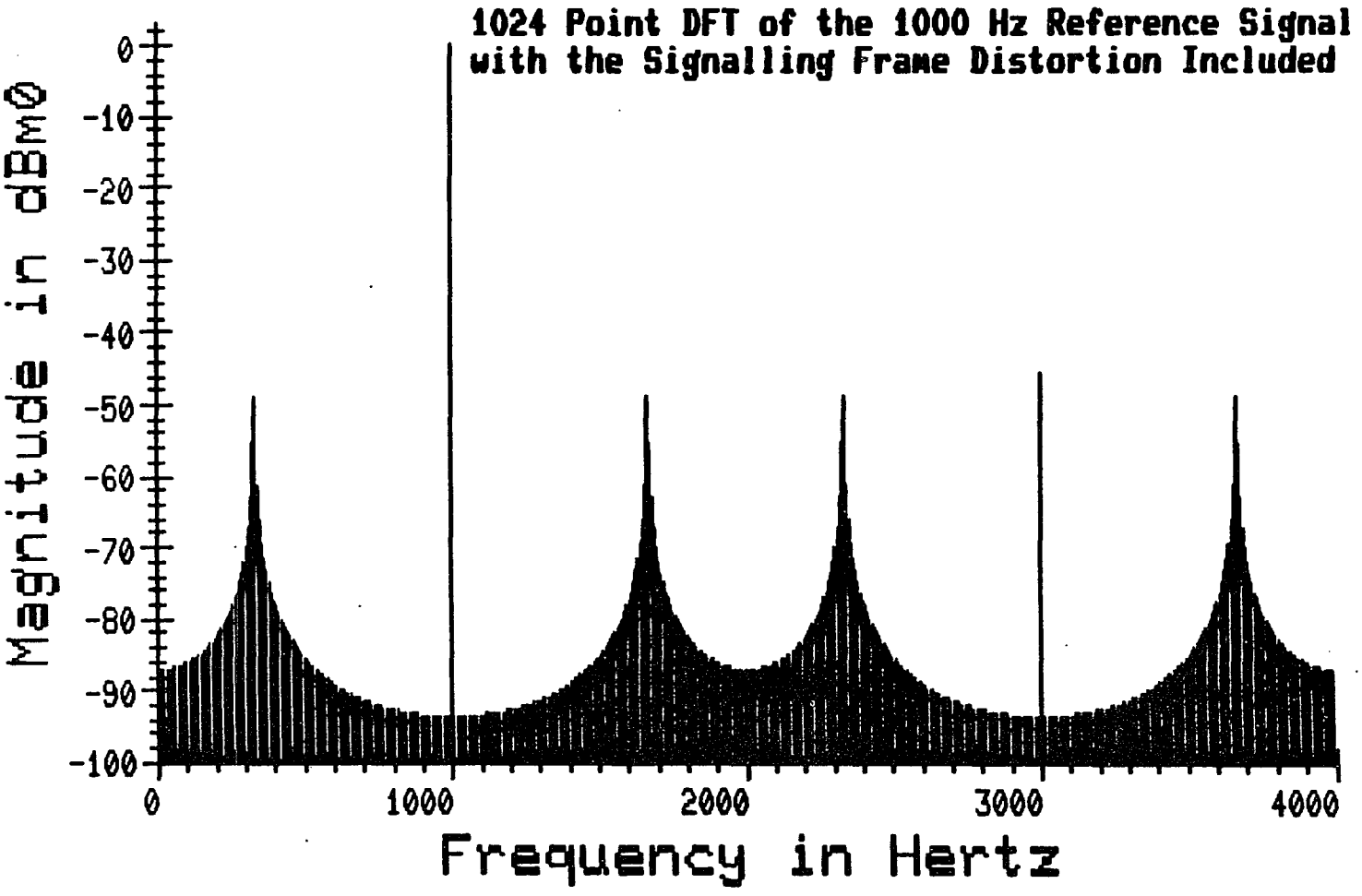
1024 Point DFT of the 1000 Hz Reference Signal
with the Signalling Frame Distortion Included
Magnitude in dBm0
0
-10
-20
-30
-40
-50
-60
-70
-80
-90
-100
0
1000
2000
3000
4000
Frequency in Hertz

Figure V-12

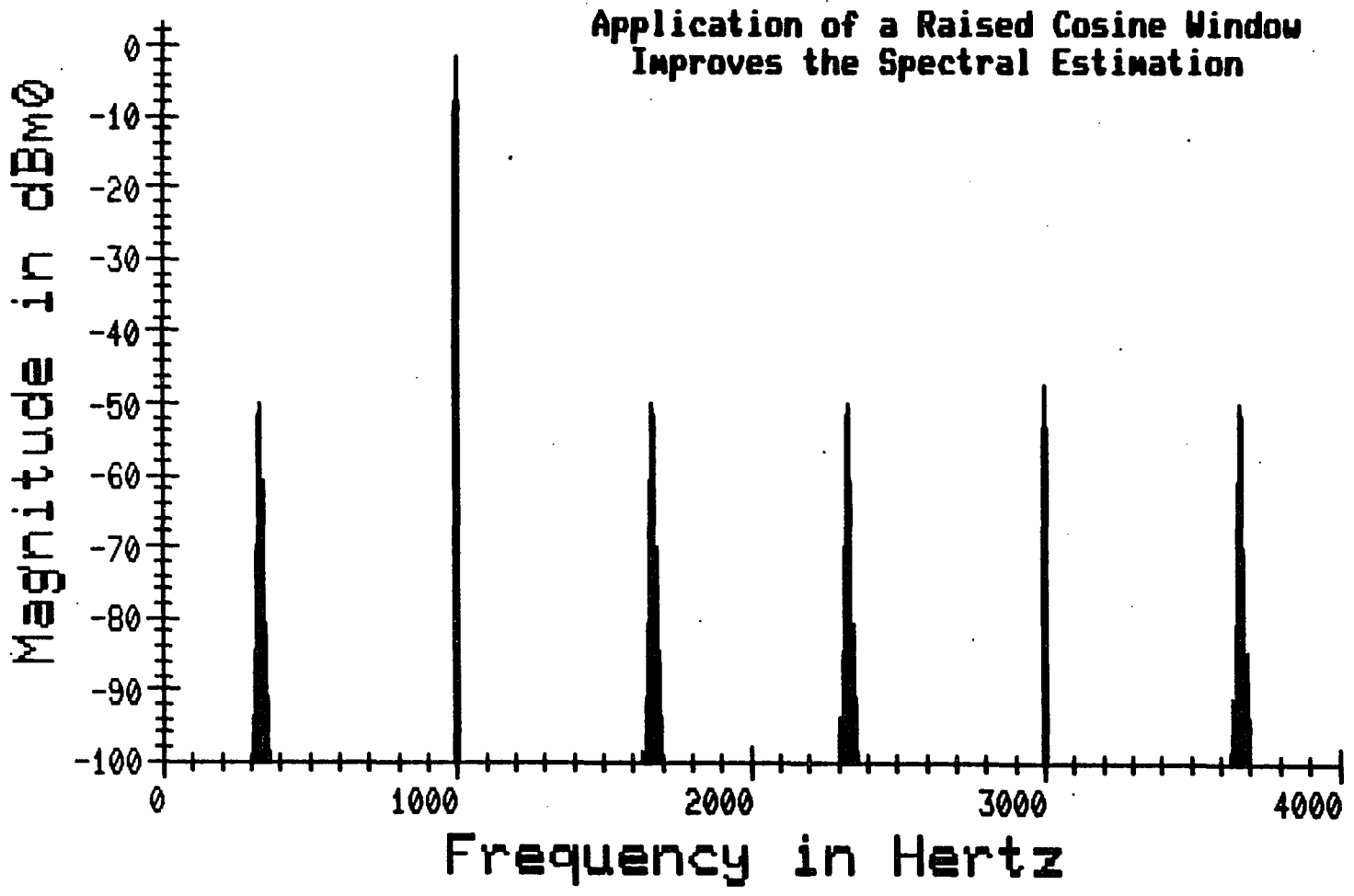
Application of a Raised Cosine Window
Improves the Spectral Estimation
Magnitude in dBm0
0
-10
-20
-30
-40
-50
-60
-70
-80
-90
-100
0
1000
2000
3000
4000
Frequency in Hertz

Figure V-13

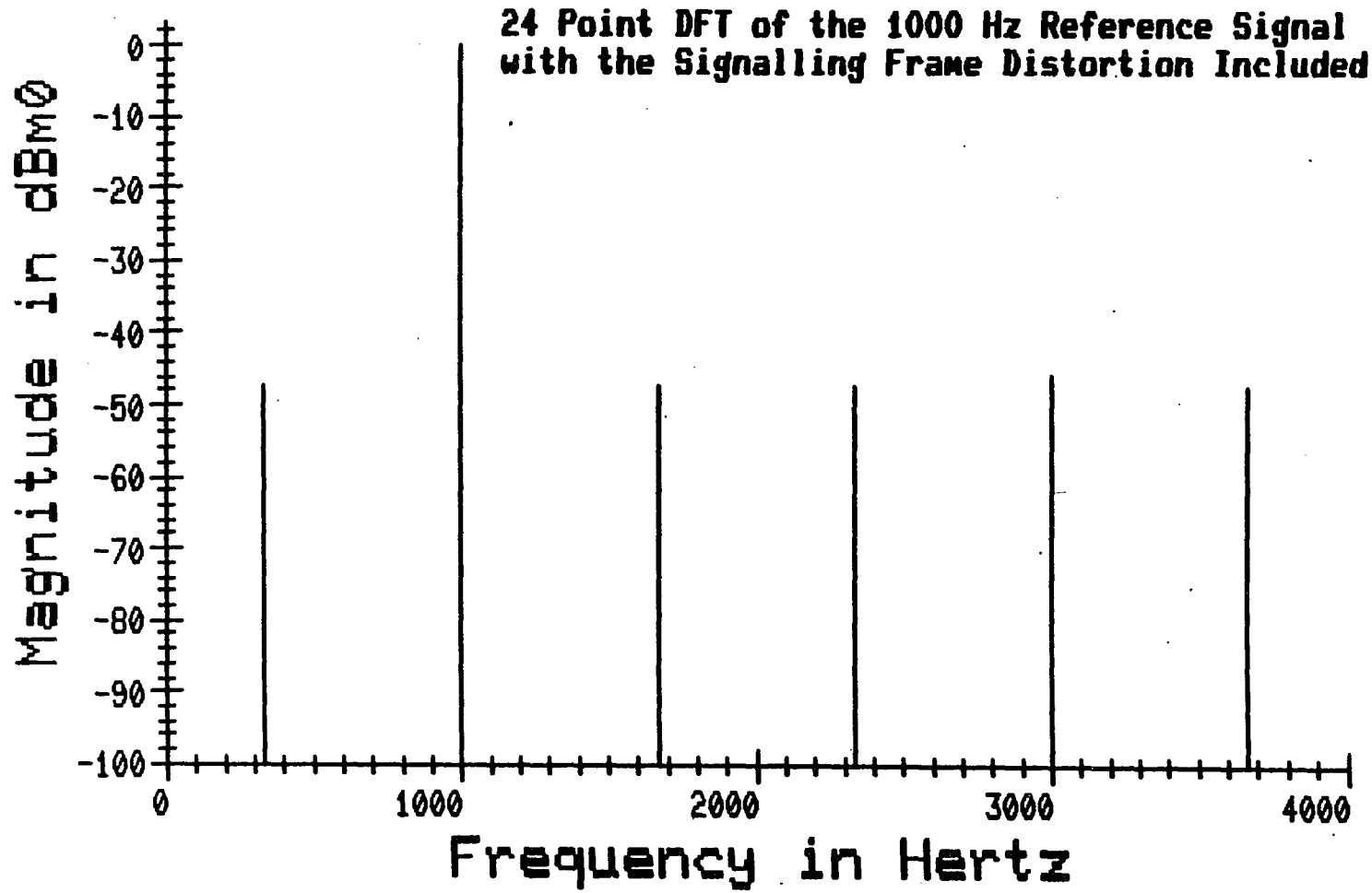
24 Point DFT of the 1000 Hz Reference Signal
with the Signalling Frame Distortion Included
Magnitude in dBm0
0
-10
-20
-30
-40
-50
-60
-70
-80
-90
-100
0
1000
2000
3000
4000
Frequency in Hertz

Figure V-14

signal were distributed evenly over the range associated with only one quantization level, then since the value assigned to that quantization level is in the middle of the range, the magnitude of the produced quantization errors would vary from zero to one half of the quantization step with an average equal to one quarter of this quantizing range. If the sampled points before quantization were randomly and evenly distributed over this range, then the resulting quantization noise would be white with a flat distribution of amplitudes. The idea of getting a signal which stays within one quantization range is rather absurd; however, if the signal covered two or more levels, the average error would still be equal to one quarter of the distance between adjacent quantization levels. In fact, almost any signal that gets sampled throughout a large number of quantization levels will result in quantization error with these white noise characteristics.

V-B The 257 Point Sampled Sine Wave

The 1000 Hz reference signal considered above is a very poor signal to use in testing quantization distortion. In generating the signal only four different levels are used, and since the magnitudes of the positive and negative values are the same, there are actually only two different magnitudes of the quantization errors generated. This certainly does not give any estimation of the typical average quantization noise which may be expected. Instead, a test signal is needed which is sampled at many different quantization levels. Because of the increased quantization errors induced at the higher levels by the compression characteristic, it is more important to get a good sampling

of the higher quantization levels used by the signal. This may be accomplished quite nicely with a sine wave signal, since about 46 percent of its samples will lie in the upper 25 percent of its range and over 66 percent will lie in the upper 50 percent of its range. The next problem is to insure that a sufficient number of these points are unique; that is, not a repetition of the same few quantization levels as was experienced with the 1000 Hz signal.

Assume for a moment that one cycle of a sine wave at 0 dBm0 is sampled at 1024 evenly spaced points and tabularized. If points are selected from the table at 8000 samples per second, then different frequencies may be generated by skipping various numbers of points in the table. Of course, an overflow, for example, of three points beyond the end of the table must be taken from the third point into the table from the beginning. In other words, indexing into the table must proceed modulo 1024. Now, if a frequency of 1000 Hz is desired, every 128th point must be taken from the table. This particular choice, however, would result in taking the same eight points over and over again, as occurred previously.

$$(128*9) \text{ modulo } 1024 = 128$$

If an increment is chosen which is mutually prime to 1024, such as 129, then as the resulting 1007.8125 Hz signal is generated, every one of the 1024 encoded points will be used and a reasonable distribution of quantization errors will result. Note, however, that since the number of points in the table, 1024, is divisible by 4, each encoded magnitude and hence each quantization error will occur 4 times, once in each quadrant of the table. This 1024 point table is,

therefore, not a very good choice. First, there are increments which should be avoided; those which are not mutually prime to 1024, and that accounts for one half of the possible increments. Secondly, only one quarter of the tabulated values generate unique quantization errors because 1024 is divisible by 4.

This leads to the conclusion that the an excellent table length should be a prime number. Then, no matter what increment is chosen, it is guaranteed to be mutually prime to the table modulus and every point in the table will be used. Also, since the table modulus will not be divisible by 2 or 4, each tabulated point will be unique. This is not to say that no two points appearing in the table will have the same value, but two points of the same value will have experienced different quantization errors.

There are 256 possible codes which may be generated in the 8 bits available in a given channel's time slot on a T1 line. Therefore, choosing a number in this range should generate a sufficiently large number of samples at the higher quantization levels. From the previous chapter, it was demonstrated that the transform of a prime number of points may be performed by doing a fast convolution with one less than that number of points. The prime number 257 is an ideal choice, since one less than this is 256, which is a power of 2 and can be efficiently transformed. The 257 point table is generated by using a FORTRAN program to calculate the values of $x(n) = A \sin[2 \pi n / 257]$, where A is the peak value of the desired sine wave referenced to 5663 for a level of 0 dBm0. Various frequencies may be generated in increments of 8000/257 = 31.1284 Hz by skipping various numbers of points in the table. Figure V-15, for example,

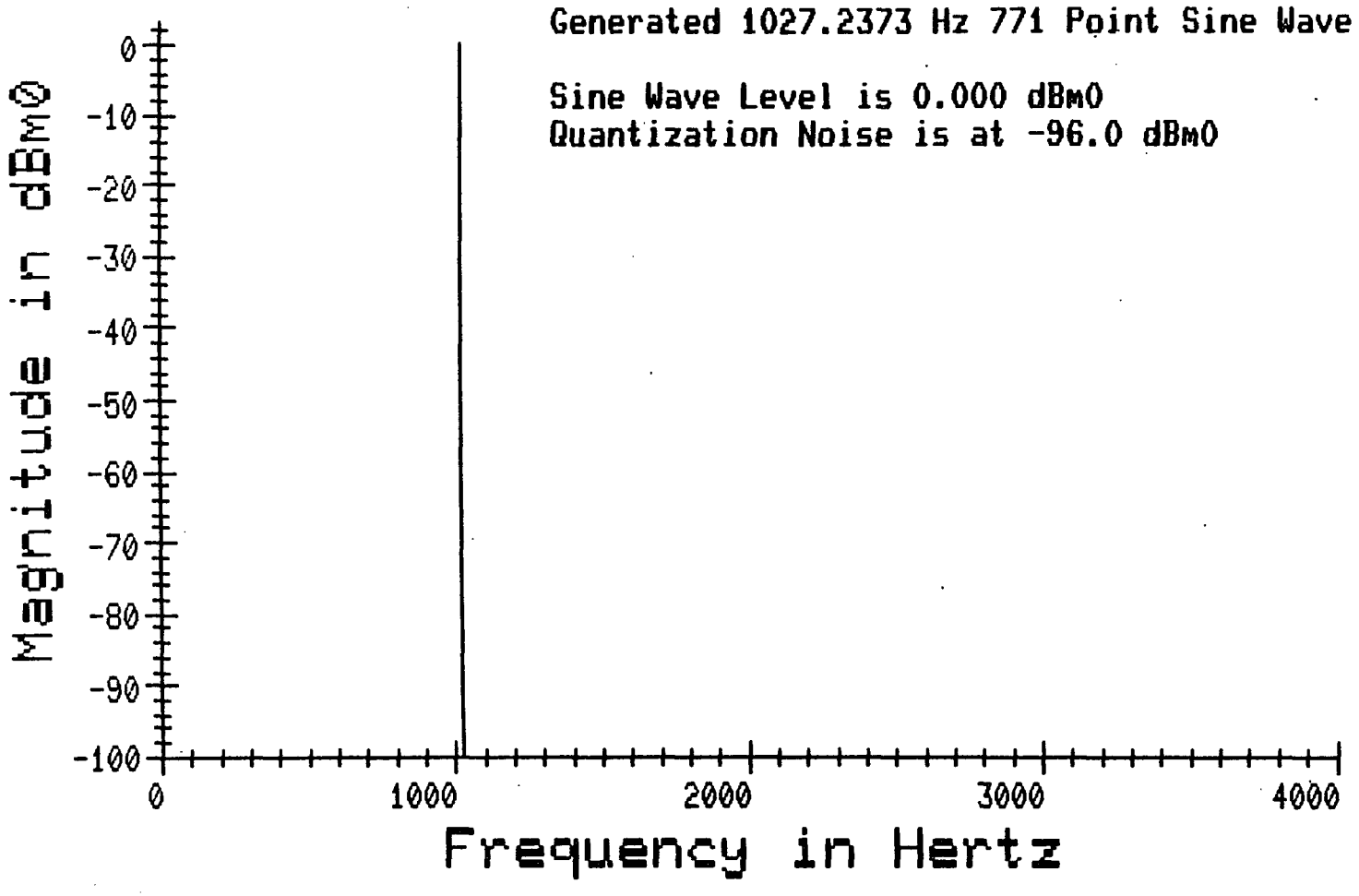
Generated 1027.2373 Hz 771 Point Sine Wave
Sine Wave Level is 0.000 dBm0
Quantization Noise is at -96.0 dBm0
Magnitude in dBm0
0
-10
-20
-30
-40
-50
-60
-70
-80
-90
-100
0
1000
2000
3000
4000
Frequency in Hertz

Figure V-15

shows the DFT of sine wave at 1027 Hz generated by transmitting every 33rd point from this table. This signal does not contain any of the added distortion generated by the signalling frames. Figure V-16 shows the effects of including this additional quantization distortion by truncating every sixth sample to only 7 bits. As expected, the frequency components of the noise are evenly distributed throughout the entire spectrum with a random distribution of amplitudes at various frequencies. Figure V-17 carries this one step further by showing the spectrum of the signal after transmission through an actual voice channel. The resulting mean and variance of the spectral components of the noise are modified as a result of the filtering action of the voice channel. Note that in each of the last two figures samples of 1542 points were taken. This is so that the number of points is divisible by both the table length of 257 and the signalling frame rate of 6. Even though truncation was performed in order to generate the signalling frame code values, the end result is the same as if rounding had been performed, because the decoded analog levels generated by these 7 bit codes are modified to lie at the midpoints of the new quantization ranges.

V-C Hardware Implementation

The hardware described here is intended to provide maximum flexiblilty to be used in this development process. Further simplications which may be made to the hardware for restricted applications are mentioned at the end of this section.

Figure V-18 shows the timing circuitry required to transmit the tabulated 8 bit words into the digital

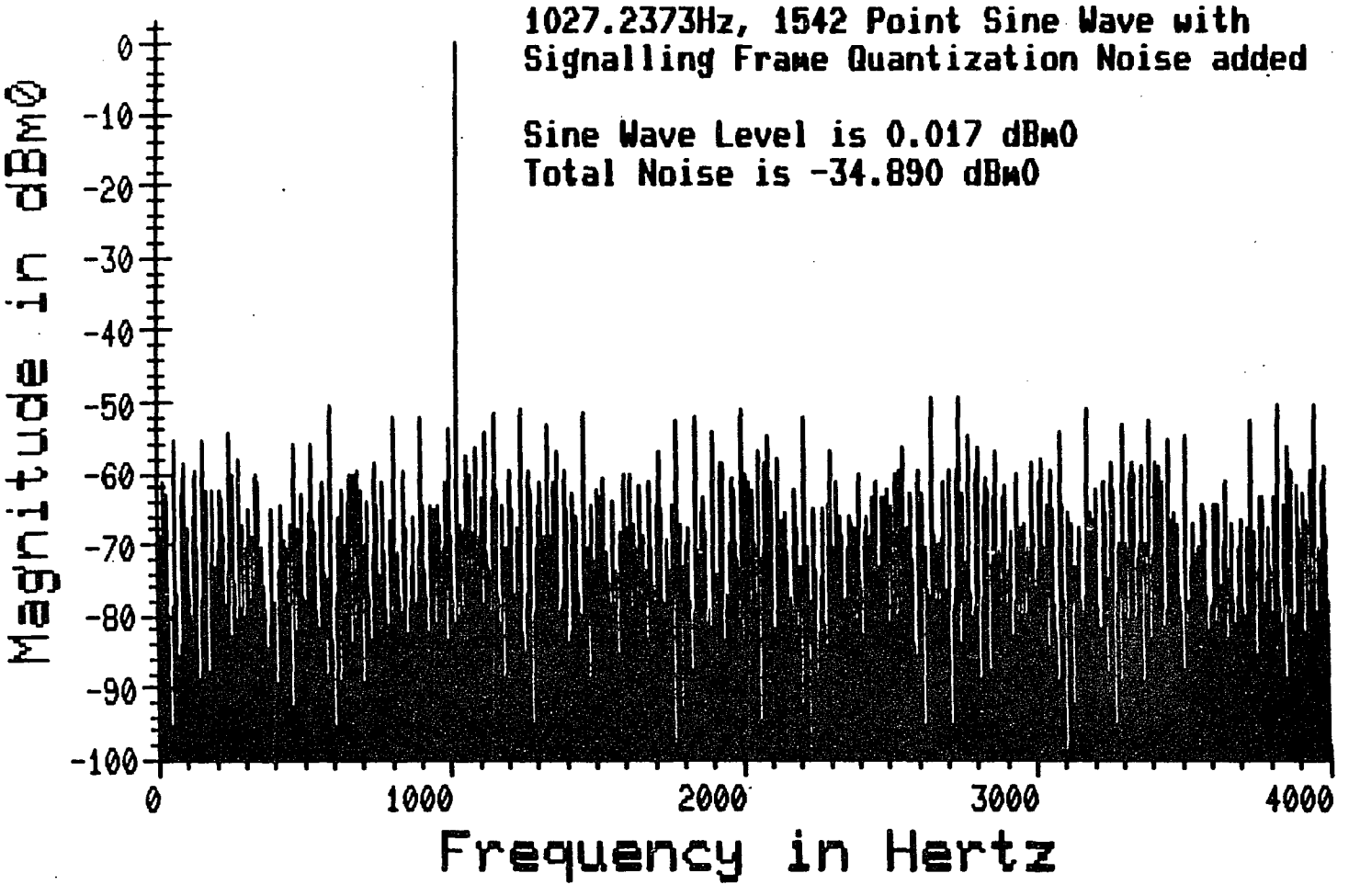
1027.2373Hz, 1542 Point Sine Wave with
Signalling Frame Quantization Noise added
Sine Wave Level is 0.017 dBm0
Total Noise is -34.890 dBm0
Magnitude in dBm0
0
-10
-20
-30
-40
-50
-60
-70
-80
-90
-100
0
1000
2000
3000
4000
Frequency in Hertz

Figure V-16

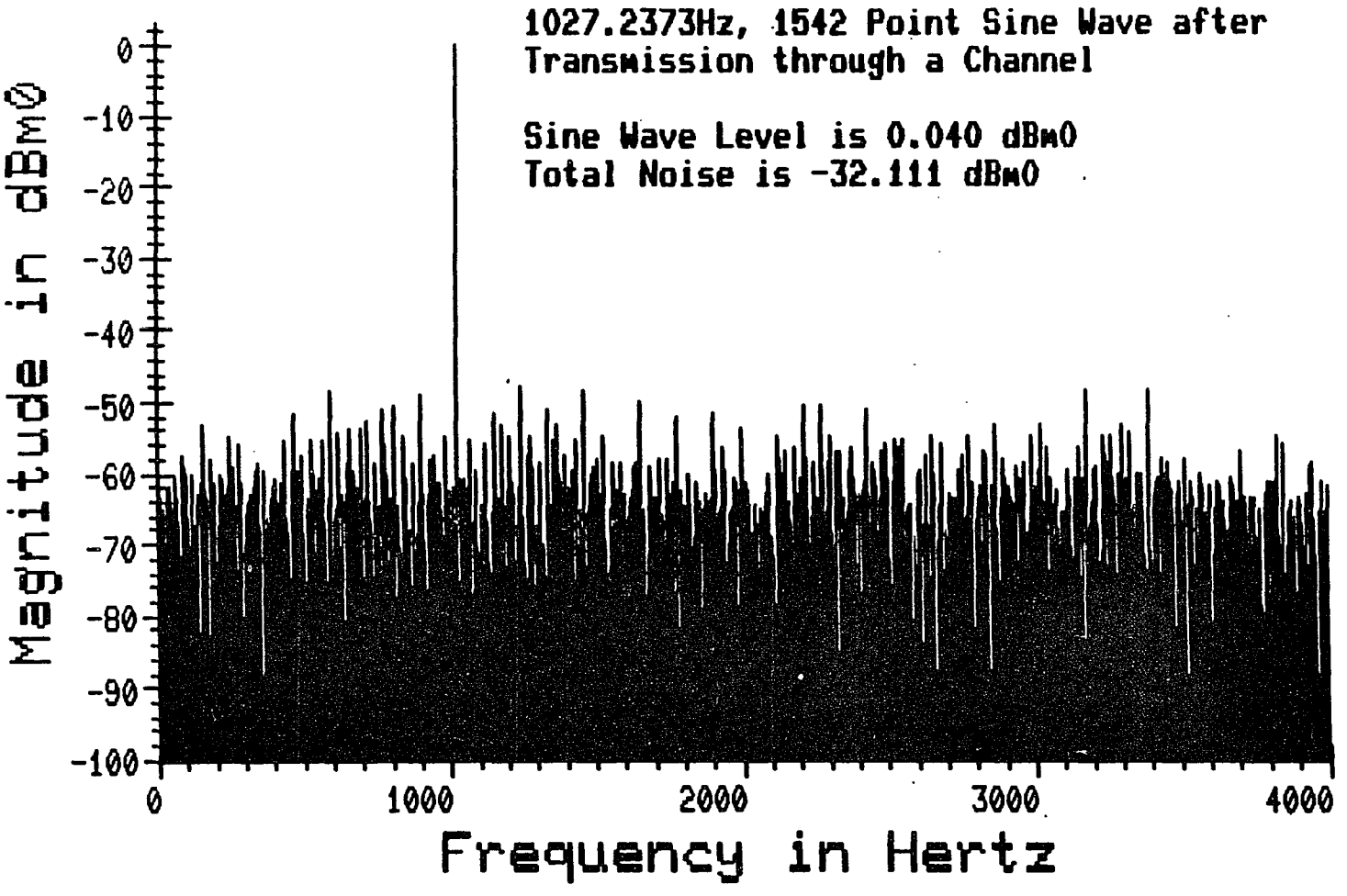
1027.2373Hz, 1542 Point Sine Wave after
Transmission through a Channel
Sine Wave Level is 0.040 dBm0
Total Noise is -32.111 dBm0
Magnitude in dBm0
0
-10
-20
-30
-40
-50
-60
-70
-80
-90
-100
0
1000
2000
3000
4000
Frequency in Hertz

Figure V-17

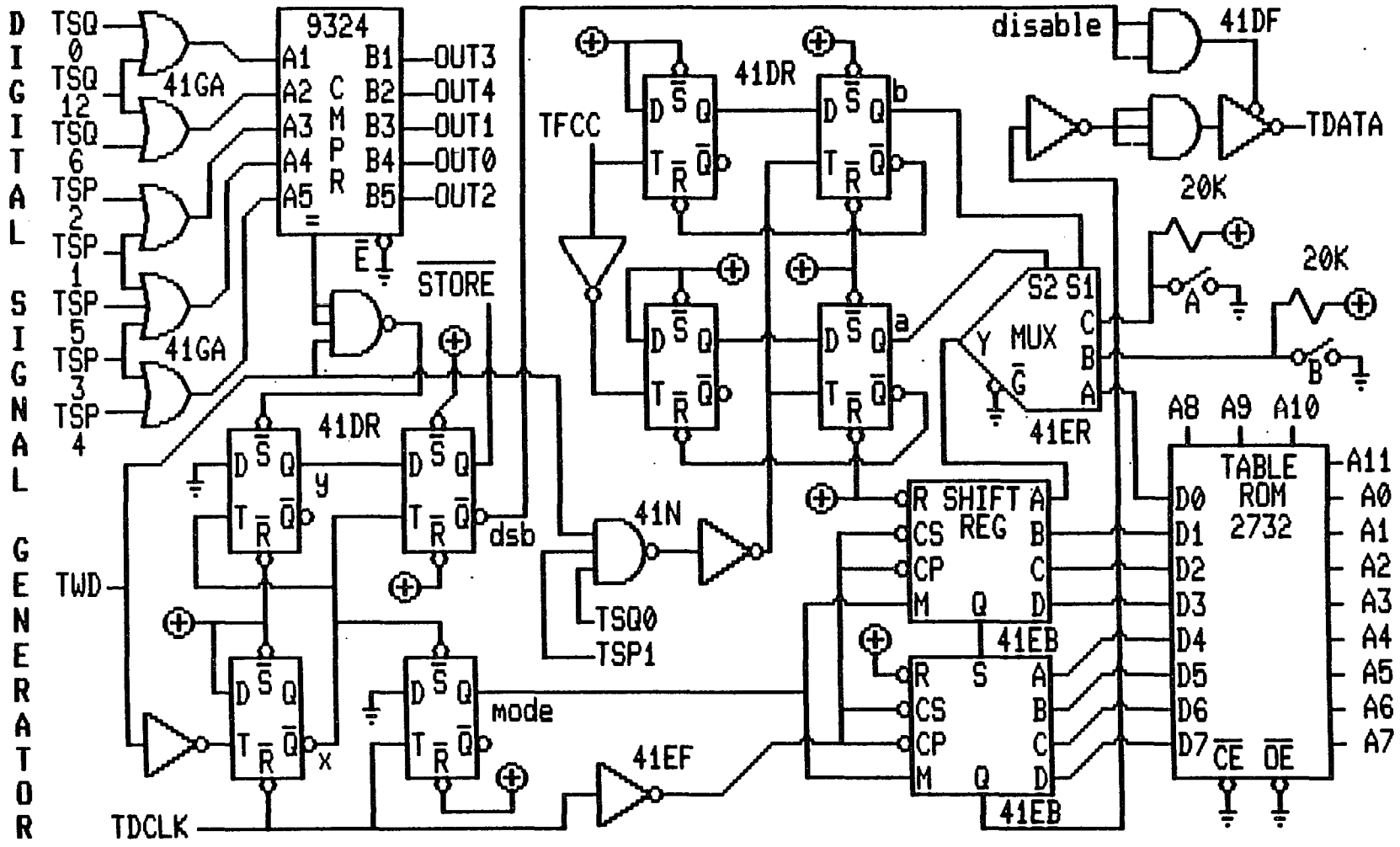
DIGITAL SIGNAL GENERATOR
TSQ 0
TSQ 12
TSQ 6
TSP 2
TSP 1
TSP 5
TSP 3
TSP 4
41GA
41GA
9324
A1 B1 OUT3
A2 C B2 OUT4
A3 M B3 OUT1
A4 P B4 OUT0
A5 R B5 OUT2
=
E
STORE
41DR
41DR
TFCC
disable
41DF
TDATA
20K
20K
A
B
S2 S1
Y MUX C
G B
A
41ER
A8 A9 A10
TABLE ROM 2732
D0 D1 D2 D3 D4 D5 D6 D7
A11 A0 A1 A2 A3 A4 A5 A6 A7
CE OE
R SHIFT A
CS REG B
CP C
M Q D
41EB
R S A
CS B
CP C
M Q D
41EB
41N
TSQ0
TSP1
41EF
TWD
TDCLK
dsb
mode
x
y
a
b

Figure V-18

interface provided in a D4 channel unit. The OR gates in the upper left hand corner of the diagram convert the standard D4 channel timing signals shown in Figure V-19 into a more concise form so that fewer bits are required to control the channel number. The resulting five signals which are fed to the comparator are shown in Figure V-20. Note that a minimum of five bits are required to uniquely specify one of twenty four channels. The codes required to select an appropriate channel are slightly cryptic as was seen in Table III-4 of Chapter 3. This encoding is left up to the computer software for the sake of keeping the hardware as simple as possible. The four flip flops at the lower left provide the timing signals which control the loading of the shift register from the table and enable the tri-state output to the TDATA bus. Figure V-21 illustrates the relationships between the two timing signals, TDCLK and TWD, supplied by the D4 hardware, and the outputs of these four flip- flops. The tabulated signal is stored in the Read-Only Memory (ROM) in the lower right hand corner of Figure V-18 and the 8 bit data is presented in parallel form to the shift registers where it is loaded and then shifted out using the TDCLK signal. The four flip-flops in the center keep track of the framing, and whenever either an A or B signalling frame occurs the appropriate multiplexer input is enabled, causing the least significant bit in the outgoing data to be replaced with the signalling information. Figure V-22 gives the timing relationships between the TFCC signal ,the channel number one sampling window, which is derived from TWD ,TSQ0 and TSP1, and the outputs of the various flip-flops. The signalling states are shown here as being controlled by switches, but these could easily be driven with a TTL level

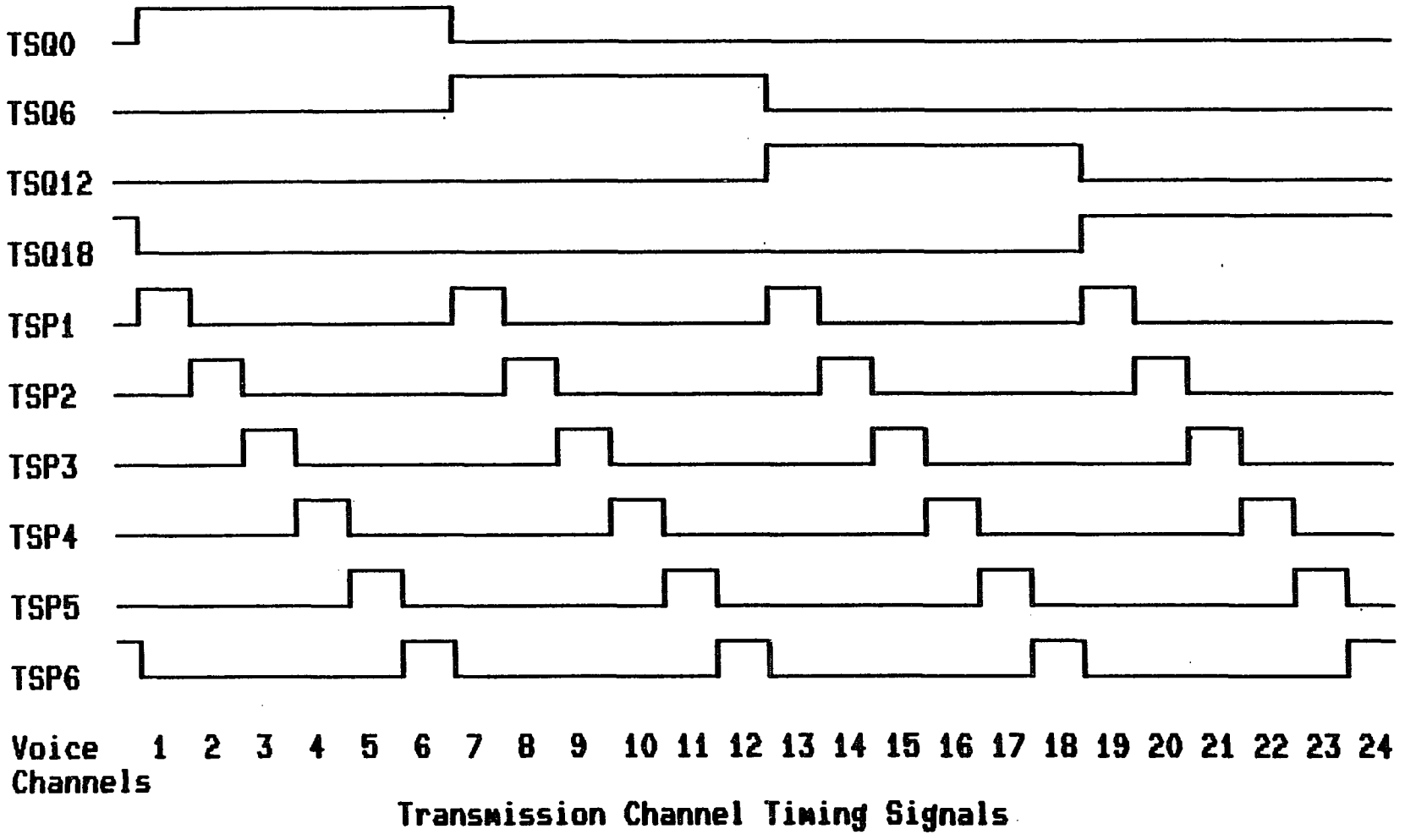
TSQ0
TSQ6
TSQ12
TSQ18
TSP1
TSP2
TSP3
TSP4
TSP5
TSP6
Voice Channels 1 2 3 4 5 6 7 8 9 10 11 12 13 14 15 16 17 18 19 20 21 22 23 24
Transmission Channel Timing Signals

Figure V-19

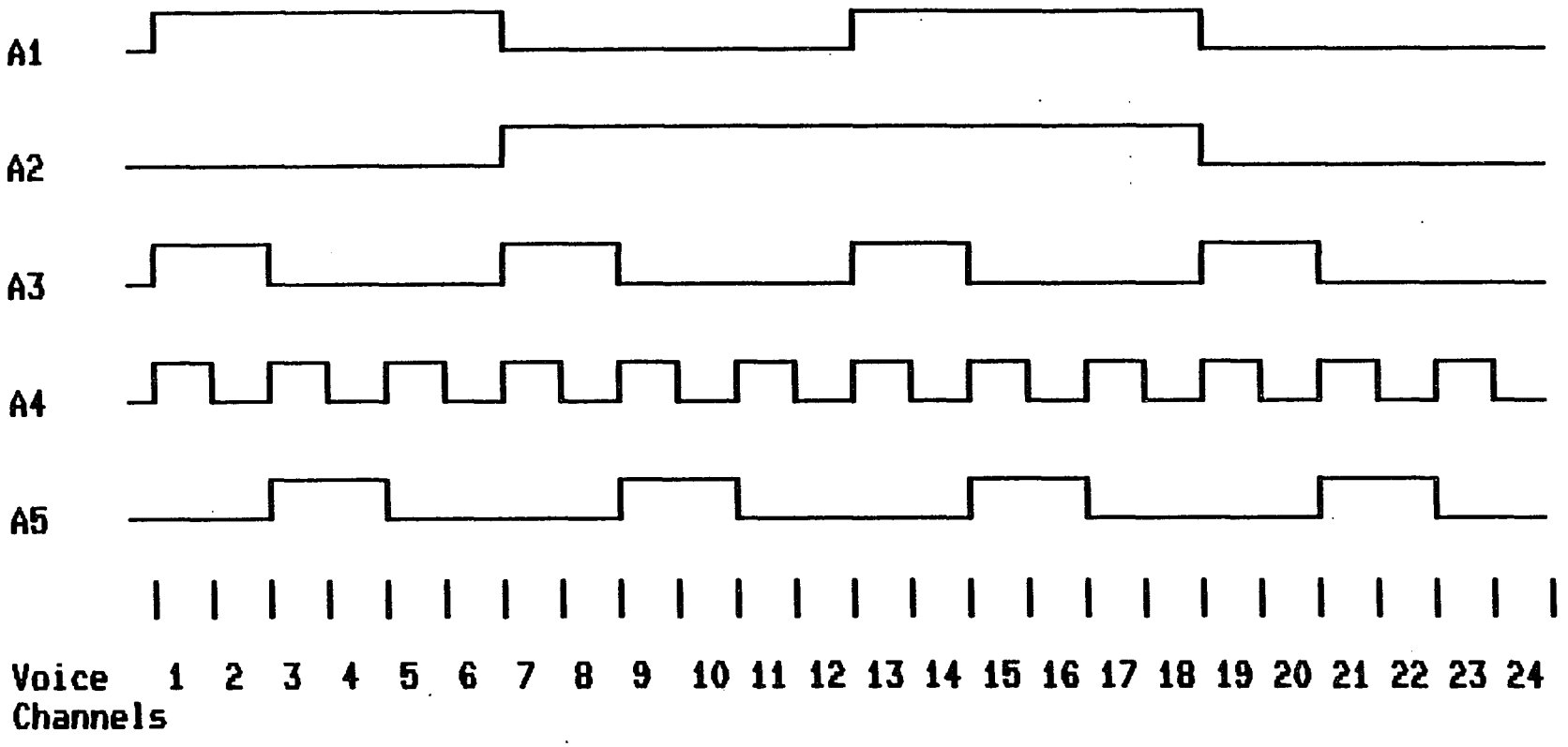

Modified Timing Signals at the Input to the Comparator

Figure V-20

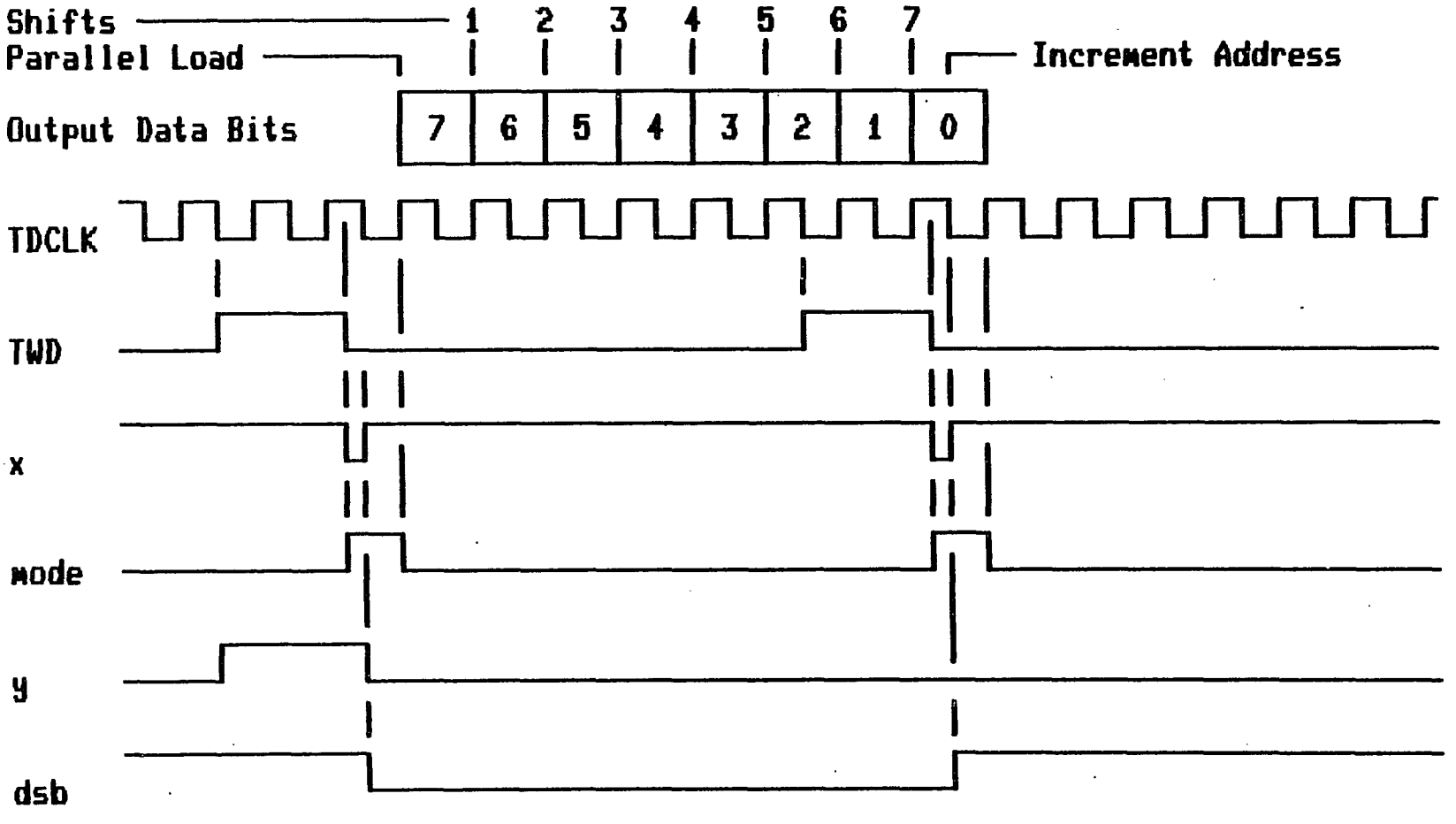

Digital Signal Generator Timing Diagram

Figure V-21

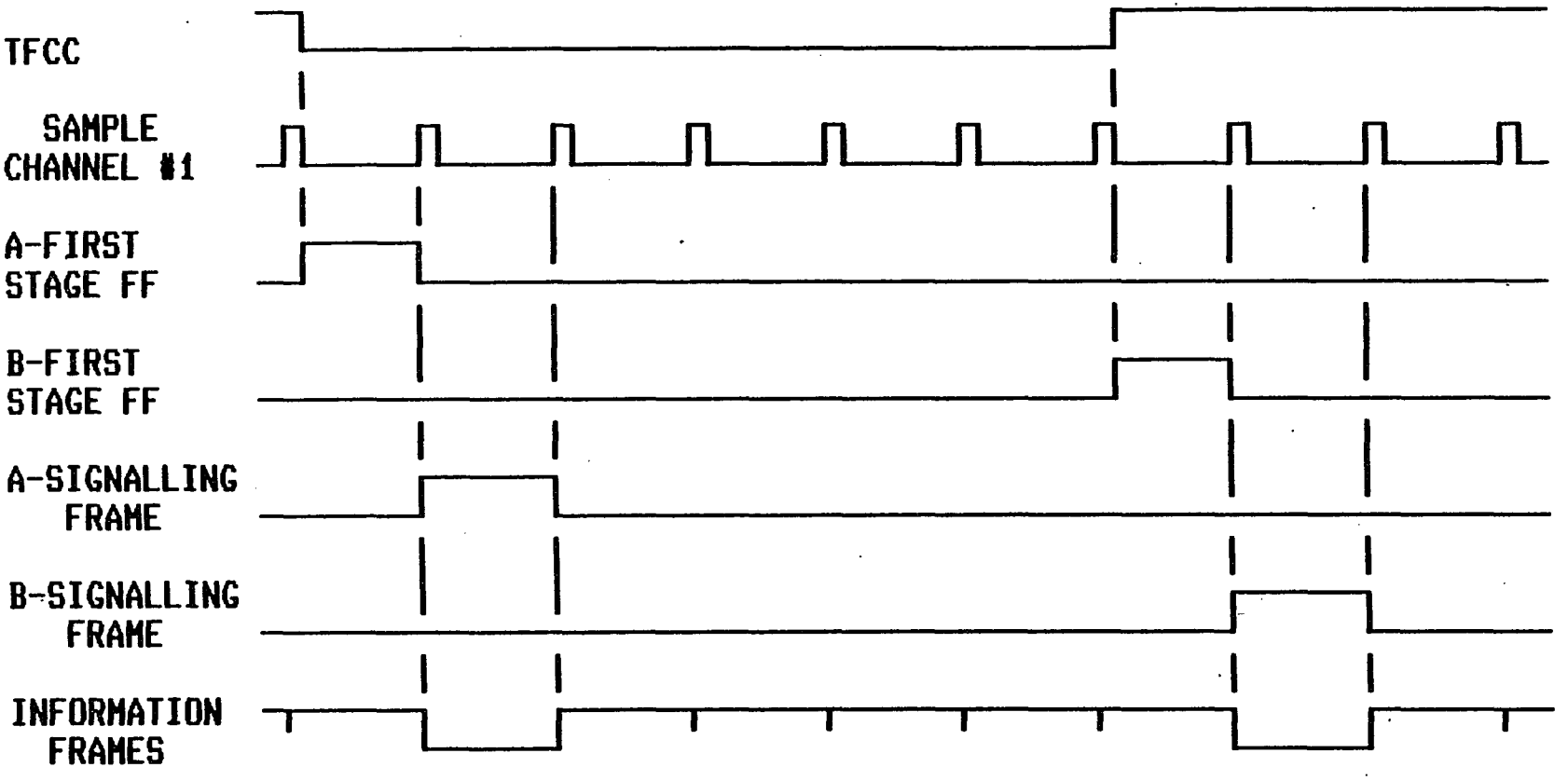

Signalling Frame Timing Diagram

Figure V-22

from the computer interface.

The address inputs to the ROM table are controlled by the modulo N adder shown in Figure V-23. Various numbers of data items may be skipped in cycling through the table by controlling the increment which is added to the ROM address, thus generating sine waves of different frequencies. The inputs I0 through I11, at the bottom, represent this increment. When an overflow occurs beyond the number of tabular values N, the ROM addresses A0 through A11 must be calculated modulo N so that a valid table entry will always be read. This is done by feeding the two's complement of the modulus N into the M0 through M11 inputs. Each time the increment is added to the last address the modulus gets subtracted from the resulting sum. If the difference is positive, then an overflow occurred and this difference is stored, instead of the direct result of the addition, as the next address. The STORE signal is used to clock the next table address into the output of the modulo N adder. The modulus is shown here as being provided by switches; however, these may be replaced by direct computer control if that is desired.

For added flexibility, the ROM memory containing the tabulated signal has been replaced by a Random Access Memory (RAM) so that various signals may be easily stored in RAM and tested prior to storage into the Erasable, Programmable, Read-Only Memory (EPROM) for continuous use. This EPROM emulator, shown in Figures V-24 and V-25, is designed to be a direct substitute for a 2732, 4K by 8 bit EPROM and, therefore, has many applications beyond this specific one. Data is stored into the RAM through a DRV11-J, bidirectional interface which has exclusive control of the write function.

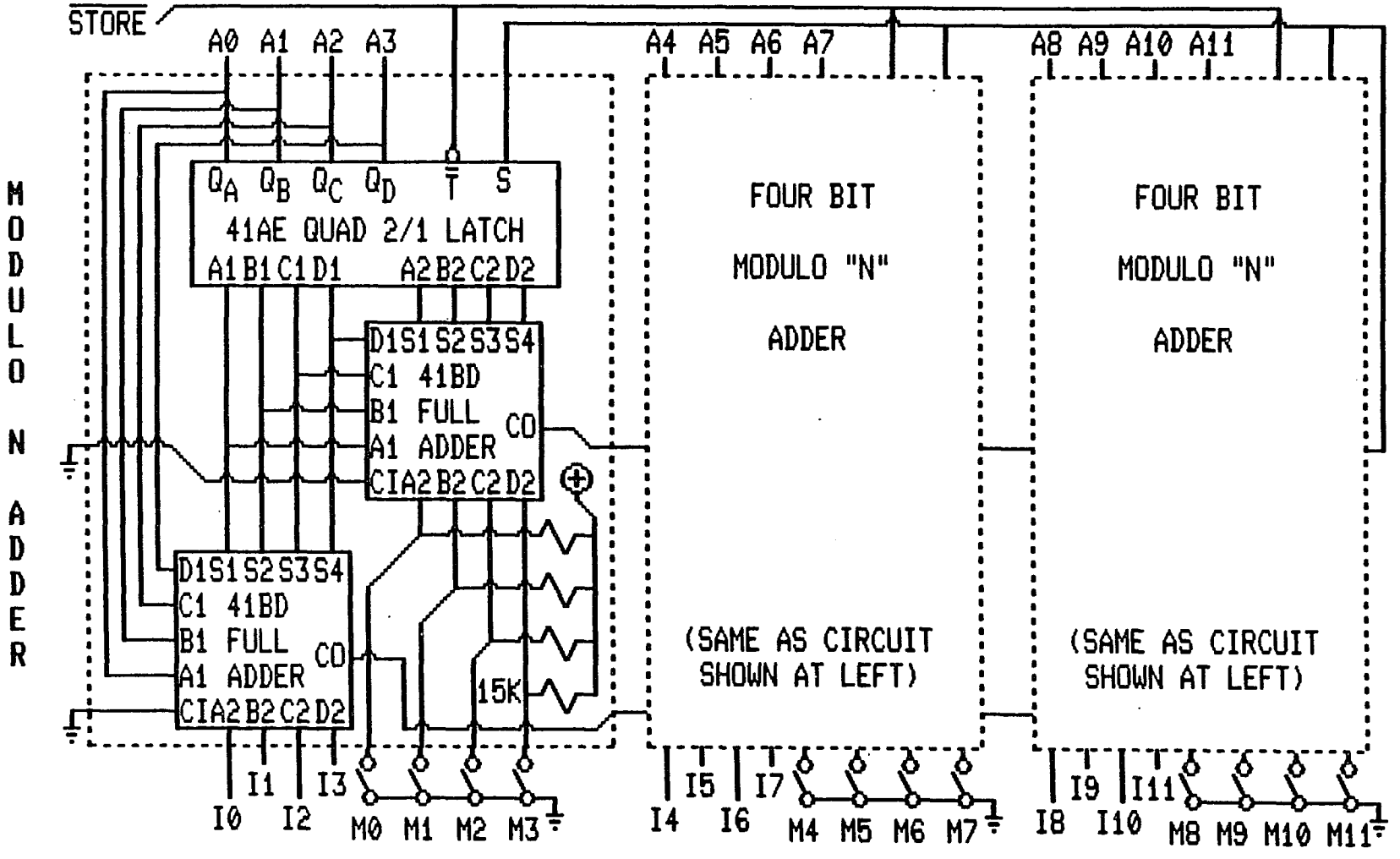
STORE
A0 A1 A2 A3
A4 A5 A6 A7
A8 A9 A10 A11
MODULO N ADDER
QA QB QC QD T̄ S
41AE QUAD 2/1 LATCH
A1 B1 C1 D1 A2 B2 C2 D2
D1 S1 S2 S3 S4
C1 41BD
B1 FULL
A1 ADDER
CI A2 B2 C2 D2
CO
15K
FOUR BIT
MODULO "N"
ADDER
(SAME AS CIRCUIT SHOWN AT LEFT)
(SAME AS CIRCUIT SHOWN AT LEFT)
I0 I1 I2 I3 M0 M1 M2 M3
I4 I5 I6 I7 M4 M5 M6 M7
I8 I9 I10 I11 M8 M9 M10 M11

Figure V-23

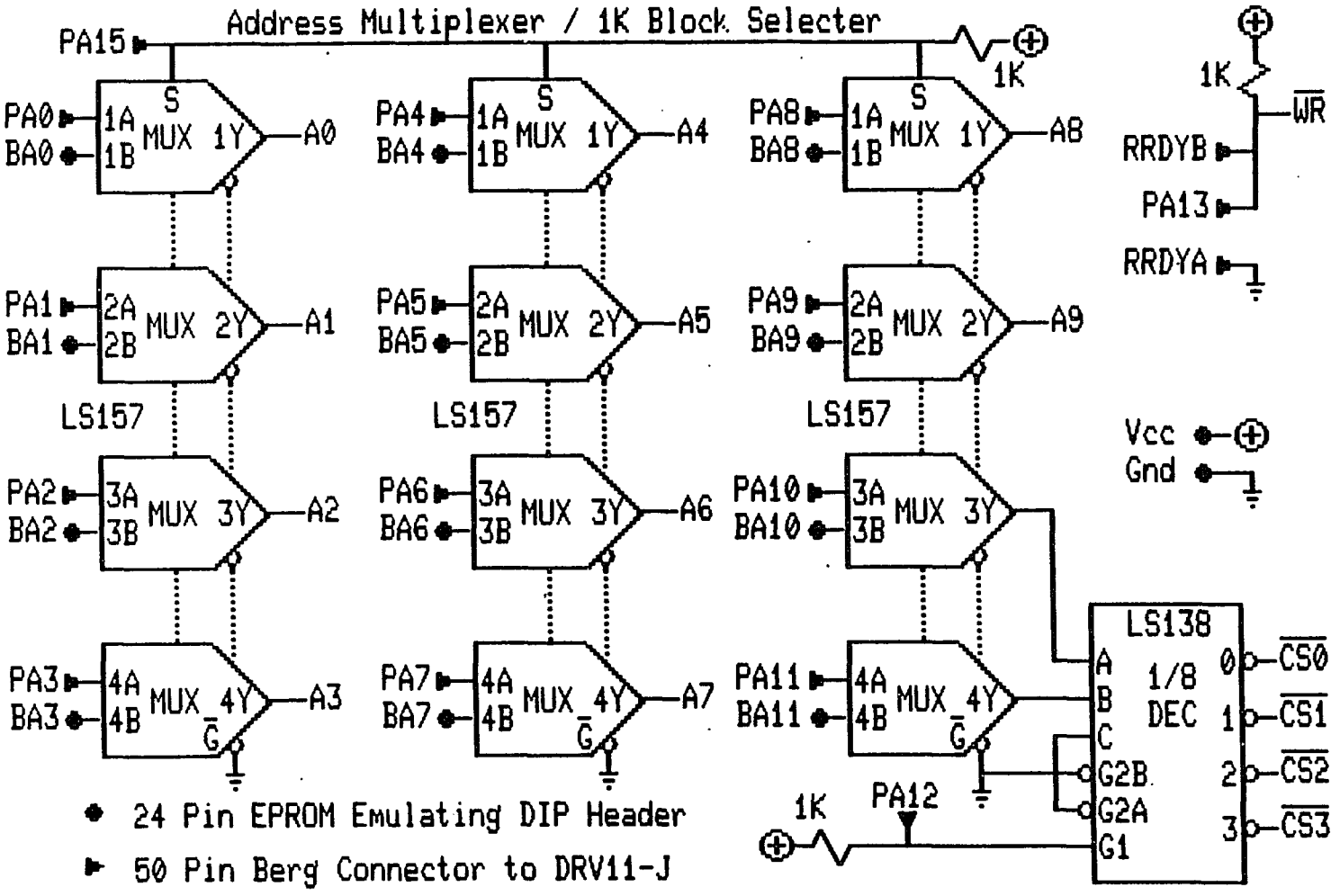
Address Multiplexer / 1K Block Selecter
PA15
1K
1K
WR
RRDYB
PA13
RRDYA
PA0
BA0
PA4
BA4
PA8
BA8
PA1
BA1
PA5
BA5
PA9
BA9
LS157
LS157
LS157
PA2
BA2
PA6
BA6
PA10
BA10
PA3
BA3
PA7
BA7
PA11
BA11
A0
A4
A8
A1
A5
A9
A2
A6
A3
A7
MUX
Vcc
Gnd
LS138
1/8 DEC
CS0
CS1
CS2
CS3
PA12
1K
24 Pin EPROM Emulating DIP Header
50 Pin Berg Connector to DRV11-J

Figure V-24

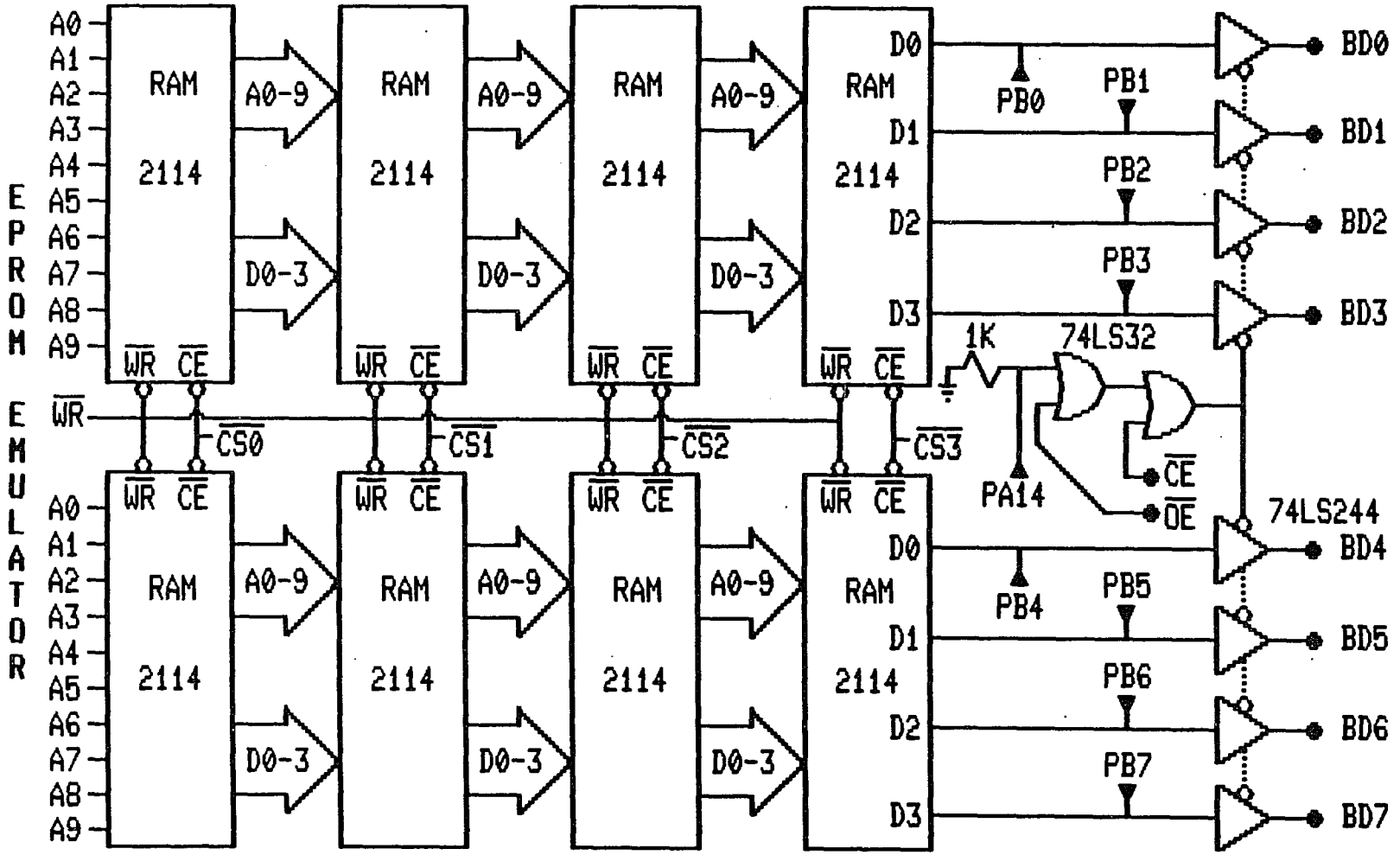
EPROM EMULATOR
A0
A1
A2
A3
A4
A5
A6
A7
A8
A9
RAM
2114
A0-9
D0-3
WR
CE
CS0
CS1
CS2
CS3
D0
D1
D2
D3
PB0
PB1
PB2
PB3
PB4
PB5
PB6
PB7
1K
74LS32
PA14
OE
74LS244
BD0
BD1
BD2
BD3
BD4
BD5
BD6
BD7

Figure V-25

Once the desired RAM locations are loaded and verified, the DRV11-J holds the write signal in a disabled state so that all further operations will be in a read- only mode. The memory is designed such that, once the loading has been completed, both of the DRV11-J ports may be switched to inputs, tri-stating the control lines, and the memory will function as ROM. At this point, the cabling from the memory to the DRV11-J may even be disconnected without disrupting the ROM operation. Figure V-26 shows the bit assignments used in writing the control software for the two DRV11-J ports.

The use of the prime number 257 as a table length has an additional advantage of making efficient use of the required storage space. This would seem incorrect at first, since the memories available contain multiples of 256 locations and the extra byte needed for the 257th location should waste the extra 255 locations. However, since most reasonable test signals may be configured so that at least one tabulated data value is zero, and since the code for a zero value is all 1's, a zero value may be eliminated and only 256 bytes stored. The address signal A8 from the modulo 257 adder will only be high when the 257th value is required from the table. Therefore, if the table is arranged so that this 257th value is zero (all 1's), this address line may be used to disable the table memory, letting the data lines float high generating the all 1's signal for the zero value. Figure V-27 shows how a 4K EPROM may be used in this way to generate up to 16 different signals using this method, assuming that each signal has at least one zero value.

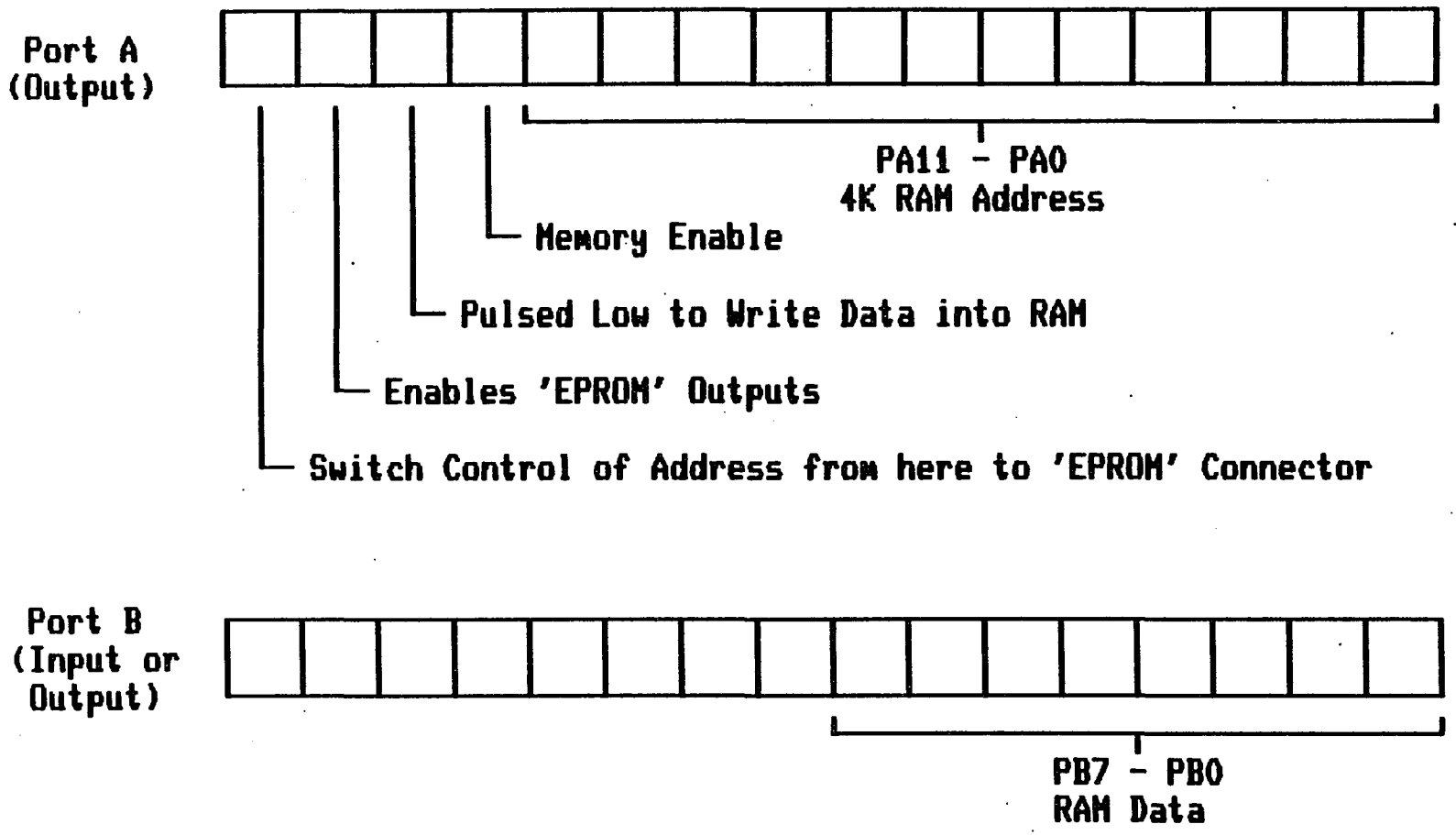

DRV11-J Port Definitions for Controlling the 2732 EPROM Emulator

Figure V-26

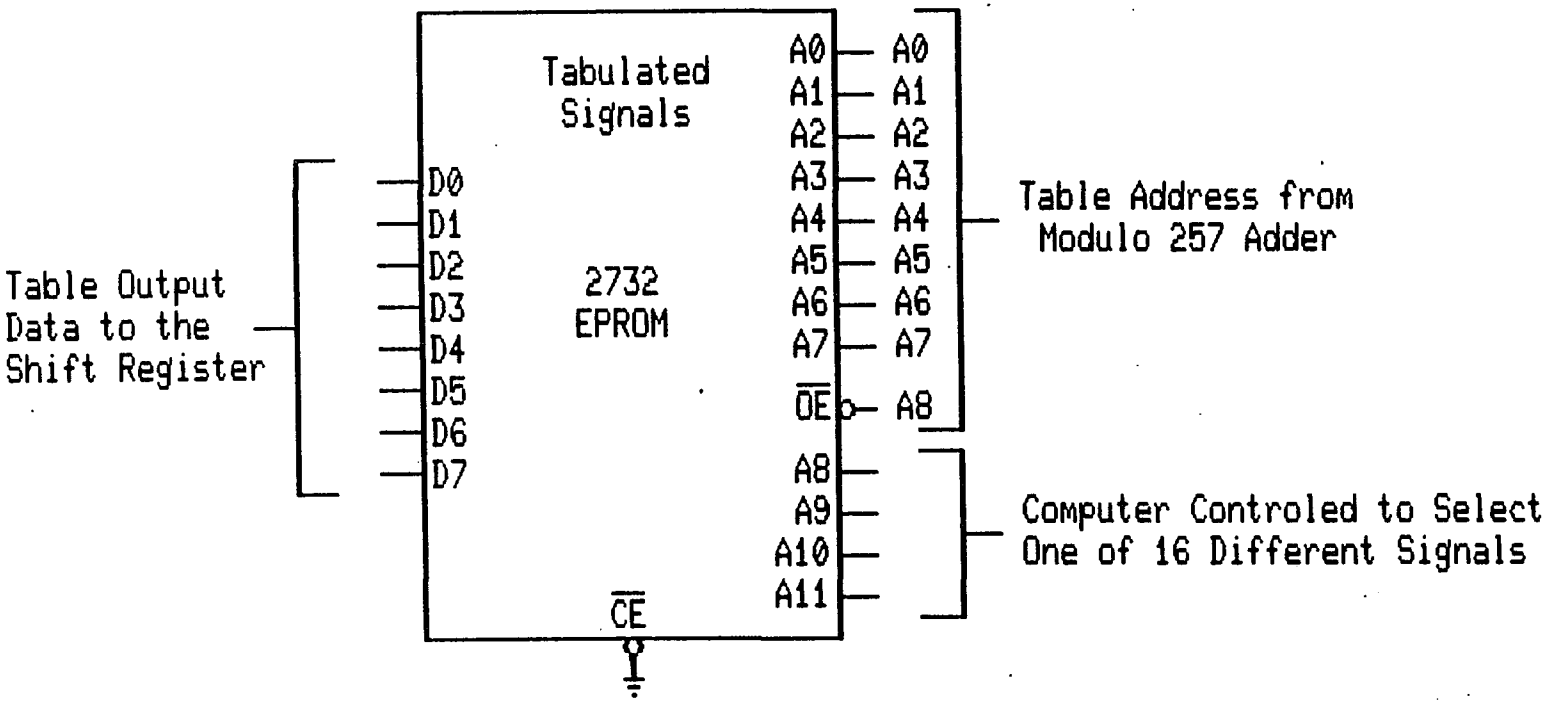

Suggested Modification for Efficient Table Storage

Figure V-27

CHAPTER 6

FAST TRANSFORM TECHNIQUES FOR DIGITAL CHANNEL MEASURMENTS

VI-A The 1542 Point Transform

VI-A.1 Selection of the Number of Points

The selection of 1542 as the number of points to be sampled and then transformed was suggested in the previous chapter; however, the reasons for this choice will be repeated here for completeness.

As demonstrated in Chapter 4, if the number of points sampled is chosen so that the frequency sample points occur exactly on any frequency components existing in a signal to be transformed, then the sinc-shaped spreading of the line spectra will not occur. For example Figure VI-1 shows a 1024 point Discrete Fourier Transform (DFT) of a test signal which was generated by taking every 33rd point from the tabulated values of a single cycle of a 0 dBm0 sine wave which has been broken into 257 evenly spaced samples. This is similar to a signal which might be generated using the digital signal generator described in Chapter 5; however, this particular test signal does not contain the quantization noise which that signal generator would produce. The frequency of this test signal may be found as

$$33 \times 3000 / 257 = 1027.24 \text{ Hz.}$$

It is assumed here that the samples are taken at the rate of 3000 per second. Note the distinct sinc-shaped distribution

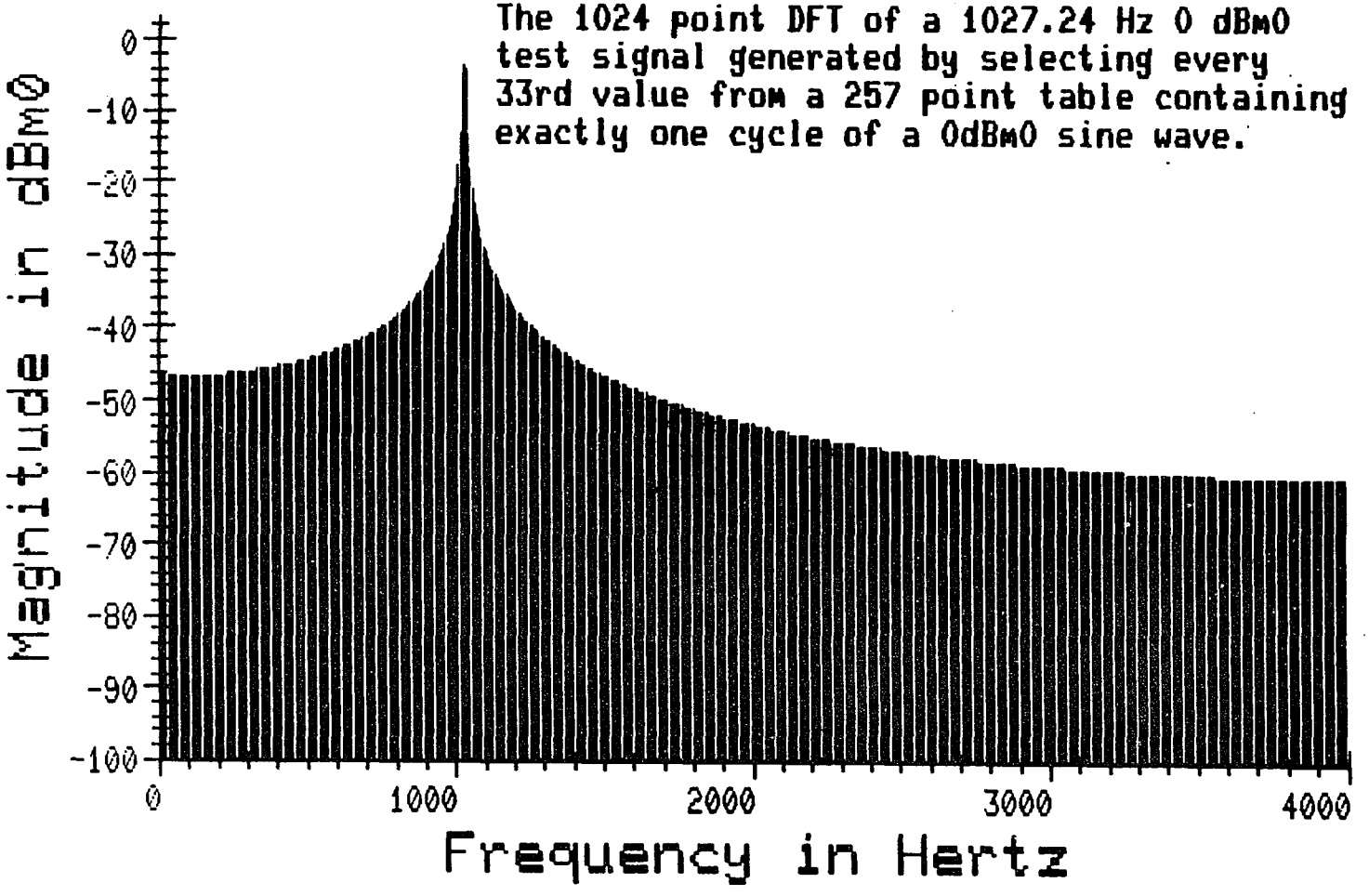
The 1024 point DFT of a 1027.24 Hz 0 dBm0
test signal generated by selecting every
33rd value from a 257 point table containing
exactly one cycle of a 0dBm0 sine wave.
Magnitude in dBm0
0
-10
-20
-30
-40
-50
-60
-70
-80
-90
-100
0
1000
2000
3000
4000
Frequency in Hertz

Figure VI-1

of the energy over the entire spectrum as was predicted in Chapter 4. In Figure VI-2, a 257 point sample of the same signal is transformed and the result shows the signal as a pure sine wave at 1027.24 Hz. Of course, this digitally generated signal would not be a single frequency sine wave until it was passed through an ideal low pass filter with a cut-off frequency of 4000 Hz. The true spectrum of the theoretical signal generated by the sample and hold output of an ideal analog to digital converter would contain an infinite number of sine wave components of equal amplitude spaced regularly at higher and higher frequencies. These additional components may be derived as shown in Chapter 4 by replicating the positive and negative frequency DFT results over and over again at 8000 Hz intervals to extend the spectrum above 4000 Hz to infinity. The next component above 1027.24 Hz will appear at 8000-1027.24=6972.76 Hz. An actual (non-ideal) low pass filter can easily be built to provide unity gain at 1027.24 Hz and, for all practical purposes, zero gain at and above 6972.76 Hz. This filter would function just as well as an ideal filter if one could be built. Now with this practical filter in place the DFT results between zero and 4000 Hz indicate correctly that the output is a pure sine wave at 1027.24 Hz.

Since this 257 point sample produced accurate results it would seem that this might be the number to use; however, as previously demonstrated, the additional quantization noise which is generated every sixth frame in the telephone transmission system will generate modulation products which do not fall exactly on the discrete frequency points of the 257 point DFT. As explained in Chapter 5, the additional distortion caused by the signalling frame generates

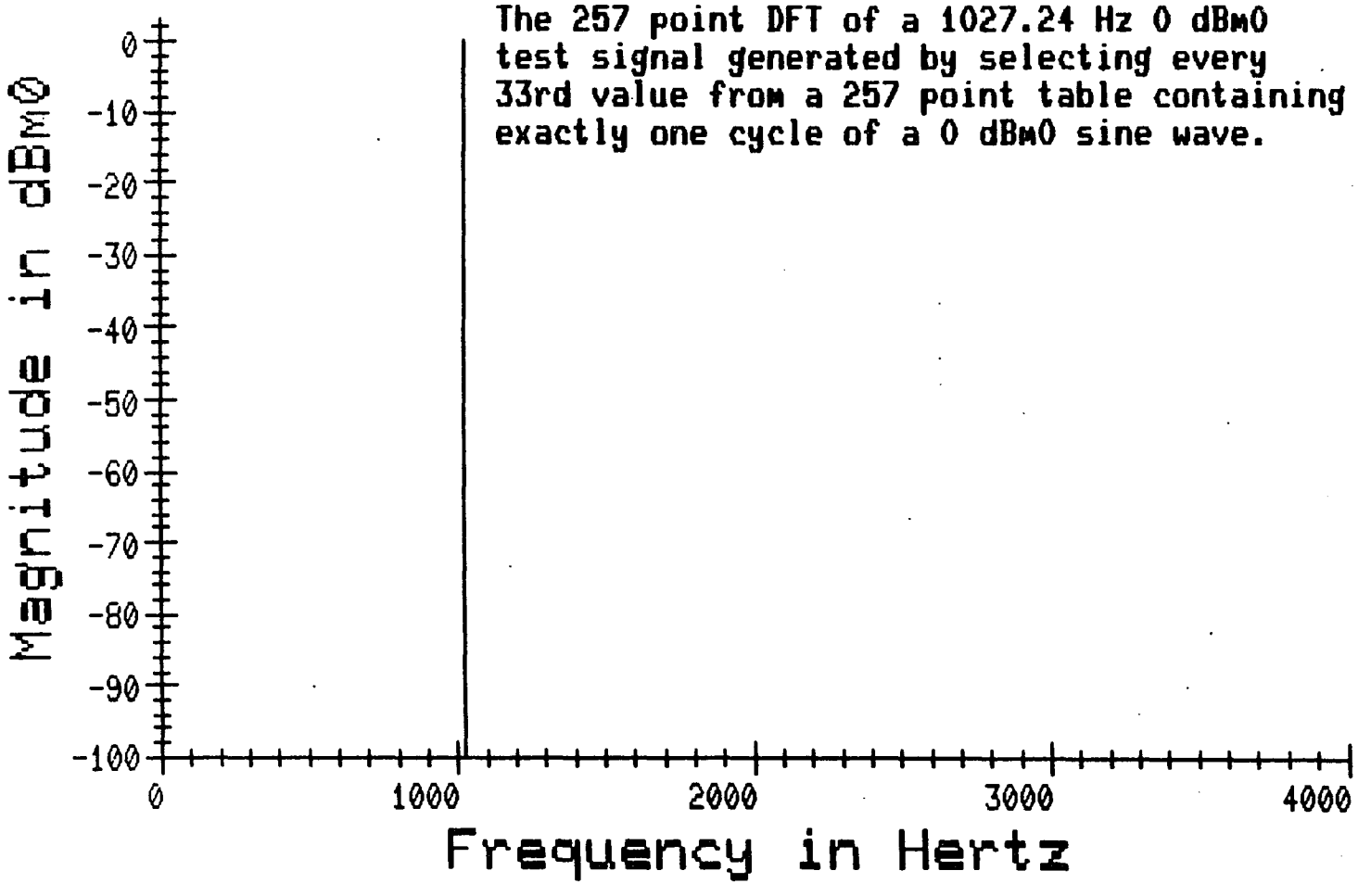
The 257 point DFT of a 1027.24 Hz 0 dBm0
test signal generated by selecting every
33rd value from a 257 point table containing
exactly one cycle of a 0 dBm0 sine wave.
Magnitude in dBm0
0
-10
-20
-30
-40
-50
-60
-70
-80
-90
-100
0
1000
2000
3000
4000
Frequency in Hertz

Figure VI-2

modulation products between the original signal frequency components and 333.33 Hz. Since the information frame quantization noise components are distributed randomly over the discrete frequencies of the 257 point DFT, five out of six of these modulation products fall at frequencies in between these discrete frequencies of the 257 point DFT. Therefore, a 257 point DFT of a signal containing these modulation products should show a large degree of correlation between adjacent frequencies due to the sinc-shaped spreading of these modulation products. Figure VI-3 shows the 257 point DFT of an actual signal after transmission through a digital telephone channel. As predicted there is a high correlation between the components at adjacent frequencies.

The use of a 1542 point DFT, which takes six times as many samples as the 257 point DFT, will detect all of these modulation products and should give a true picture of the actual frequency components which make up the signal. Figure VI-4 shows the actual results of transforming a 1542 point sample of a 1027.24 Hz signal after transmission through a channel. Here it is seen that the amplitudes of the quantization noise products appear much more random than in the previous figure.

The best way to determine the accuracy of these spectral measurement techniques is to conduct a series of experiments and analyze the results statistically to see how well they converge. Table VI-1 lists the results of twenty experiments performed on a single channel using a test signal of 0 dBm0 at 1027.24 Hz. Twenty independent samples were taken within a ten minute time interval and each was analyzed using a 1542 point DFT to determine the level of

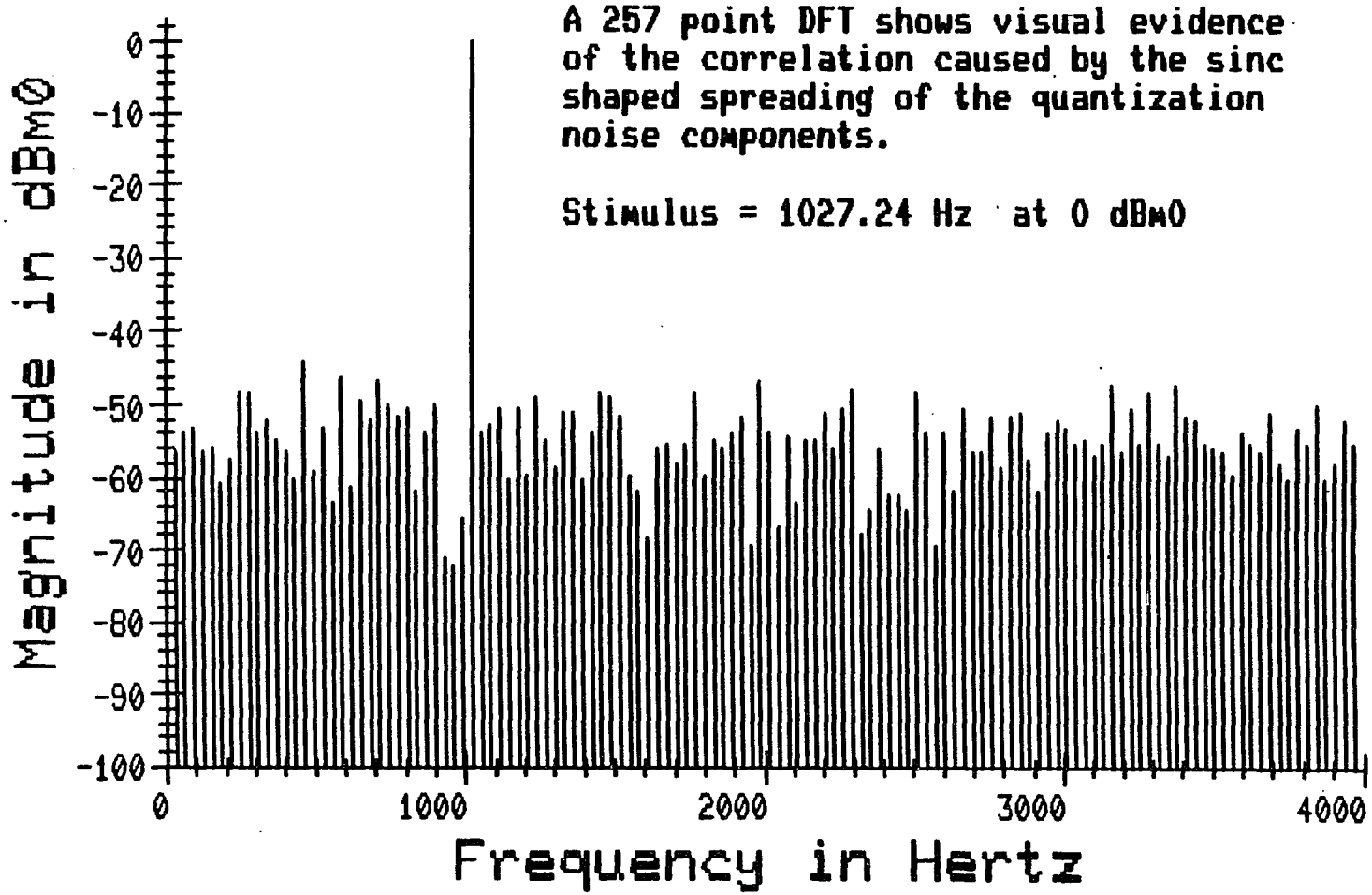
A 257 point DFT shows visual evidence of the correlation caused by the sinc shaped spreading of the quantization noise components.
Stimulus = 1027.24 Hz at 0 dBm0
Magnitude in dBm0
0
-10
-20
-30
-40
-50
-60
-70
-80
-90
-100
0
1000
2000
3000
4000
Frequency in Hertz

Figure VI-3

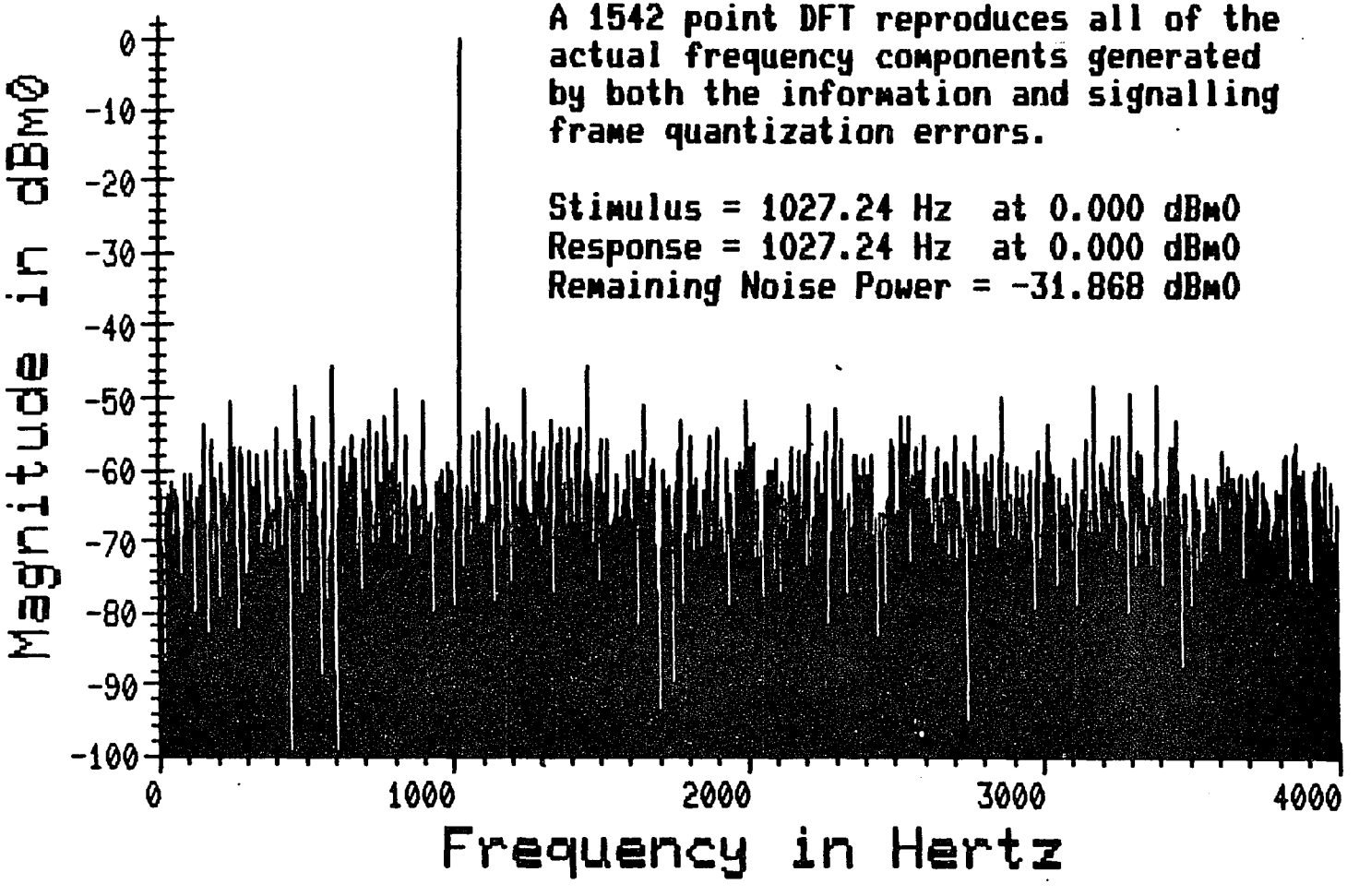
A 1542 point DFT reproduces all of the actual frequency components generated by both the information and signalling frame quantization errors.
Stimulus = 1027.24 Hz at 0.000 dBm0
Response = 1027.24 Hz at 0.000 dBm0
Remaining Noise Power = -31.868 dBm0
Magnitude in dBm0
0
-10
-20
-30
-40
-50
-60
-70
-80
-90
-100
0
1000
2000
3000
4000
Frequency in Hertz

Figure VI-4

TABLE VI-1. Results of 20 Experiments on a Single Channel where Signal Level and Quantization Noise are Measured Using 1542 Point Samples

EXPERIMENT NUMBER	SIGNAL LEVEL	NOISE LEVEL	EXPERIMENT NUMBER	SIGNAL LEVEL	NOISE LEVEL
1	-0.008	-31.835	11	-0.005	-31.819
2	-0.007	-31.828	12	-0.005	-31.812
3	-0.005	-31.815	13	-0.005	-31.835
4	-0.008	-31.821	14	-0.006	-31.842
5	-0.006	-31.813	15	-0.006	-31.829
6	-0.007	-31.833	16	-0.006	-31.815
7	-0.007	-31.840	17	-0.006	-31.813
8	-0.005	-31.818	18	-0.005	-31.821
9	-0.006	-31.818	19	-0.007	-31.814
10	-0.006	-31.810	20	-0.006	-31.817

STATISTICS:

SIGNAL LEVEL		QUANTIZATION NOISE LEVEL	
MEAN	= -0.0061	MEAN	= -31.822
STANDARD DEVIATION	= 0.0010	STANDARD DEVIATION	= 0.010

the 1027.24 Hz signal and the remaining quantization noise. The statistics show that there is a 68 percent certainty that the measurement of the signal level is accurate to within 0.001 dB and a 99 percent certainty that the actual value is within 0.003 dB of the measured value. Also, the quantization noise has a 68 percent probability of being within 0.01 dB of the measured value and a 99 percent probability of being within 0.03 dB.

Similar experiments were run using the 257 point DFT. Table VI-2 shows the results of twenty experiments on the same channels with the same stimulus and taken during the same time period. Here the variation in the measurements has increased considerably. From the statistics shown the measurement of the signal level can be expected to be accurate to within 0.0037 dB 68 percent of the time and within 0.0111 dB 99 percent of the time. The accuracy of the noise measurements may be expected to be accurate to within 0.11 dB 68 percent of the time and within 0.33 dB 99 percent of the time.

Since the measurement limits on transmission through a channel are given to tenths of a dB and limits on noise are given to the nearest dB, either of these two methods will yield sufficiently accurate results. This is because the stimulus occurs at one of the discrete frequencies of either transform and the desired noise measurement is of the total noise power over the entire spectrum, not at individual frequencies. The point-by-point results of the 257 point should not be taken as a true representation of the actual frequency components in the received signal. Figures VI-5,6 and 7 show three independent measurements on a given channel. In comparing these results, it is seen that there is

TABLE VI-2. Results of 20 Experiments on a Single Channel where Signal Level and Quantization Noise are Measured Using 257 Point Samples

EXPERIMENT NUMBER	SIGNAL LEVEL	NOISE LEVEL	EXPERIMENT NUMBER	SIGNAL LEVEL	NOISE LEVEL
1	-0.006	-31.783	11	-0.007	-31.841
2	-0.005	-31.944	12	-0.008	-31.828
3	-0.004	-31.844	13	-0.004	-31.791
4	-0.004	-31.844	14	-0.004	-31.800
5	-0.012	-31.469	15	-0.004	-31.800
6	-0.012	-31.974	16	-0.004	-31.800
7	-0.000	-31.746	17	-0.002	-31.848
8	-0.008	-31.928	18	-0.010	-31.967
9	-0.002	-31.773	19	-0.010	-31.967
10	-0.003	-31.850	20	-0.013	-31.806

STATISTICS:

SIGNAL LEVEL	QUANTIZATION NOISE LEVEL
MEAN = -0.0061	MEAN = -31.8302
STANDARD DEVIATION = 0.0037	STANDARD DEVIATION = 0.1100

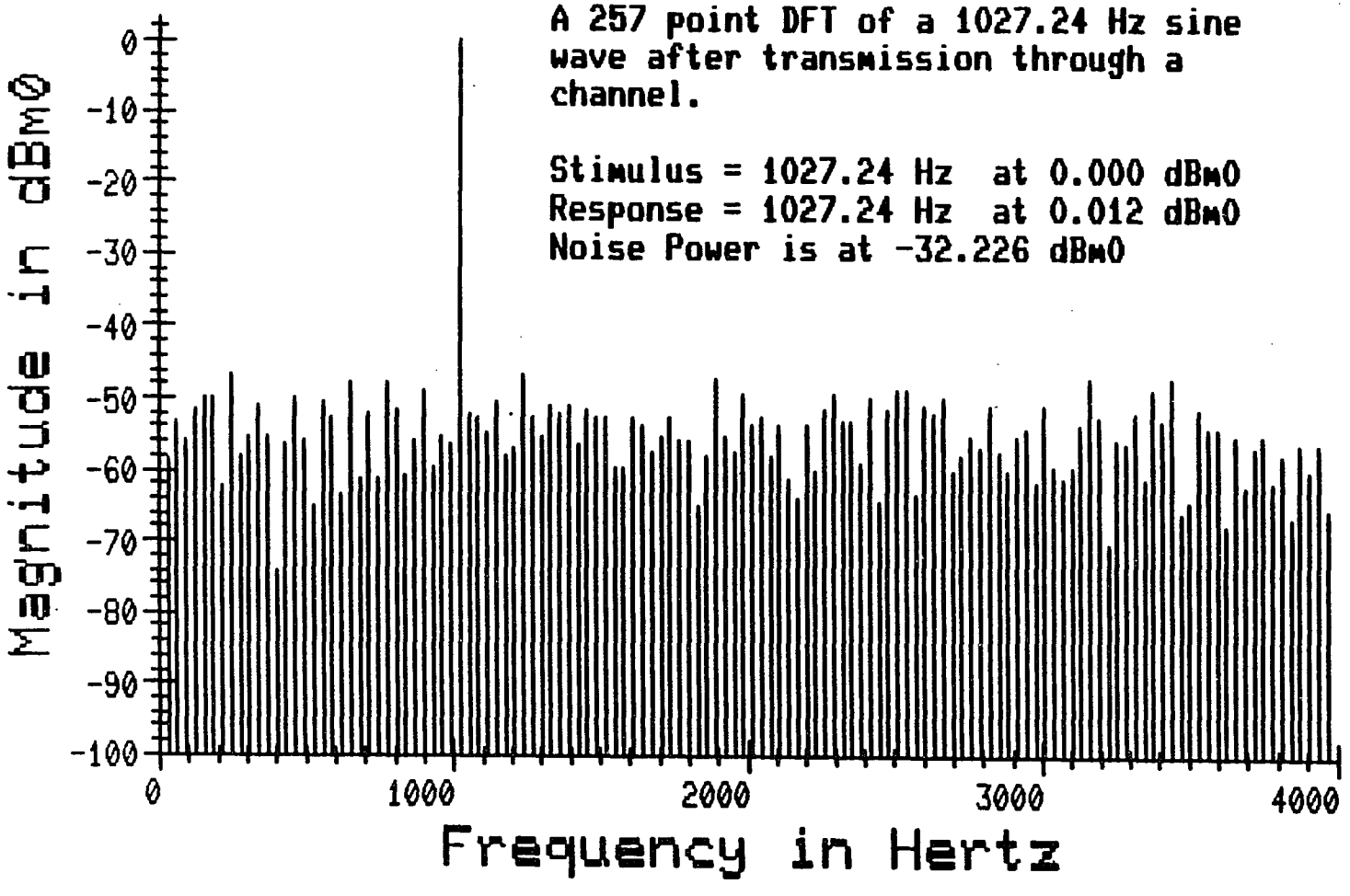
A 257 point DFT of a 1027.24 Hz sine wave after transmission through a channel.
Stimulus = 1027.24 Hz at 0.000 dBm0
Response = 1027.24 Hz at 0.012 dBm0
Noise Power is at -32.226 dBm0
Magnitude in dBm0
0
-10
-20
-30
-40
-50
-60
-70
-80
-90
-100
0
1000
2000
3000
4000
Frequency in Hertz

Figure VI-5

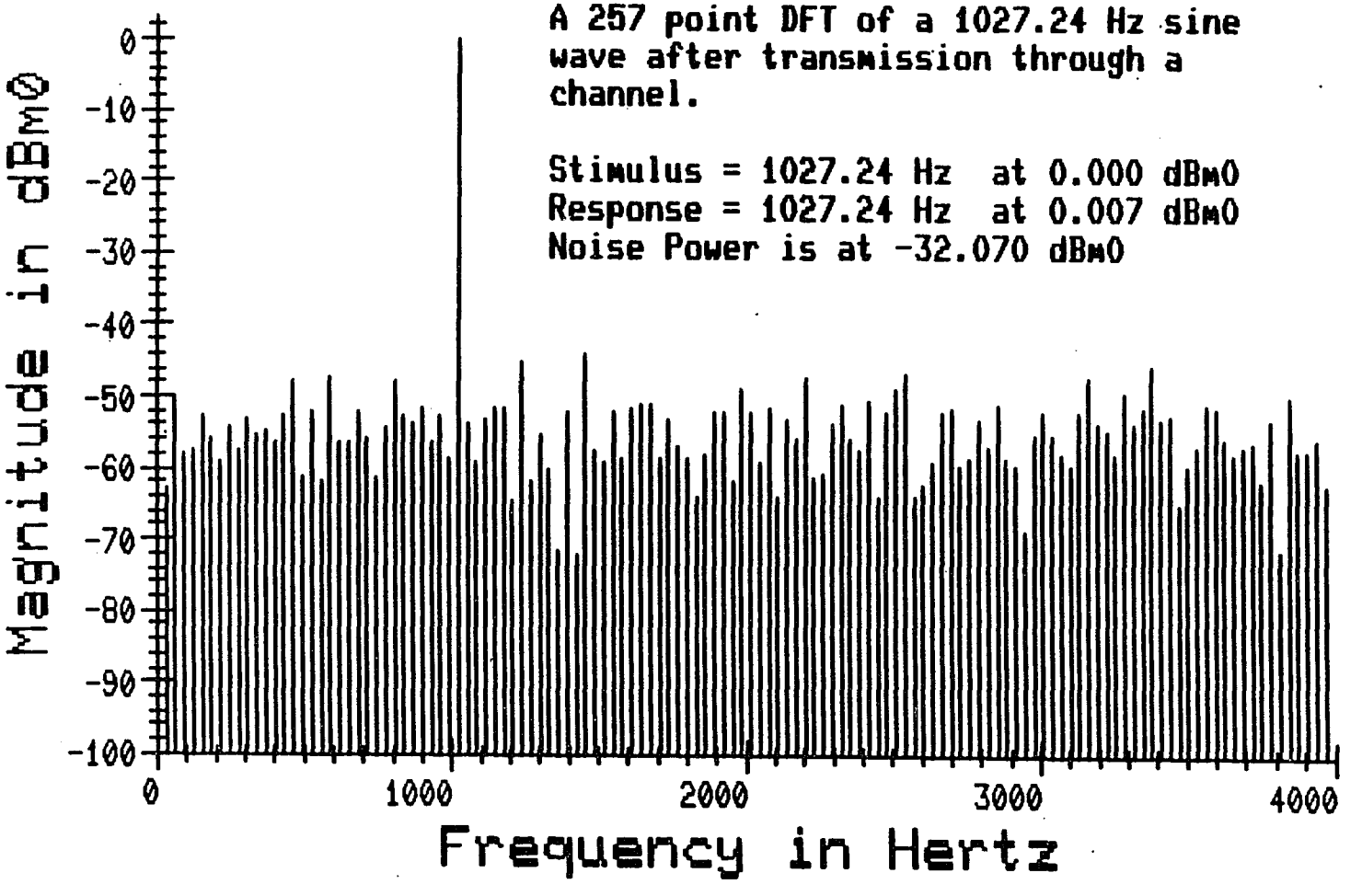
A 257 point DFT of a 1027.24 Hz sine wave after transmission through a channel.
Stimulus = 1027.24 Hz at 0.000 dBm0
Response = 1027.24 Hz at 0.007 dBm0
Noise Power is at -32.070 dBm0
Magnitude in dBm0
0
-10
-20
-30
-40
-50
-60
-70
-80
-90
-100
0
1000
2000
3000
4000
Frequency in Hertz

Figure VI-6

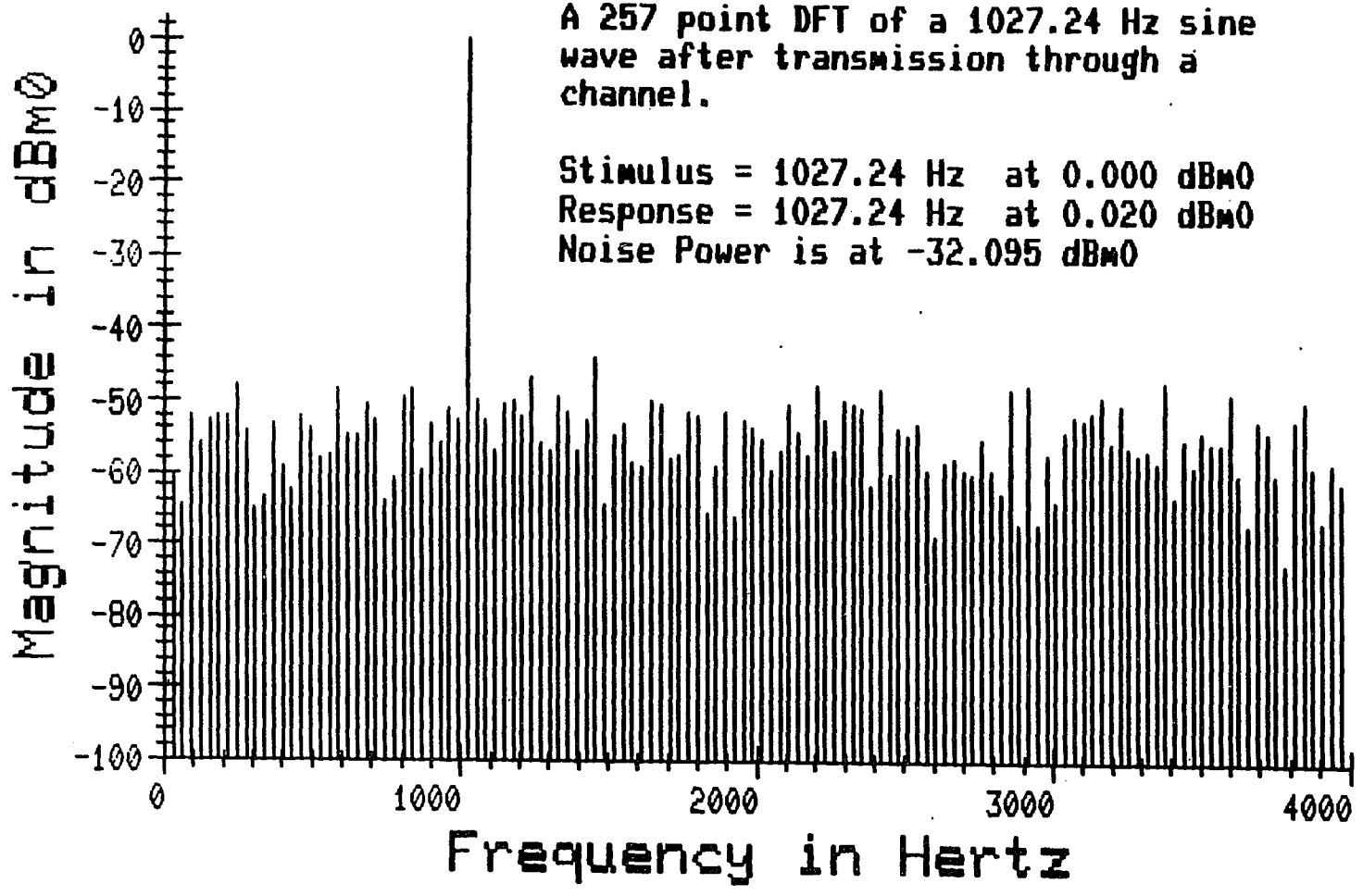
A 257 point DFT of a 1027.24 Hz sine wave after transmission through a channel.
Stimulus = 1027.24 Hz at 0.000 dBm0
Response = 1027.24 Hz at 0.020 dBm0
Noise Power is at -32.095 dBm0
Magnitude in dBm0
0
-10
-20
-30
-40
-50
-60
-70
-80
-90
-100
0
1000
2000
3000
4000
Frequency in Hertz

Figure VI-7

little or no correlation between the noise components from one measurement to the next. Since most of the noise generated is due to the quantization distortion and, hence, is deterministic and periodic by nature, then a better correlation between successive measurements should be expected. The discrepancy results from the fact that the noise is periodic at 1542 sample intervals and the 257 point transform doesn't use a sample large enough to capture all of its characteristics. Figures VI-8,9 and 10 show the results of three independent measurements on the same channel a before but this time 1542 point samples are analyzed. The obvious correlation between these three DFT's give further evidence that the actual frequency components of the signal are being reported.

Of course, the choice of 1542 as a sample size is valid only because a 257 point table is being used to generate the stimulus and the sampling and signal generation processes are synchronized. If any other table length is used, accurate results may be derived from a sample size which is evenly divisible by both the table length and the signalling frame rate of six. The table length of 257 was chosen because it provides sufficient sample points at the higher amplitudes, is prime and has the added advantage of being efficiently transformed. As explained in Chapter 4, any prime number of points may be transformed by performing a fast convolution on one less than that number of points. The number 256, which is one less than 257, is a power of two and therefore provides for a very efficient DFT.

VI-A.2 Software Implementation

The 1542 point Discrete Fourier Transform (DFT) has

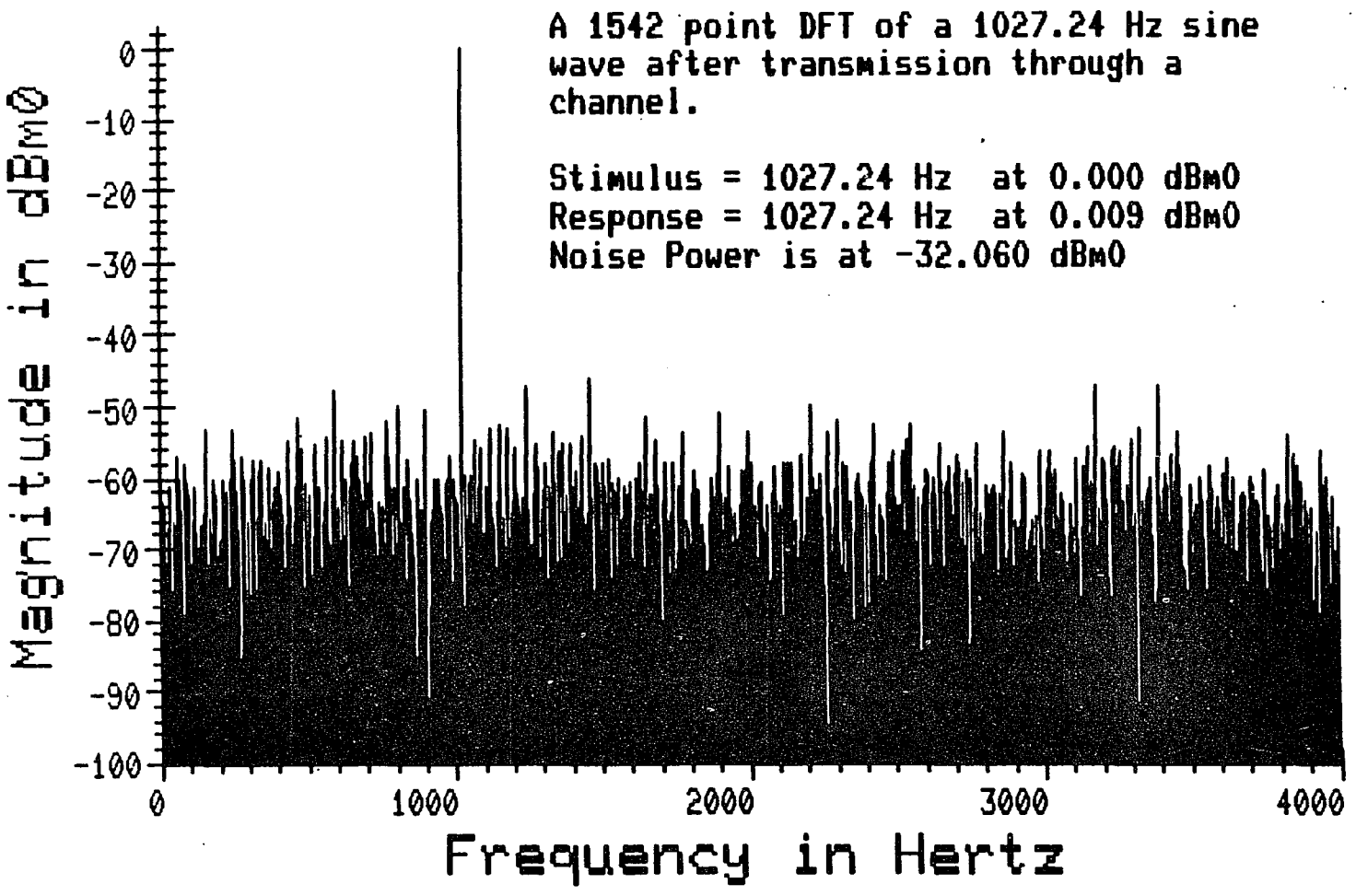
A 1542 point DFT of a 1027.24 Hz sine wave after transmission through a channel.
Stimulus = 1027.24 Hz at 0.000 dBm0
Response = 1027.24 Hz at 0.009 dBm0
Noise Power is at -32.060 dBm0
Magnitude in dBm0
0
-10
-20
-30
-40
-50
-60
-70
-80
-90
-100
0
1000
2000
3000
4000
Frequency in Hertz

Figure VI-8

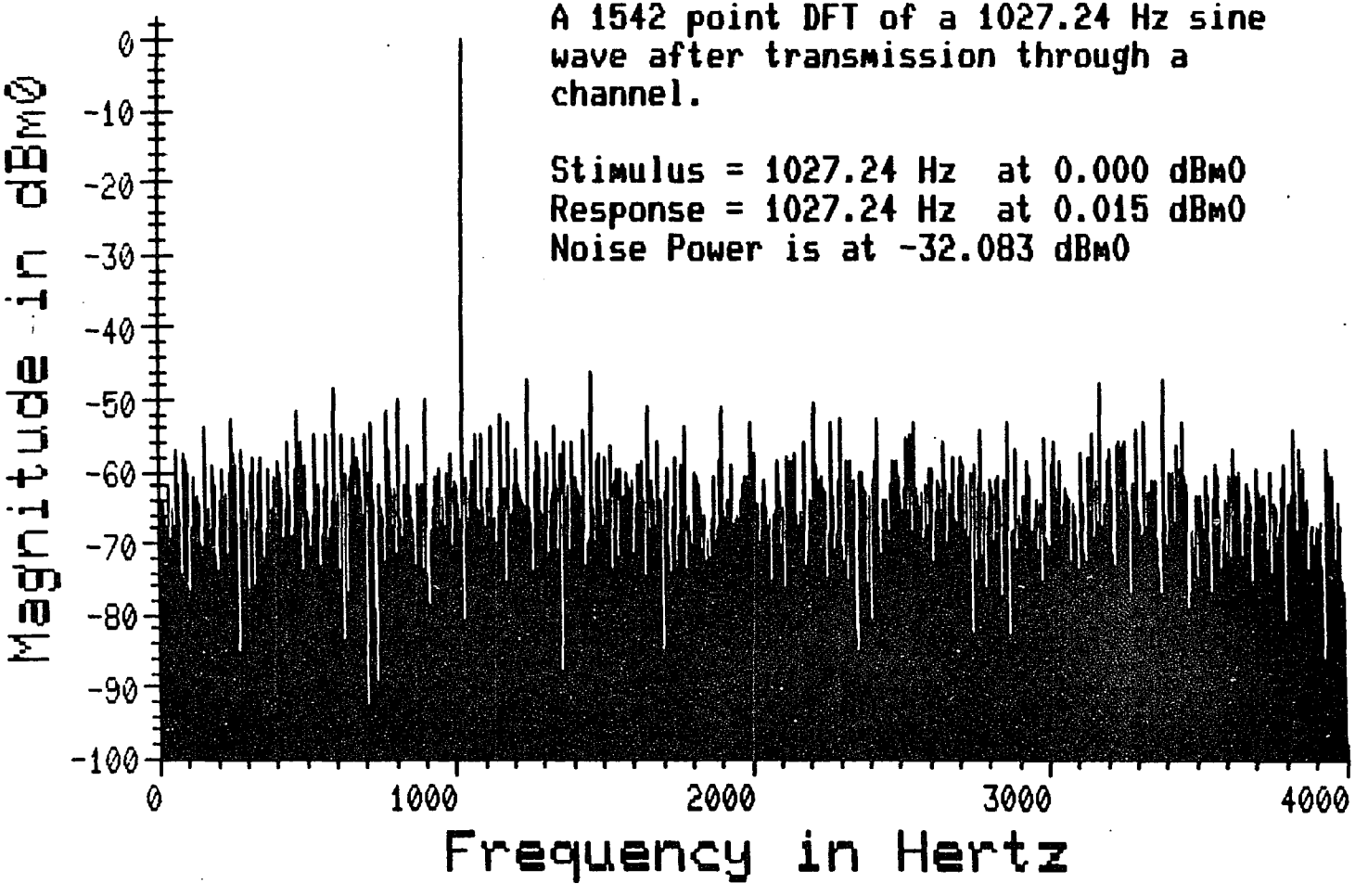
A 1542 point DFT of a 1027.24 Hz sine wave after transmission through a channel.
Stimulus = 1027.24 Hz at 0.000 dBm0
Response = 1027.24 Hz at 0.015 dBm0
Noise Power is at -32.083 dBm0
Magnitude in dBm0
0
-10
-20
-30
-40
-50
-60
-70
-80
-90
-100
0
1000
2000
3000
4000
Frequency in Hertz

Figure VI-9

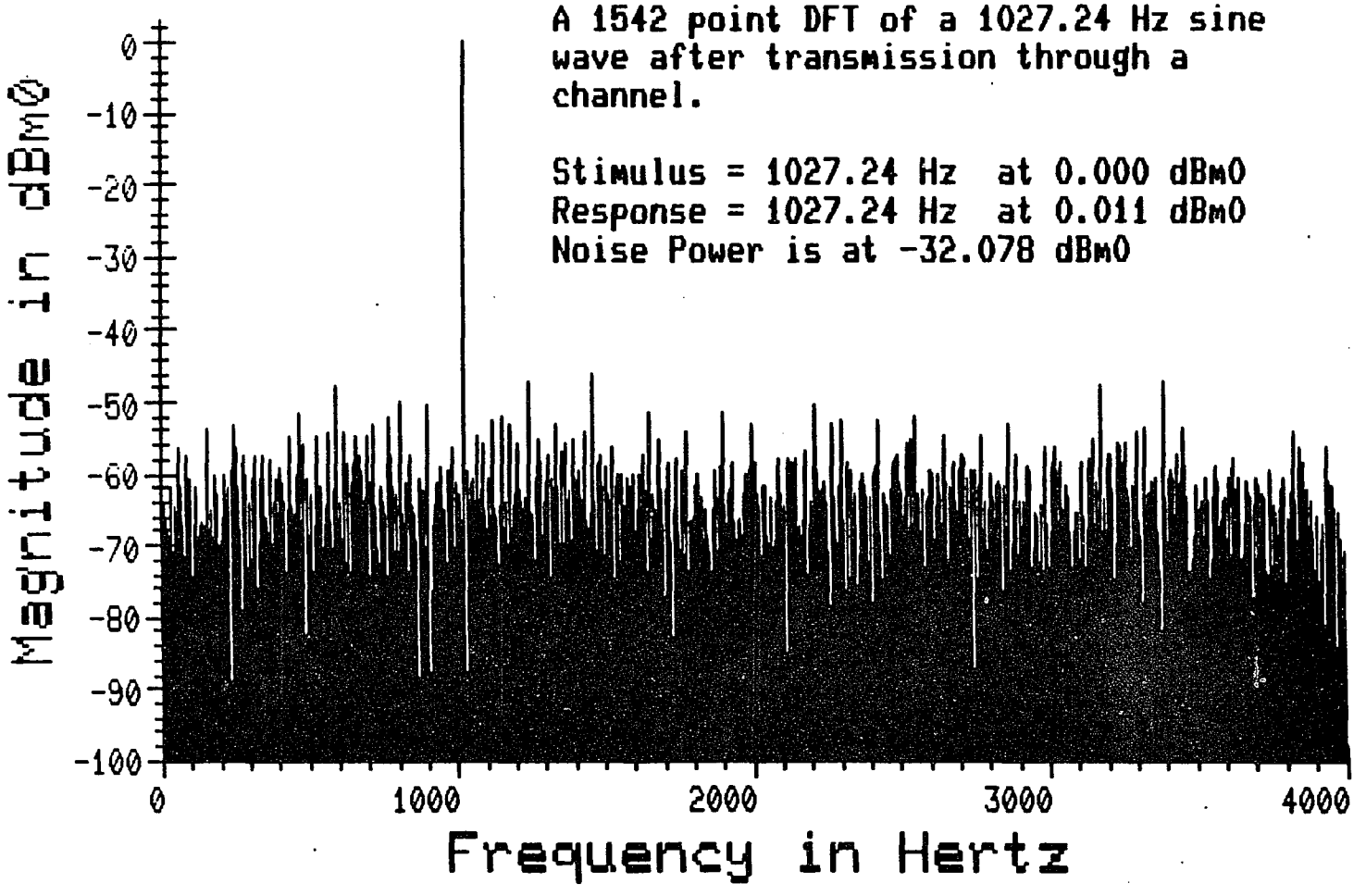
A 1542 point DFT of a 1027.24 Hz sine wave after transmission through a channel.
Stimulus = 1027.24 Hz at 0.000 dBm0
Response = 1027.24 Hz at 0.011 dBm0
Noise Power is at -32.078 dBm0
Magnitude in dBm0
0
-10
-20
-30
-40
-50
-60
-70
-80
-90
-100
0
1000
2000
3000
4000
Frequency in Hertz

Figure VI-10

been implemented in three distinct steps, each corresponding to one of its three prime factors of 2, 3 and 257. All of the measurements taken will be of real data points so the doubling algorithm is used to separate the even and odd numbered points into two sets of 771 points each. Then the two-at-a-time algorithm is used to transform both of these 771 point sequences simultaniously. Once the two 771 point transforms have been separated the doubling algorithm is used to put them back together forming the desired 1542 point transform. Figure VI-11 is the flow chart for the program which performs these operations. Note that this program may also be used to perform the Inverse Fourier Transform (IFT) of a conjugate even DFT. Figure VI-12 shows the flow chart of the program segment which performs the 771 point Fast Fourier Transform (FFT). Here the points are separated into three groups of 257 points each. Each group is individually transformed. Then a three-way combination is performed to merge the results into the 771 point transform of the original points. Figure VI-13 shows the flow chart of the 257 point prime transform algorithm. First, the points are shuffled in the order given by the prime root of 257 in preparation for performing the fast convolution. The first point is temporarily left out and the remaining 256 points are transformed using a common radix two algorithm. The convolution proceeds as the result is multiplied by the transform of the radix 257 rotation factors which has been precalculated and also divided by 256 in preparation for the inverse transform. The first point which was left out is added to each of the 256 values and the 256 point IFT is performed. This completes the convolution and the result is the 257 point transform of the data. This 1542 point

Flow Chart of the 1542 Point Fast Fourier Transform Algorithm

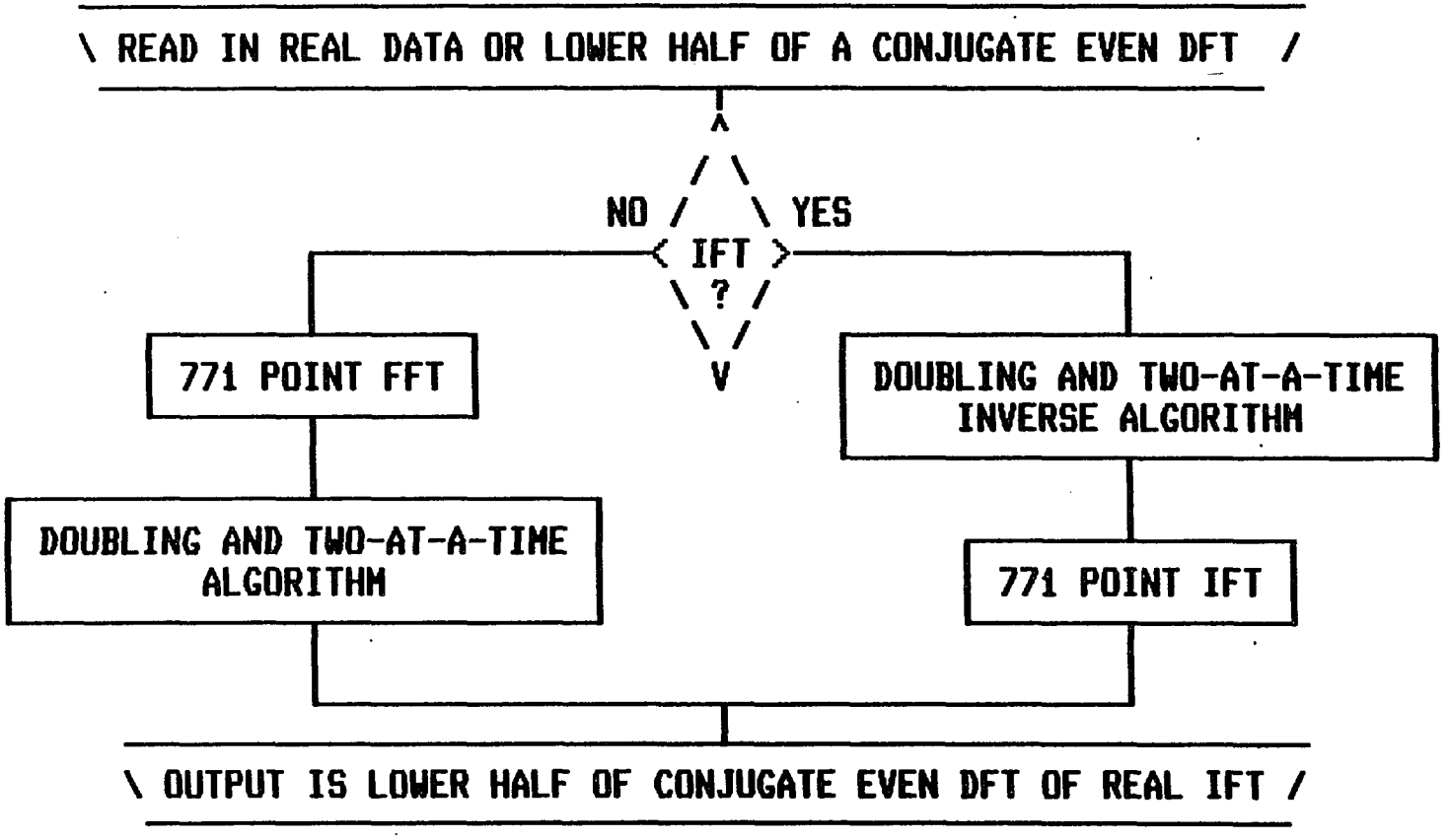

Figure VI-11

Flow Chart for the 771 Point Fast Fourier Transform Subroutine

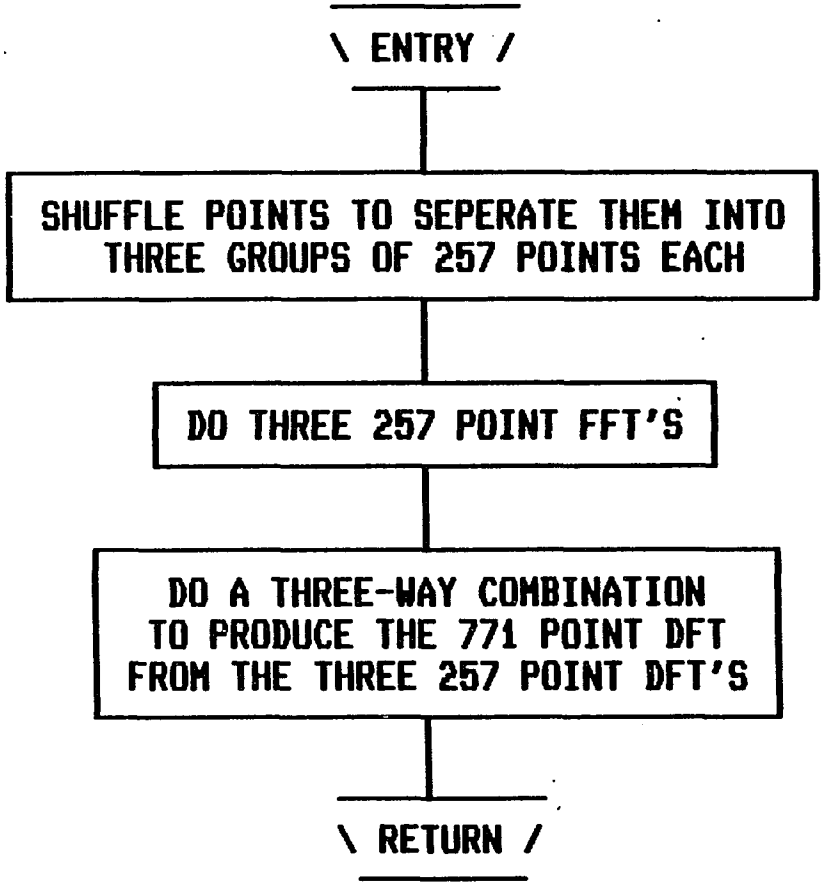

Figure VI-12

Flow Chart for the 257 Point Fast Fourier Transform Subroutine

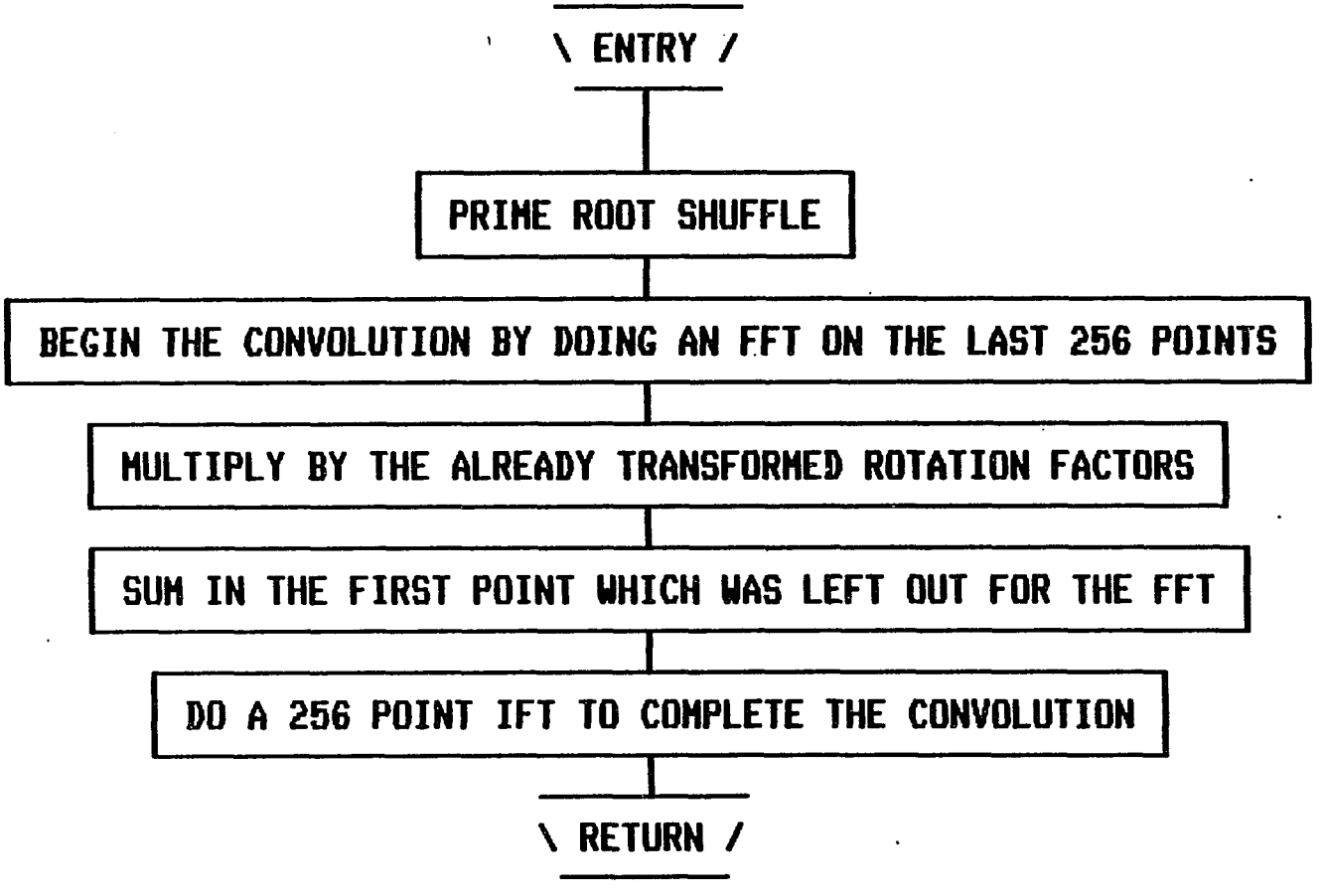

Figure VI-13

transform is reasonably efficient requiring about 6000 floating point multiplications compared to about 4000 for a comperable 2048 point FFT or 1700 for a 1024 point FFT.

Since the transform is modularized, various sections may be used directly to produce 771 and 257 point FFT's.

VI-B Use of Radix Two Transforms

Sometimes the stimulus which is used to analyze a transmission channel will not be derived from a synchronized source but from some other analog signal generator. In this case the 1542 point FFT will not produce accurate results. Therefore it is just as well to use a radix two FFT which will provide a greater computational efficiency. Figure VI-14 is a 1542 point FFT of an actual measurement taken using an analog signal source with a frequency near 1027 Hz. Although the sinc-shaped spreading seen here is minimal, the results are still distorted enough to produce a significant error in the measurement.

The use of data windows, as described in the next section, greatly improves the accuracy of these spectral measurements [2,3,4]. In situations where precise spectral measurements are not required and computational time is important, radix two FFT's in conjunction with data windows may be used to reduce the number of required floating point multiplications.

VI-C Data Windows

VI-C.1 Previously Developed Windows

Data windows in general are used to reduce the effects of taking a finite length sample from the middle of a

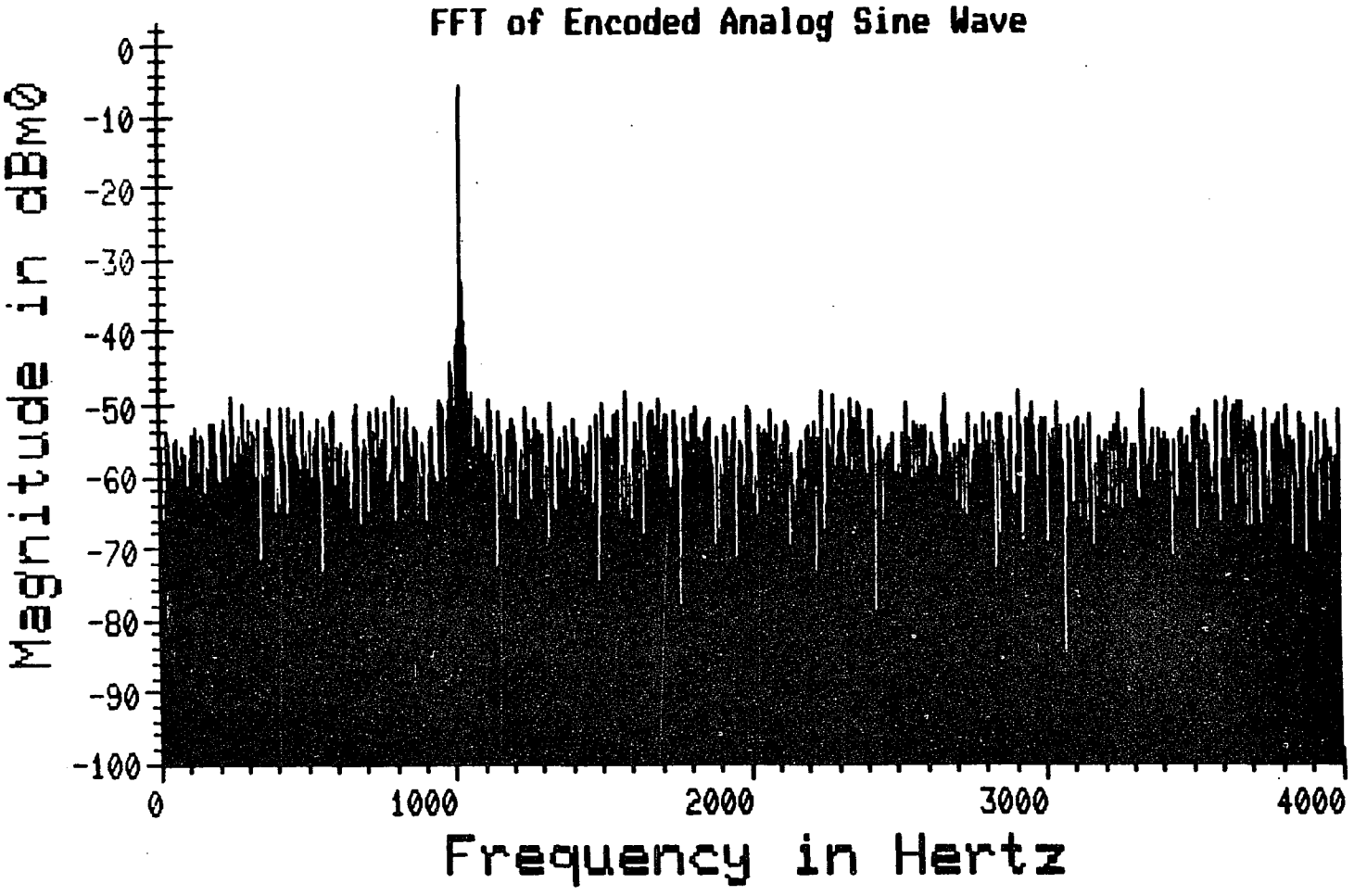
FFT of Encoded Analog Sine Wave
Magnitude in dBm0
0
-10
-20
-30
-40
-50
-60
-70
-80
-90
-100
0
1000
2000
3000
4000
Frequency in Hertz

Figure VI-14

continuous signal. As shown in Chapter 4, the sinc-shaped spreading of the spectra results from the sampling process having effectively multiplied the signal by a rectangular pulse in time. The effect of this multiplication results in the convolution of the signal's spectrum with the sinc-shaped spectrum of this rectangular pulse. The data windows in the time domain attempt to taper the edges of this rectangular sampling window which in the frequency domain results in less spreading of the spectrum. It is instructive to take a signal example which exhibits this sinc-shaped spreading such as that shown in Figure VI-15 and try each of the various data windows to see how it improves the spectral estimate. Figure VI-16 is the phase plot for this same spectrum. It is interesting to notice the 180 degree phase shift which occurs at the peak of the response as predicted in Chapter 4.

Two data windows are suggested by Peter D. Welch in [3]. The first has the triangular shape of $1-|t|$ where t ranges from minus to plus one as shown in Figure VI-17. This window, called the Parzen window, has the transform shown in Figure VI-18 and when applied to the example signal produces the DFT shown in Figure VI-19. This window shows a marked improvement over the unwindowed case but the energy is still spread over a significant frequency range.

The second data window has the shape $1-t^2$ where t again ranges from minus to plus one. This window, shown in Figure VI-20 has the transform shown in Figure VI-21 and when applied to the signal produces the spectrum of Figure VI-22. This window shows only a very slight improvement over the first window.

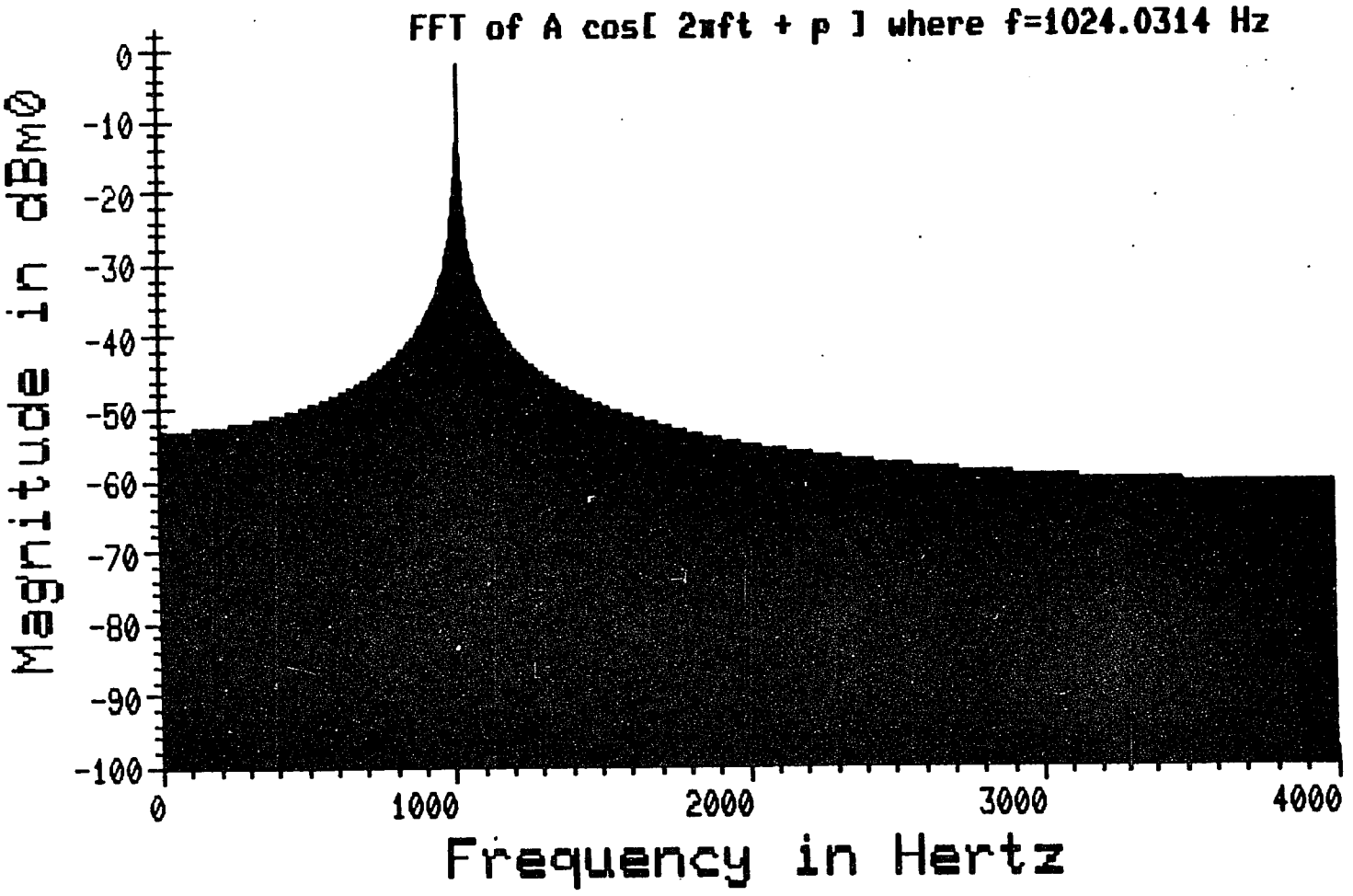
FFT of A cos[2πft + p] where f=1024.0314 Hz
Magnitude in dBm0
0
-10
-20
-30
-40
-50
-60
-70
-80
-90
-100
0
1000
2000
3000
4000
Frequency in Hertz

Figure VI-15

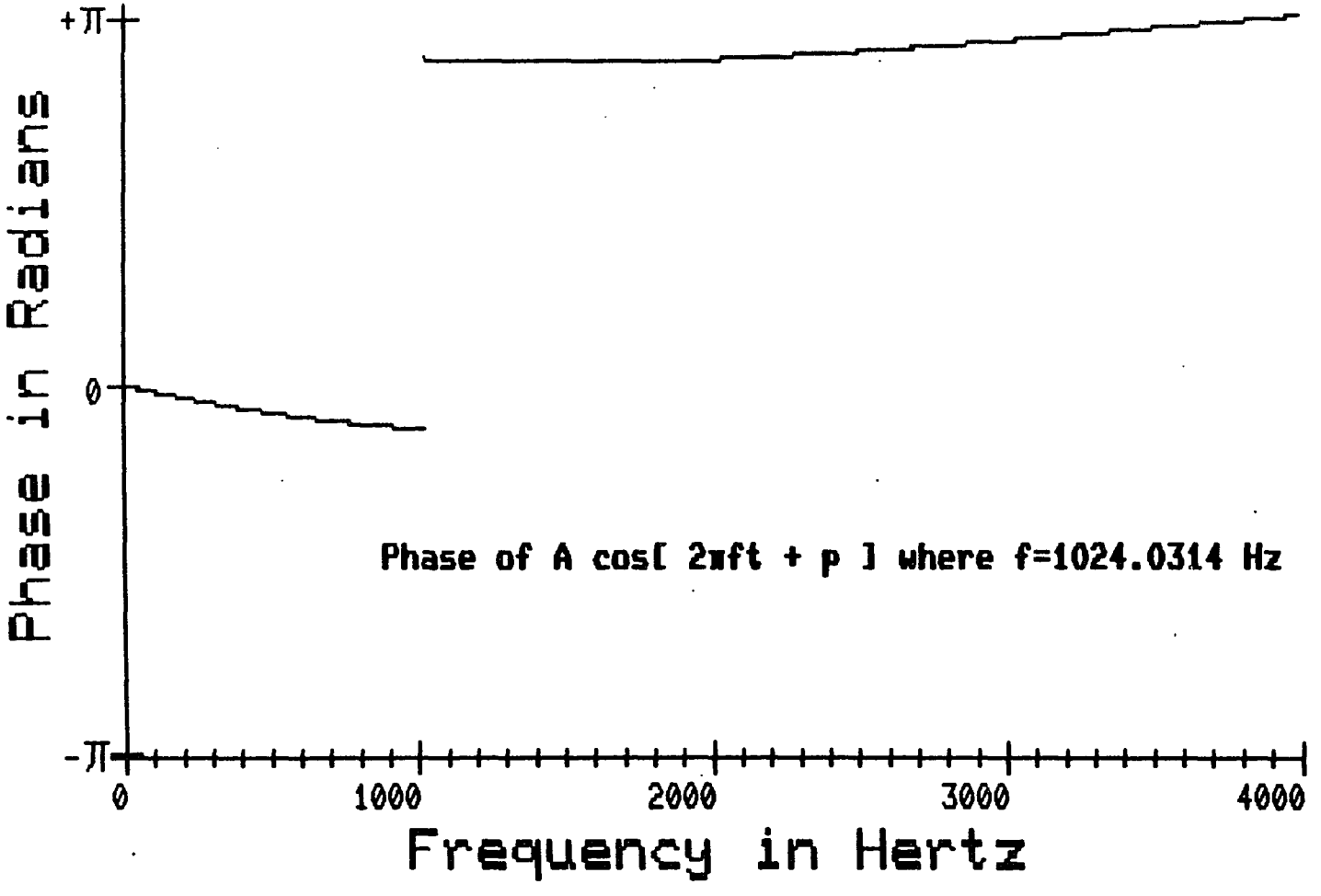
+π
0
-π
Phase in Radians
Phase of A cos[2πft + p] where f=1024.0314 Hz
0
1000
2000
3000
4000
Frequency in Hertz

Figure VI-16

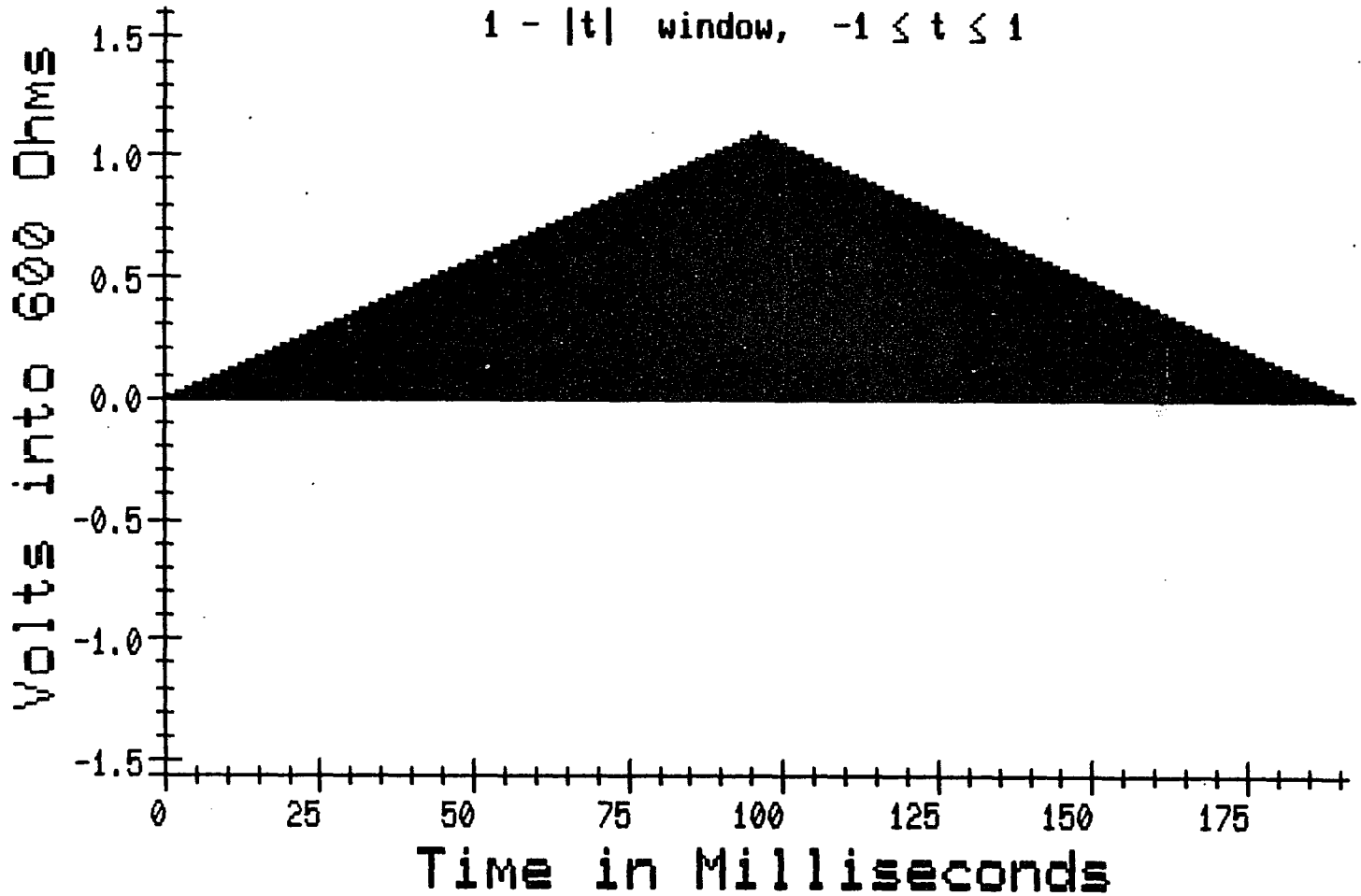
1 - |t| window, -1 ≤ t ≤ 1
Volts into 600 Ohms
1.5
1.0
0.5
0.0
-0.5
-1.0
-1.5
0
25
50
75
100
125
150
175
Time in Milliseconds

Figure VI-17

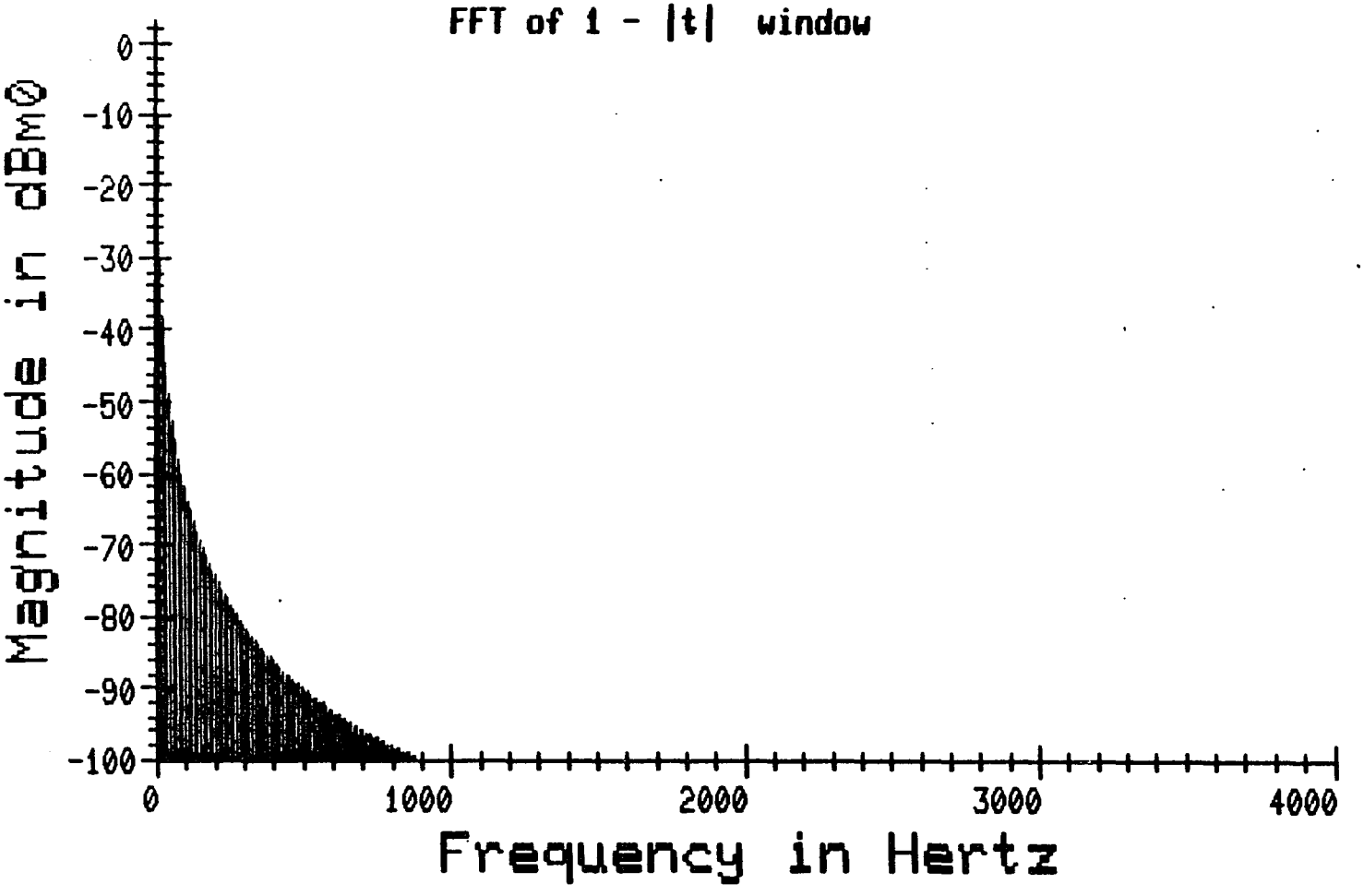
FFT of 1 - |t| window
Magnitude in dBm0
0
-10
-20
-30
-40
-50
-60
-70
-80
-90
-100
0
1000
2000
3000
4000
Frequency in Hertz

Figure VI-18

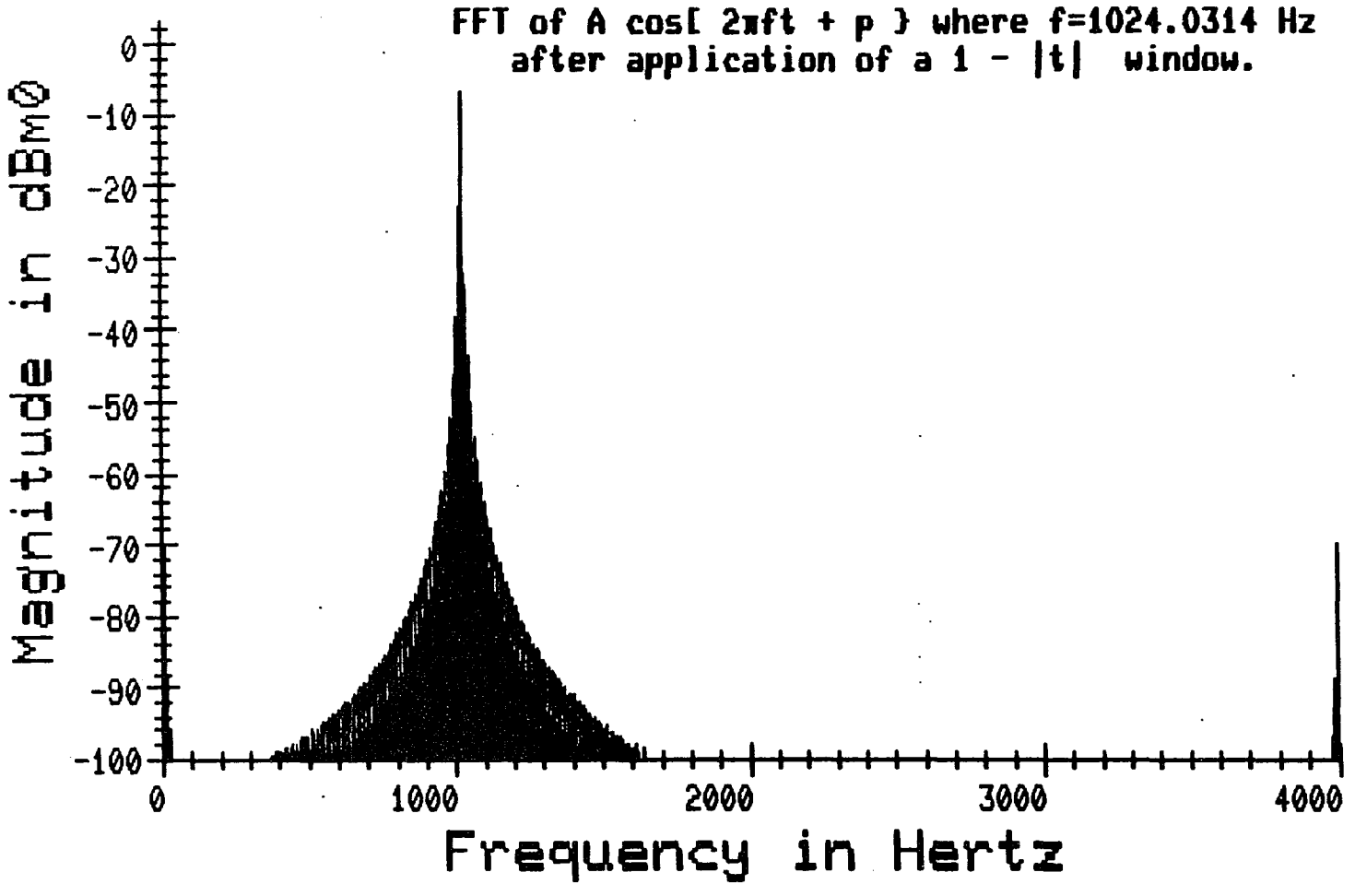
FFT of A cos[2πft + p] where f=1024.0314 Hz
after application of a 1 - |t| window.
Magnitude in dBmØ
0
-10
-20
-30
-40
-50
-60
-70
-80
-90
-100
0
1000
2000
3000
4000
Frequency in Hertz

Figure VI-19

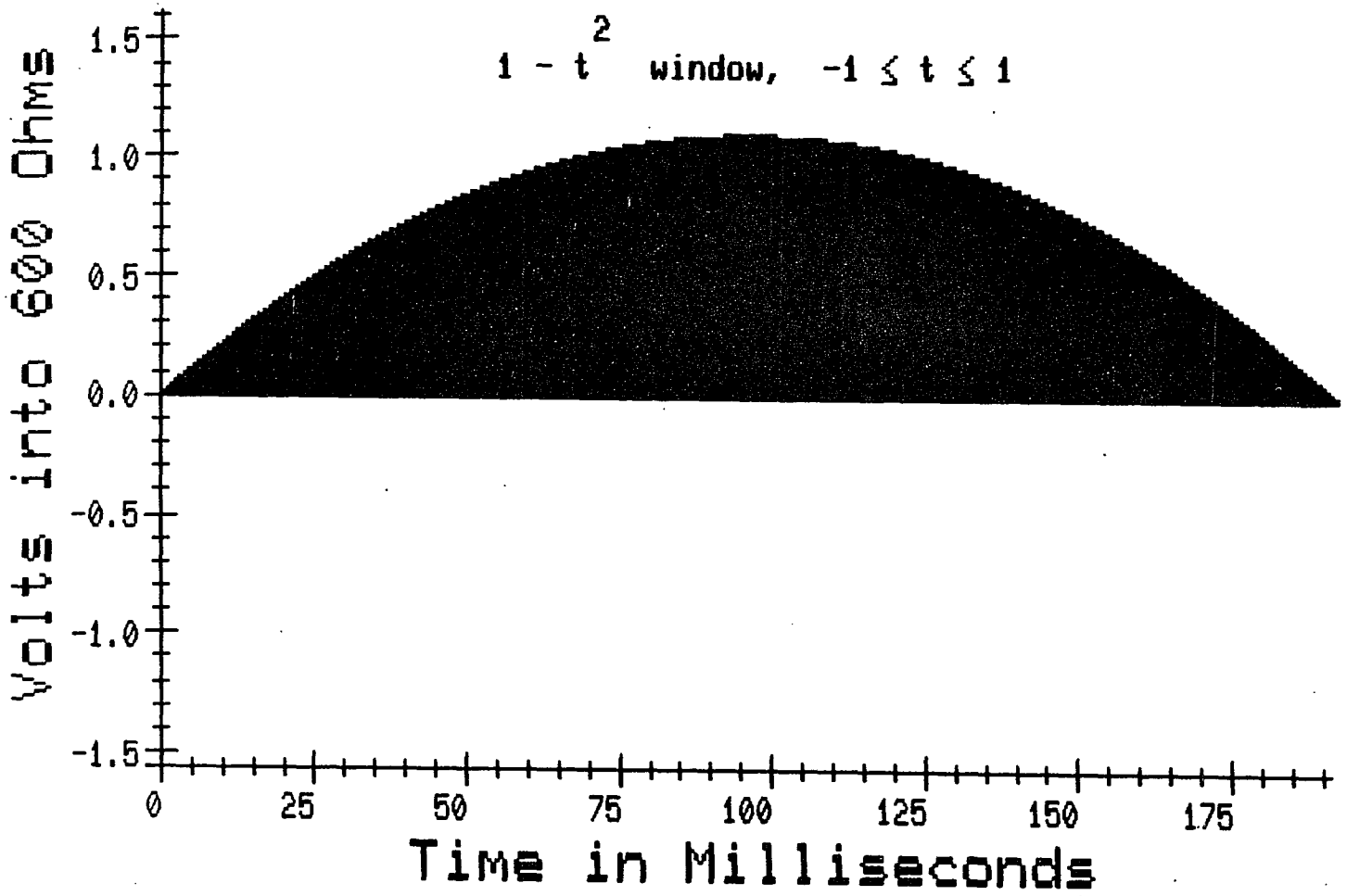
$1 - t^2$ window, $-1 \leq t \leq 1$
Volts into 600 Ohms
1.5
1.0
0.5
0.0
-0.5
-1.0
-1.5
0
25
50
75
100
125
150
175
Time in Milliseconds

Figure VI-20

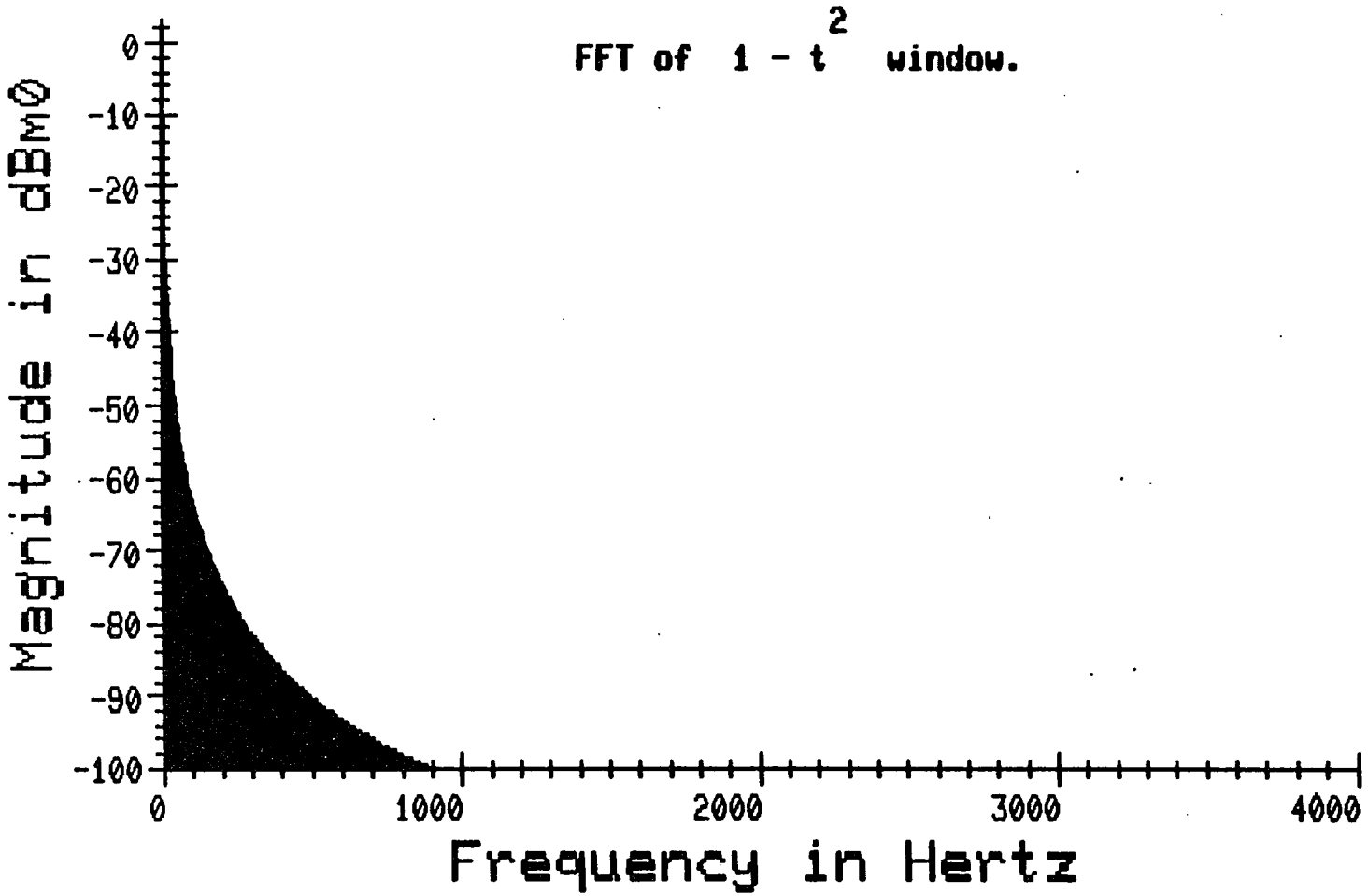
FFT of 1 - t^2 window.
Magnitude in dBm0
0
-10
-20
-30
-40
-50
-60
-70
-80
-90
-100
0
1000
2000
3000
4000
Frequency in Hertz

Figure VI-21

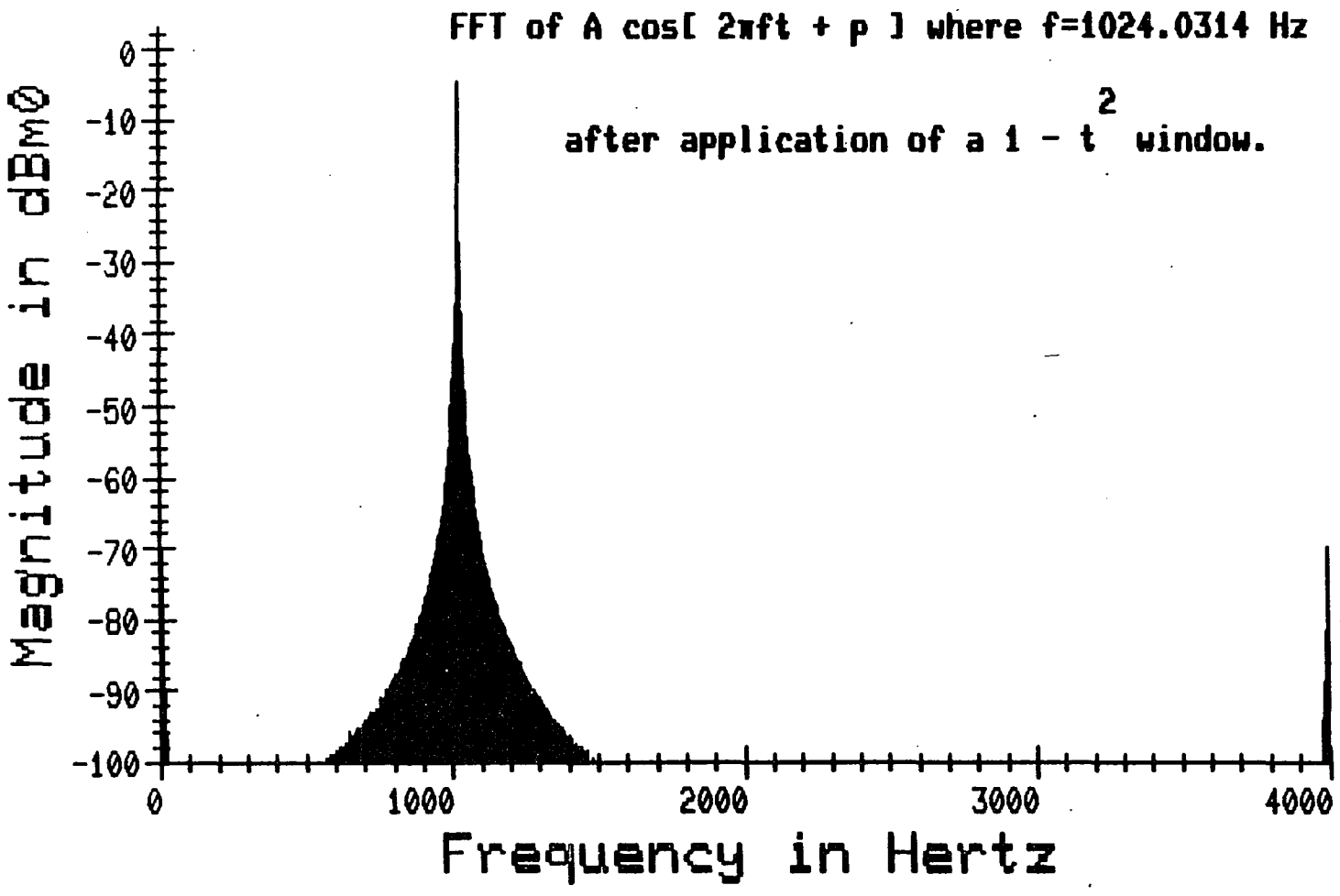
FFT of A cos[2πft + p] where f=1024.0314 Hz
after application of a 1 - t^2 window.
Magnitude in dBm0
0
-10
-20
-30
-40
-50
-60
-70
-80
-90
-100
0
1000
2000
3000
4000
Frequency in Hertz

Figure VI-22

Another window commonly used is the Hanning or raised cosine or cosine arch spectral window as shown in Figure VI-23. This window has a DFT consisting of a component at zero frequency and negative real components of half that height at next discrete frequencies above and below zero. This window shows a marked improvement as shown in Figure VI-24 by concentrating more of the power into a narrower spike.

VI-C.2 New Data Windows

The raised cosine window seems to be going in the right direction; that is, improving the concentration of the spectral energy around the actual frequency of the signal. A closer inspection of the mathematical operation performed by this window in the frequency domain leads to an interpretation which may be extrapolated to form a series of new windows.

Figure VI-25 shows the DFT of this raised cosine window. Remember that the windowing operation may be performed in the frequency domain by convolving this function with the DFT of the signal in question. This convolution operation is rather simple in this case since only three components must be multiplied and summed to produce each point in the output spectrum. Figure VI-25 shows a graphic representation of what is done at each point in the convolution. Effectively the two points R and T on either side of the frequency in question are averaged to produce a straight line approximation U of the value in the middle. Then this value U is subtracted from the actual value S at this frequency producing the output value V. This procedure is effectively attempting to approximate the 1/x

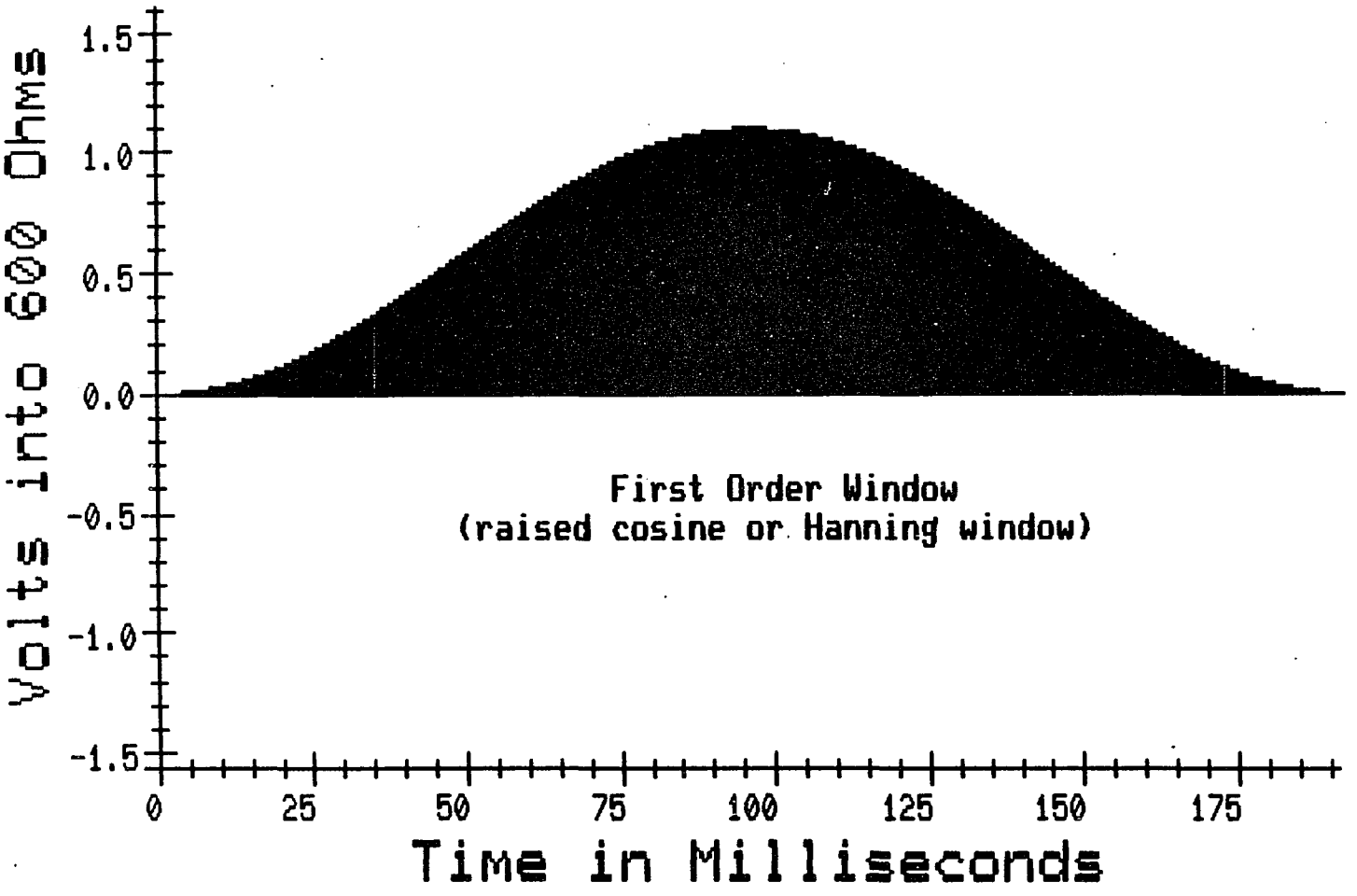
Volts into 600 Ohms
1.5
1.0
0.5
0.0
-0.5
-1.0
-1.5
0
25
50
75
100
125
150
175
Time in Milliseconds
First Order Window
(raised cosine or Hanning window)

Figure VI-23

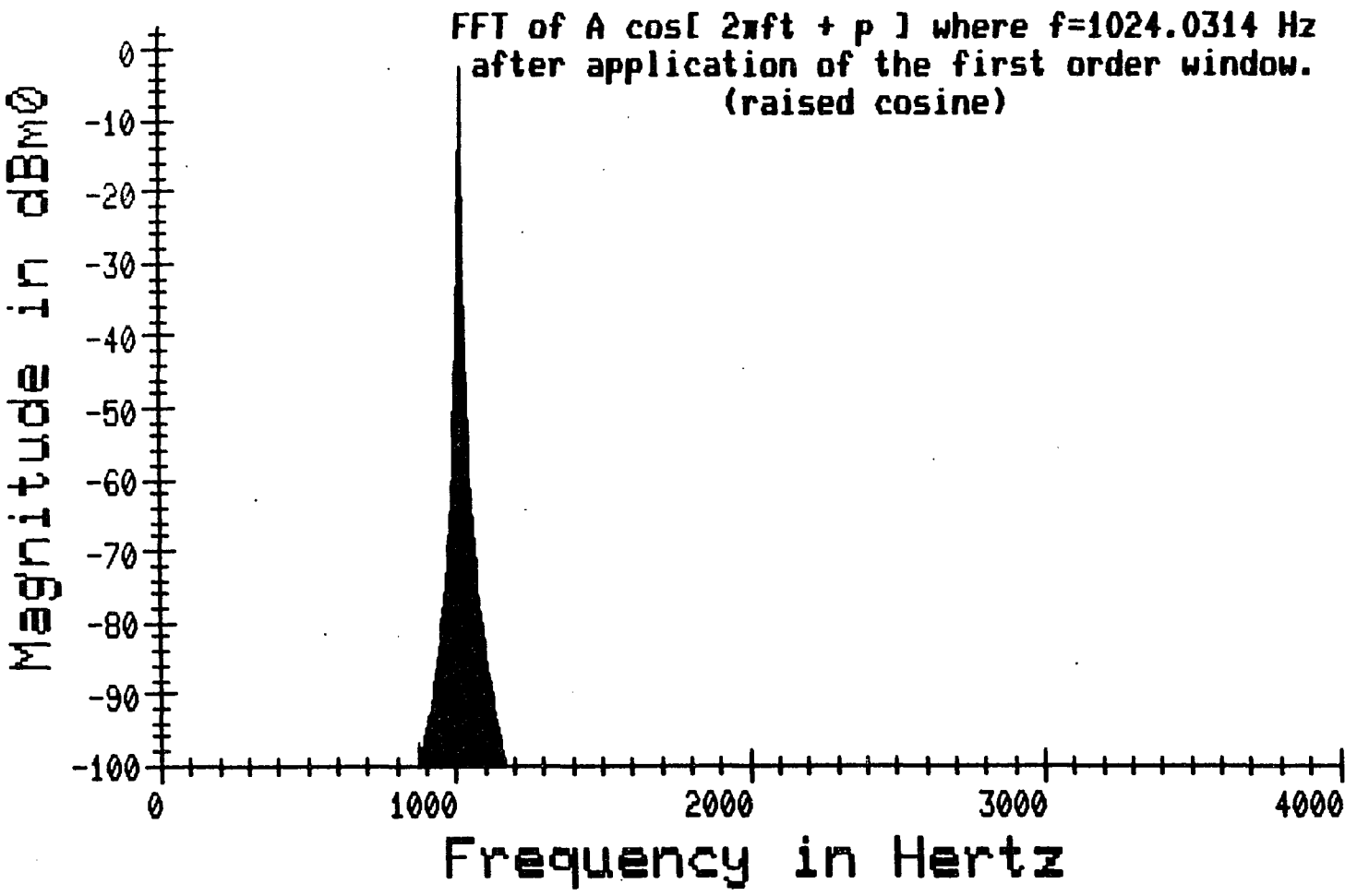
FFT of A cos[2πft + p] where f=1024.0314 Hz
after application of the first order window.
(raised cosine)
Magnitude in dBm0
0
-10
-20
-30
-40
-50
-60
-70
-80
-90
-100
0
1000
2000
3000
4000
Frequency in Hertz

Figure VI-24

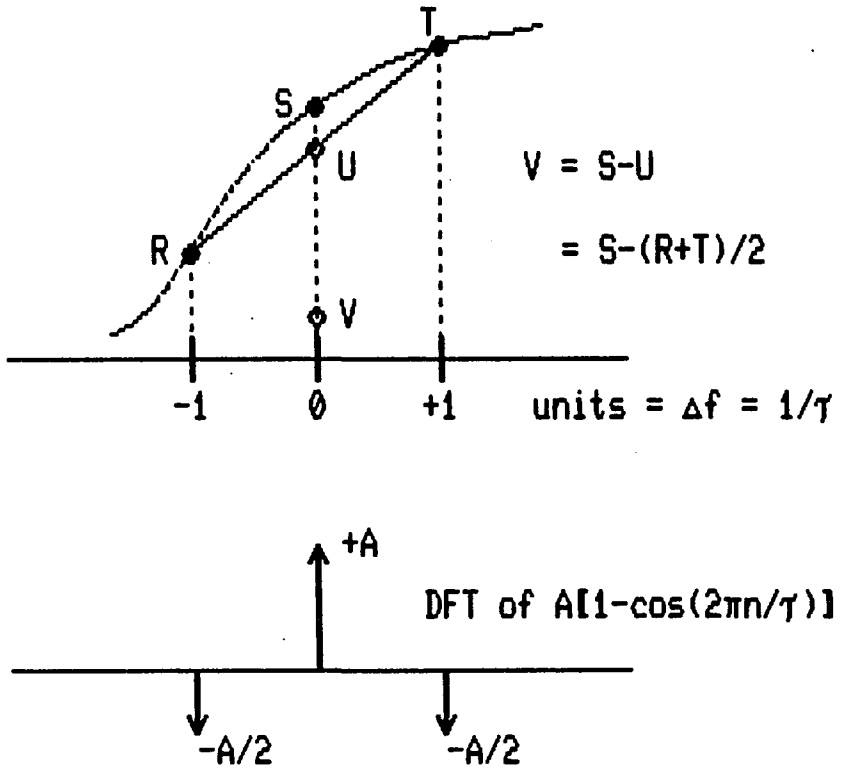

Application of the Hanning Window in the Frequency Domain

Figure VI-25

shape of the sinc-shaped curve with a straight line and remove some of the correlation between adjacent points. Note that near the peak of the example spectrum the shape becomes less linear and even has a point of discontinuity right at the peak. This will cause the error in the linear approximation, and hence the output values, to approach a maximum at this point. Since this operation is linear the propagation of the signal and noise through this 'filter' can be determined. Simply put, the power will propagate the same as the variance or as the square of the coefficients. Thus summing the squares of the coefficients yields

$$\frac{A^2}{4} + A^2 + \frac{A^2}{4} = \frac{3\,A^2}{2} \quad .$$

If the net power gain desired is one, then setting this equal to one and solving for A will result in the correct value to use for the weighting of the data window.

$$A = \sqrt{2/3} \quad .$$

This raised cosine window used a linear approximation to improve the spectral estimation so why not extend this by approximating the 1/x curve with higher order polynomials in an attempt to improve the spectral estimation even further. First the coefficients must be symmetrically placed on either side of the center value so that the inverse DFT and the resulting data window will be real. The next window then would include an extra point on each side of the center value as shown in Figure VI-26. This is being referred to as a third order window because 1/x is being approximated by a third order curve. Let x be the frequency point and y be the value of the input DFT at the frequency x. Then the third order equation would be

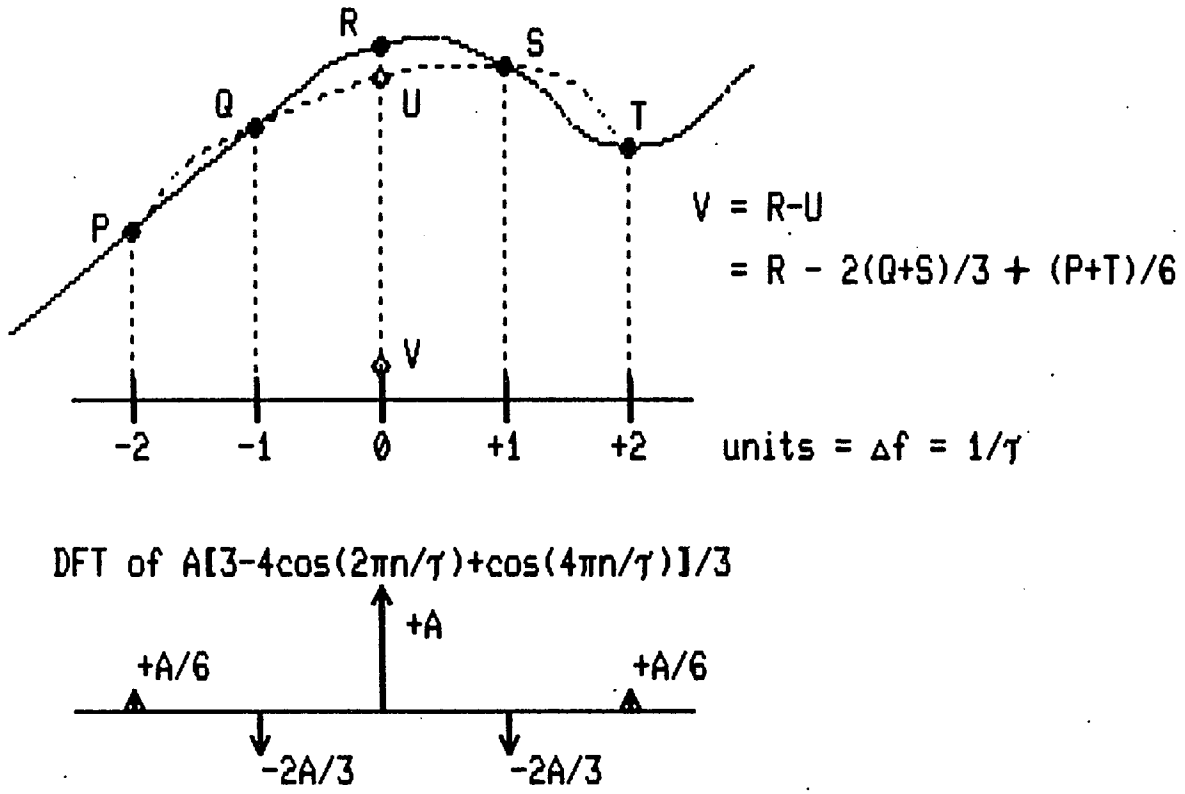

Application of a Third Order Window in the Frequency Domain

Figure VI-26

$$y = a x^3 + b x^2 + c x + d$$

Substituting each of the points P, Q, S and T into the equation will allow the coefficients to be determined.

$$P = -8\,a + 4\,b - 2\,c + d$$
$$Q = -a + b - c + d$$
$$S = a + b + c + d$$
$$T = 8\,a + 4\,b + 2\,c + d$$

Note that substituting x=0 into the equation gives the value of U=d. Therefore the above system of equations must be solved only for d. This solution results in

$$U = d = 2(Q + S)/3 - (P + T)/6$$

and the resulting output value V is given by

$$V = R - U = R - 2(Q + S)/3 + (P + T)/6.$$

This translates into the DFT shown in Figure VI-26 and the actual window in the time domain is

$$A[\ 1 - 2\cos(2\pi\, n/t)/3 + \cos(4\pi\, n/t)/6\ ]$$

To maintain a unity power gain through the windowing process the value of A must be determined.

$$1 = \frac{A^2}{36} + \frac{4\,A^2}{9} + A^2 + \frac{4\,A^2}{9} + \frac{A^2}{36} = \frac{35\,A^2}{18}$$

$$A = \sqrt{18/35}$$

The window so generated looks in the time domain as shown in Figure VI-27 and produces the spectral estimate of Figure VI-28 when applied to the example signal. It is observed

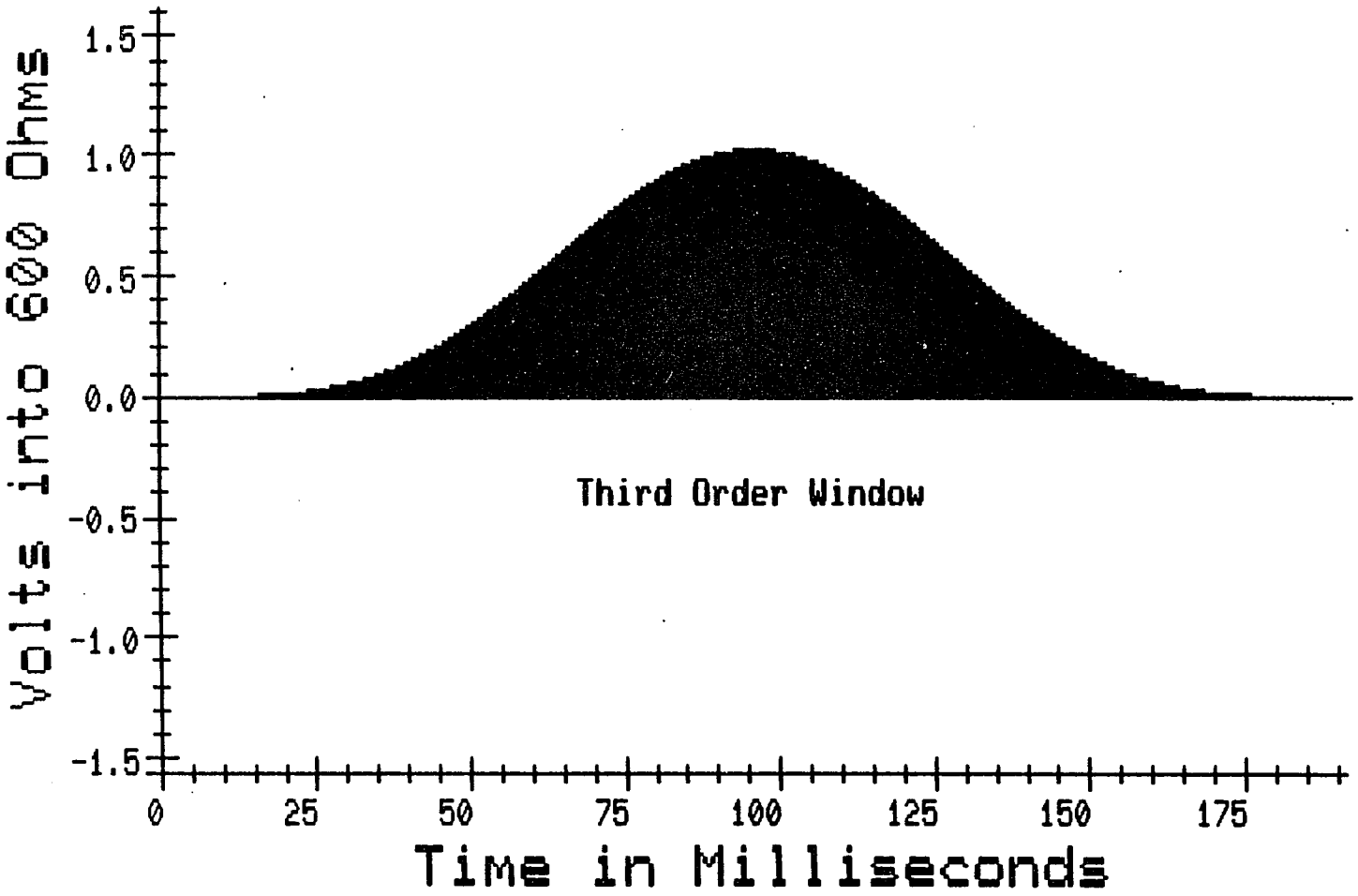
Volts into 600 Ohms
1.5
1.0
0.5
0.0
-0.5
-1.0
-1.5
Third Order Window
0
25
50
75
100
125
150
175
Time in Milliseconds

Figure VI-27

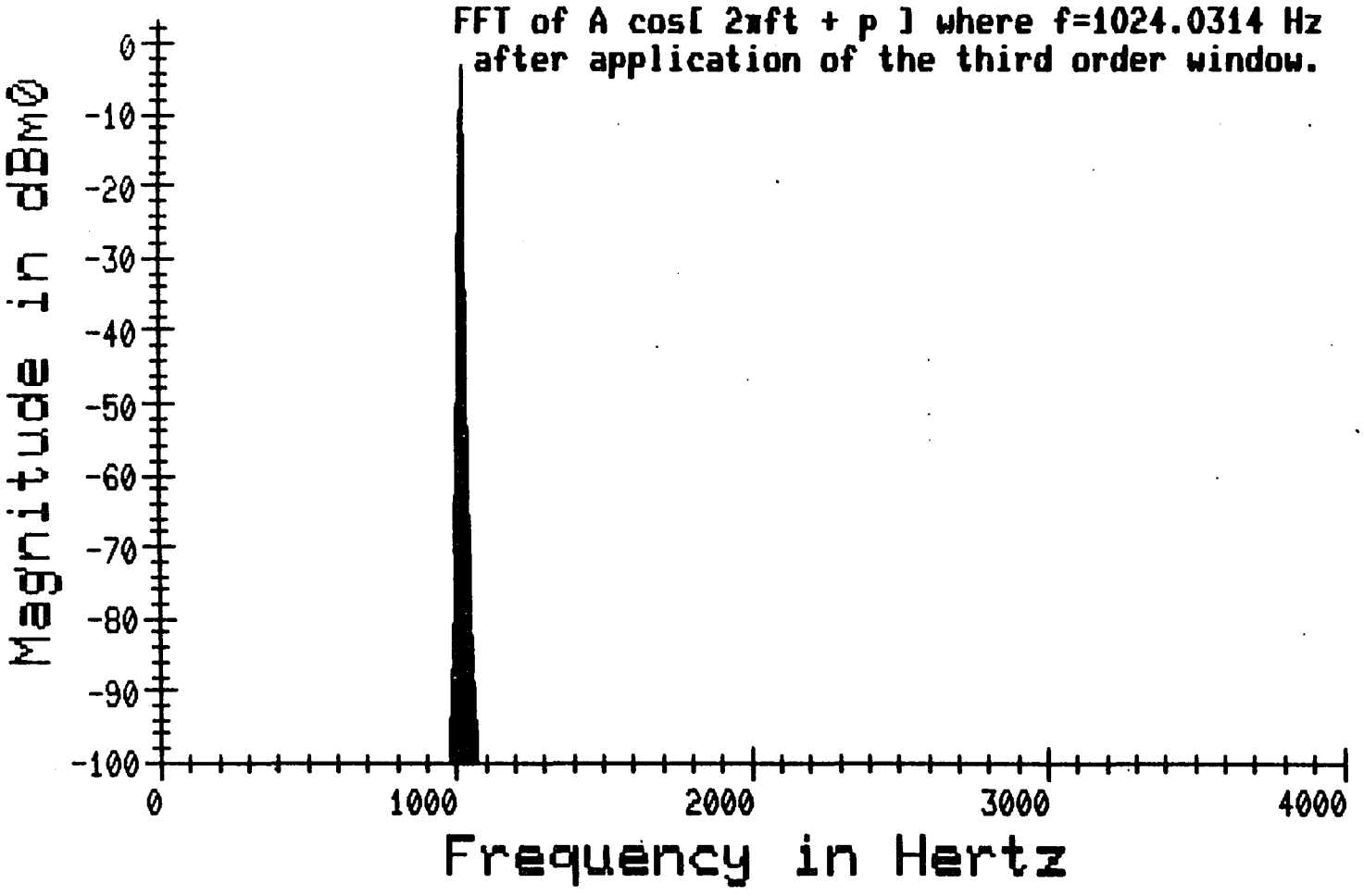
FFT of A cos[2πft + p] where f=1024.0314 Hz
after application of the third order window.
Magnitude in dBm0
0
-10
-20
-30
-40
-50
-60
-70
-80
-90
-100
0
1000
2000
3000
4000
Frequency in Hertz

Figure VI-28

that the spectral energy here is even more concentrated near the actual sine wave frequency.

This procedure may be carried out further to approximate the 1/x curve with any odd order polynomial producing a series of data windows. Figure VI-29 shows the time domain representation of the fifth order window which further narrows the spread of the spectral energy as shown in Figure VI-30. Figures VI-31 and 32 show the seventh order window and its effect on the spectrum. This improvement in the spectral estimation may seem to continue; however, the utility of the windows does not necessarily continue to improve for a practical application. Note, for example, in the extreme case of the nineteenth order window of Figure VI-33 and its effect in Figure VI-34 that the upper portion of the spectral spike continues to widen as the order of the window increases. The effect of this may be seen by taking an actual signal including the quantization noise and trying out the various windows.

VI-C.3 Application of Data Windows

Figure VI-35 shows the DFT of an actual channel response to the example signal which was used above. Note again the sinc-shaped spreading of the main spike which tends to obscure the quantization noise at least in the immediate vicinity. Figure VI-36 shows the effect on the time domain signal of the application of the raised cosine or first order window. Application of this window in the frequency domain, shown in Figure VI-37, drastically shrinks the spectral spreading and makes the adjacent noise much less obscure. Only eight spectral lines in the main signal spike protrude above the level of the remaining noise. If

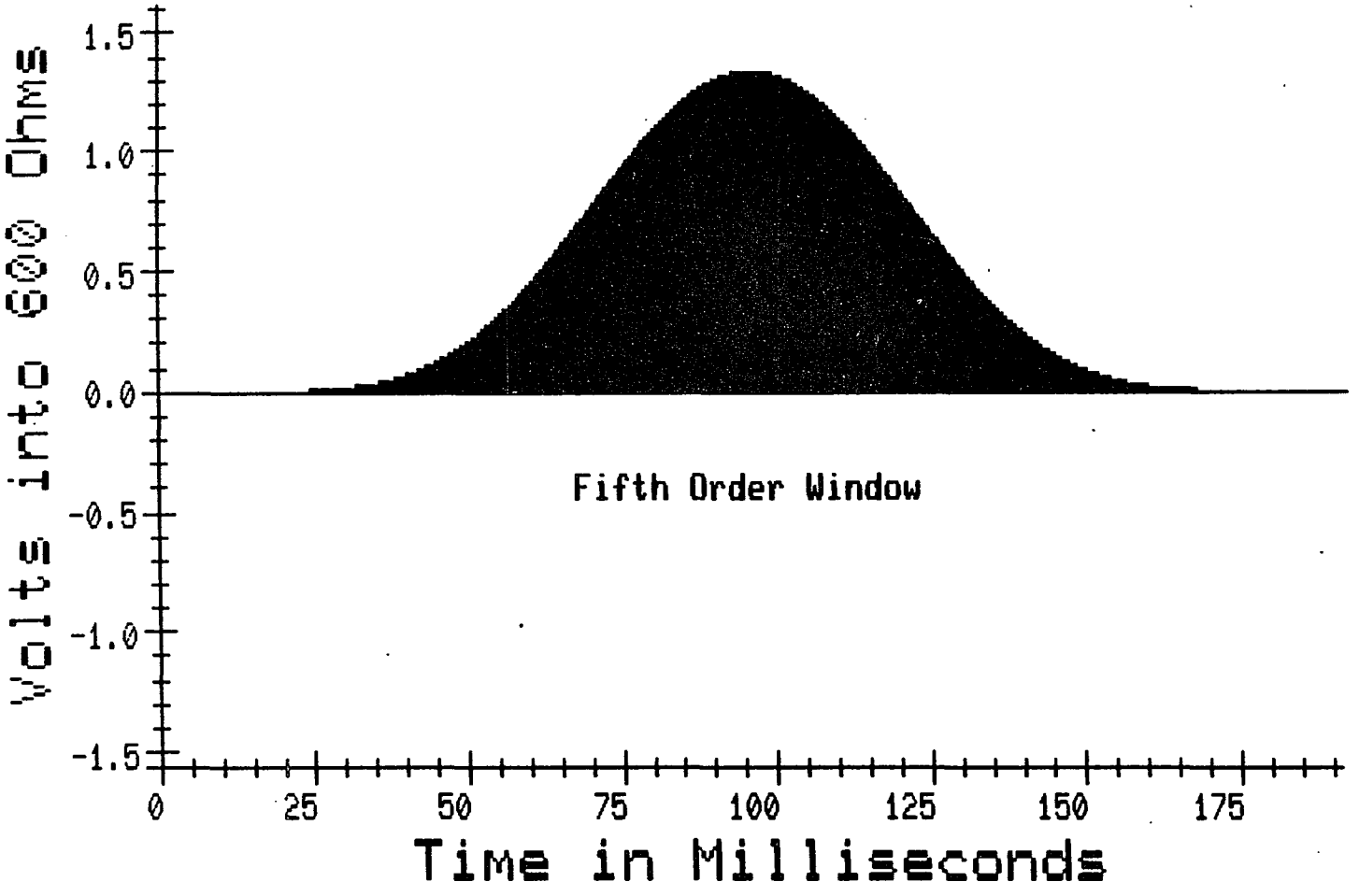
Volts into 600 Ohms
1.5
1.0
0.5
0.0
-0.5
-1.0
-1.5
Fifth Order Window
0
25
50
75
100
125
150
175
Time in Milliseconds

Figure VI-29

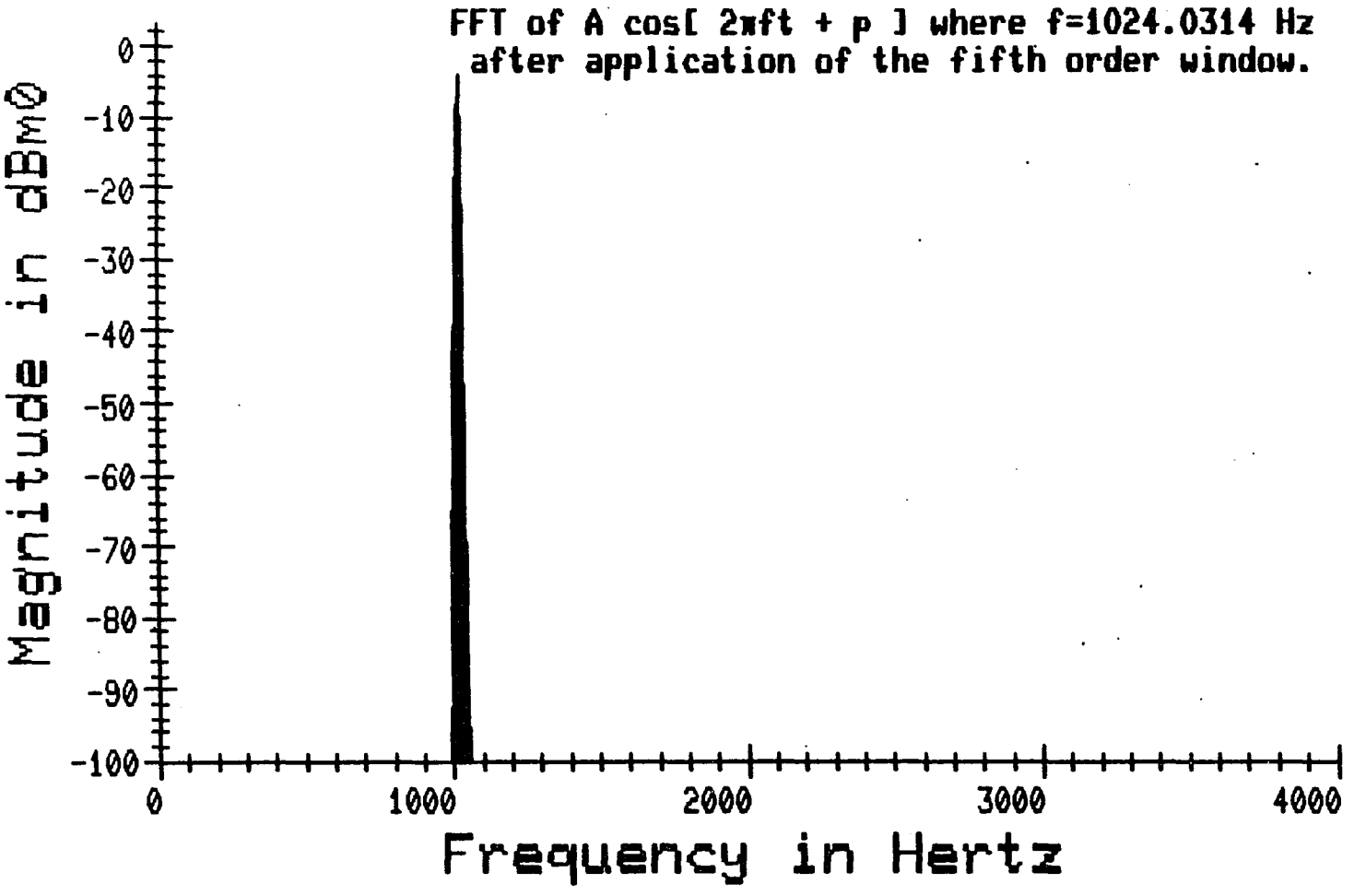
FFT of A cos[2πft + p] where f=1024.0314 Hz
after application of the fifth order window.
Magnitude in dBm0
0
-10
-20
-30
-40
-50
-60
-70
-80
-90
-100
0
1000
2000
3000
4000
Frequency in Hertz

Figure VI-30

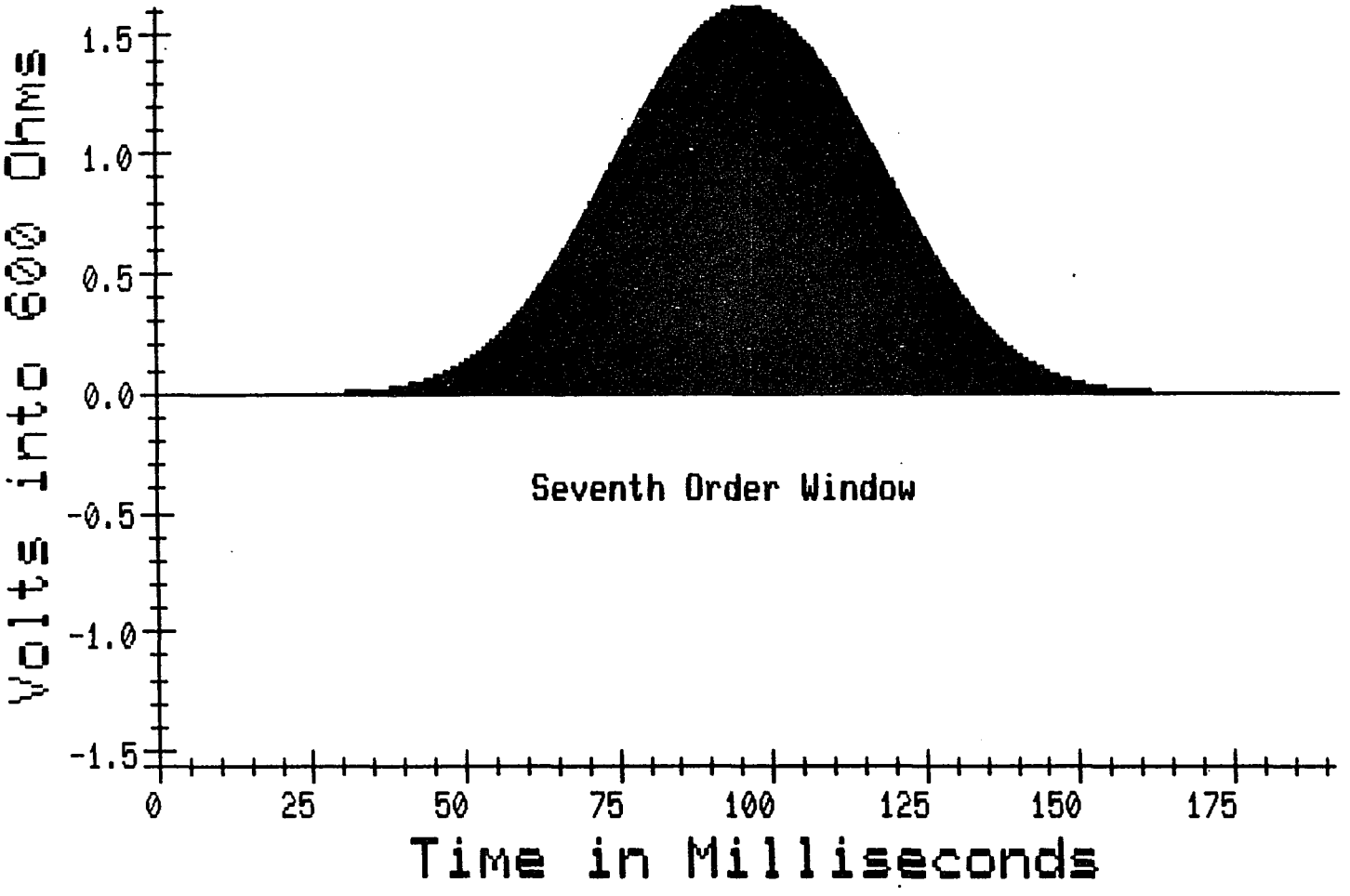
Volts into 600 Ohms
1.5
1.0
0.5
0.0
-0.5
-1.0
-1.5
0
25
50
75
100
125
150
175
Time in Milliseconds
Seventh Order Window

Figure VI-31

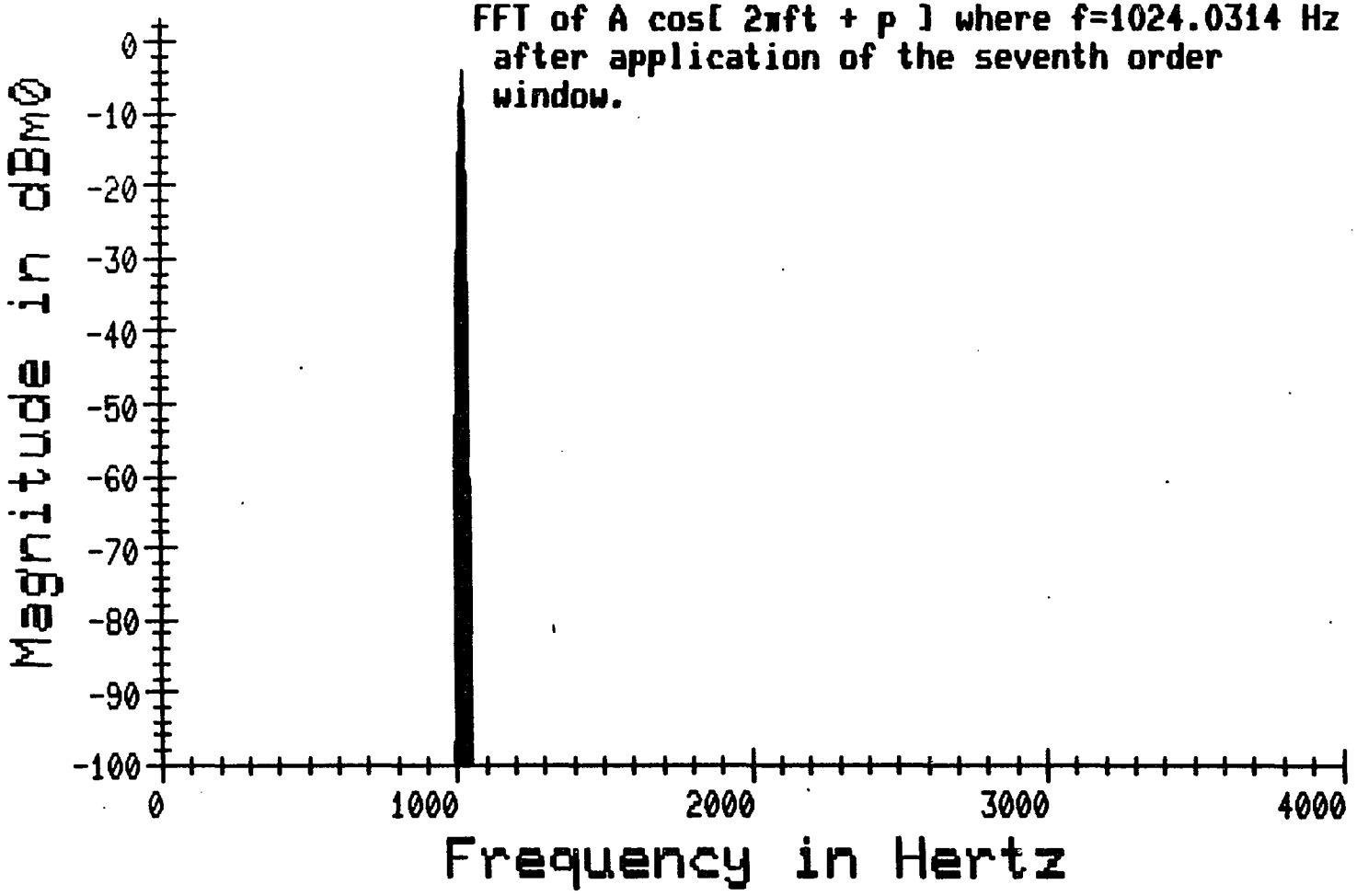
FFT of A cos[2πft + p] where f=1024.0314 Hz
after application of the seventh order
window.
Magnitude in dBmΩ
0
-10
-20
-30
-40
-50
-60
-70
-80
-90
-100
0
1000
2000
3000
4000
Frequency in Hertz

Figure VI-32

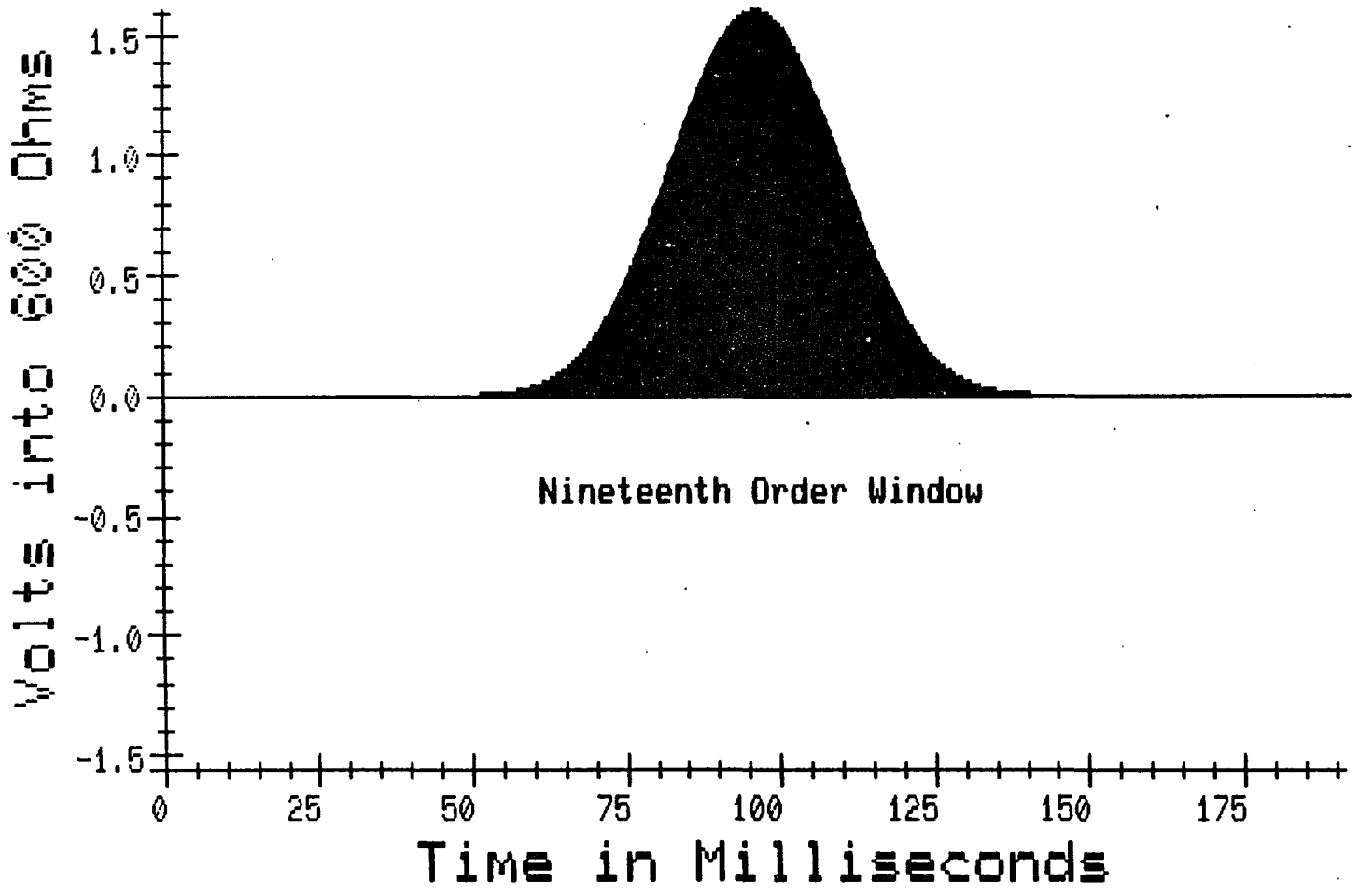
Volts into 600 Ohms
1.5
1.0
0.5
0.0
-0.5
-1.0
-1.5
Nineteenth Order Window
0
25
50
75
100
125
150
175
Time in Milliseconds

Figure VI-33

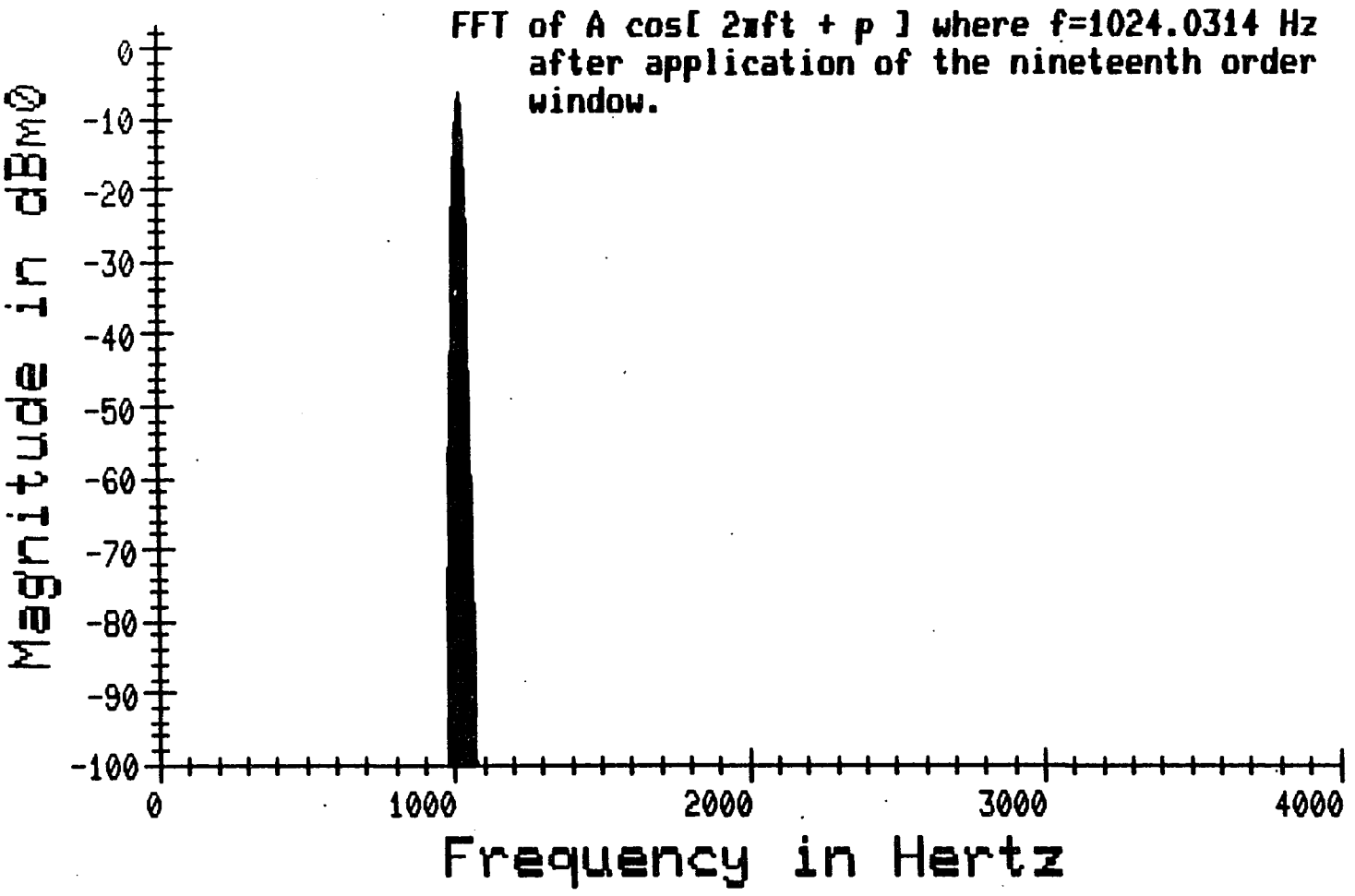
FFT of A cos[2πft + p] where f=1024.0314 Hz
after application of the nineteenth order
window.
Magnitude in dBmΩ
0
-10
-20
-30
-40
-50
-60
-70
-80
-90
-100
0
1000
2000
3000
4000
Frequency in Hertz

Figure VI-34

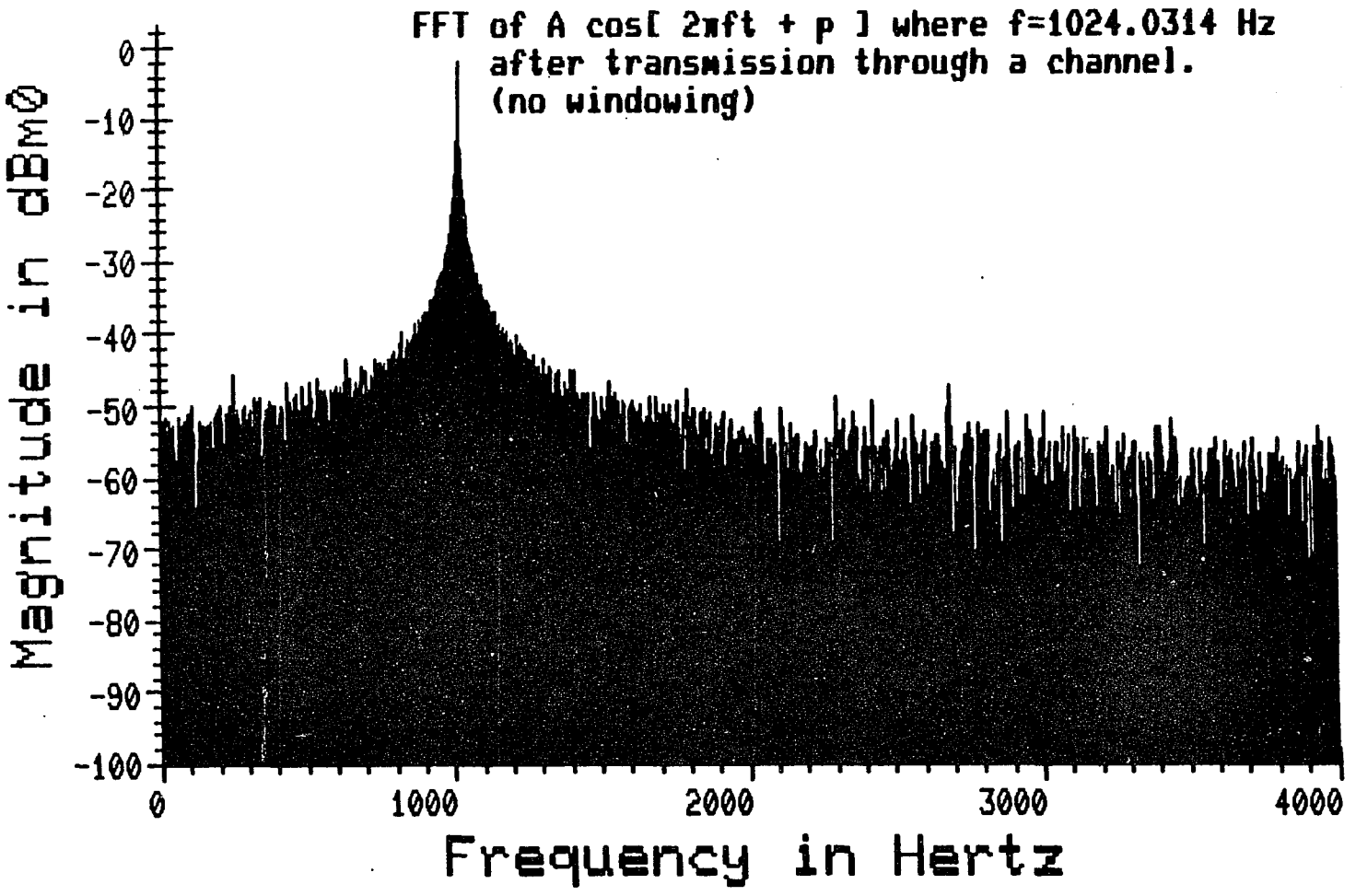
FFT of A cos[2πft + p] where f=1024.0314 Hz
after transmission through a channel.
(no windowing)
Magnitude in dBm0
0
-10
-20
-30
-40
-50
-60
-70
-80
-90
-100
0
1000
2000
3000
4000
Frequency in Hertz

Figure VI-35

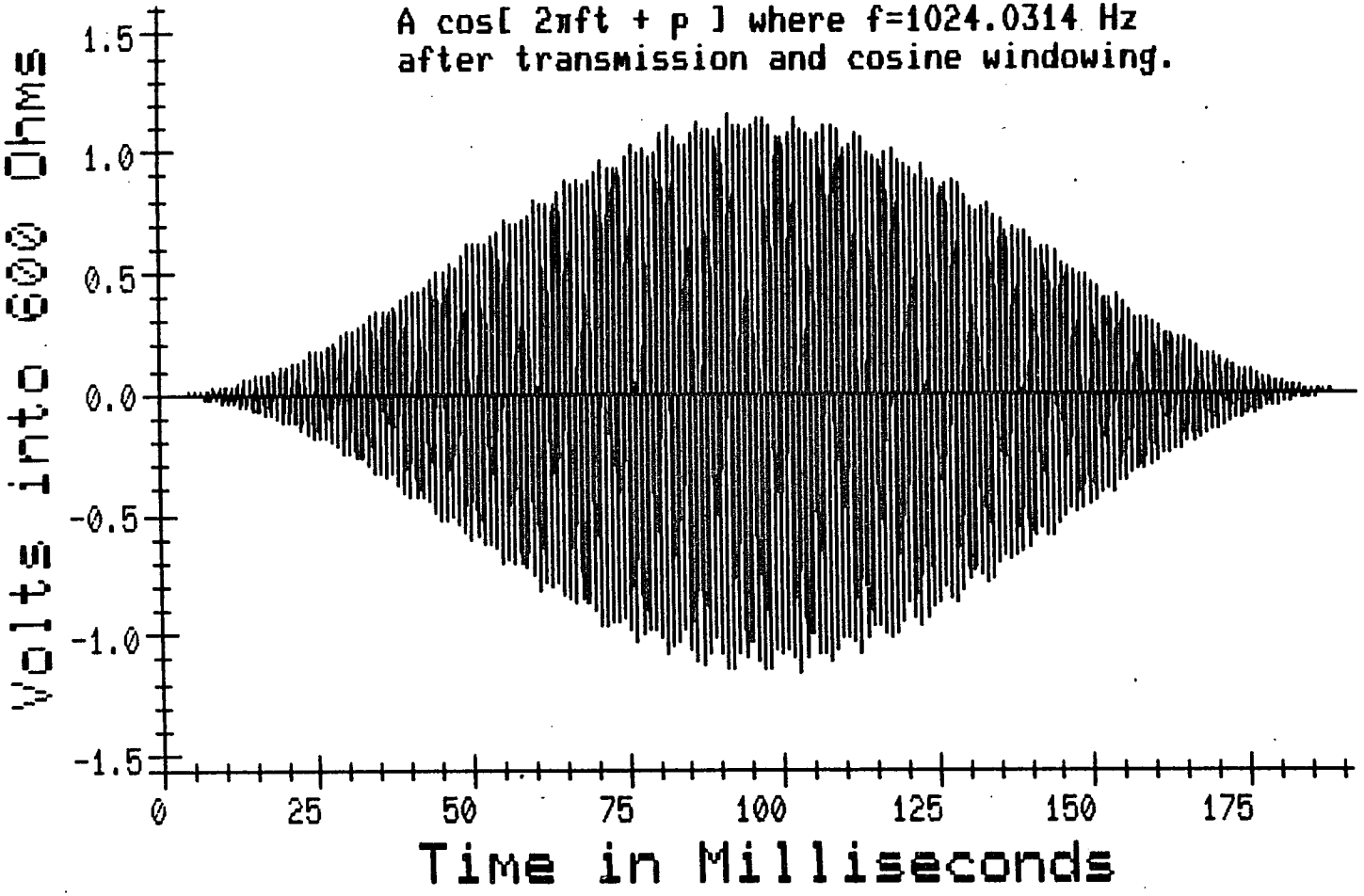
A cos[2πft + p] where f=1024.0314 Hz
after transmission and cosine windowing.
Volts into 600 Ohms
1.5
1.0
0.5
0.0
-0.5
-1.0
-1.5
0
25
50
75
100
125
150
175
Time in Milliseconds

Figure VI-36

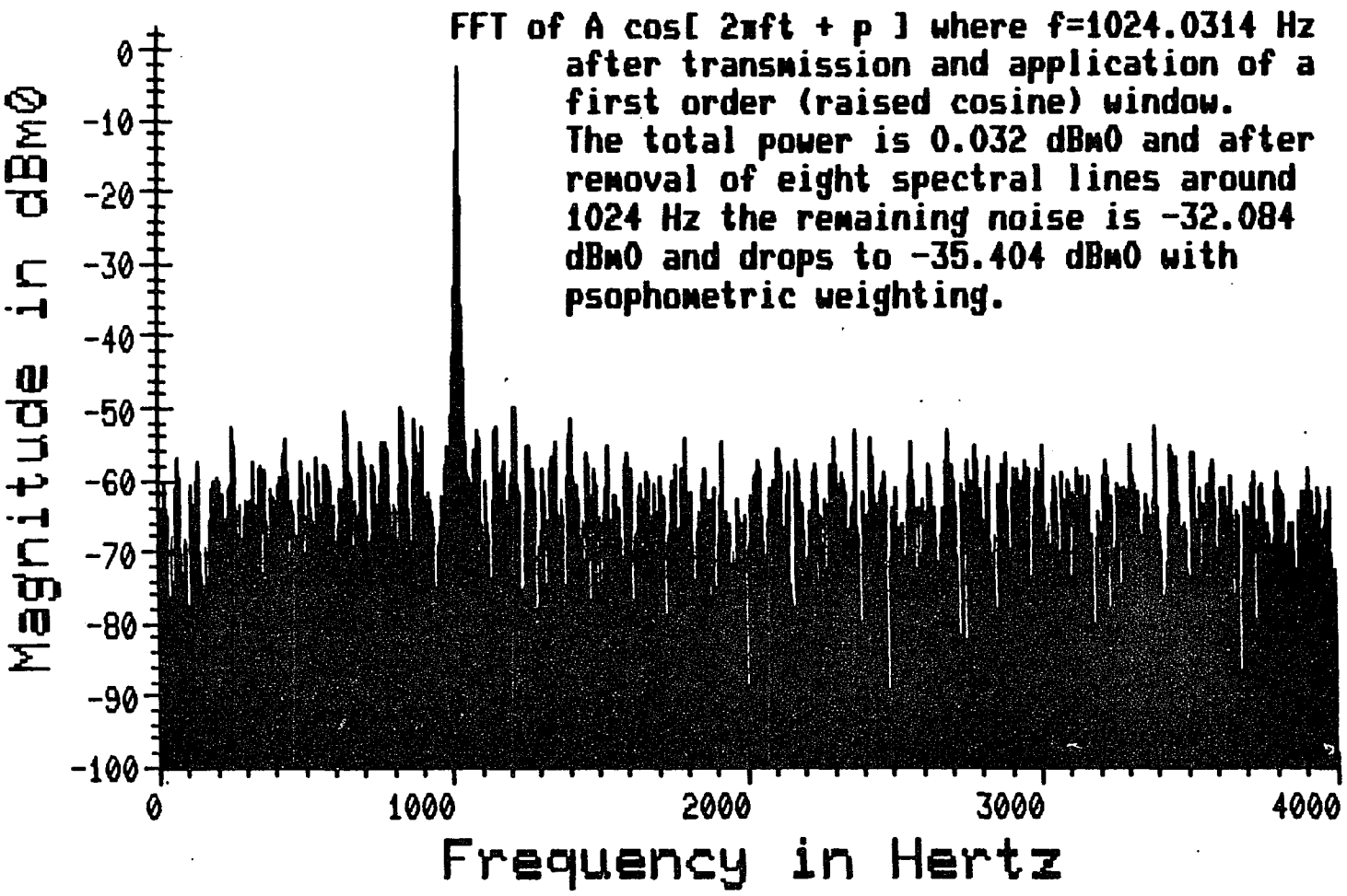
FFT of A cos[2πft + p] where f=1024.0314 Hz
after transmission and application of a
first order (raised cosine) window.
The total power is 0.032 dBm0 and after
removal of eight spectral lines around
1024 Hz the remaining noise is -32.084
dBm0 and drops to -35.404 dBm0 with
psophometric weighting.
Magnitude in dBm0
0
-10
-20
-30
-40
-50
-60
-70
-80
-90
-100
0
1000
2000
3000
4000
Frequency in Hertz

Figure VI-37

the power in these eight lines is totalled the signal appears to have a level of 0.032 dBm0 and the remaining noise power totals to -32.084 dBm0. Noise measurements are normally made with a psophometric weighting which will be described in the next chapter. Notice that the noise spikes appear to have become more correlated. This is due to the 'filtering' action caused by the application of the window. Since only the total noise power is of concern here, this correlation will not effect the measurement. Figure VI-38 shows the result of applying the third order window. Here the majority of the signal power is contained in only six spectral lines. The removal of fewer lines should improve the estimate of the noise power slightly since less noise is being masked by the signal. The widening of the upper part of the spectral spike as higher order windows are used becomes evident in Figure VI-39 where the fifth order window is applied. Here the energy in the main spike is once again spread into eight spectral lines which protrude above the noise. It would seem then that the higher order windows will only be useful when the expected quantization noise is much lower than it is here. Where there are only eight bits used here to transmit the data, it is not difficult to imagine an application where the quantization noise is considerably reduced and higher order windows may be useful.

Figure VI-40 shows the application of the seventh order window. As expected further widening of the main spike is experienced. Figure VI-41 is included to illustrate the extreme case where a nineteenth order window is employed. Note the continued widening of the main spike and the extreme correlation of the quantization noise; however, even under these conditions a reasonable estimation of the signal

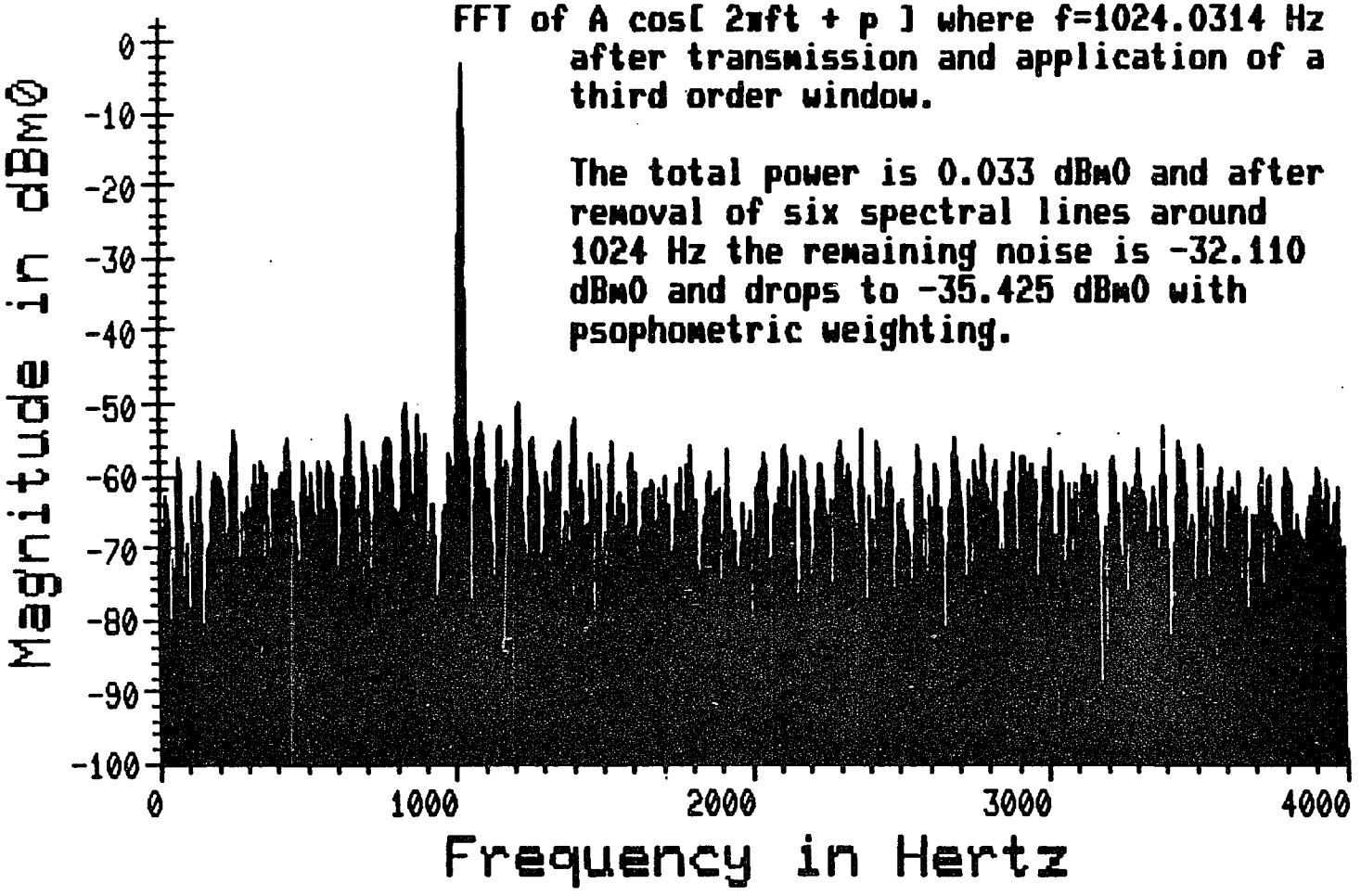
FFT of A cos[2πft + p] where f=1024.0314 Hz after transmission and application of a third order window.
The total power is 0.033 dBm0 and after removal of six spectral lines around 1024 Hz the remaining noise is -32.110 dBm0 and drops to -35.425 dBm0 with psophometric weighting.
Magnitude in dBm0
0
-10
-20
-30
-40
-50
-60
-70
-80
-90
-100
0
1000
2000
3000
4000
Frequency in Hertz

Figure VI-38

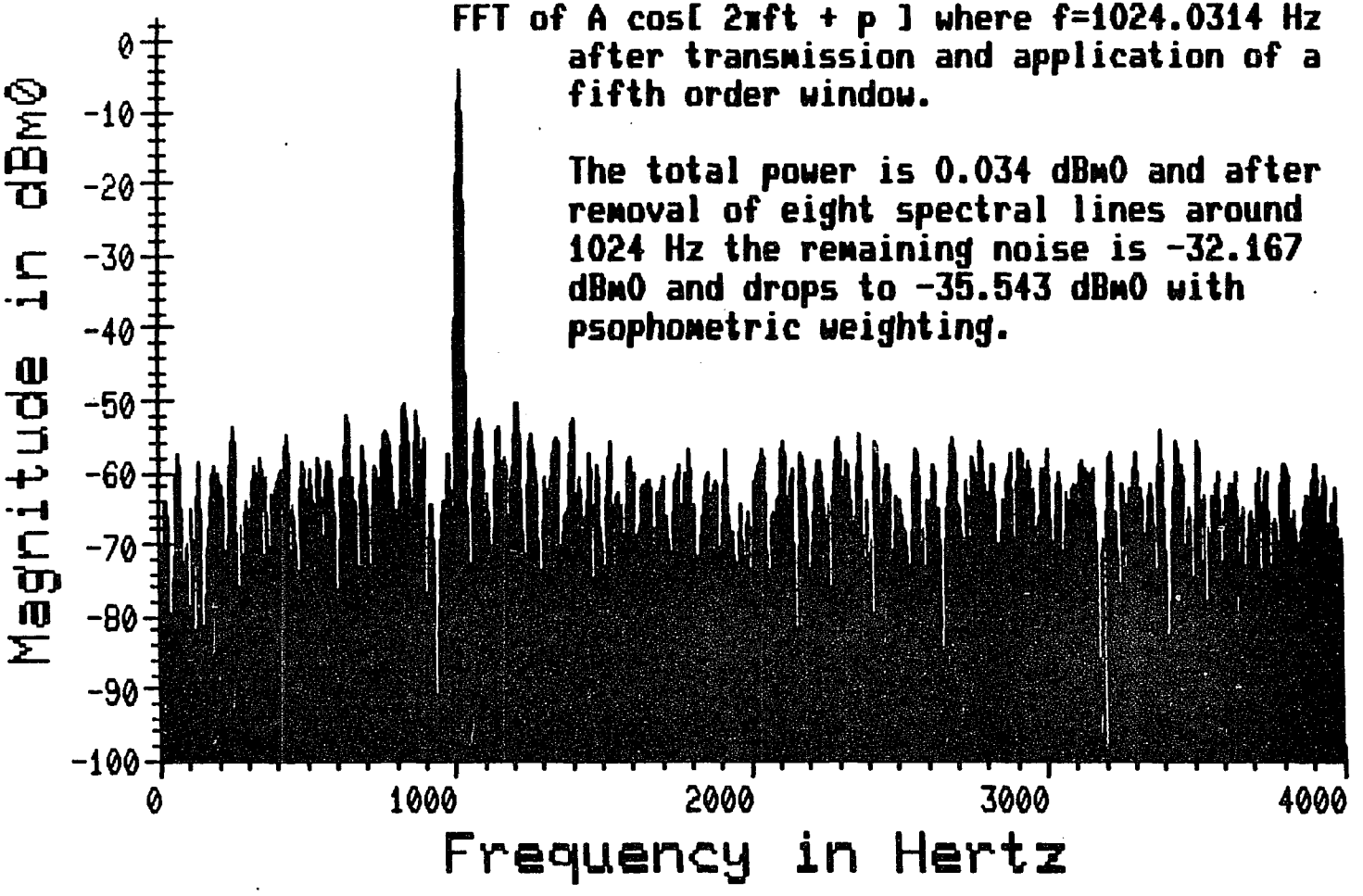
FFT of A cos[2πft + p] where f=1024.0314 Hz after transmission and application of a fifth order window.
The total power is 0.034 dBm0 and after removal of eight spectral lines around 1024 Hz the remaining noise is -32.167 dBm0 and drops to -35.543 dBm0 with psophometric weighting.
Magnitude in dBm0
0
-10
-20
-30
-40
-50
-60
-70
-80
-90
-100
0
1000
2000
3000
4000
Frequency in Hertz

Figure VI-39

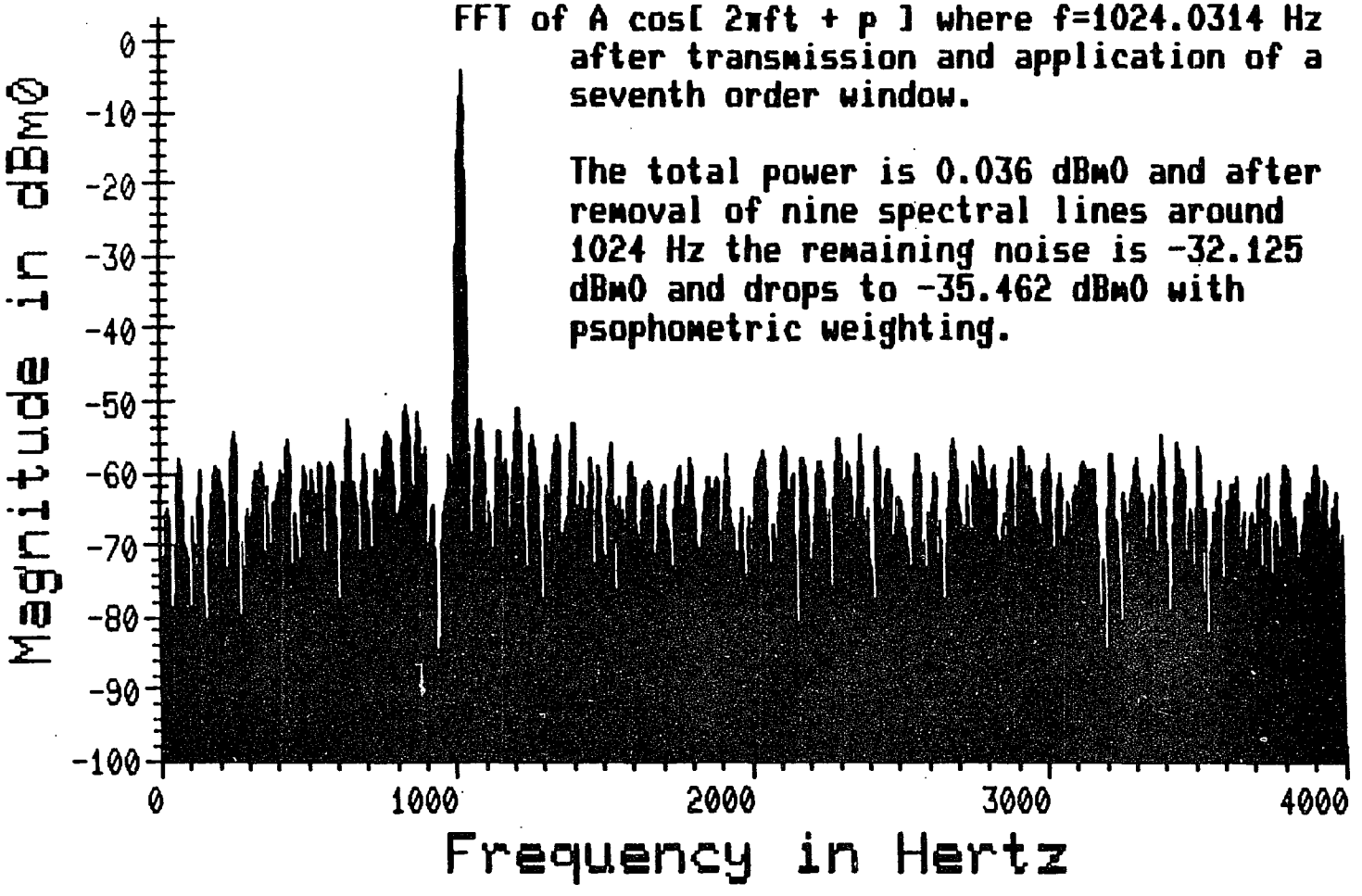
FFT of A cos[2πft + p] where f=1024.0314 Hz after transmission and application of a seventh order window.
The total power is 0.036 dBm0 and after removal of nine spectral lines around 1024 Hz the remaining noise is -32.125 dBm0 and drops to -35.462 dBm0 with psophometric weighting.
Magnitude in dBm0
0
-10
-20
-30
-40
-50
-60
-70
-80
-90
-100
0
1000
2000
3000
4000
Frequency in Hertz

Figure VI-40

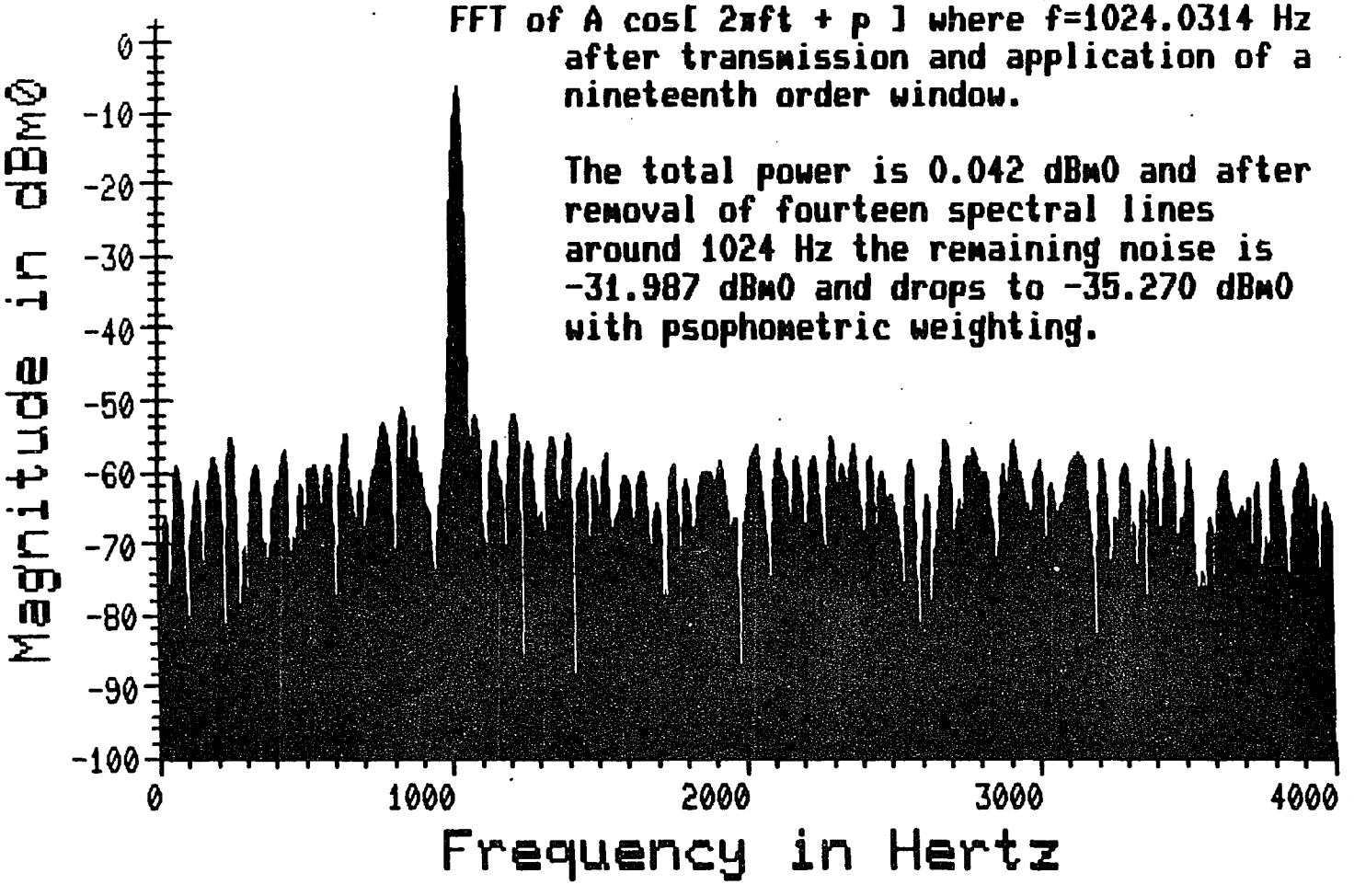
FFT of A cos[2πft + p] where f=1024.0314 Hz
after transmission and application of a
nineteenth order window.
The total power is 0.042 dBm0 and after
removal of fourteen spectral lines
around 1024 Hz the remaining noise is
-31.987 dBm0 and drops to -35.270 dBm0
with psophometric weighting.
Magnitude in dBm0
0
-10
-20
-30
-40
-50
-60
-70
-80
-90
-100
0
1000
2000
3000
4000
Frequency in Hertz

Figure VI-41

power and the noise level is obtained.

As a check on the validity of these estimates and on the propagation of the correct power levels through these windows, another signal which could be properly measured without windowing was subjected to the same operations. Figure VI-42 shows this signal after transmission through the channel. The series of Figures VI-43, 44 and 45 show the effects of applying some of the data windows to this signal. The signal was measured to within 0.007 dB even in the extreme case and the noise was measured to within 0.36 dB. Obviously the best choice in this case is to use no window at all, but in the general case the third order window is sufficient. A nice demonstration of the use of the data window is seen in Figures VI-46 and 47 where four sine wave components combine to obscure each other and the surrounding noise; however, the third order window brings them out and restores the adjacent noise. This last example was included to illustrate that these techniques work just as well on other than single sine wave signals.

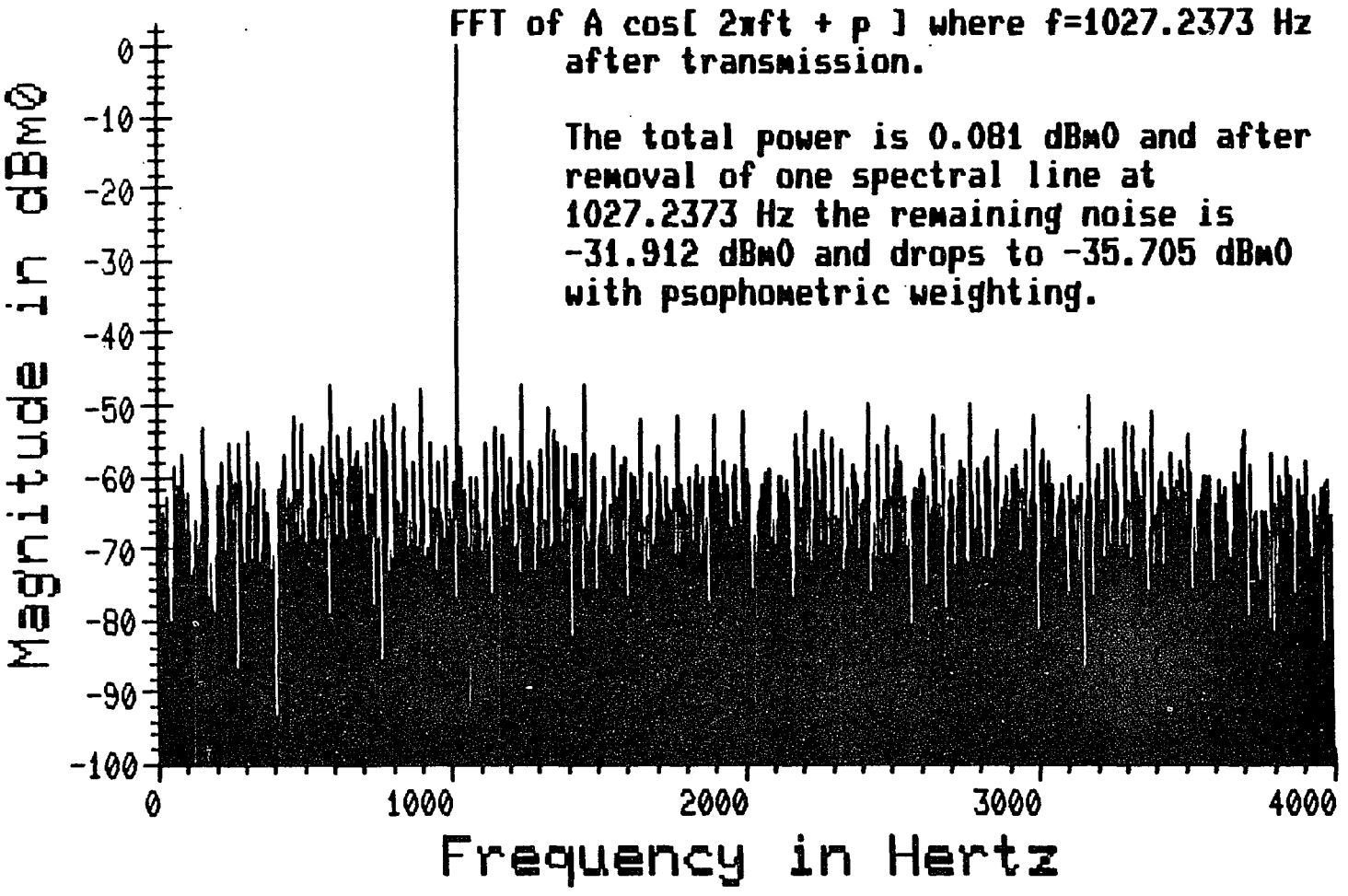
FFT of A cos[2πft + p] where f=1027.2373 Hz
after transmission.
The total power is 0.081 dBm0 and after
removal of one spectral line at
1027.2373 Hz the remaining noise is
-31.912 dBm0 and drops to -35.705 dBm0
with psophometric weighting.
Magnitude in dBm0
0
-10
-20
-30
-40
-50
-60
-70
-80
-90
-100
0
1000
2000
3000
4000
Frequency in Hertz

Figure VI-42

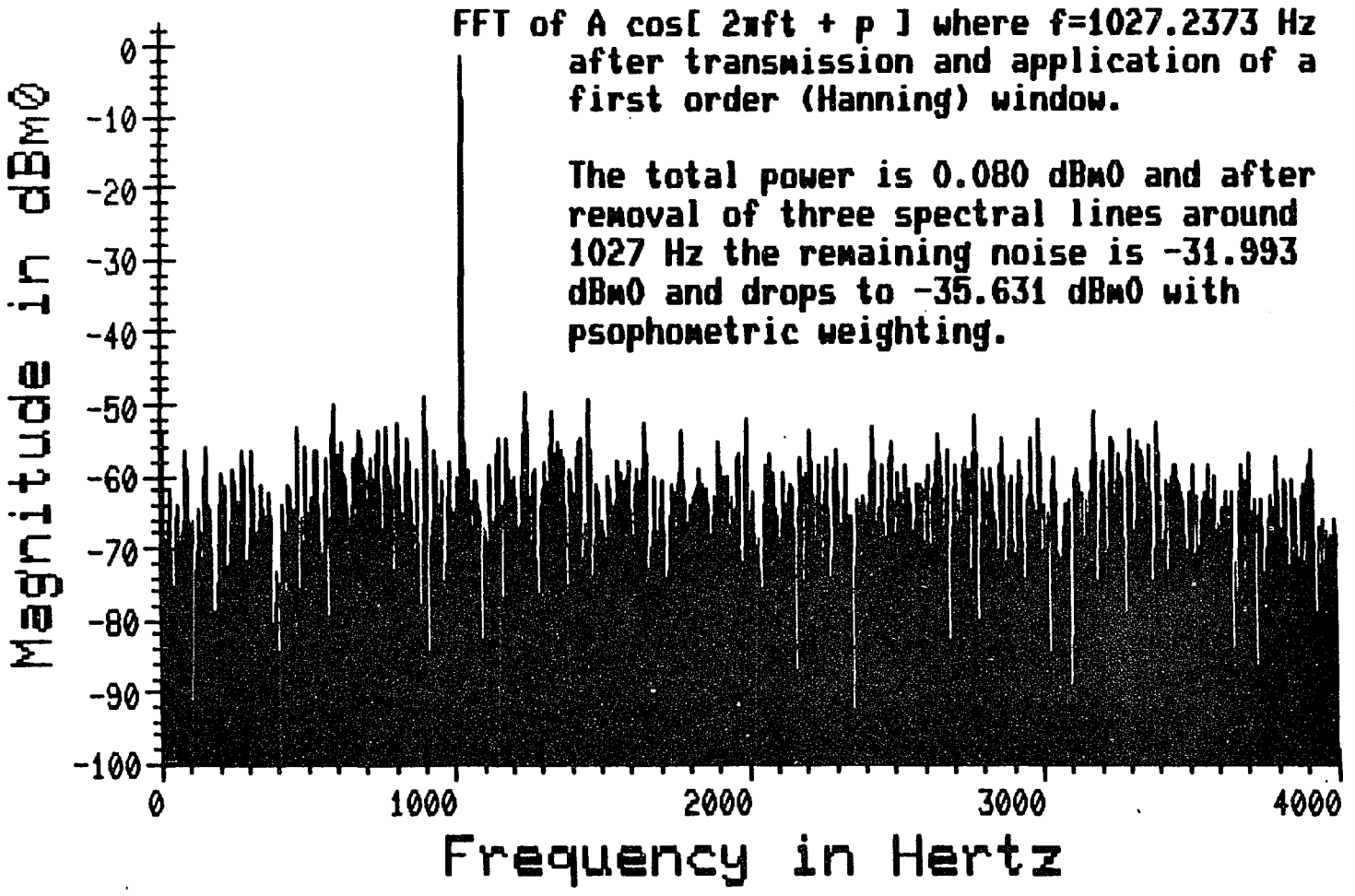
FFT of A cos[2πft + p] where f=1027.2373 Hz after transmission and application of a first order (Hanning) window.
The total power is 0.080 dBm0 and after removal of three spectral lines around 1027 Hz the remaining noise is -31.993 dBm0 and drops to -35.631 dBm0 with psophometric weighting.
Magnitude in dBm0
0
-10
-20
-30
-40
-50
-60
-70
-80
-90
-100
0
1000
2000
3000
4000
Frequency in Hertz

Figure VI-43

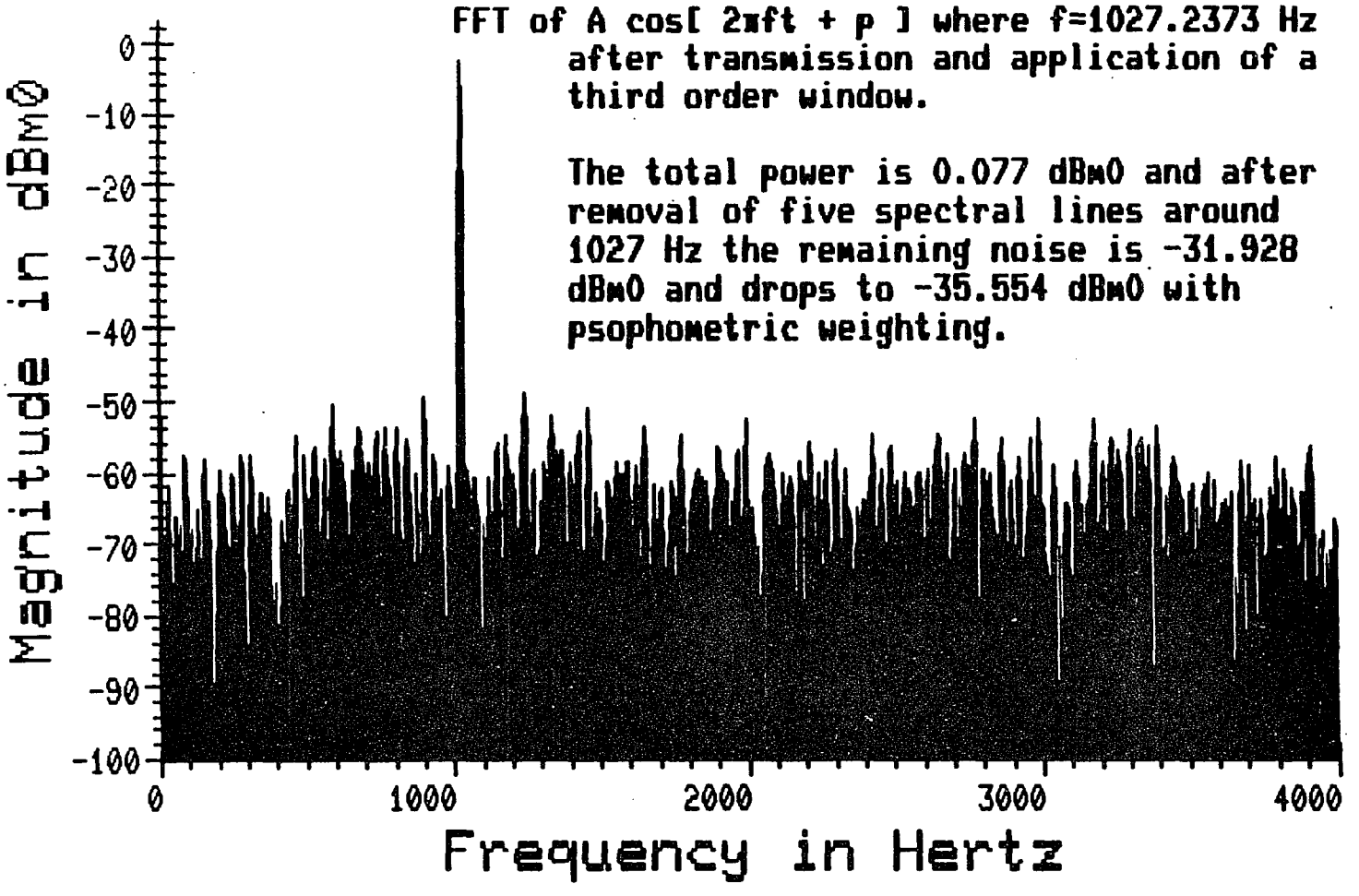
FFT of A cos[2πft + p] where f=1027.2373 Hz
after transmission and application of a
third order window.
The total power is 0.077 dBm0 and after
removal of five spectral lines around
1027 Hz the remaining noise is -31.928
dBm0 and drops to -35.554 dBm0 with
psophometric weighting.
Magnitude in dBm0
0
-10
-20
-30
-40
-50
-60
-70
-80
-90
-100
0
1000
2000
3000
4000
Frequency in Hertz

Figure VI-44

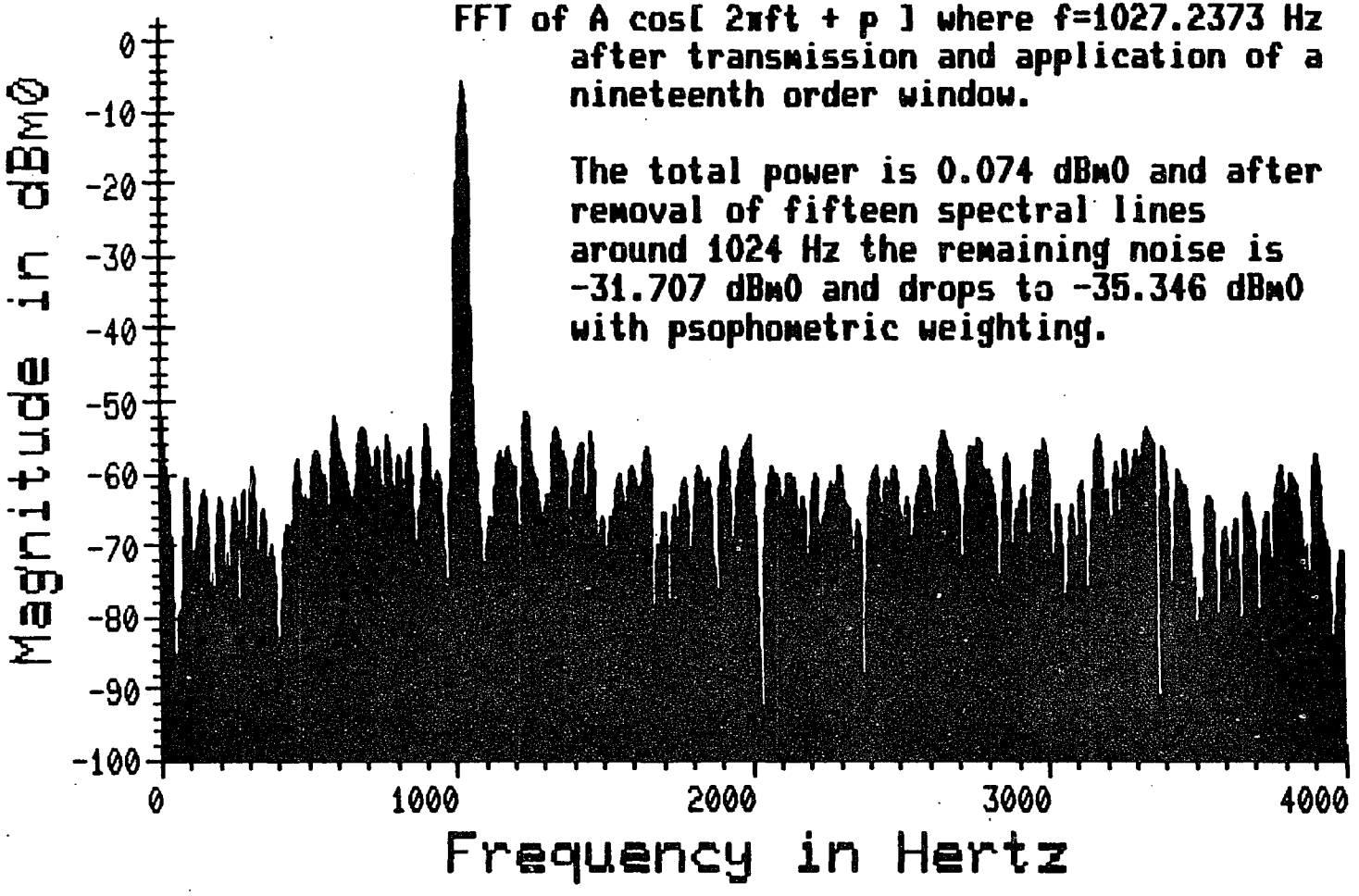
FFT of A cos[2πft + p] where f=1027.2373 Hz
after transmission and application of a
nineteenth order window.
The total power is 0.074 dBm0 and after
removal of fifteen spectral lines
around 1024 Hz the remaining noise is
-31.707 dBm0 and drops to -35.346 dBm0
with psophometric weighting.
Magnitude in dBm0
0
-10
-20
-30
-40
-50
-60
-70
-80
-90
-100
0
1000
2000
3000
4000
Frequency in Hertz

Figure VI-45

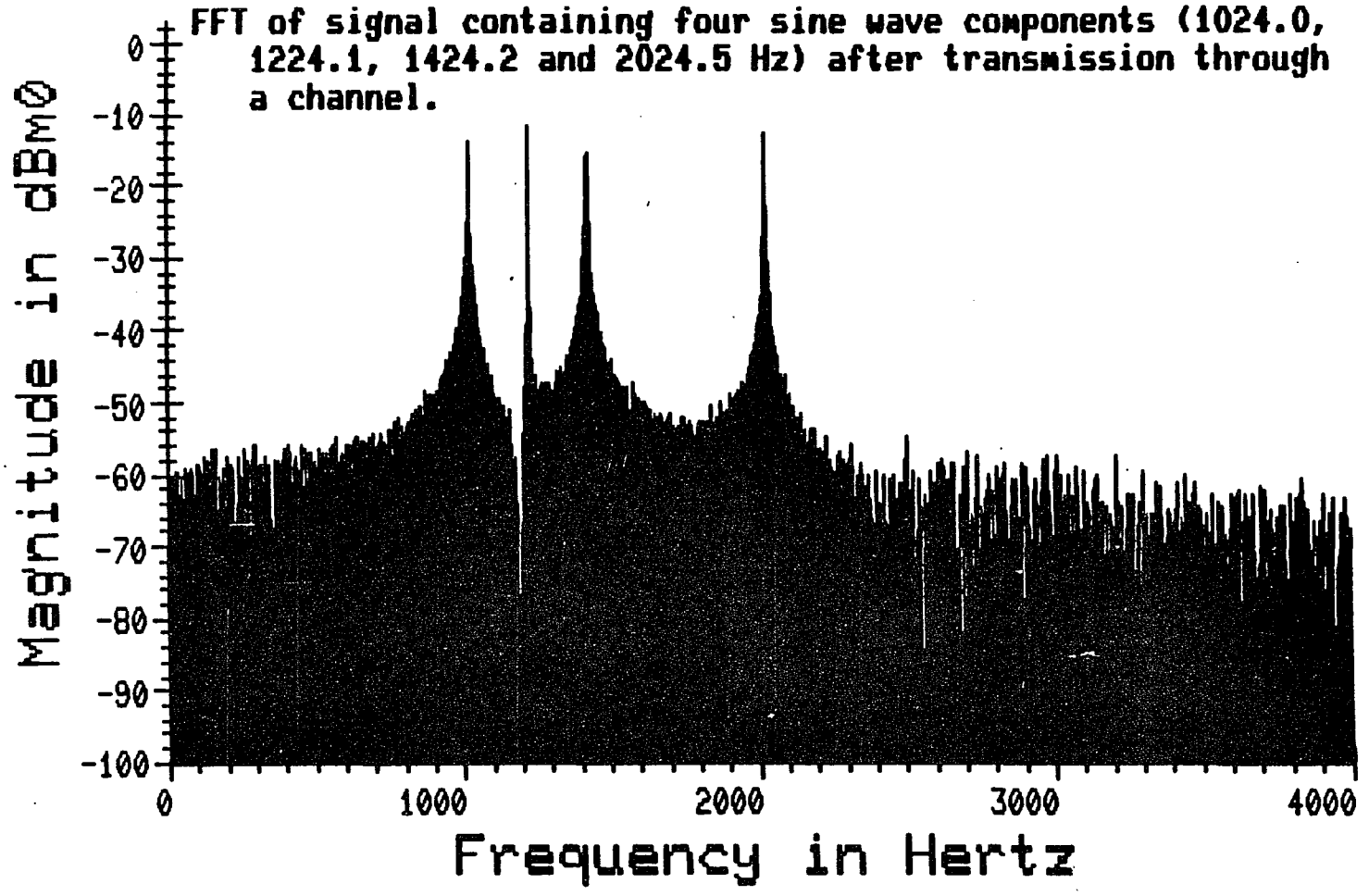
FFT of signal containing four sine wave components (1024.0, 1224.1, 1424.2 and 2024.5 Hz) after transmission through a channel.
Magnitude in dBm0
0
-10
-20
-30
-40
-50
-60
-70
-80
-90
-100
0
1000
2000
3000
4000
Frequency in Hertz

Figure VI-46

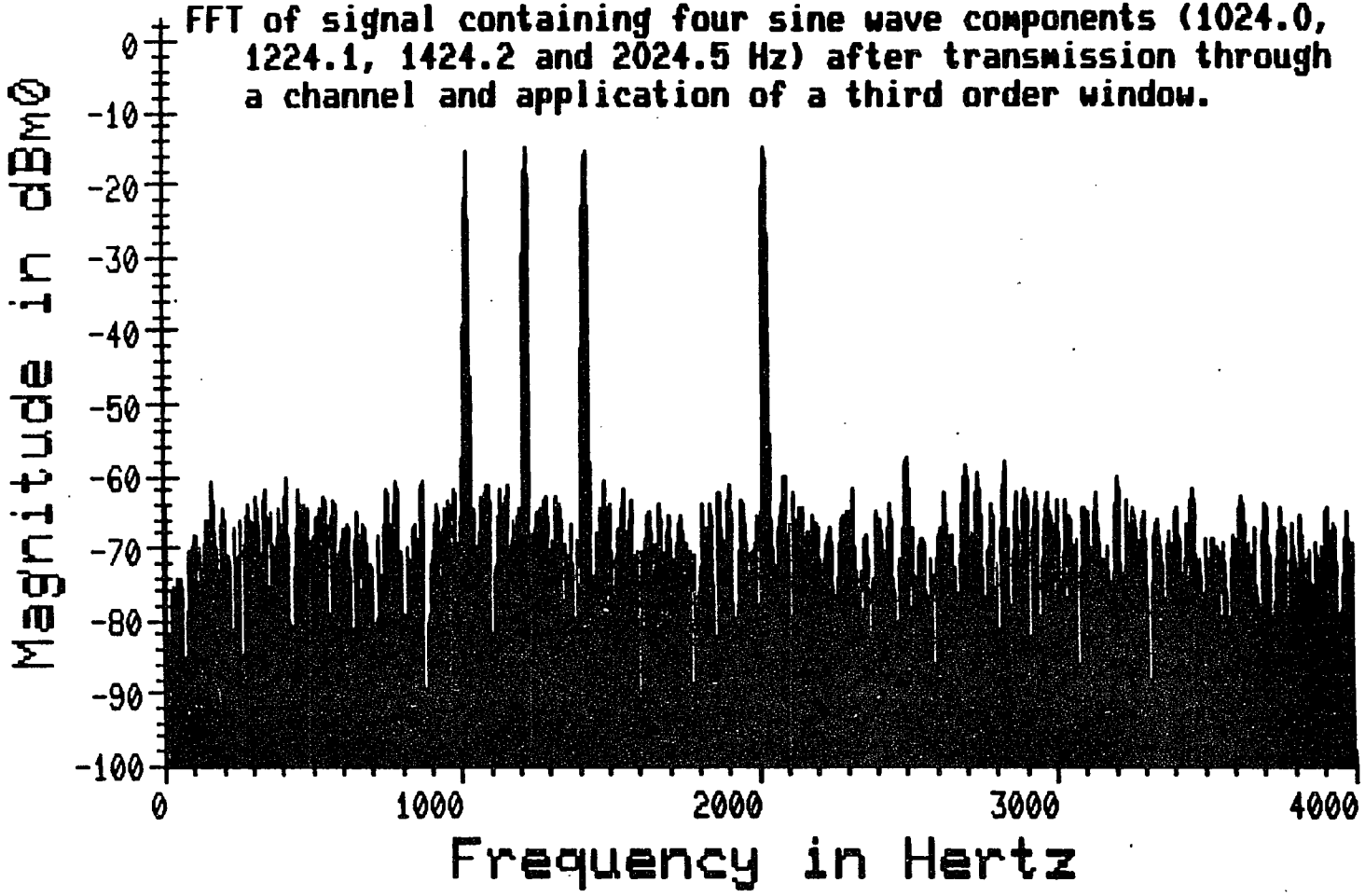
FFT of signal containing four sine wave components (1024.0, 1224.1, 1424.2 and 2024.5 Hz) after transmission through a channel and application of a third order window.
Magnitude in dBm0
0
-10
-20
-30
-40
-50
-60
-70
-80
-90
-100
0
1000
2000
3000
4000
Frequency in Hertz

Figure VI-47

CHAPTER 7

MEASUREMENTS ON DIGITAL TRANSMISSION CHANNELS

VII-A Frequency Response Measurements

VII-A.1 Individual Frequency Measurements

In Chapter 3 it was indicated that an acceptable evaluation of the frequency response of a telephone digital transmission channel may be derived from only four measurements at appropriate frequencies. This may be accomplished by generating the 257 point sampled representation of a single cycle sine wave and storing it in the signal generator ROM as explained in Chapter 5. Then four different frequencies may be generated, one at a time, transmitted through a channel and evaluated using the FFT procedures of Chapter 6. An additional short-cut may be taken here, since all of the pertinent information is contained in one spectral value. Rather than calculating the entire DFT using the given FFT techniques, the value at this single frequency may be calculated by

$$X(k) = \sum_{n=0}^{N-1} x(n)\, W_N^{-nk}$$

using only the one desired value of k. This requires a maximum of N-1 complex multiplications. If 257 points are sampled this reduces the number of multiplications from the 1023 required to do the FFT to only 256. For the 1542 point case the reduction is from 3670 to 1541. This process would have to be repeated four times to obtain the required

measurements at the four different frequencies.

A better method is to generate 257 samples of a composite signal containing all four frequency components. These samples are stored in the signal generator ROM and output one at a time, in order, without skipping over any of them. The resulting time domain signal would appear similar to Figure VII-1 where frequencies of 186.77, 311.28, 1027.24 and 3019.46 Hz are generated at -9 dBm0 each. This signal was transmitted through a telephone channel and the 257 point sample shown in Figure VII-2 was taken. The resulting FFT, shown in Figure VII-3, gives the frequency responses at the desired four points. This process required 1023 complex multiplications, compared to 256 times 4 or 1024 which would be required to repeat the single frequency measurement four times. If a 1542 sample is taken of the same channel output, as shown in Figure VII-4, the resulting FFT of Figure VII-5 requires only 3670 multiplications instead of 4 times 1541 or 6164. Note that the results of these two FFT's differ by less than a tenth of a dB in each case, indicating that the 257 point result will suffice here. This will be true in each case where the signal generator is modulo 257 and a detail frequency analysis is not required for the quantization noise; however, if the true frequency content of the noise is desired, then the 1542 point FFT must be used.

An extrapolation of this technique would indicate that more frequency components could be added to the test signal to increase the number of frequency response measurement points. This would not increase the number of multiplications required; however, the power in each signal would have to be reduced so that the channel will not be

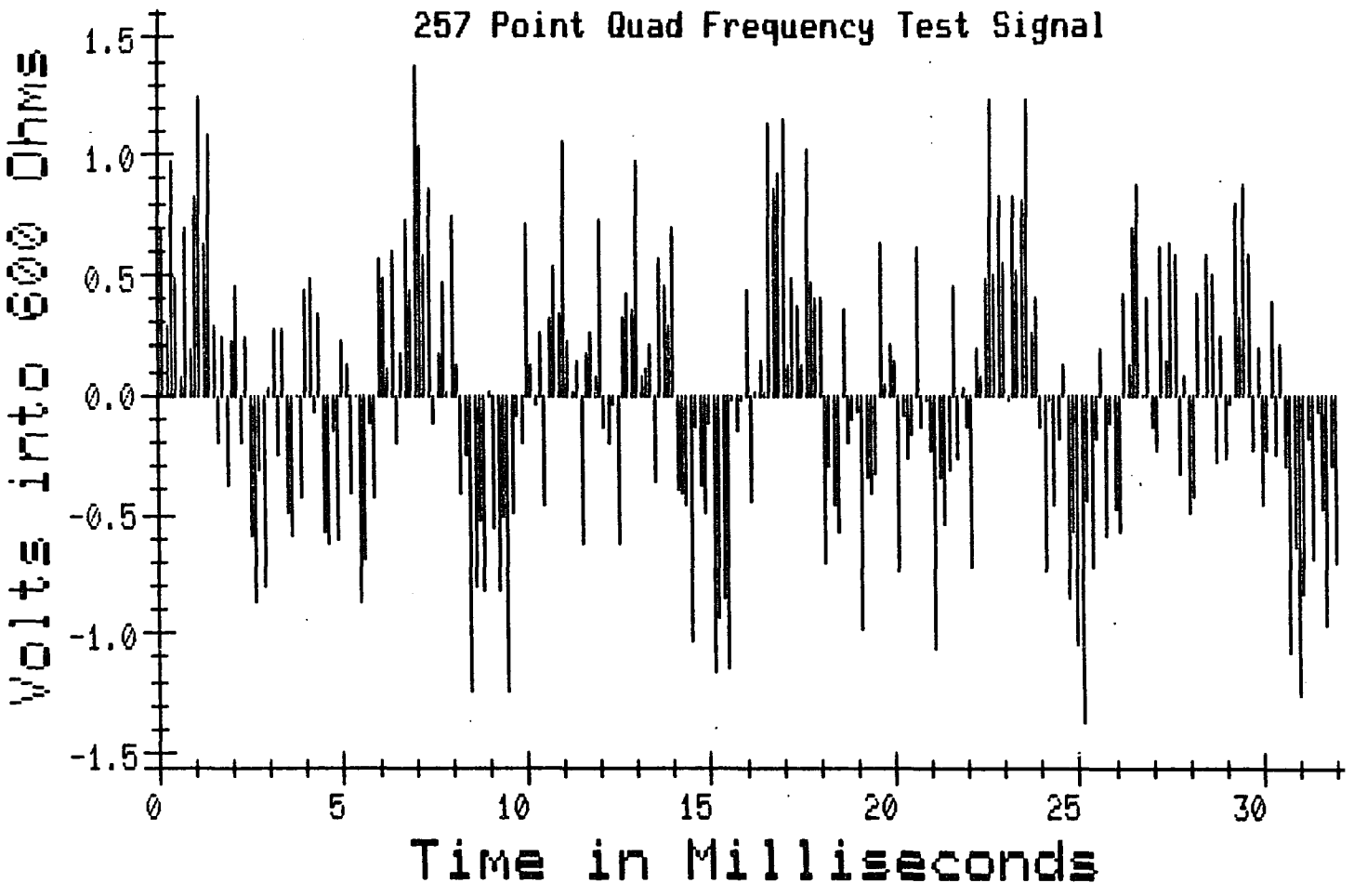
257 Point Quad Frequency Test Signal
Volts into 600 Ohms
1.5
1.0
0.5
0.0
-0.5
-1.0
-1.5
0
5
10
15
20
25
30
Time in Milliseconds

Figure VII-1

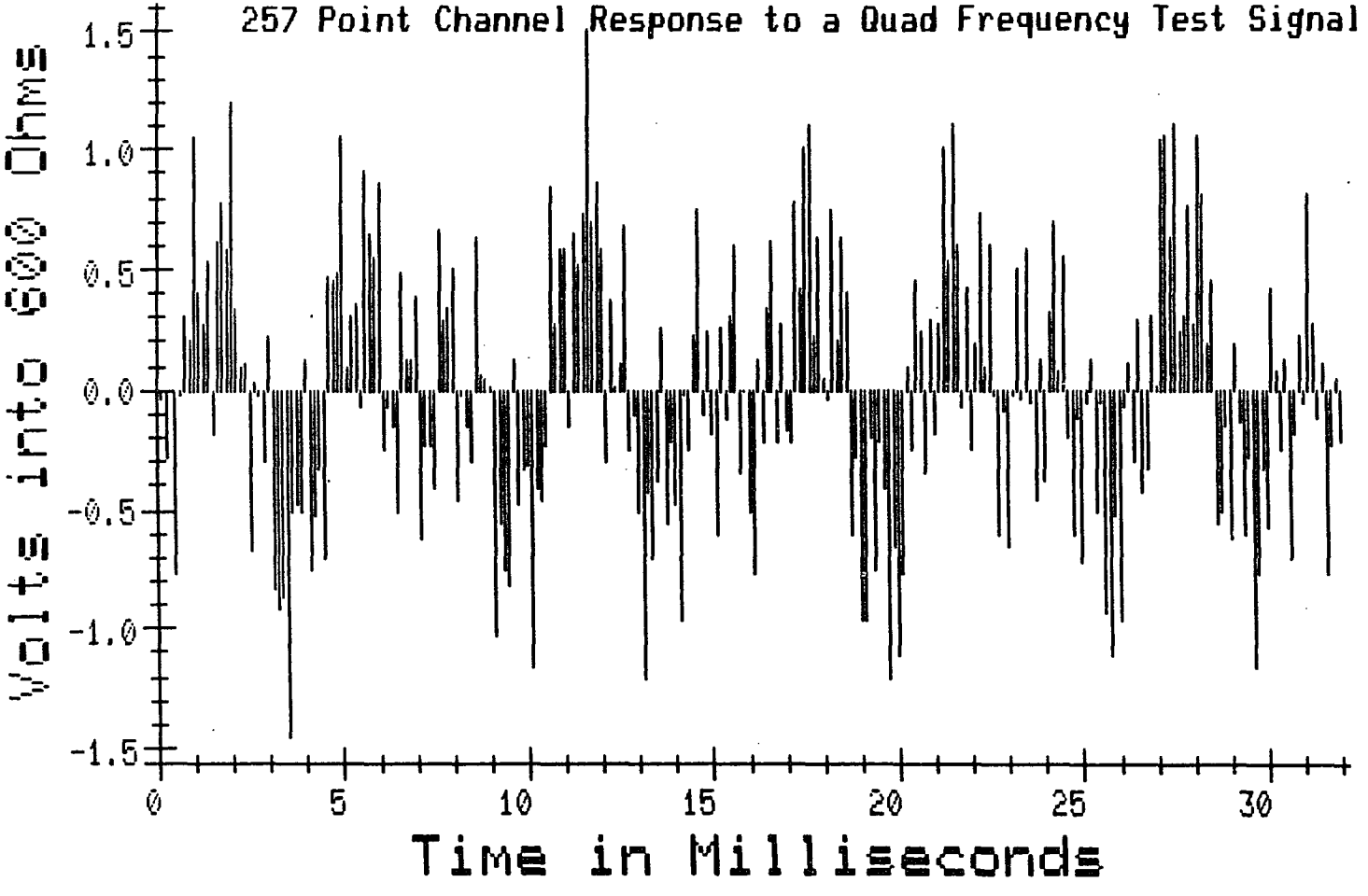
257 Point Channel Response to a Quad Frequency Test Signal
Volts into 600 Ohms
1.5
1.0
0.5
0.0
-0.5
-1.0
-1.5
0
5
10
15
20
25
30
Time in Milliseconds

Figure VII-2

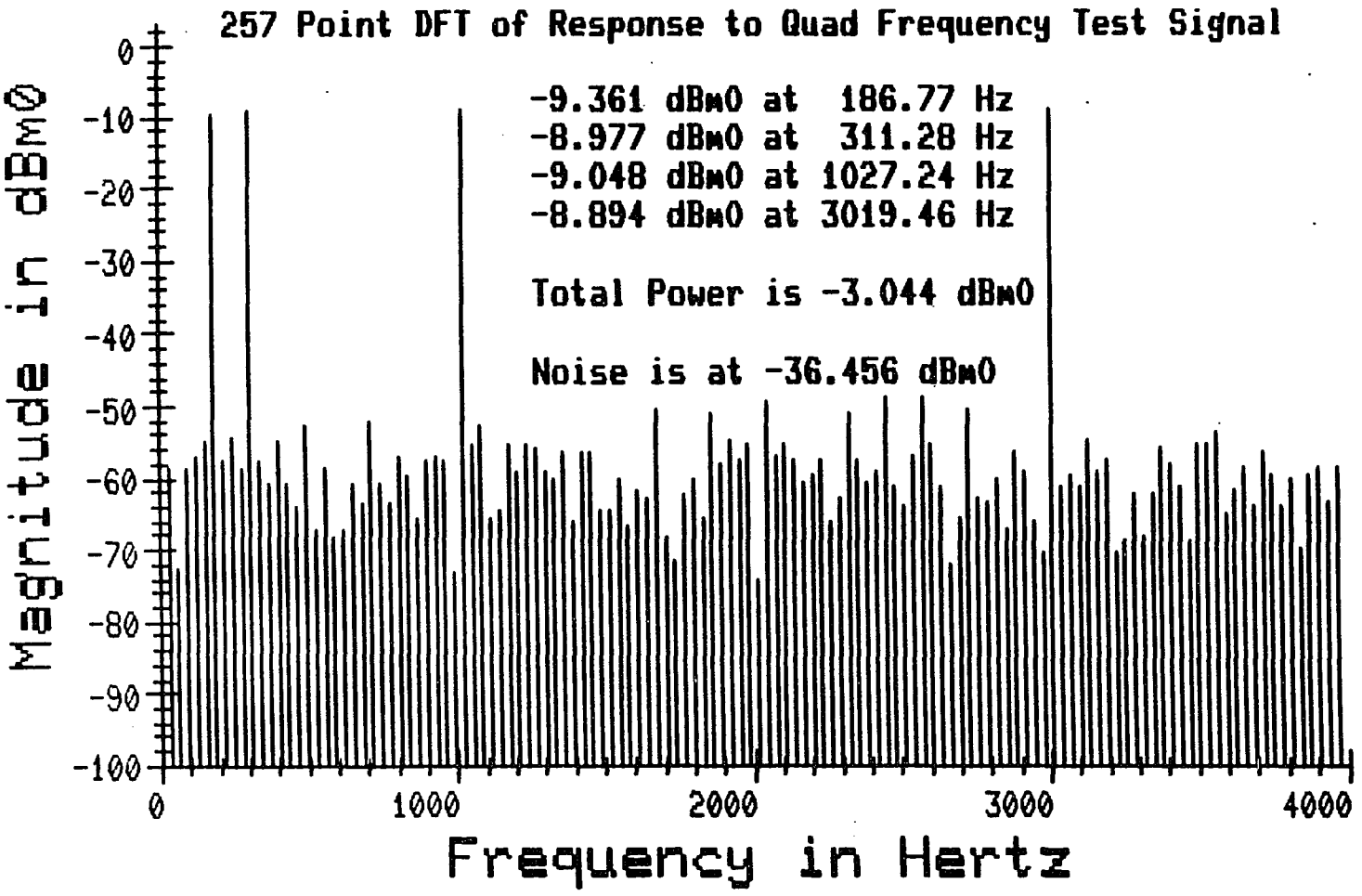
257 Point DFT of Response to Quad Frequency Test Signal
-9.361 dBm0 at 186.77 Hz
-8.977 dBm0 at 311.28 Hz
-9.048 dBm0 at 1027.24 Hz
-8.894 dBm0 at 3019.46 Hz
Total Power is -3.044 dBm0
Noise is at -36.456 dBm0
Magnitude in dBm0
0
-10
-20
-30
-40
-50
-60
-70
-80
-90
-100
0
1000
2000
3000
4000
Frequency in Hertz

Figure VII-3

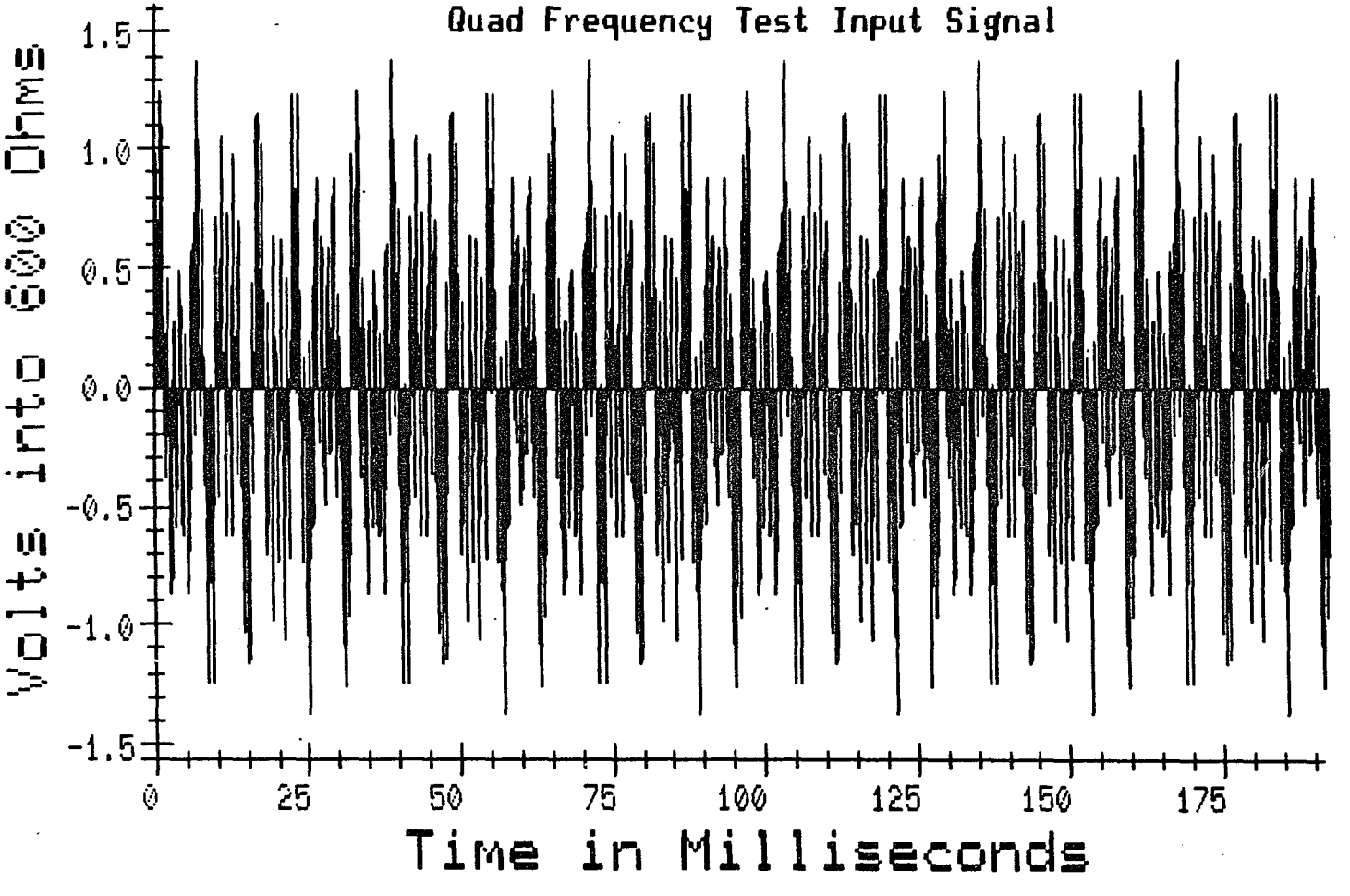
Quad Frequency Test Input Signal
Volts into 600 Ohms
1.5
1.0
0.5
0.0
-0.5
-1.0
-1.5
0
25
50
75
100
125
150
175
Time in Milliseconds

Figure VII-4

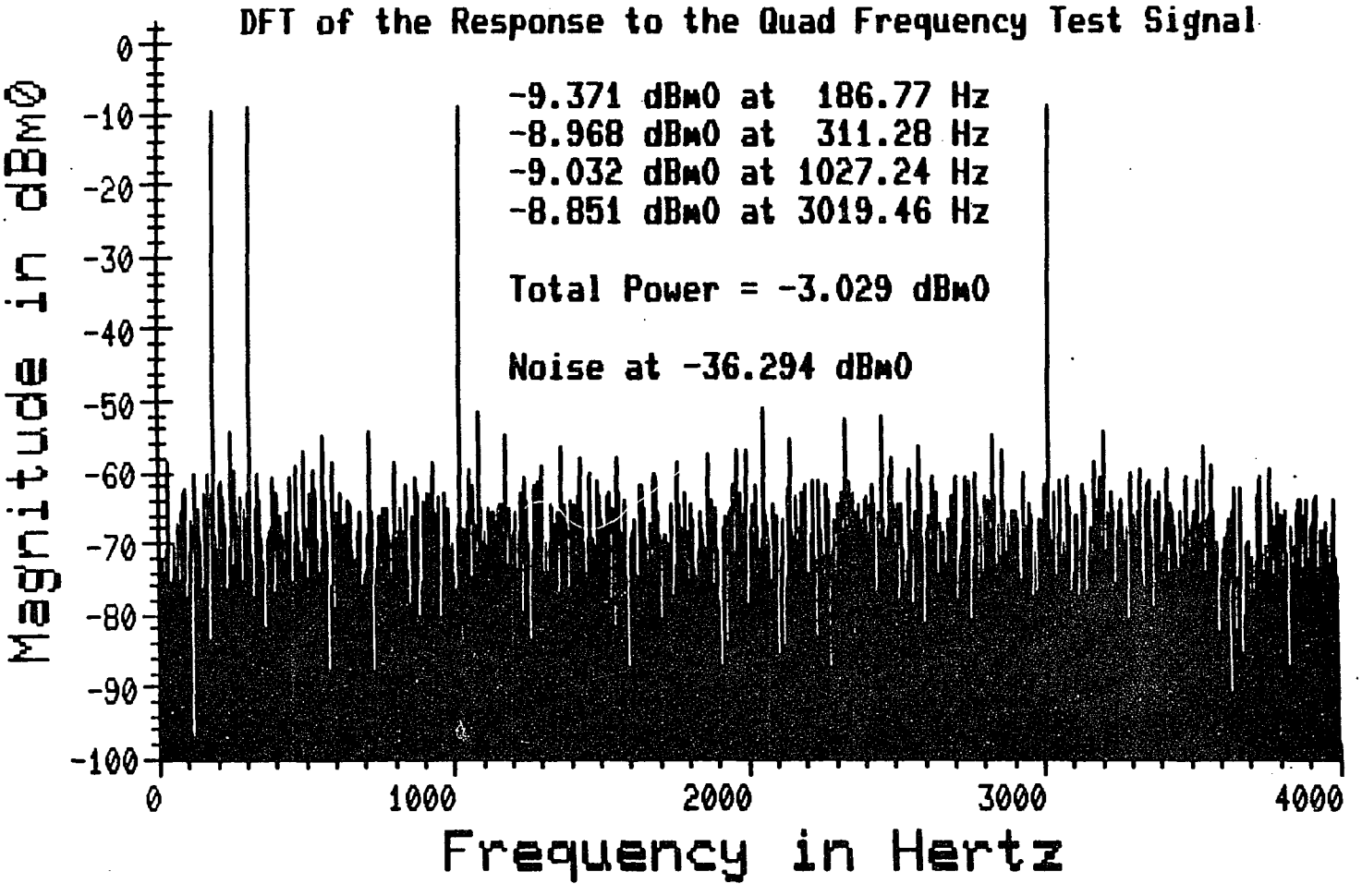
DFT of the Response to the Quad Frequency Test Signal
-9.371 dBm0 at 186.77 Hz
-8.968 dBm0 at 311.28 Hz
-9.032 dBm0 at 1027.24 Hz
-8.851 dBm0 at 3019.46 Hz
Total Power = -3.029 dBm0
Noise at -36.294 dBm0
Magnitude in dBm0
0
-10
-20
-30
-40
-50
-60
-70
-80
-90
-100
0
1000
2000
3000
4000
Frequency in Hertz

Figure VII-5

over driven. In the case of the single frequency signal, up to a 3.2 dBm0 signal may be used. If y signals of equal amplitude are to be used, this level must be reduced to

$$3.2 \text{ dBm0} - \log_{10} y$$

For the quad-frequency signal, this results in approximately 3.2 - 12 = -8.8 dBm0. That is why a -9 dBm0 signal was selected. The disadvantage to using more frequency components at lower levels is that the level of the quantization noise, which will stay relatively constant, begins to obscure the measurements and less accurate results must be expected. Note that the noise power is distributed over more discrete frequencies in the 1542 point case resulting in an increase in the measurement accuracy.

VII-A.2 Impulse Response

Another means of determining the frequency response of a channel is from its impulse response. Although ideal impulses do not exist in the real analog world, they may be easily approximated in the digital sense. Figure VII-6 shows a 1542 point time slice of six impulses spaced 257 points apart. In the practical sense, this signal is not time limited and is periodic so it will have a continuous Fourier transform. As shown in Chapter 4 this continuous transform may be found by replicating its DFT; or in this case the DFT will give the portion of this continuous transform between zero and 4000 Hz. Taking the DFT of these impulses results in the discrete spectrum of Figure VII-7. Note that each frequency component is at the same level. If this signal is transmitted through a channel, the result will be the frequency response of the channel sampled at 257 different

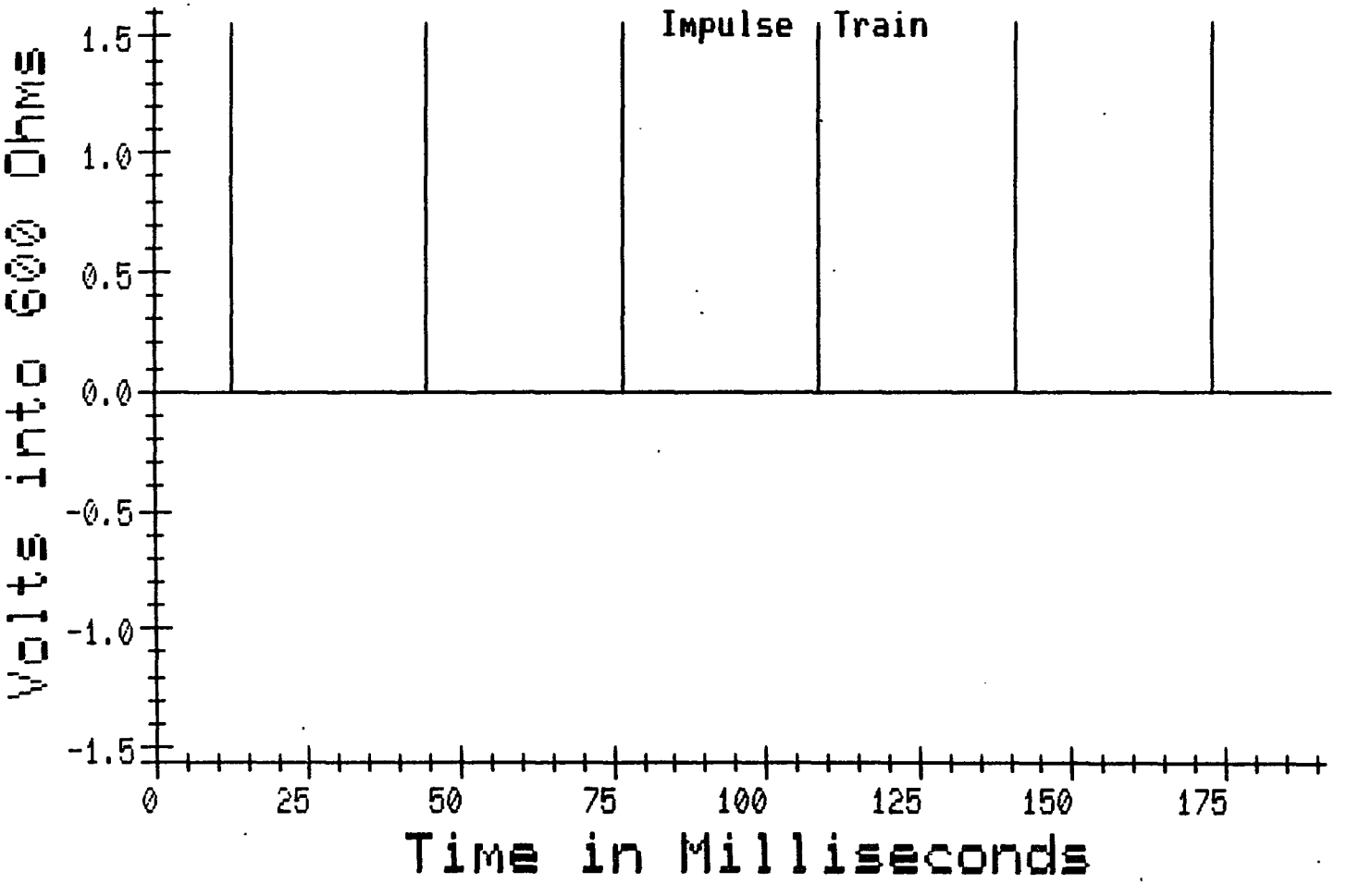
Impulse Train
Volts into 600 Ohms
1.5
1.0
0.5
0.0
-0.5
-1.0
-1.5
0
25
50
75
100
125
150
175
Time in Milliseconds

Figure VII-6

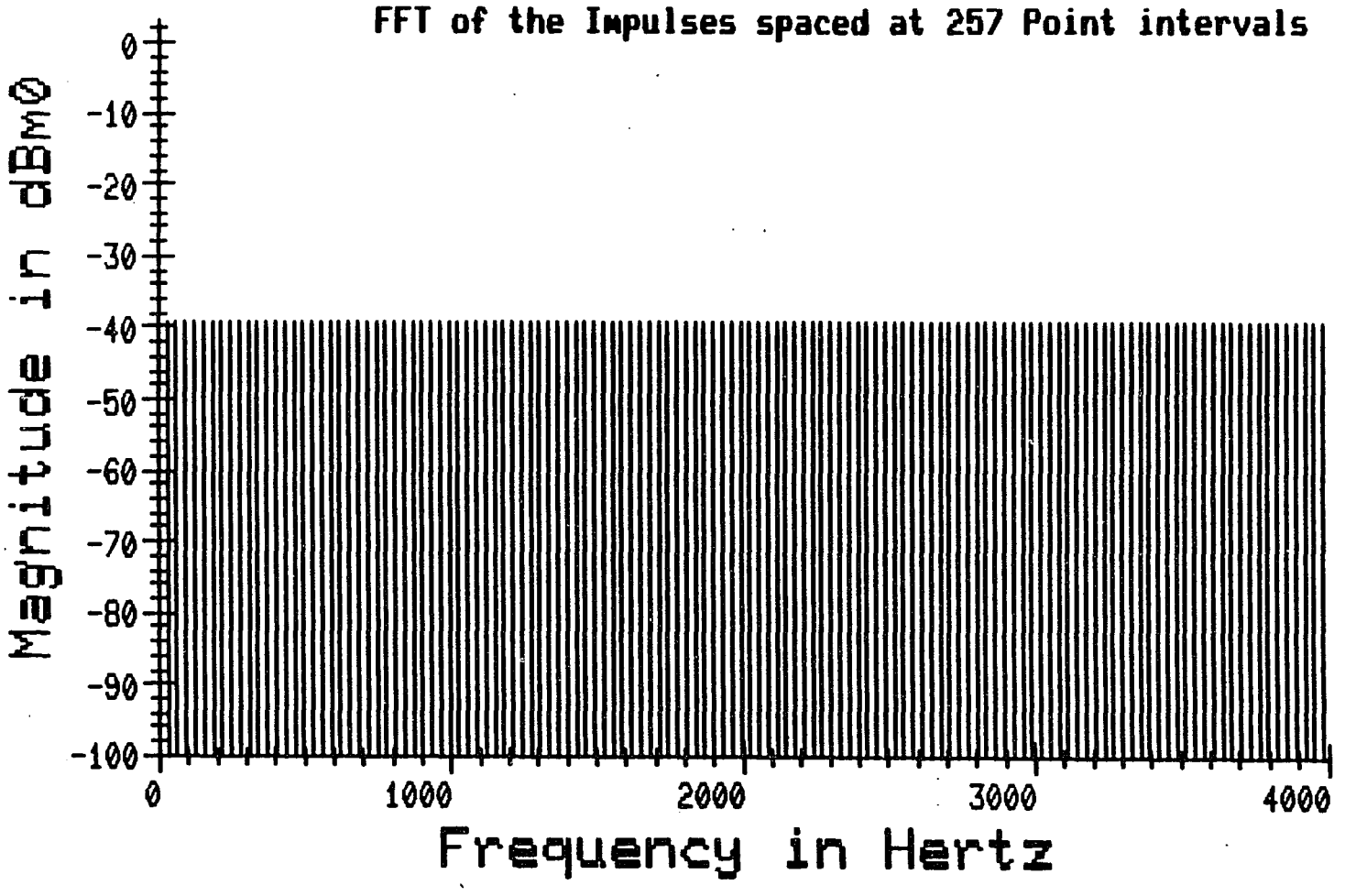
FFT of the Impulses spaced at 257 Point intervals
Magnitude in dBm0
0
-10
-20
-30
-40
-50
-60
-70
-80
-90
-100
0
1000
2000
3000
4000
Frequency in Hertz

Figure VII-7

points spaced 8000/257 = 31.13 Hz apart over the range from -4000 Hz to +4000 Hz. Since each negative frequency component of a transform of real points is the same as the complex conjugate of the positive frequency component, it will suffice to show only the positive frequency portion.

The mu-law encoding scheme, used in the telephone transmission system under consideration here, does not have the same transfer characteristic during the signalling frames as during the information frames. This causes every sixth impulse to be slightly modified having the same effect as an additional but small impulse every 1542 samples. The DFT of this small impulse is shown in Figure VII-8 and the superposition of these two signals results in the DFT shown in Figure VII-9. This, in essence, is the spectrum of the test signal which is used to generate the impulse response. It is obvious from this analysis that a 1542 point DFT must be performed in order to detect all of the frequency components of the resulting signal; however, if a certain amount of inaccuracy may be tolerated, then a 257 point DFT may suffice. Figure VII-10 shows the actual time domain response of a channel to this impulse train. Figure VII-11 is the 1542 point DFT of this response. The frequency response of the channel is seen clearly outlined by every sixth discrete frequency point and the quantization noise is seen distributed among all of the frequency points. The quantization noise is down about 40 dB below the signal over most of the spectrum, so the measurements should be accurate to within $10^{-40/20} = 0.01$ dB. Near 4000 Hz the noise margin degrades to about 15 dB resulting in an accuracy of about $10^{-15/20} = 0.18$ dB.

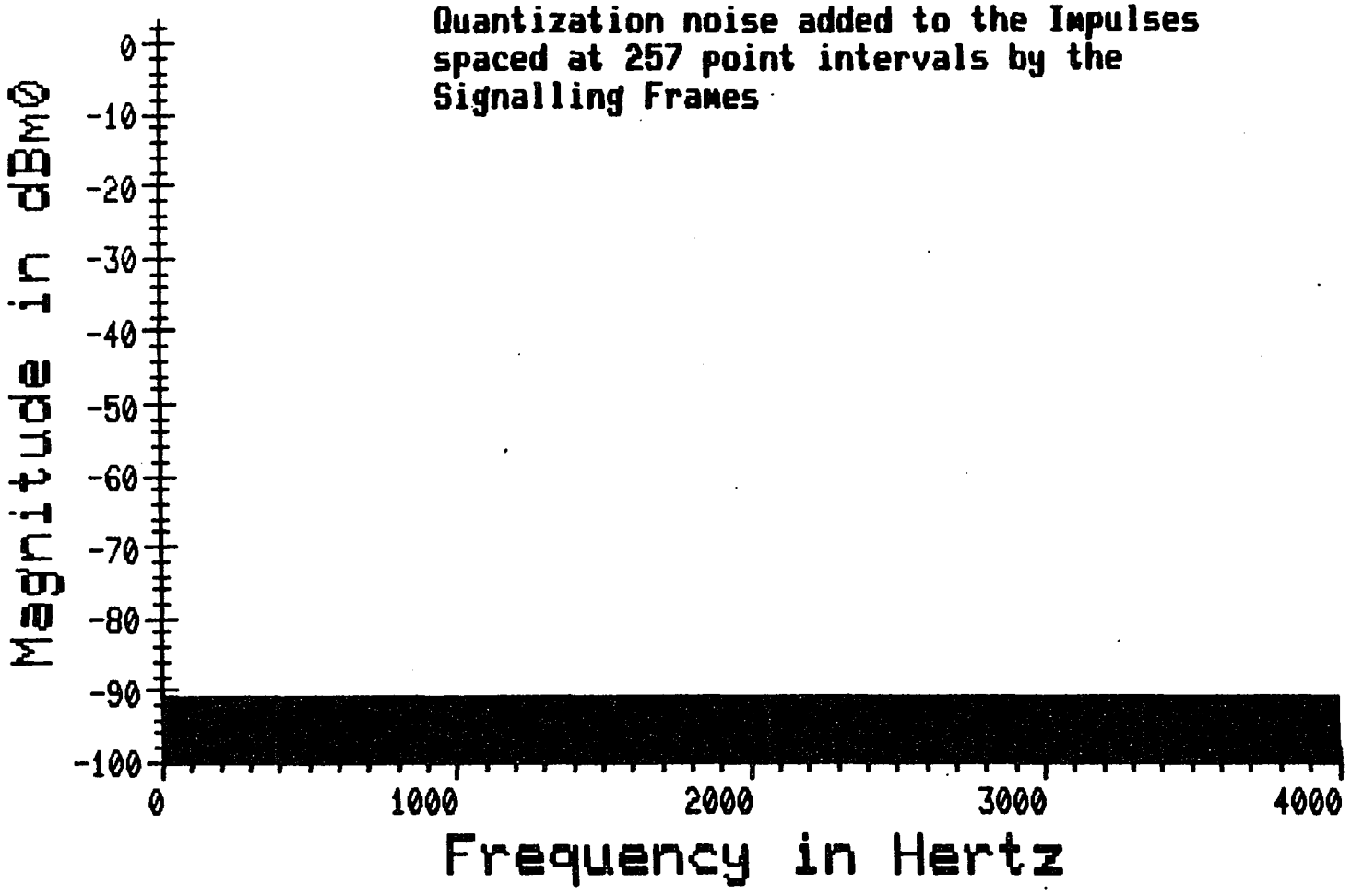
Quantization noise added to the Impulses
spaced at 257 point intervals by the
Signalling Frames
Magnitude in dBm0
0
-10
-20
-30
-40
-50
-60
-70
-80
-90
-100
0
1000
2000
3000
4000
Frequency in Hertz

Figure VII-8

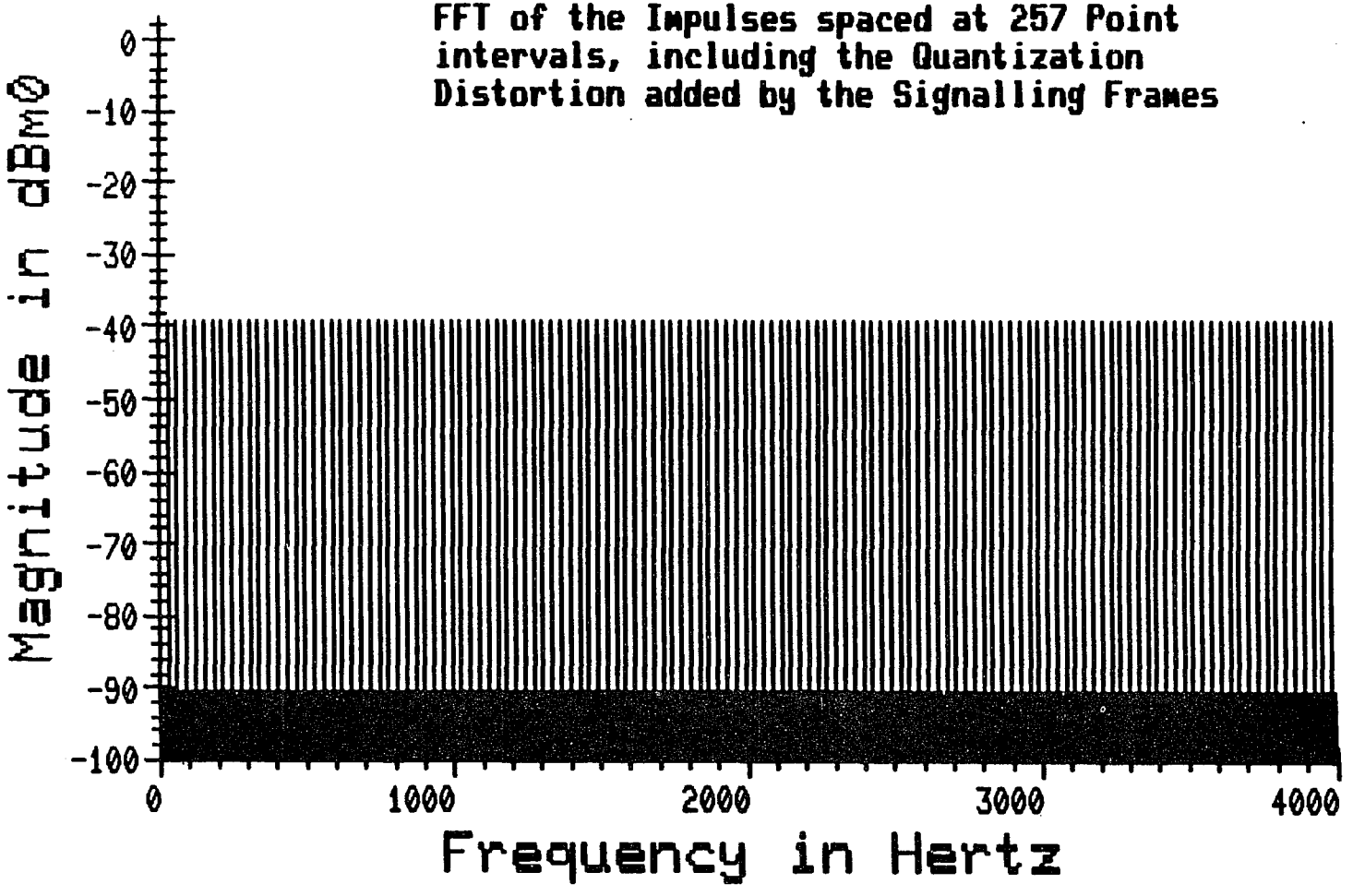
FFT of the Impulses spaced at 257 Point intervals, including the Quantization Distortion added by the Signalling Frames
Magnitude in dBm0
0
-10
-20
-30
-40
-50
-60
-70
-80
-90
-100
0
1000
2000
3000
4000
Frequency in Hertz

Figure VII-9

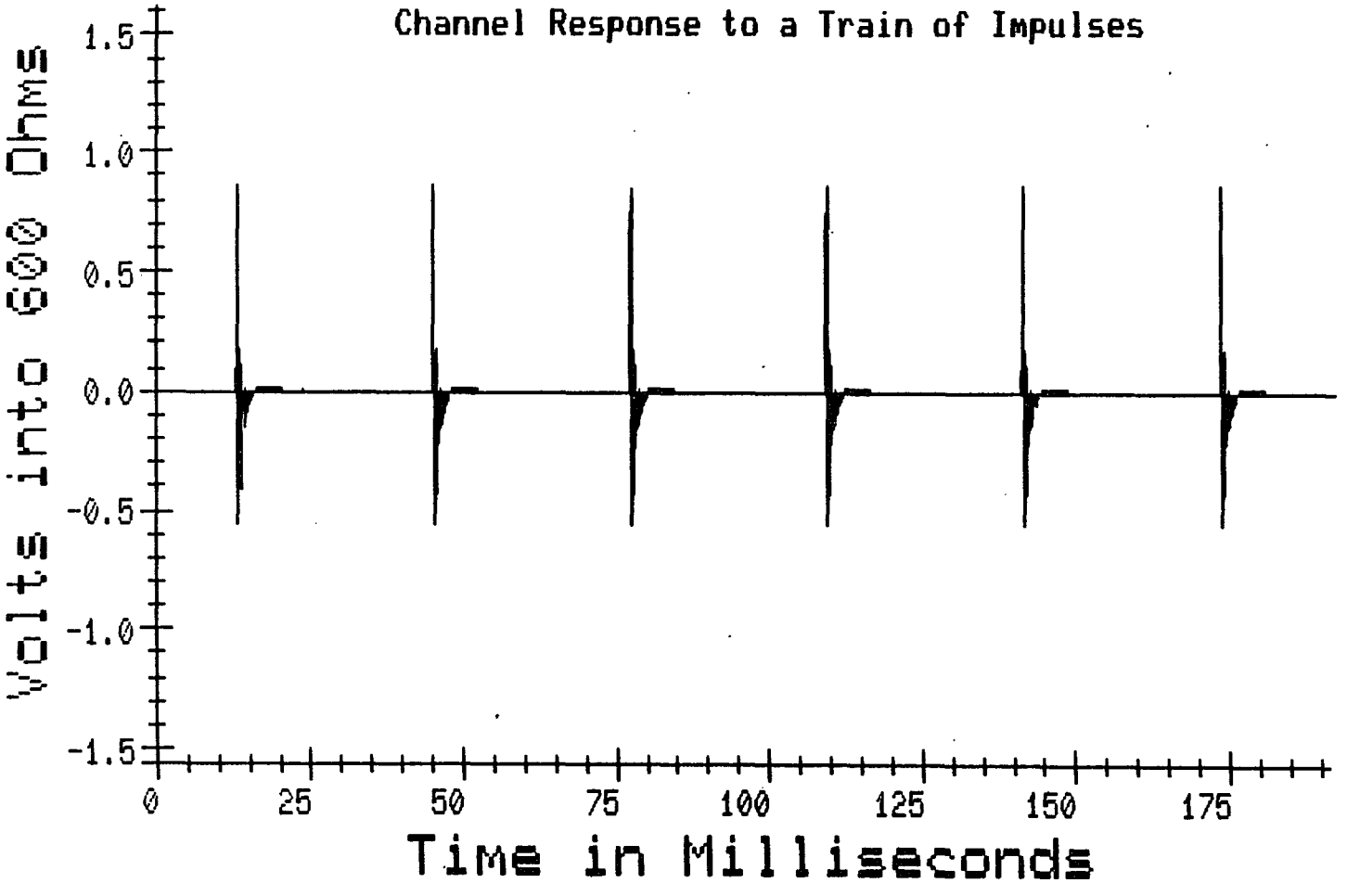

Figure VII-10

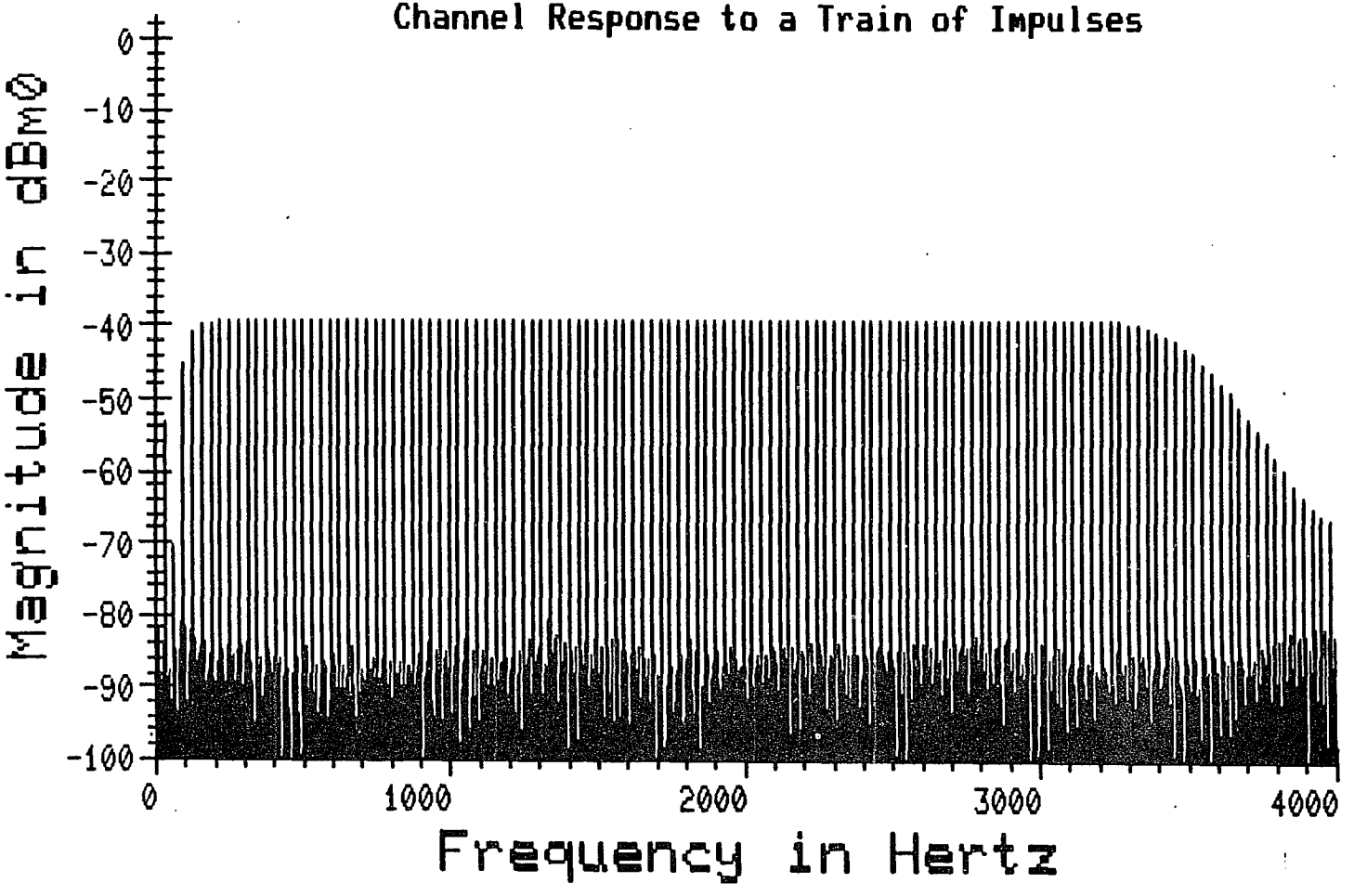

Figure VII-11

Figure VII-12 shows the 257 point DFT of the channel's response to this same signal. The quantization noise power is concentrated into 1/6 as many discrete frequencies, increasing the noise level by about 15.6 dB. This brings the noise to about the same level as the signal near 4000 Hz. As a result of this, the measurement near 4000 Hz is not dependable. As mentioned in Chapter 3, it is desirable to take a frequency response measurement as near as possible to 4000 Hz to insure that the signal is being attenuated by at least 28 dB, insuring sufficient out-of-band signal suppression. For this reason it is suggested that an additional measurement be made with a sine wave stimulus of 3984.44 Hz at 0 dBm0. Figure VII-13 shows the typical results of such a measurement. Once again, it should be mentioned here that the entire DFT need not be calculated to obtain this single frequency component. An interesting and useful phenomenon may be observed in this DFT result. The quantization noise seen here has an envelope which approximates the frequency response curve of the channel unit. This is the result of the quantized 0 dBm0 signal being decoded by the receive unit and correctly converted into a 0dBm0, 3984.44 Hz signal including noise at about -32 dBm0. The signal is then shaped by the receive and transmit filters before being reconverted into digital form. The 3984.44 Hz signal at this point has been attenuated by about 28 dB so that any additional quantization noise generated at the transmitter should be down an additional 28 dB below the noise that was generated at the receiver. Therefore, the noise seen here is the receiver quantization noise, shaped by the frequency response of the analog portion of the channel. This might be used as a tool to

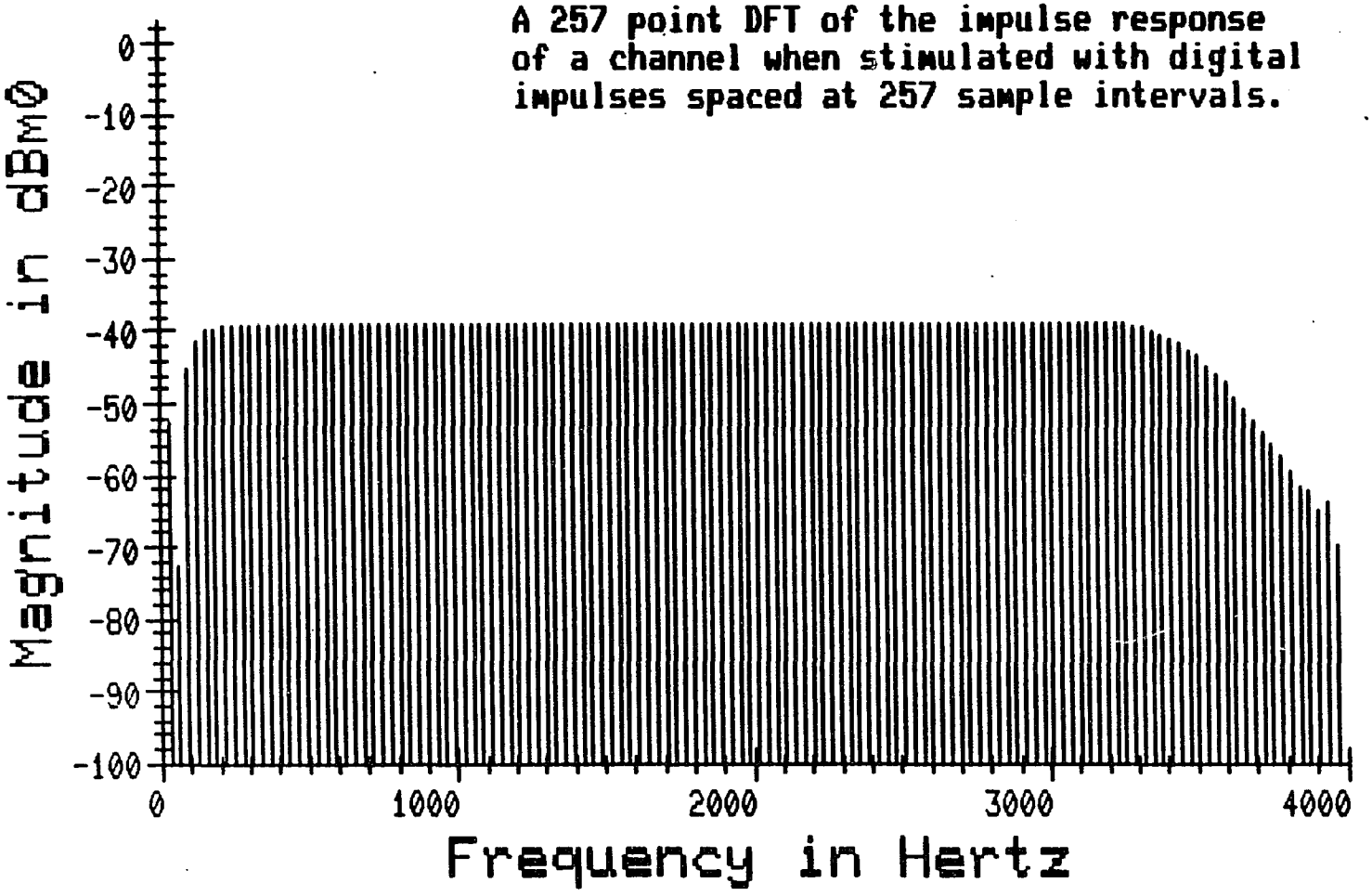

Figure VII-12

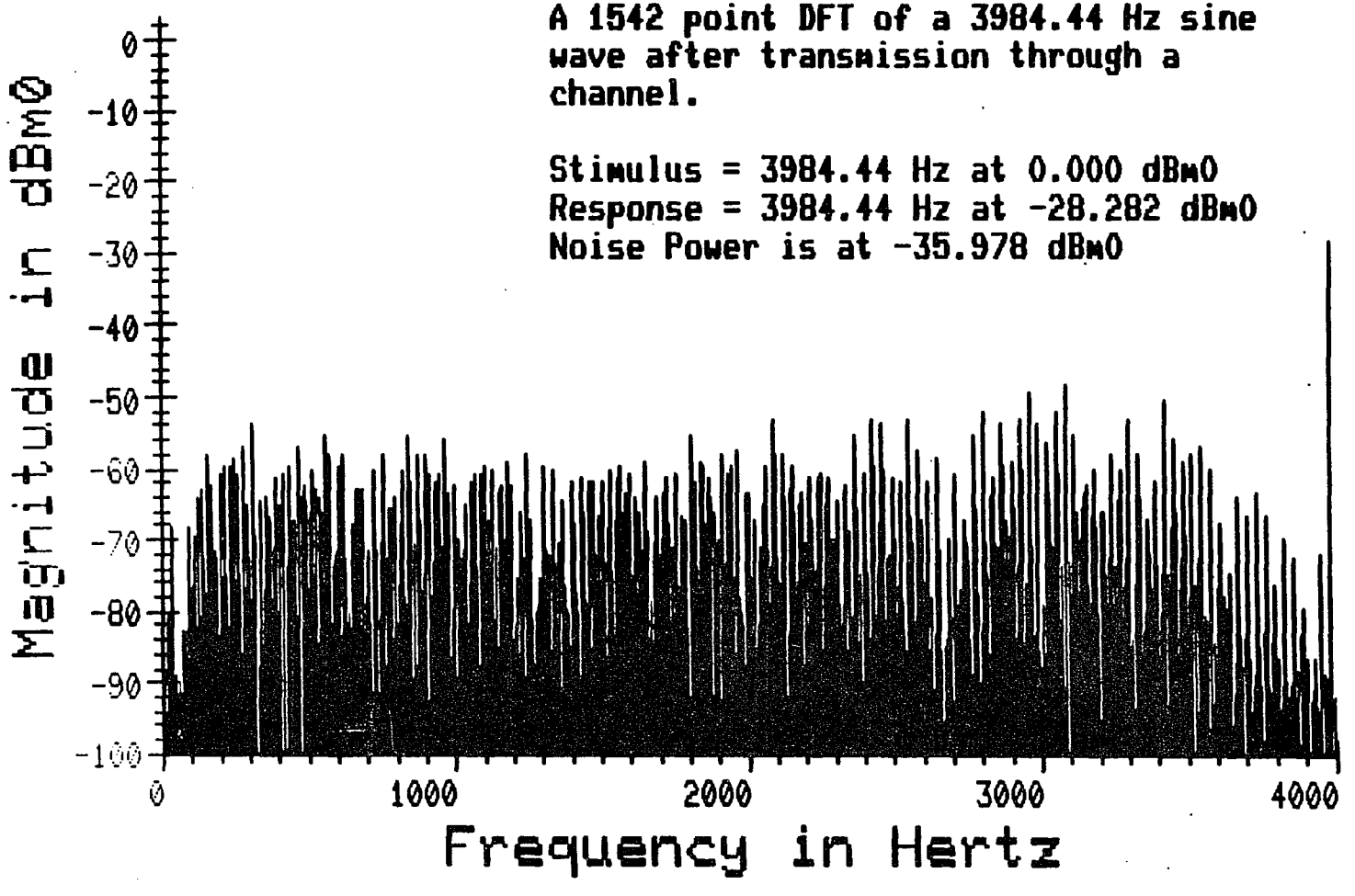

Figure VII-13

determine whether a particular noise problem is being caused by the transmitter or the receiver portion of a channel. Again, the 257 point DFT of this data, shown in Figure VII-14 yields similar quantitative results; however, the envelope does not show the shaping of the channel's frequency response as distinctly due to the skewing of the noise components which fall at frequencies not distinguished by this DFT.

The channel appears to exhibit even more attenuation at a frequency of 62.26 Hz than it does near 4000 Hz. It would seem that this may be an even better signal to use when trouble-shooting a noise problem. Figure VII-15 shows such a measurement made on a different channel. Since the 62.26 Hz component is attenuated by 34 dB, the remaining noise is all generated in the receiver with the transmit quantization noise affecting this reading by only about 0.15 dB.

The phase response of a channel may be easily derived from its impulse response as the phase portion of the DFT. Figure VII-16 shows the phase response of the DFT whose magnitude was given in Figure VII-11. Only the values at every sixth discrete frequency represent the response of the channel; the others are just the phase of the quantization noise and are insignificant. This phase may have undergone a considerable linear shift due to the time relationship of the first sample taken and the actual beginning of the impulse response. This shift may be easily removed by a computer program and the results compared to the acceptable limits as shown in Figure VII-17.

VII-A.3 Gold Code Signals

Another signal which may be useful if it is desired to

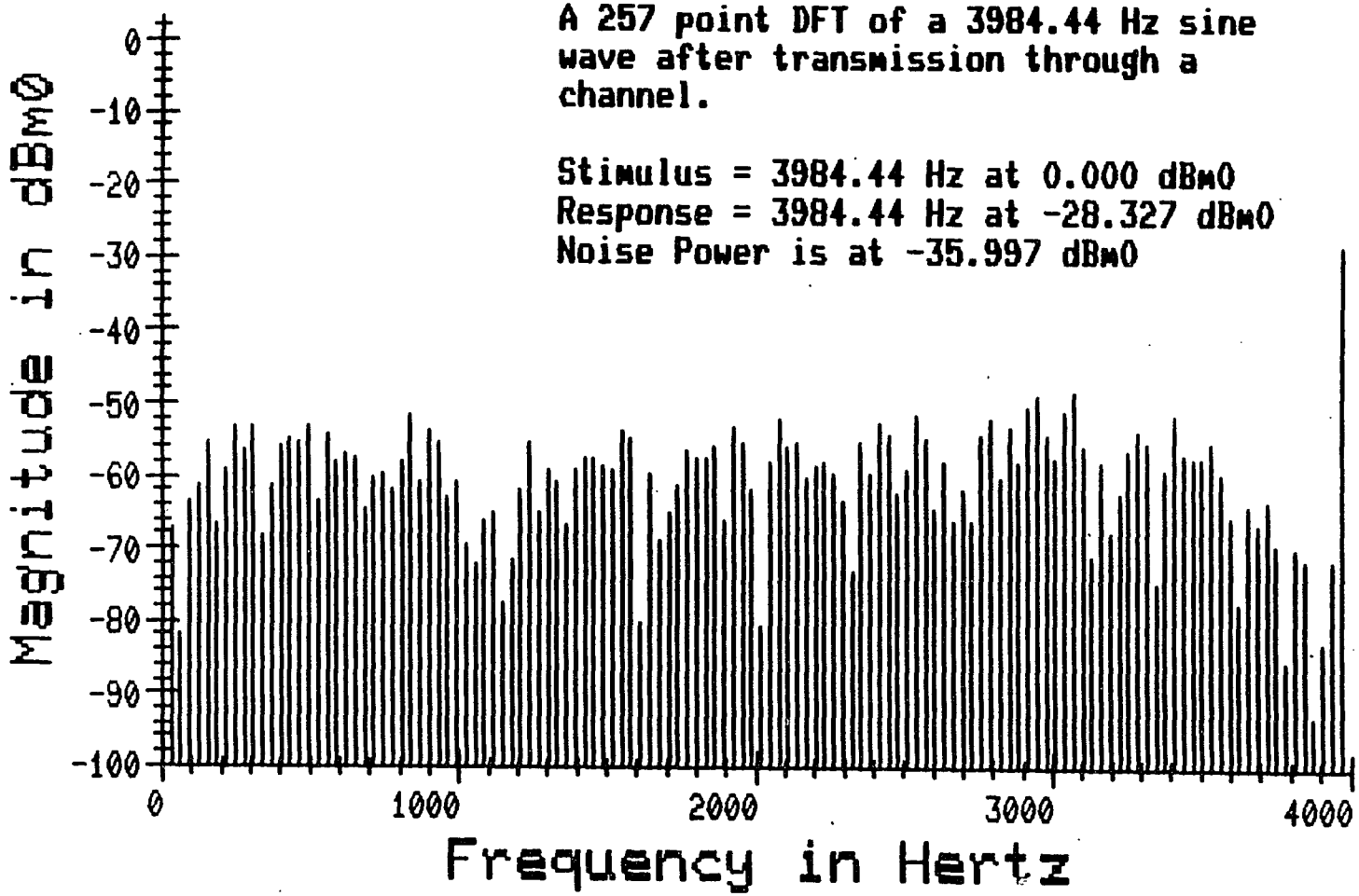

Figure VII-14

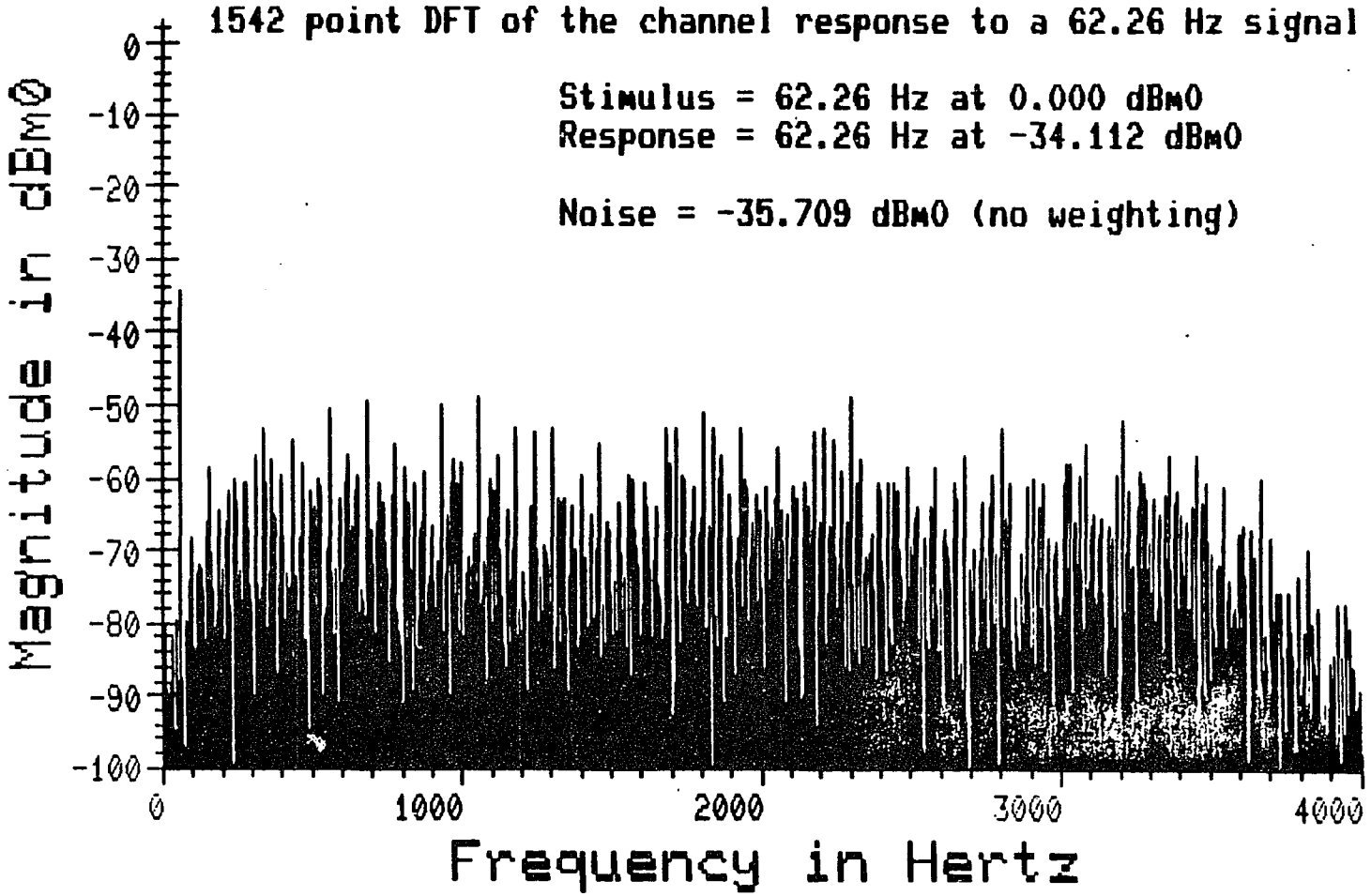

Figure VII-15

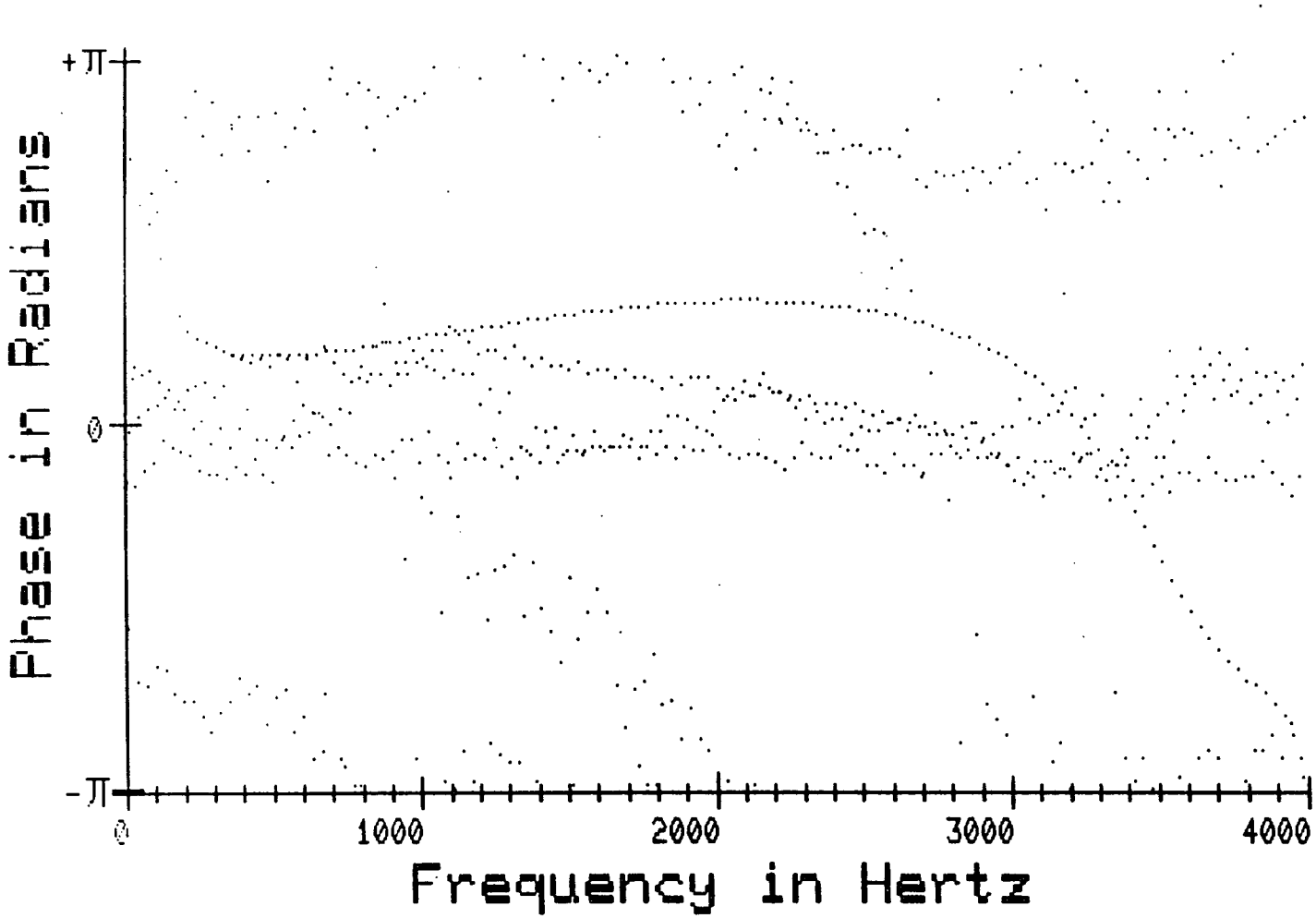

Phase response to digital impulses with 257 point spacings.

Figure VII-16

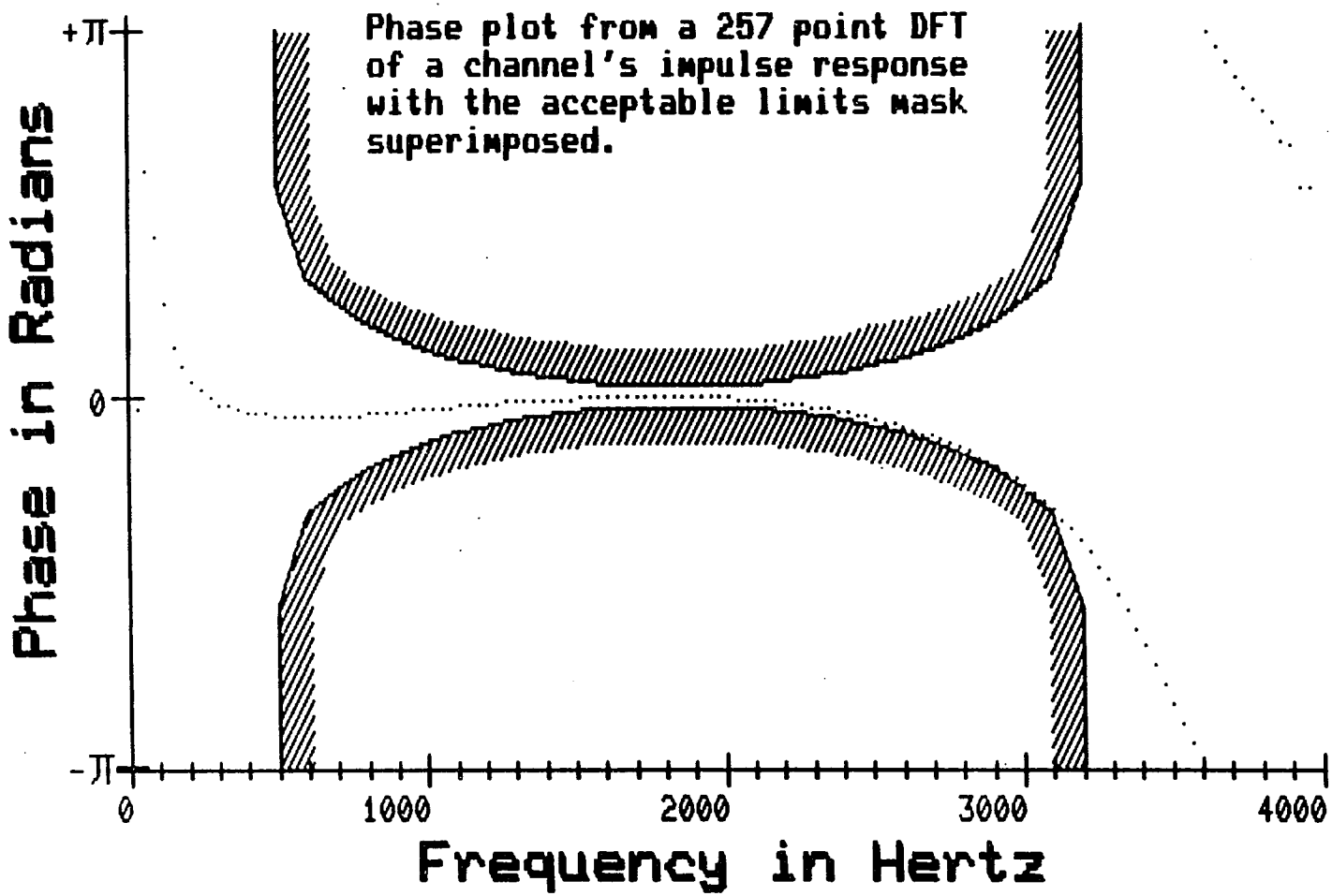

Figure VII-17

measure the frequency response of channel at a higher power level is shown in Figure VII-18. This is a 511 point Gold code sequence generated by simulating a nine bit shift register with feedback, where the taps are specified by a Gold code [16]. This signal does not lend itself to analysis using the 257 or 1542 point FFT's; however, this family of signals should be mentioned because of their distinct characteristics. Figure VII-19 shows the frequency content of this signal as flat, just as that of the impulse. This signal may be transmitted at a much higher average power level since the energy is spread evenly in time instead of being concentrated into a single pulse. Figure VII-20 is the time domain response of a channel to this signal and Figure VII-21 is its DFT. Notice that this DFT displays the same shape as the impulse response which was shown in Figure VII-12, except that the power level is much higher. These sequences may only be generated with lengths of one less than a power of two, but may prove useful as a noise source with a flat spectrum.

VII-B Gain Tracking and Distortion

The gain tracking measurements are intended to insure that the decoding characteristic is truly the inverse of the encoding characteristic, resulting in a linear system. These measurements are made by varying the amplitude of a single frequency source and evaluating the response to insure that the amplitudes track accordingly. The use of a single frequency tone allows the frequency response characteristics of the analog portions of the channel to be ignored. Measurements at the different power levels must be made separately so that this independence may be maintained.

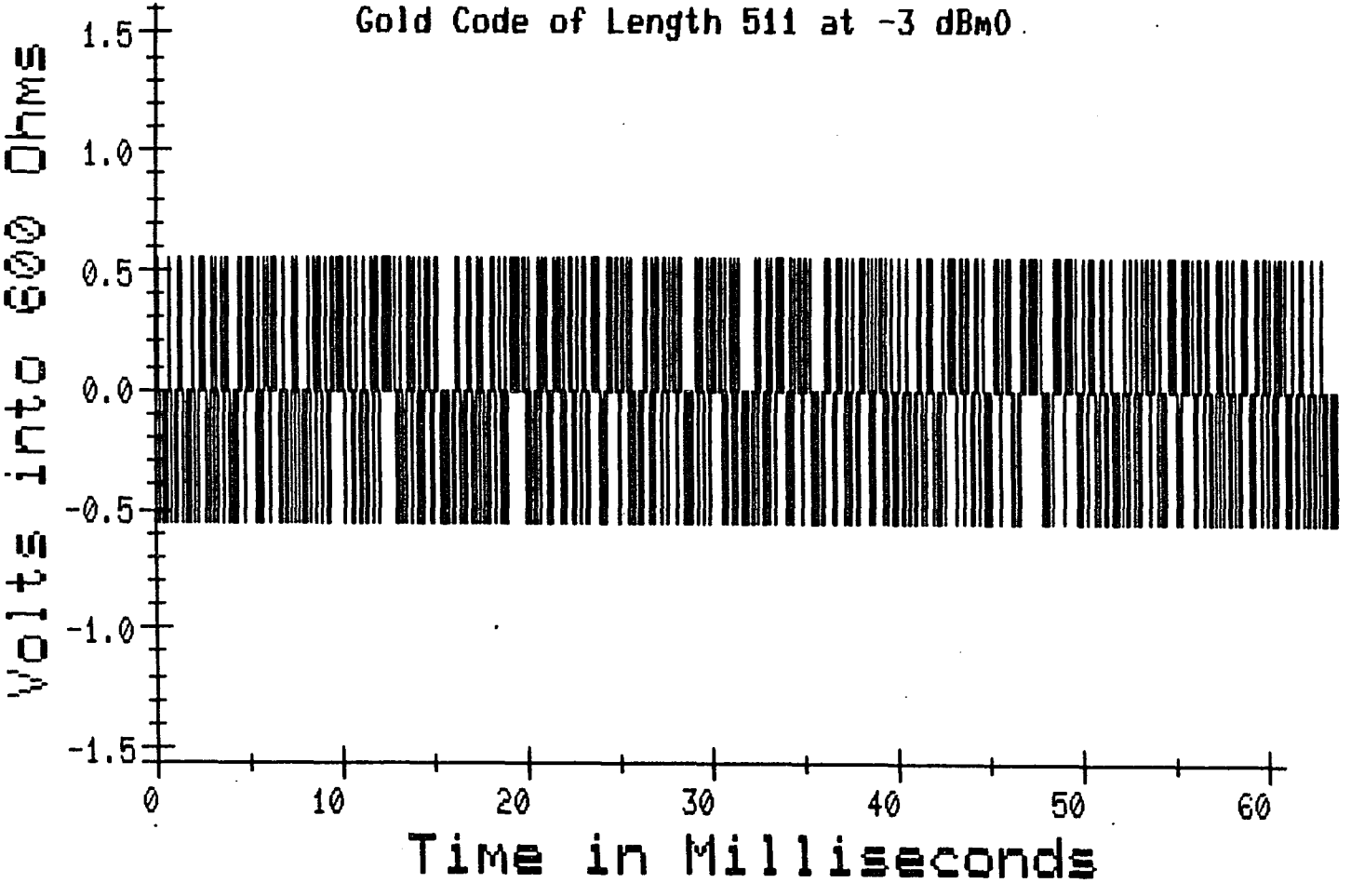

Figure VII-18

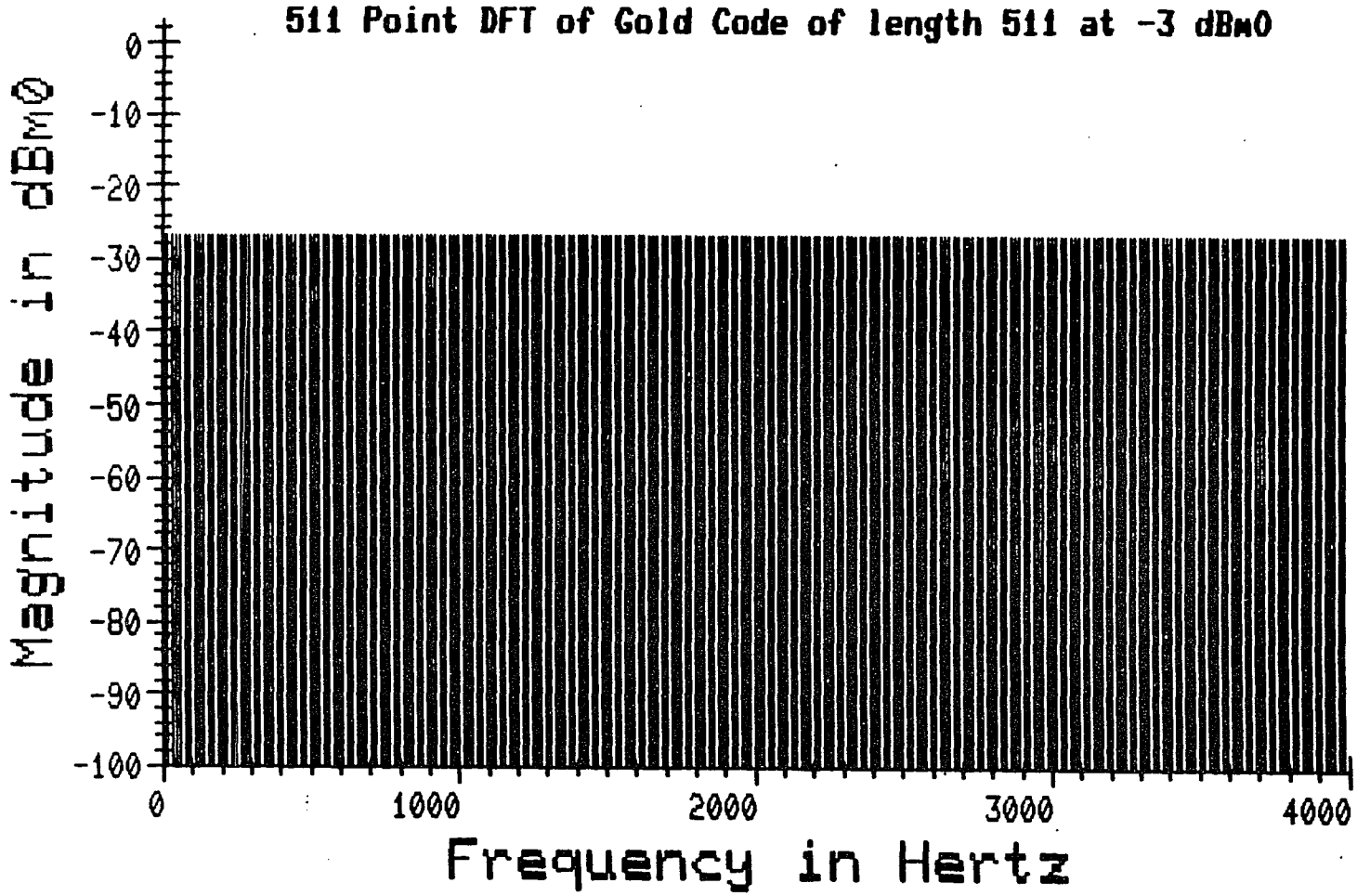

Figure VII-19

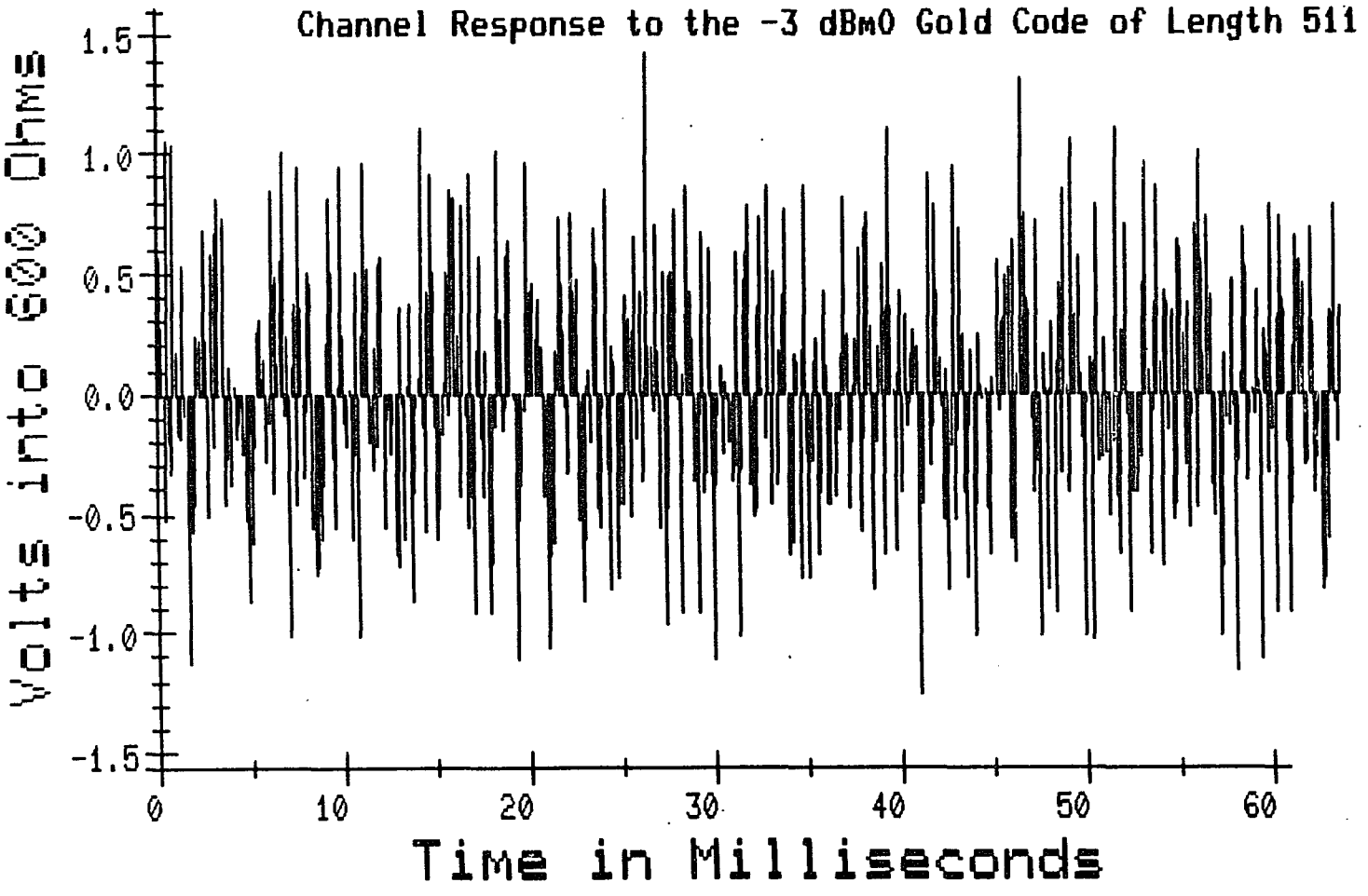

Figure VII-20

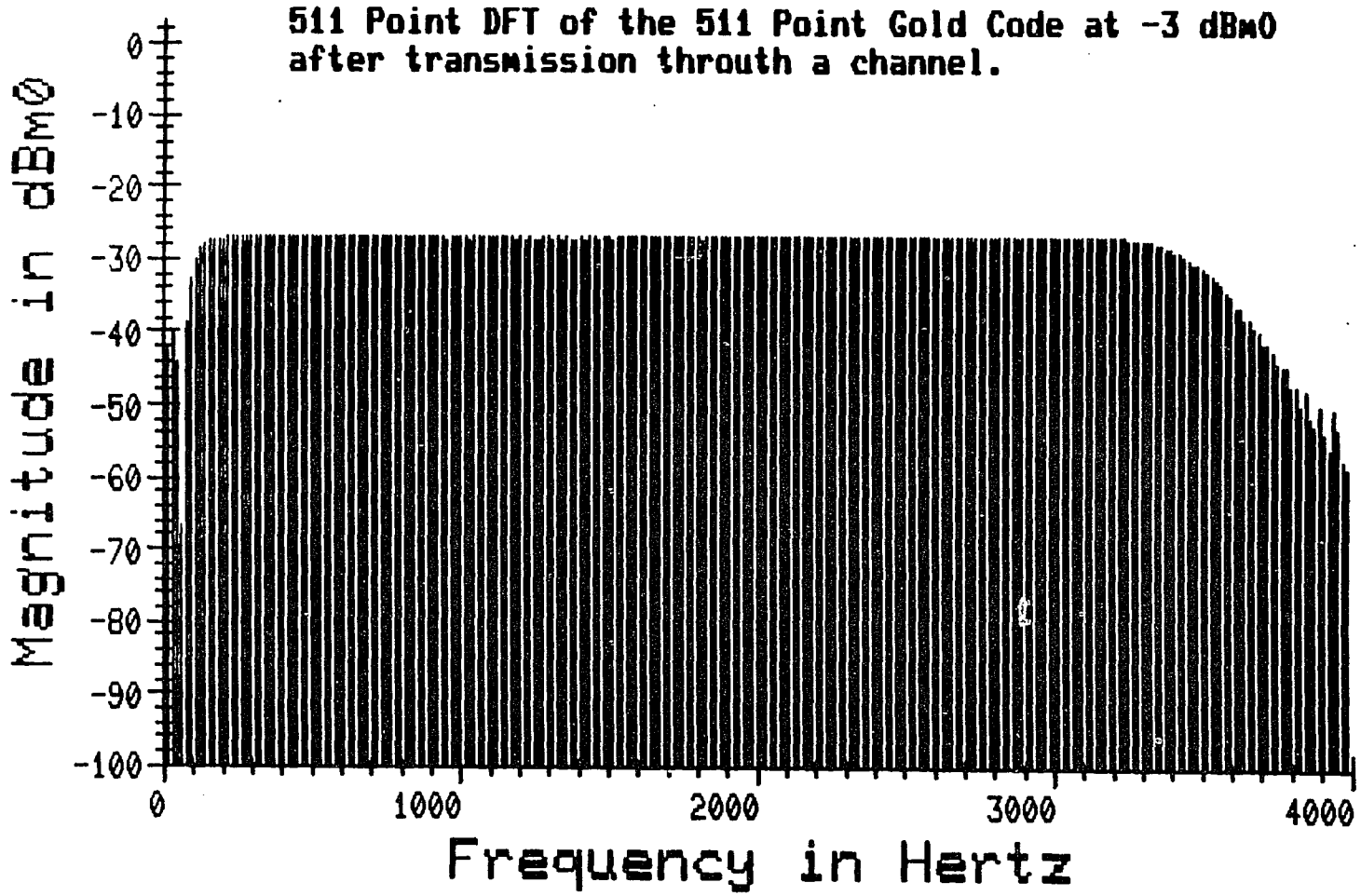

Figure VII-21

Figure VII-22 illustrates the response of a channel to a 1027.24 Hz sine wave at 0 dBm0. As noted previously, all of the signal power is contained in one spectral line. The power in this line of 0.020 dBm0 represents the gain of the channel at this power level and frequency. The remainder of the power in this spectrum represents the quantization distortion generated in the transmission process. In this case, when the noise is totaled the result is a level of -32.120 dBm0. This appears to exceed the requirement of -35 dBm0; however, the specification is that the noise be passed through a psophometric filter prior to evaluation. Figure VII-23 shows the frequency response characteristic of this filter. This psophometric weighting may be easily applied to the channel response by simply multiplying a digitized version of this filter response by the DFT of the channel response. The result is the spectrum of Figure VII-24. The noise here has dropped to -35.810 dBm0p which acceptably satisfies the requirement.

As a check on the validity of these measurements, a signal of 1024.03 Hz at 0 dBm0 was used to test a given channel. This frequency is very close to the 1020 Hz signal used in the common analog test equipment for testing the channels. After transmission through the channel and cosine windowing, the DFT of the signal was calculated as shown in Figure VII-25. The power in the eight spectral lines around 1024 Hz was totaled at 0.005 dBm0. Psophometric weighting was applied to the spectrum as shown in Figure VII-26 and then the noise which remained after the exclusion of these eight lines was totaled as -35.403 dBm0p. Analog measurements made on this channel using a notch filter to remove the 1020 Hz signal and a psophometric filter resulted

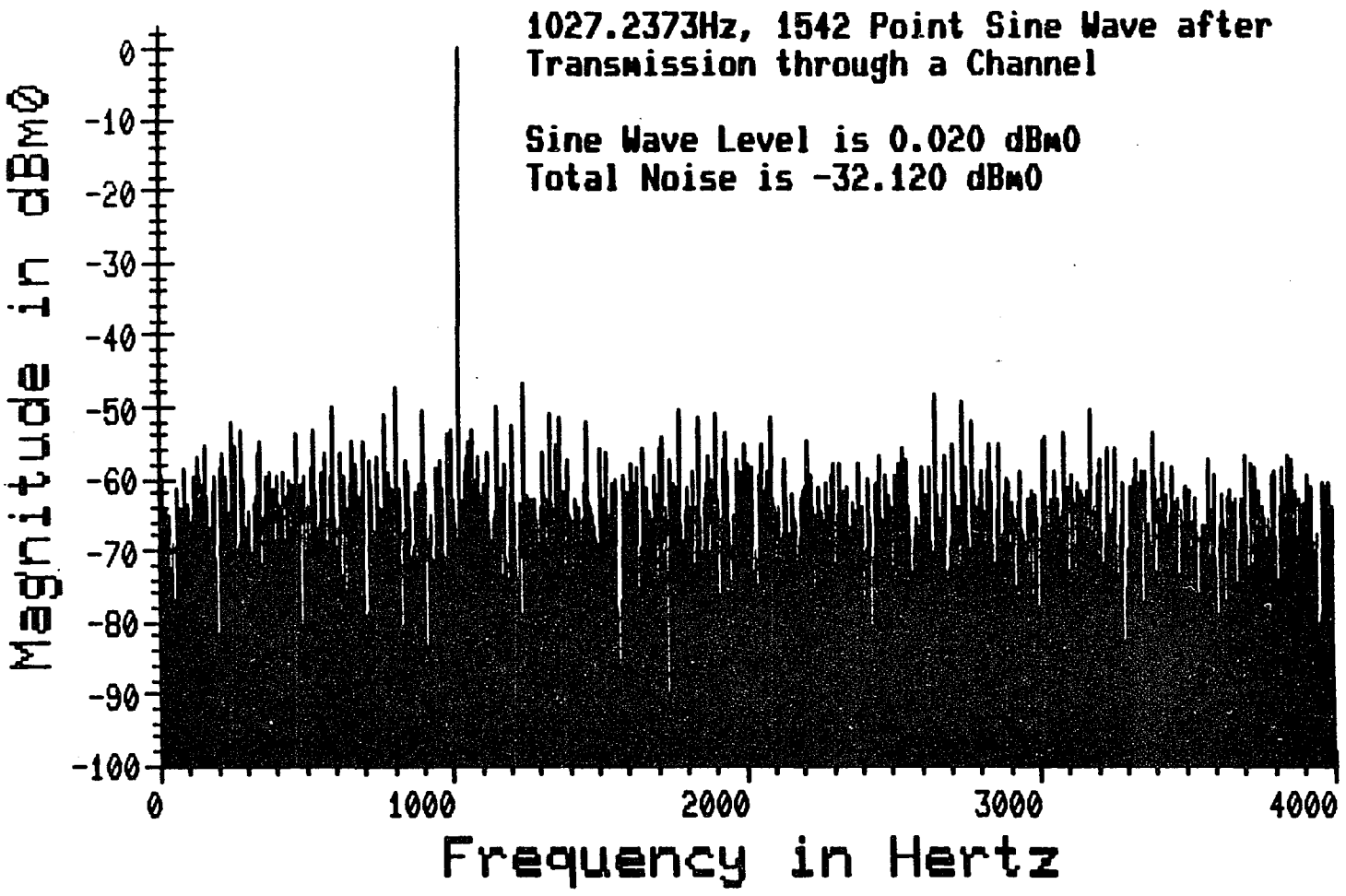

Figure VII-22

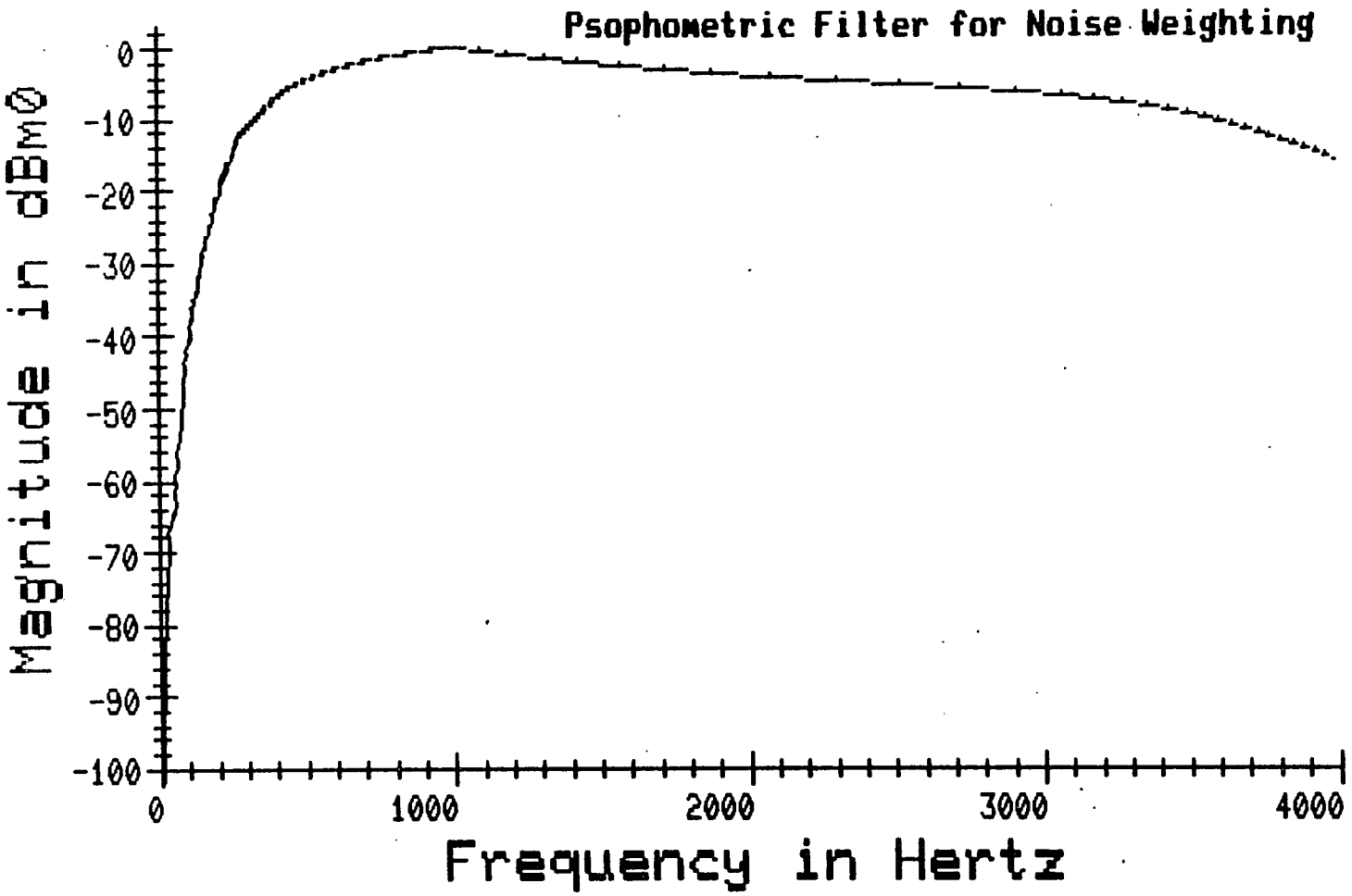

Figure VII-23

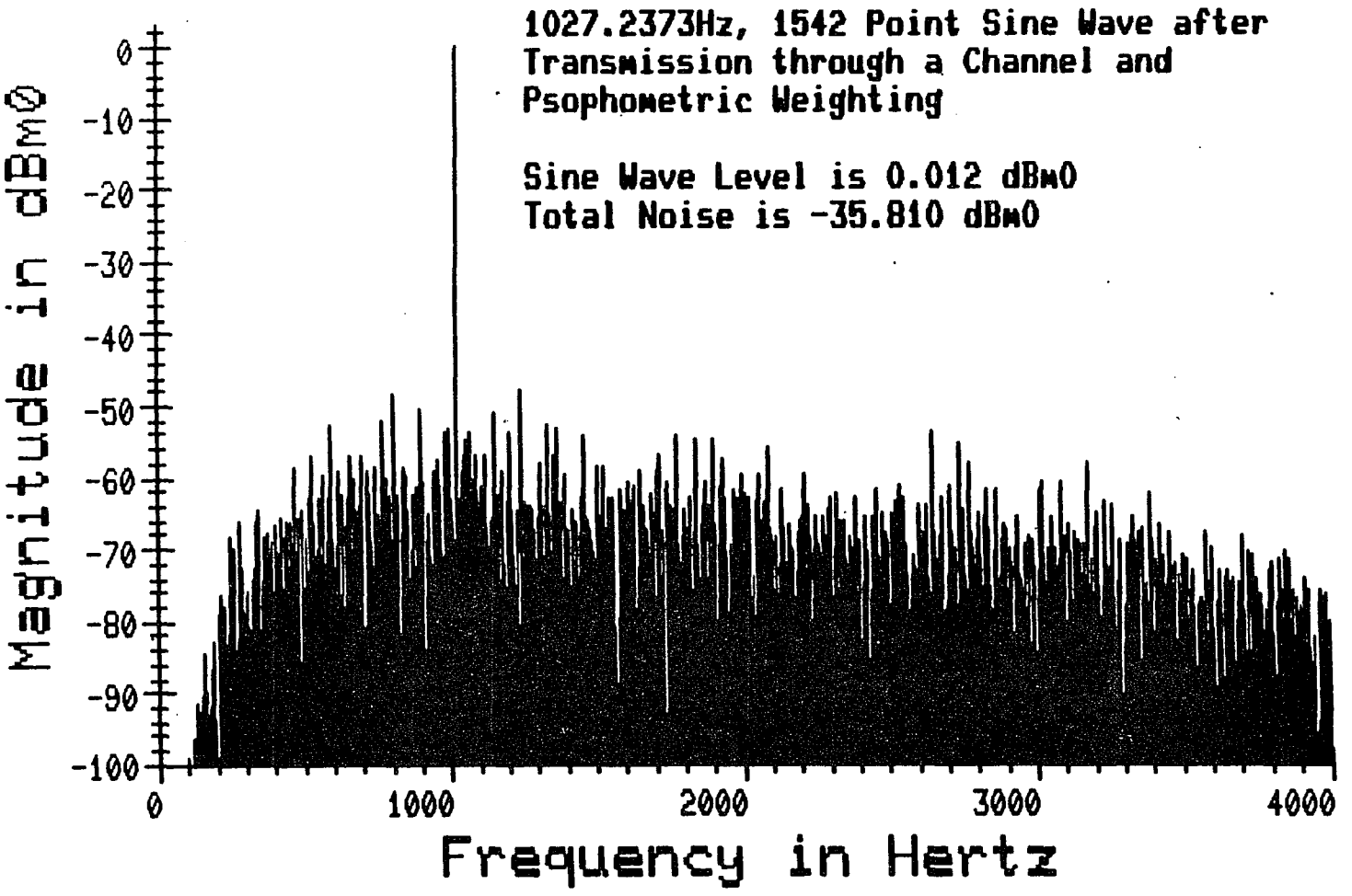

Figure VII-24

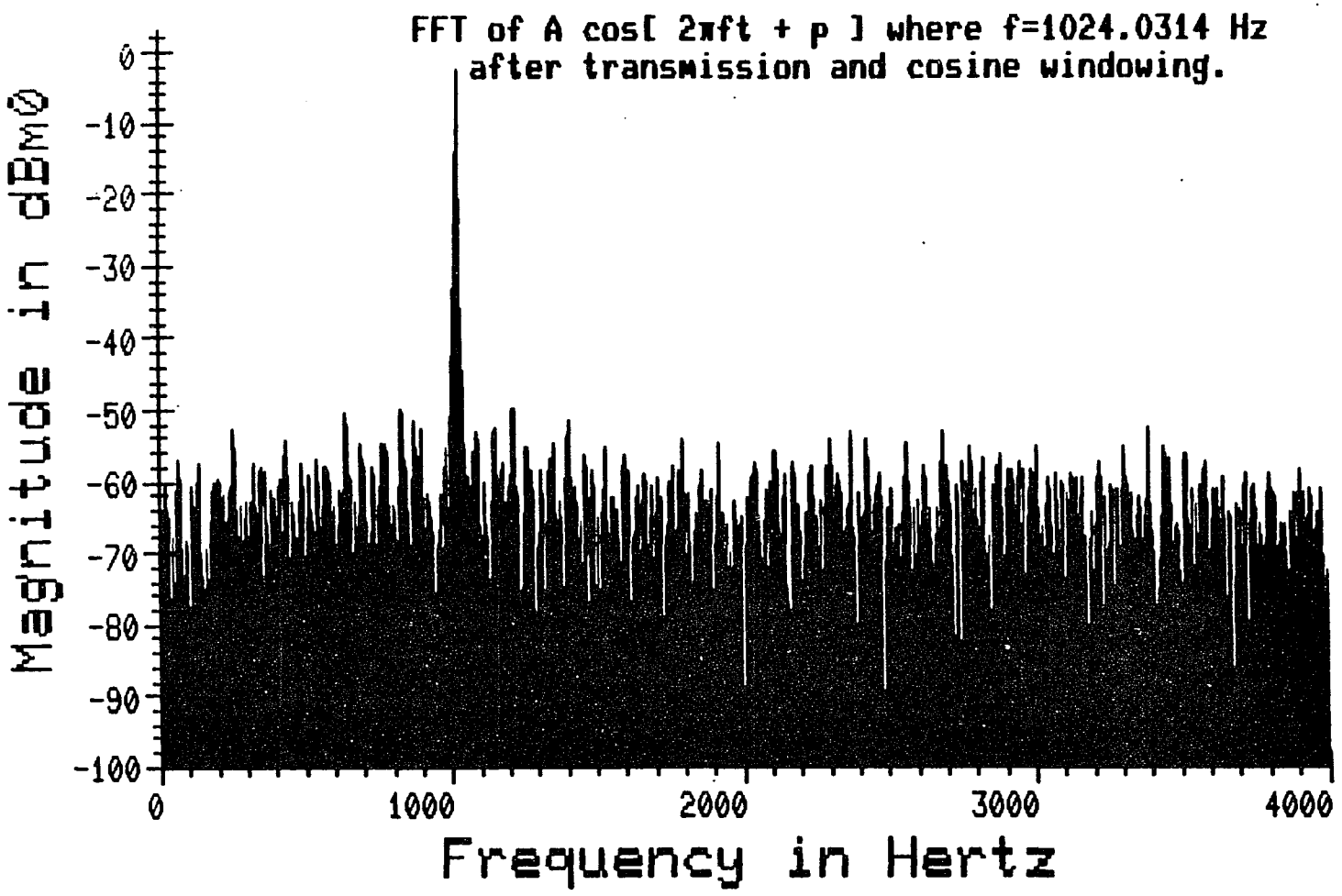

Figure VII-25

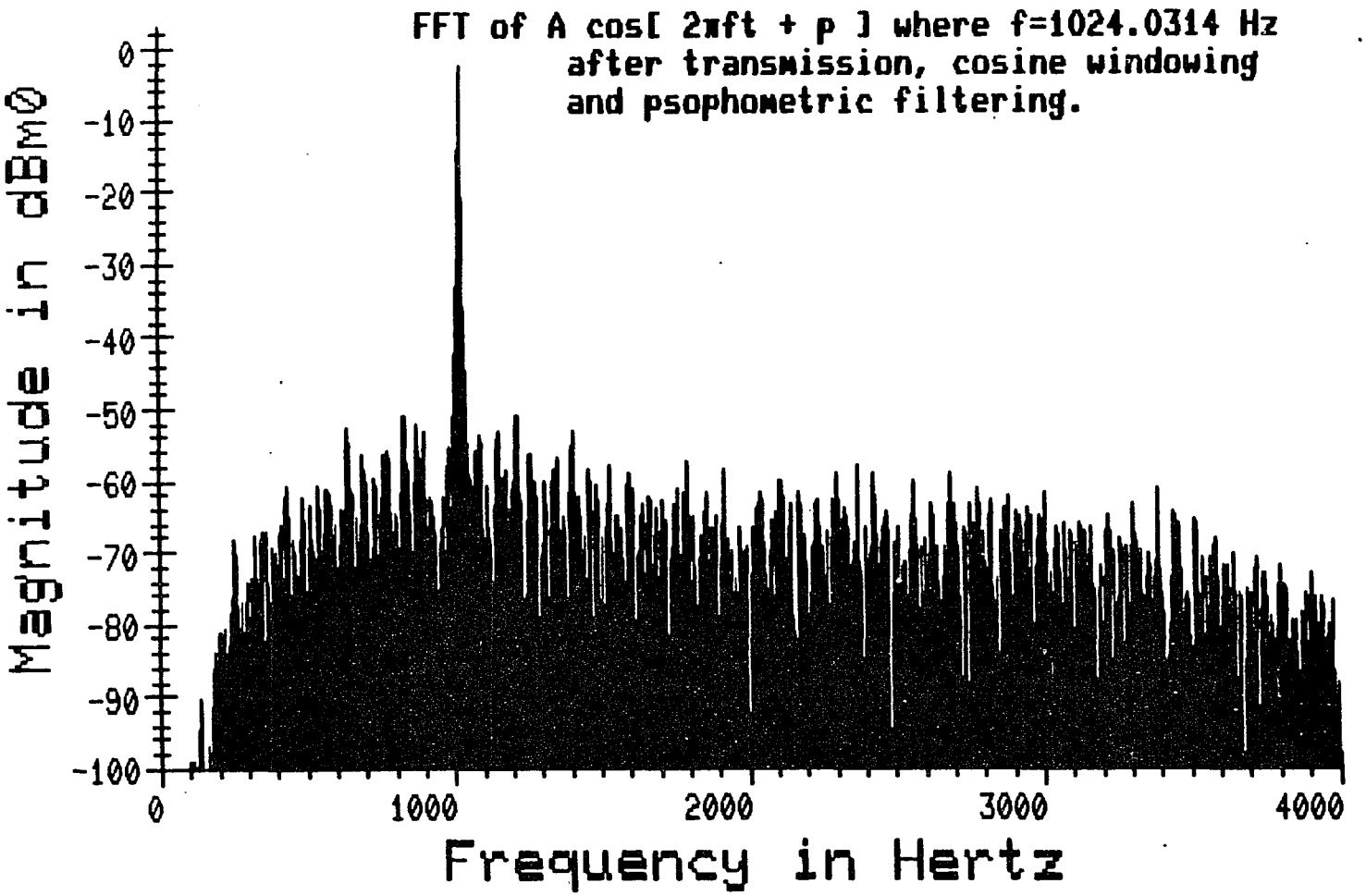

Figure VII-26

in an RMS reading of 0.0132 volts at 600 ohms, which translates to -35.4 dBm0p and compares nicely with the results derived digitally.

Figure VII-27 shows a 1542 point measurement with the stimulus at -10 dBm0. The results show a gain of 0.005 dB and the noise is down by -45.677 + 9.995 = -35.682 dB. The results of a 257 point measurement, shown in Figure VII-28, indicate a gain of 0.008 dB and a noise margin of -36.416 dB. This 1 dB difference is the largest discrepancy which was seen in any of the comparisons. Subsequent measurements show a discrepancy of about 0.3 dB which is closer to the error that is expected. This discrepancy is assumed to be just due to the measurement variability and will probably happen about once in a few thousand measurements.

Figures VII-29 and 30 show 1542 and 257 point measurements taken with the stimulus at -20 dBm0. The results show transmission losses of 0.033 dB and 0.011 dB respectively and noise margines of -35.964 dB and -35.665. Similarly, close agreement between the two measurements is exhibited in Figures VII-31 and 32 at a signal level of -30 dBm0. The transmission loss is at 0.048 dB and 0.058 dB, while the noise margins are -35.669 dB and -35.770 dB.

At the -40 dBm0 signal level, only the lower two straight line sections of the compression characteristic are used. From this point on, the noise margin degrades rapidly. The transmission losses of 0.042 dB and 0.073 dB still remain consistent, as shown in Figures VII-33 and 34, while the noise margins have dropped to -31.037 dB and -31.026 dB respectively.

The close agreements between the more accurate 1542 point measurements and the 257 point measurements indicate

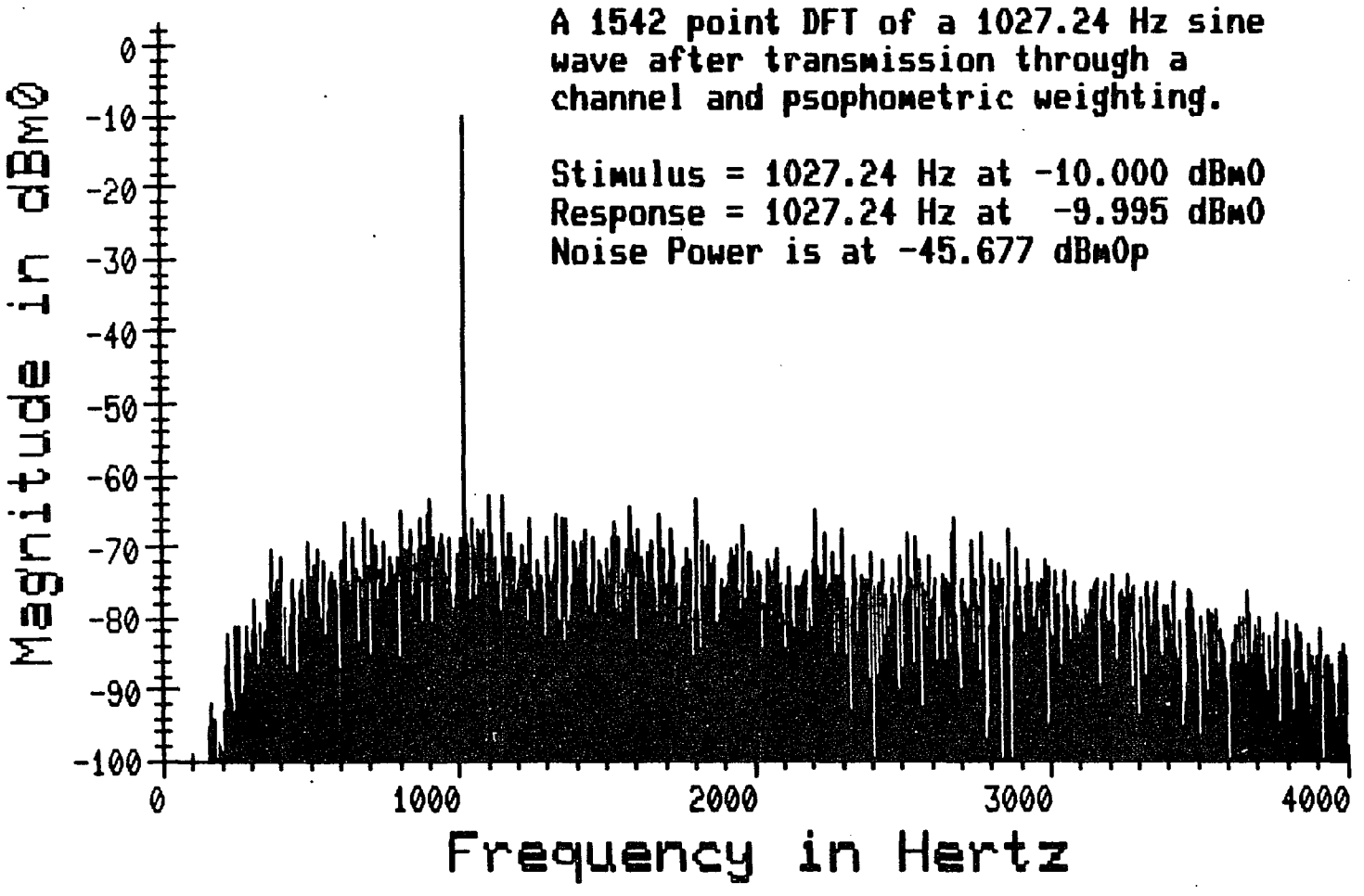

Figure VII-27

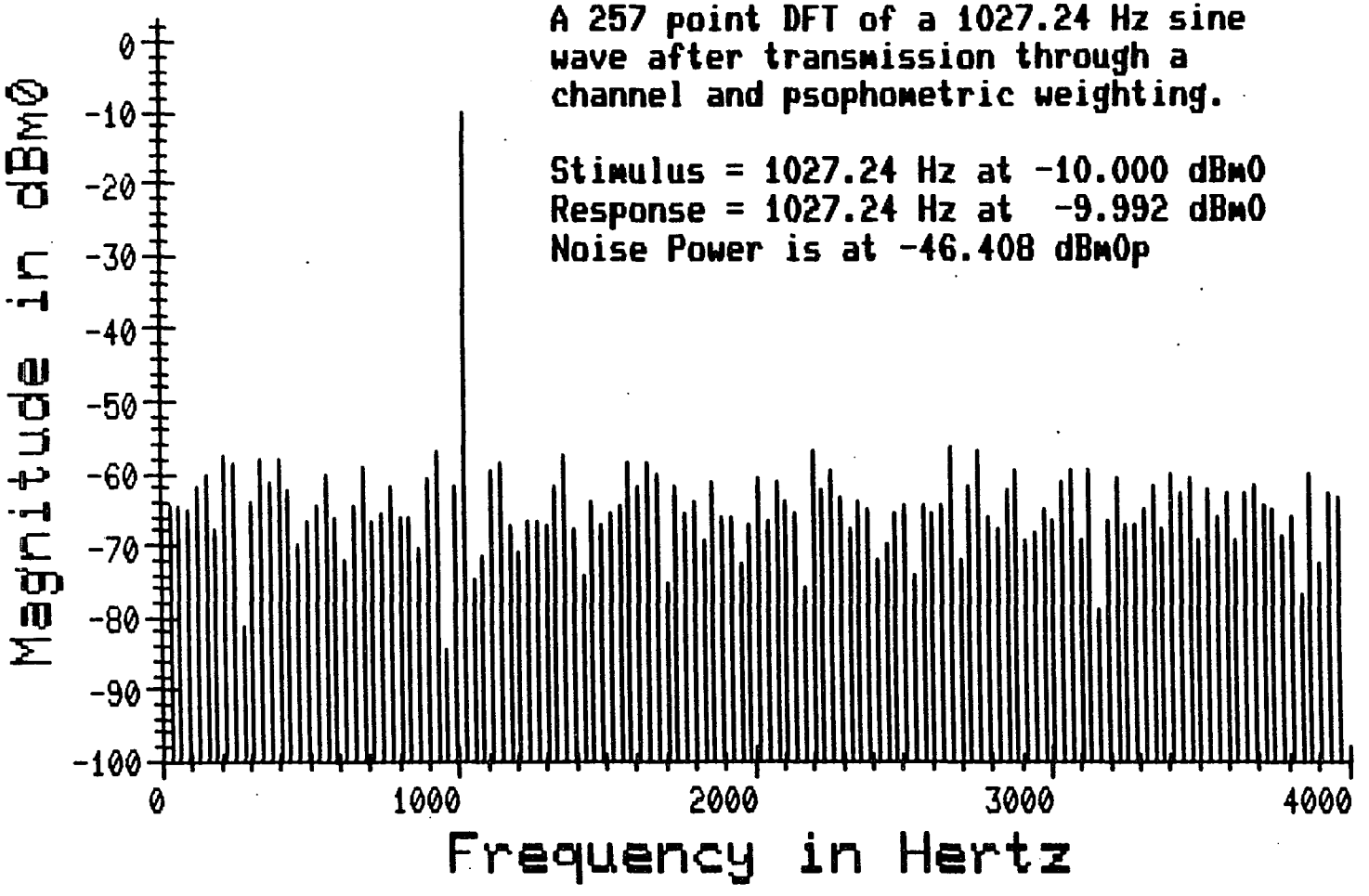

Figure VII-28

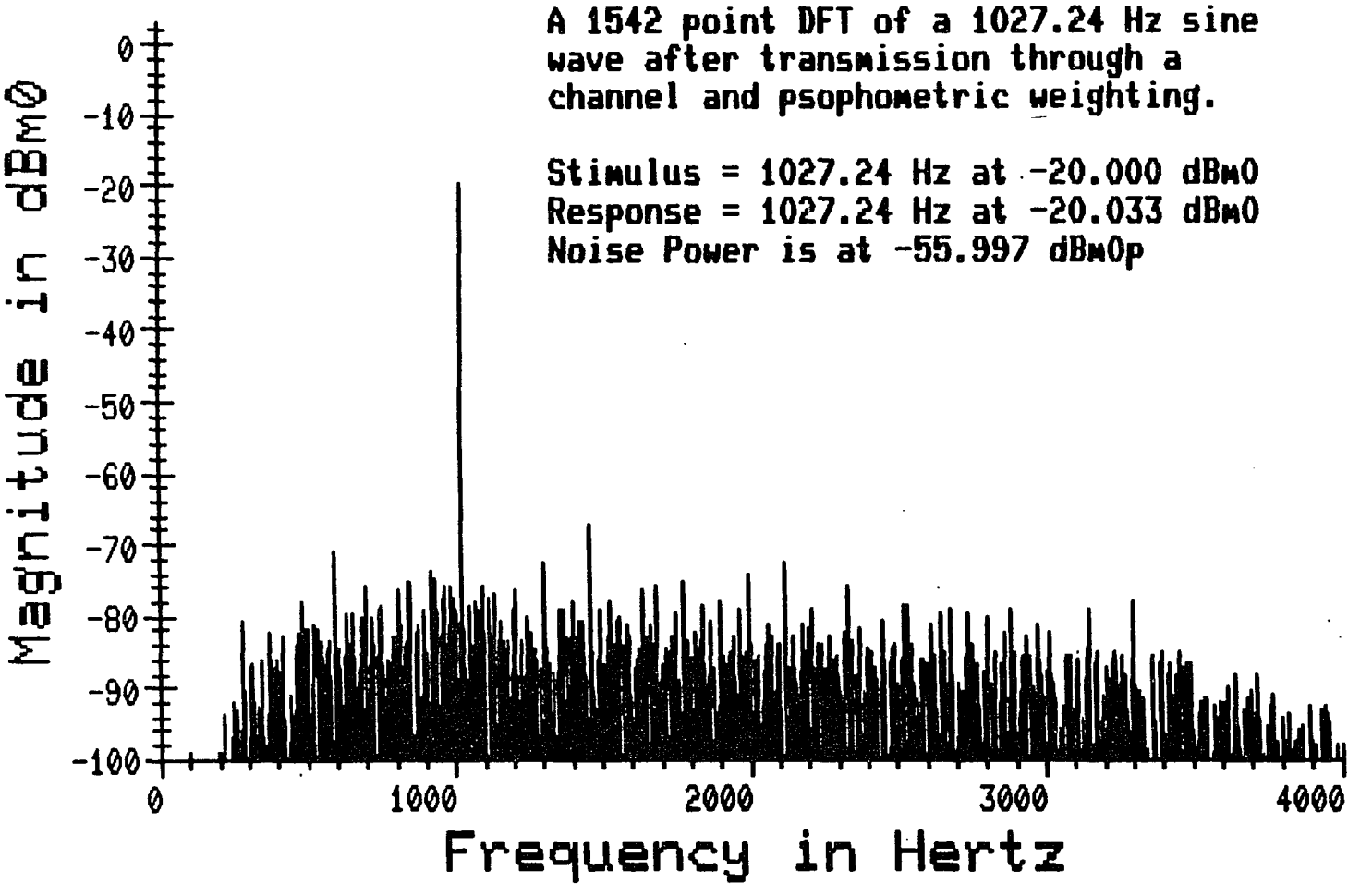

Figure VII-29

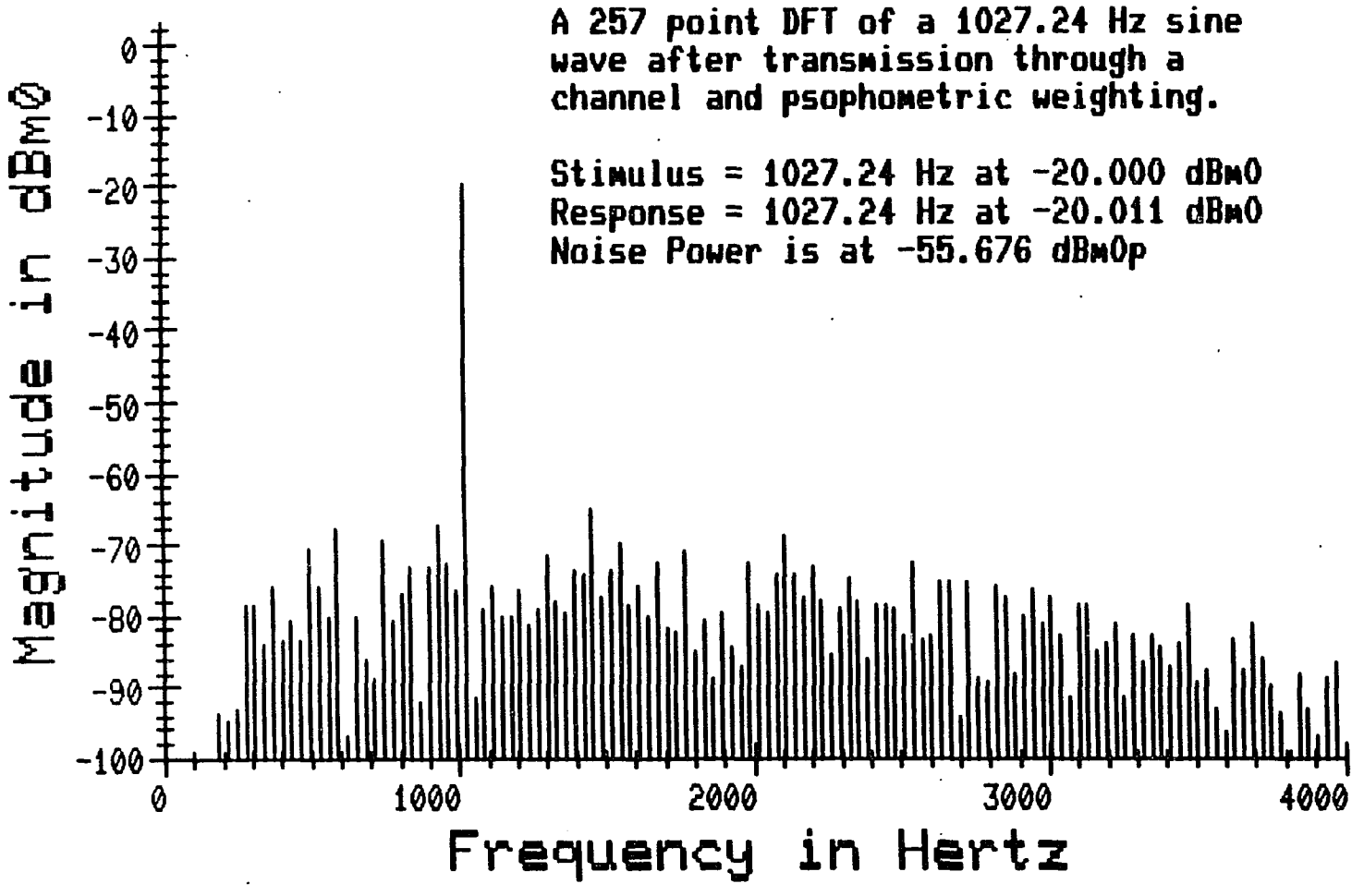

Figure VII-30

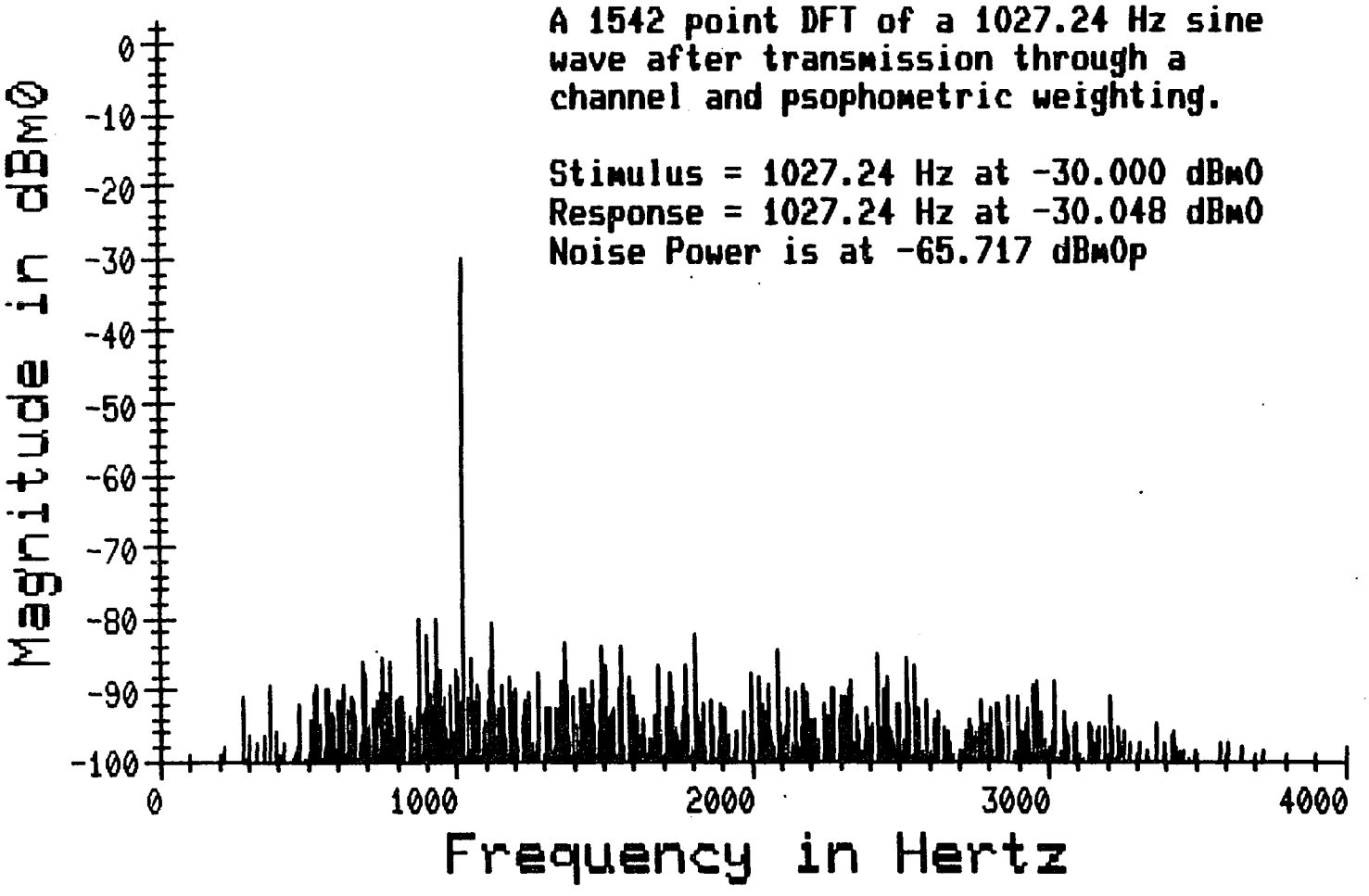

Figure VII-31

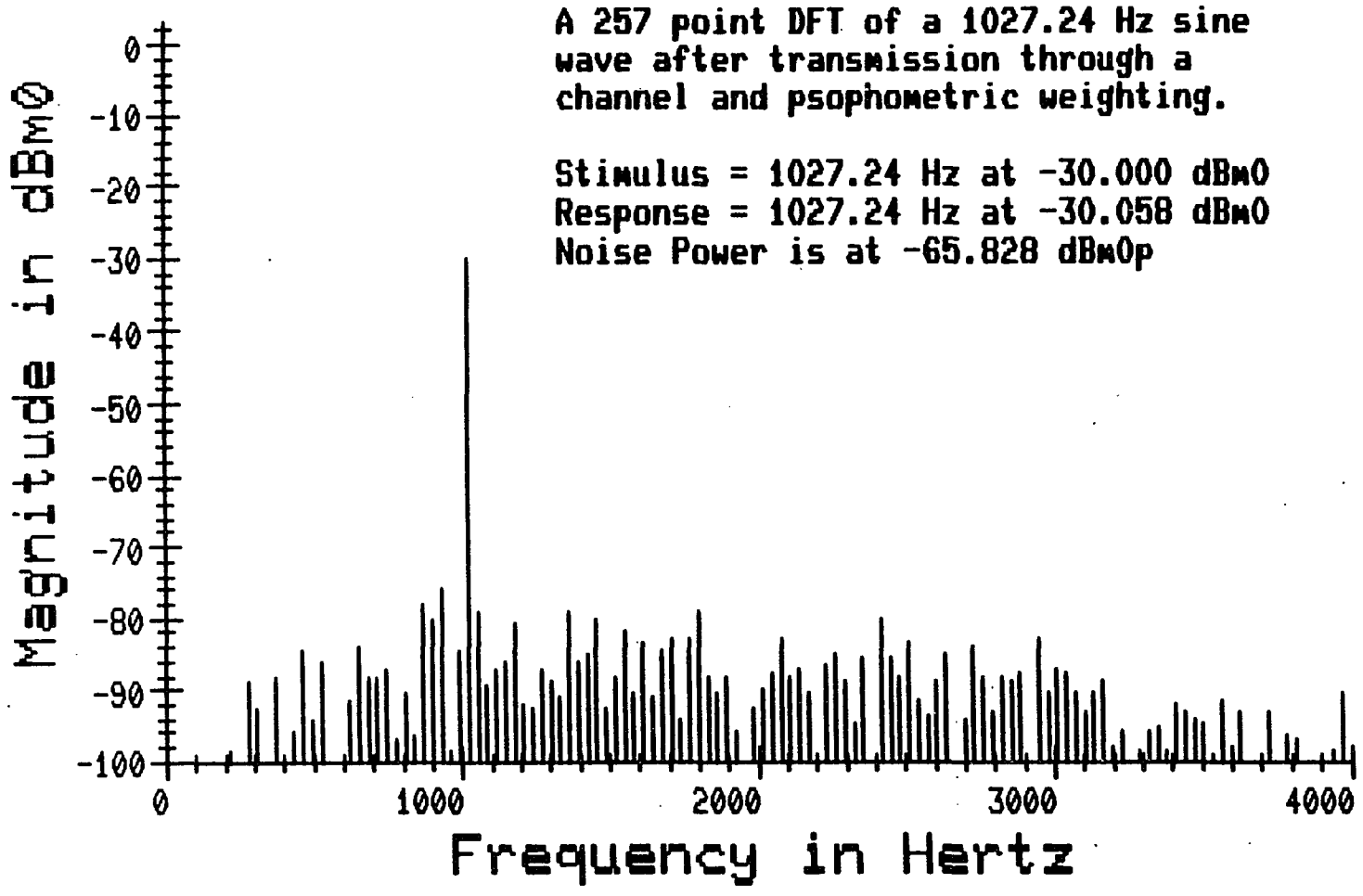

Figure VII-32

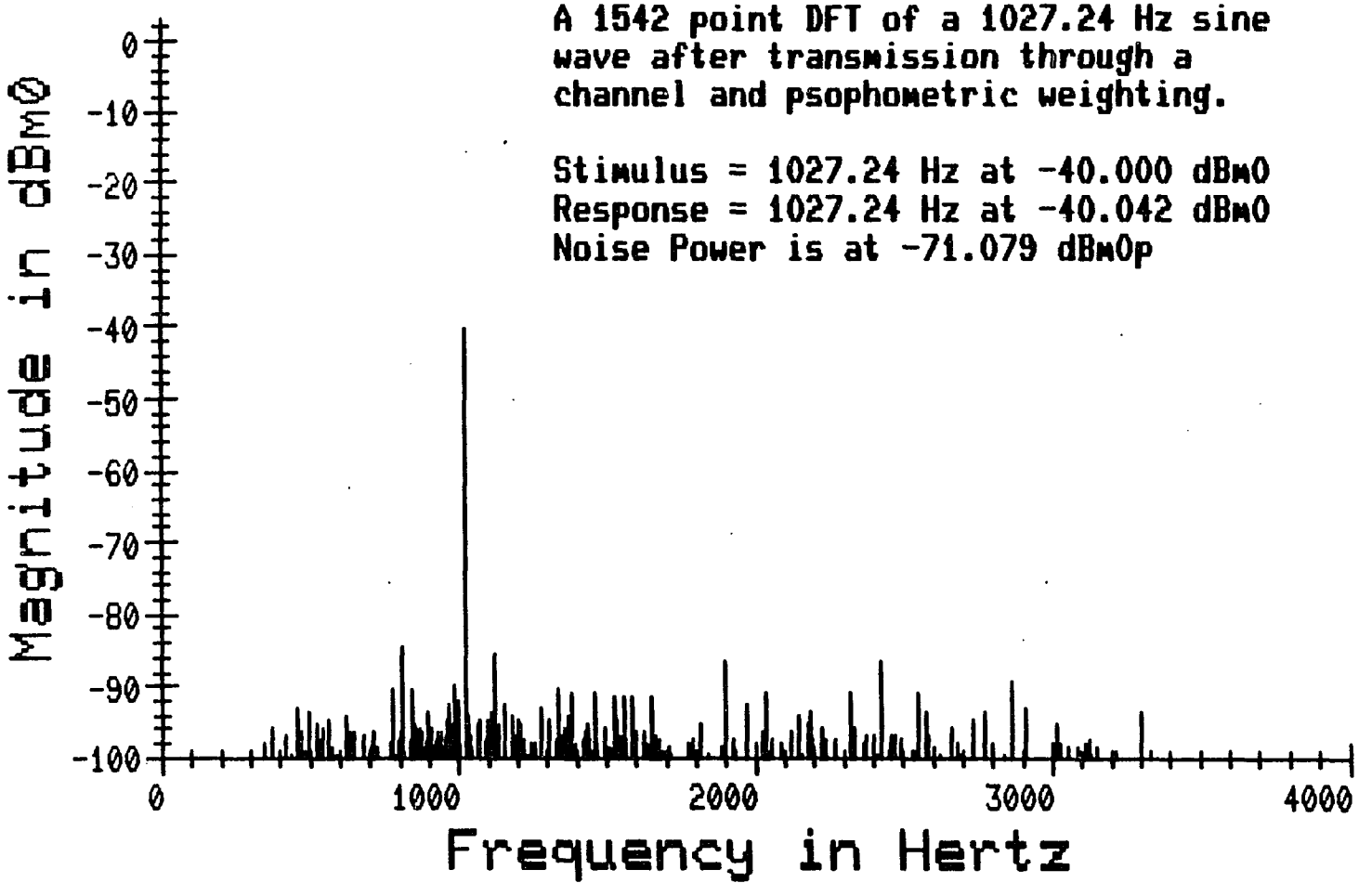

Figure VII-33

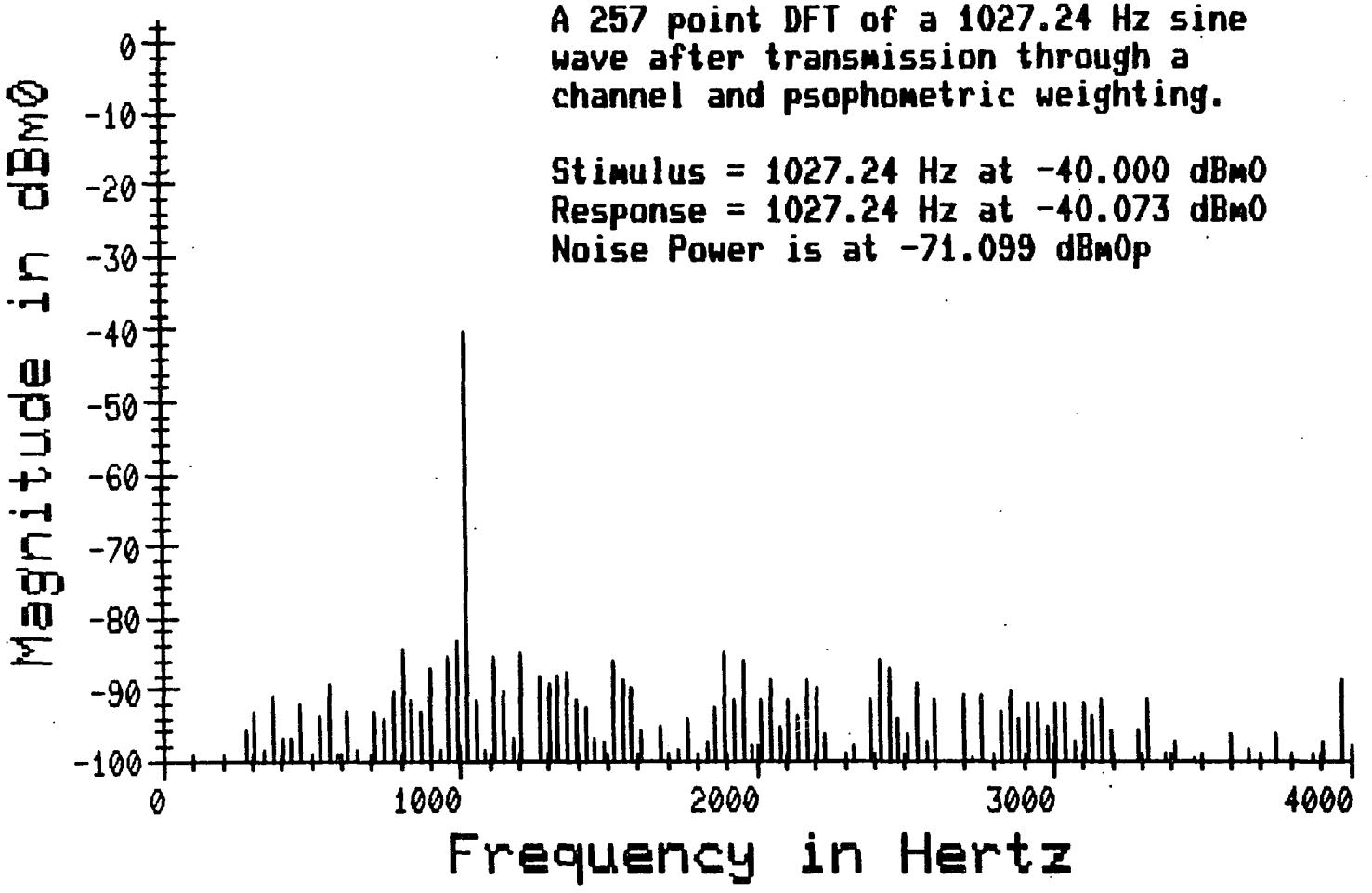

Figure VII-34

that most of the testing may be satisfactorally done with the fewer number of points. This results in almost a ten to one decrease in the number of complex multiplications which must be performed. If a failure is detected with this smaller sample, it is suggested that either more measurements be made with 257 points and the results averaged or, preferably, a measurement be made with 1542 points. The 1542 point measurement is about an order of magnitude more accurate and gives a true picture of the actual frequency distribution of the quantization noise. If graphic results are to be examined visually then this more correct spectrum will be important.

VII-C Crosstalk

Crosstalk measurements are generally performed by transmitting a signal on an adjacent channel and checking for the presence of that signal in the test channel. Figure VII-35 is the DFT result of just such a crosstalk measurement. If the measurements are to be made in this manner, the short-cut mentioned at the beginning of this chapter may be used to calculate the DFT result for just the one expected frequency component. Crosstalk measurements are usually made to both adjacent channels. This may be accomplished by transmitting tones of two different frequencies in each of the adjacent channels and inspecting the DFT results for the presence of either of these components as seen in Figure VII-36. An extrapolation of this technique might be to transmit different frequencies on each of the twenty-three other channels simultaneously, then the DFT results from just one measurement on the test channel will display the crosstalk from all of the other

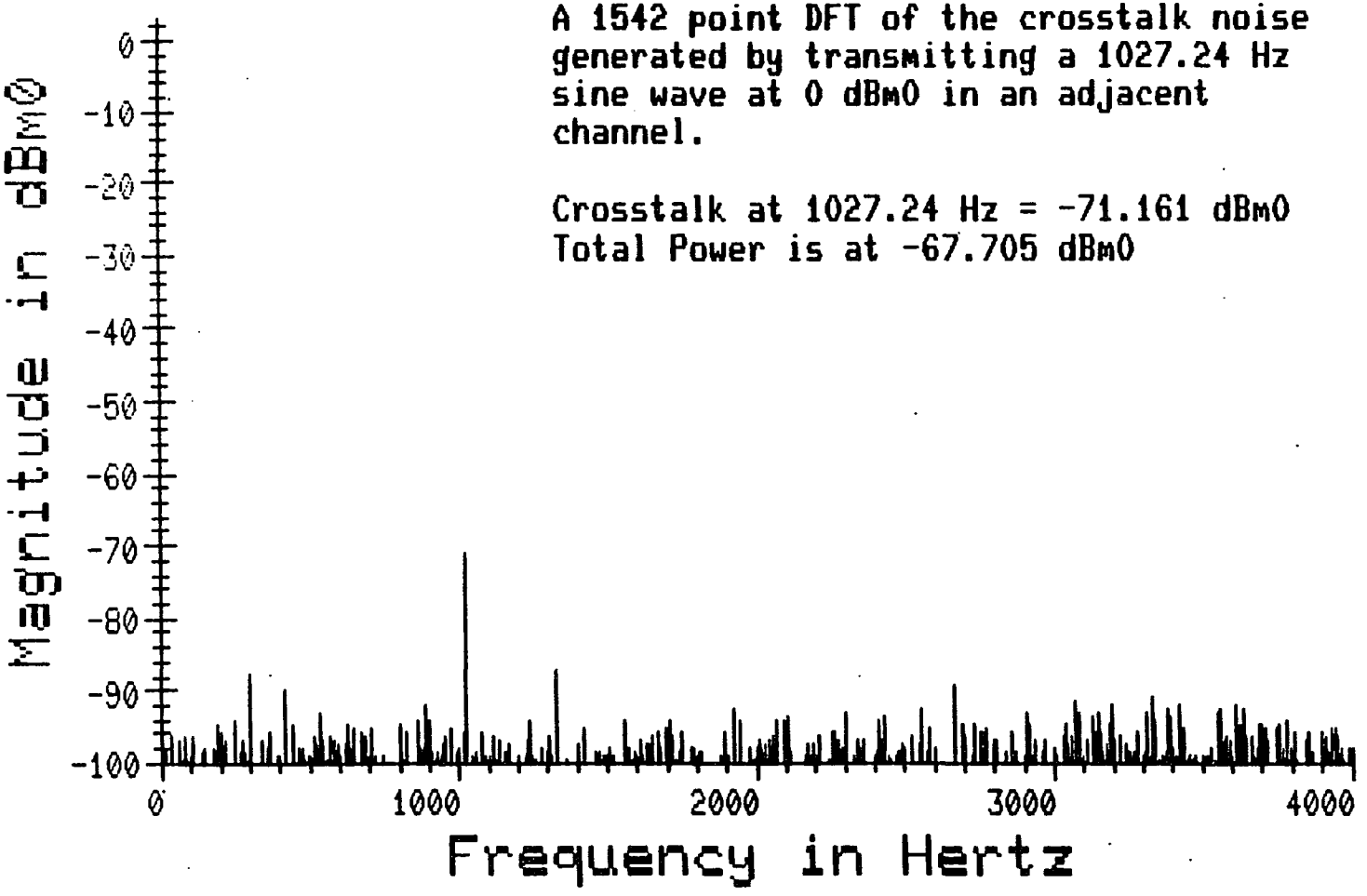

Figure VII-35

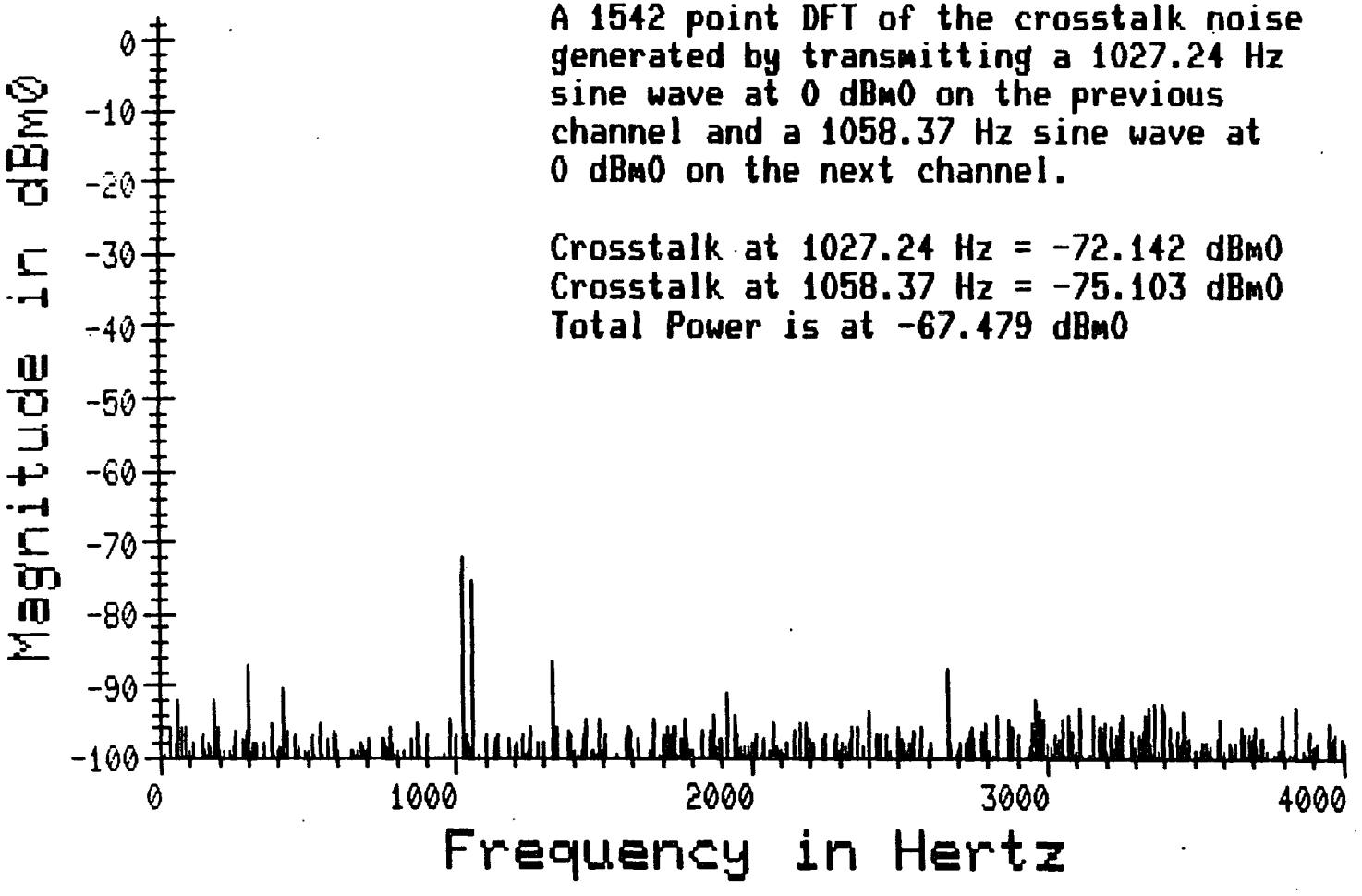

Figure VII-36

channels.

VII-D Intermodulation Distortion

An intermodulation measurement evaluates the linearity of the voice channel. To perform this test a signal consisting of two frequency components each at or below -4 dBm0 is encoded into the signal generator's 257 word ROM. The signal is transmitted through a channel and the DFT results are evaluated, as shown in Figure VII-37, for intermodulation of the two signals. The effect of a nonlinearity in the channel may be demonstrated by over-driving it as shown in Figure VII-38. Here it is obvious that the largest modulation components will be adjacent to the two source frequency components; thus, evaluation of one of these will suffice.

VII-E Idle Circuit Noise

Since there is not a code value representing a true zero for the signalling frame, some quantization noise will be present, even in a completely idle circuit. This noise accounts for an absolute minimum possible noise level of -87.7 dBm0 or 2.4 dBrn0 where 0 dBrn0 = -90 dBm0, which is the one nanowatt reference level. Noise measurements may be made with either a psophometric filter, in which case the units of dBm0p are used, or with a c-message weighting, which has a frequency taper slightly different from that of the psophometric filter and the units are specified as dBrnc0. Figure VII-39 shows a typical noise measurement. This could also be derived directly from the measured data by simply totalling the power in the time domain signal.

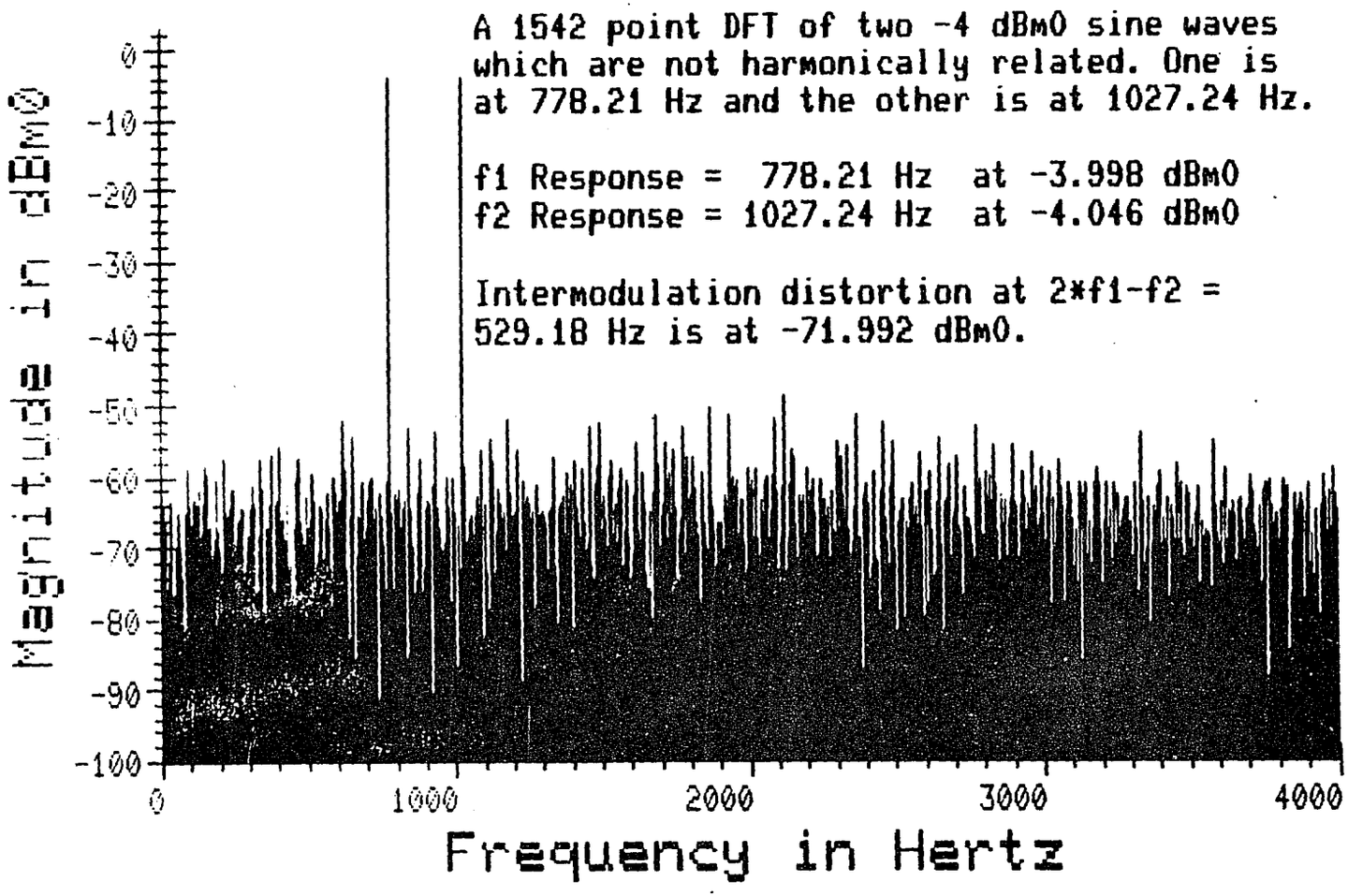

Figure VII-37

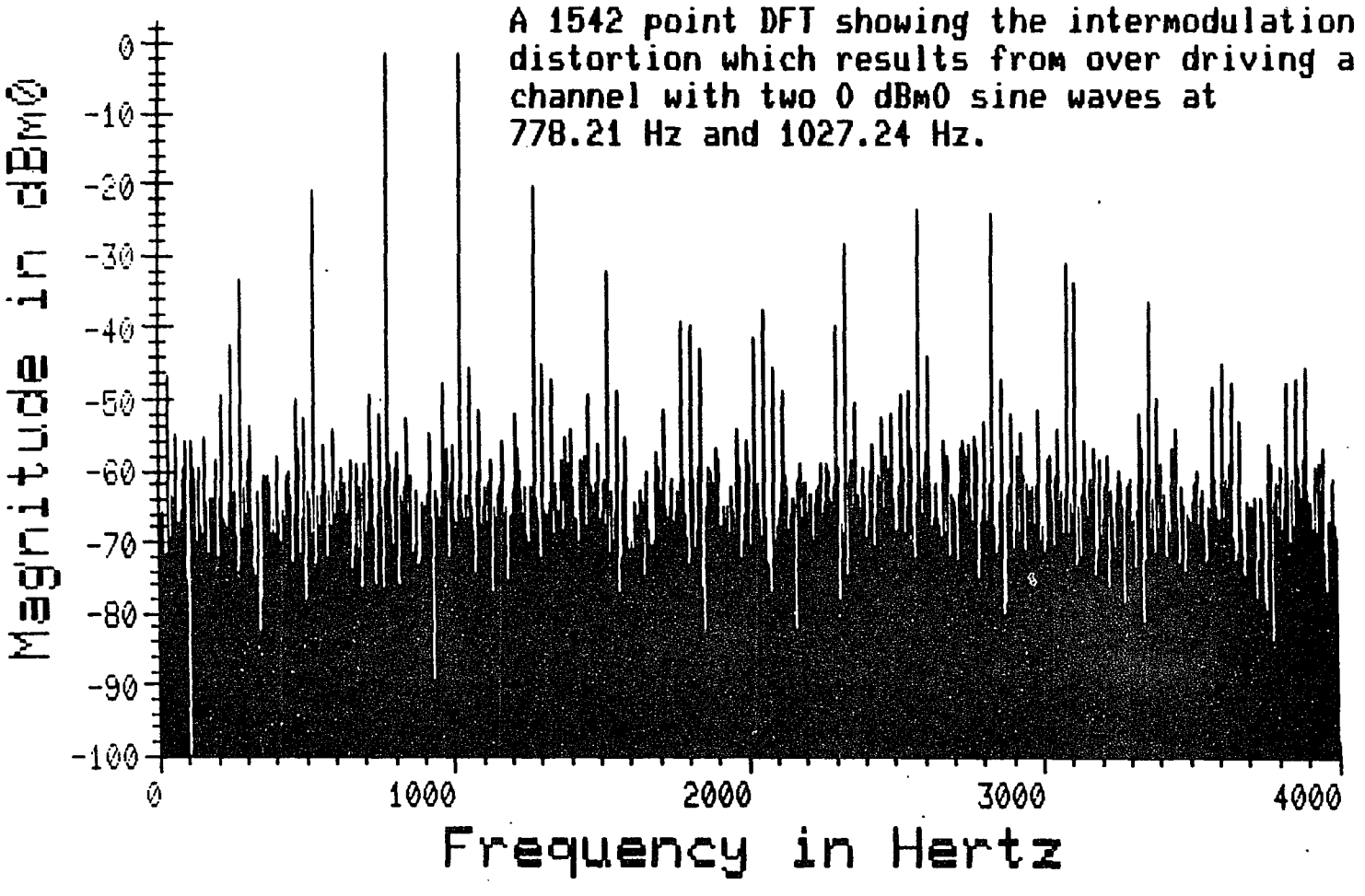

Figure VII-38

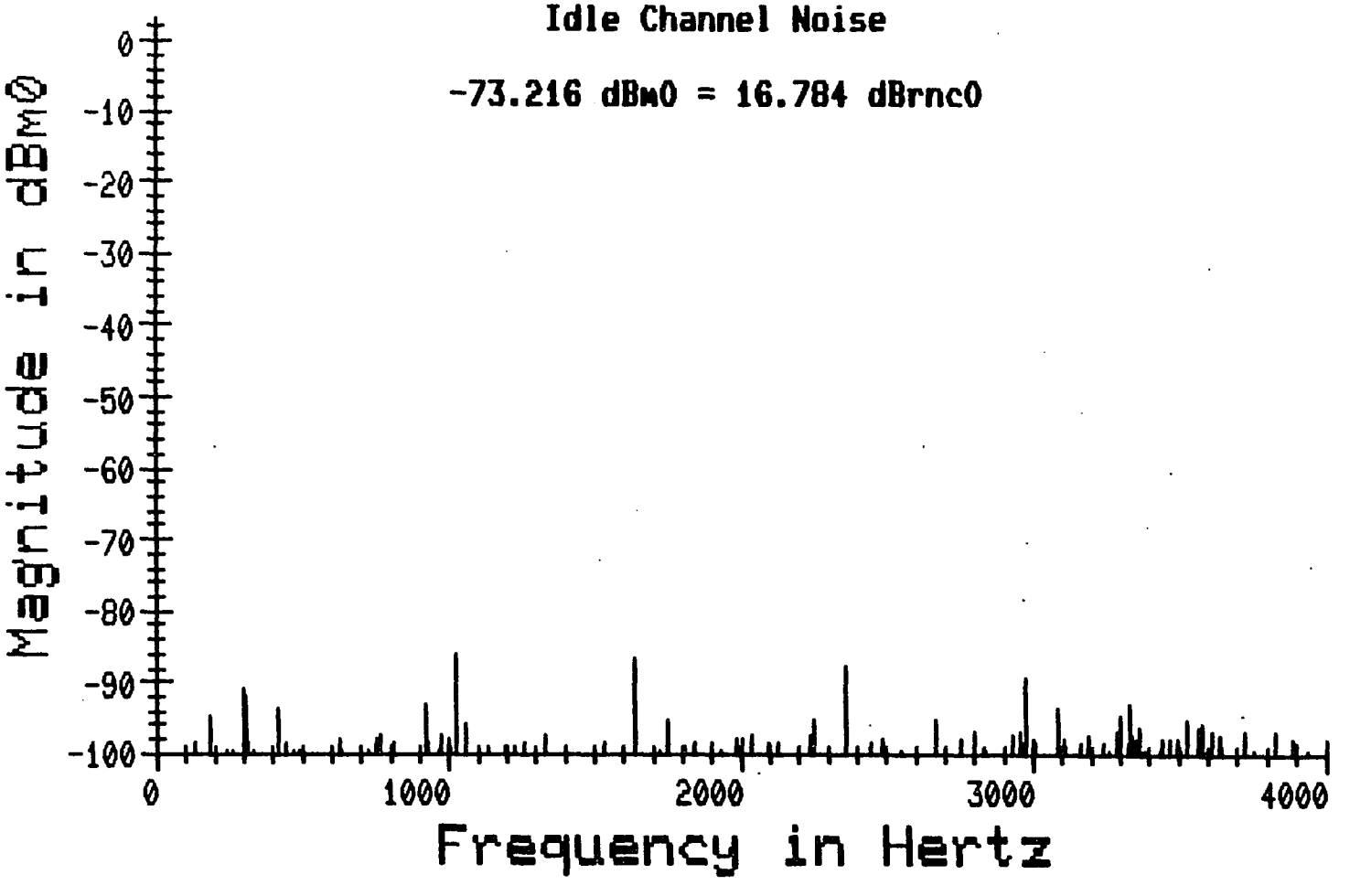

Figure VII-39

CHAPTER 8

CONCLUSIONS

VIII-A Areas for Future Investigation

Possible areas of future investigation may involve the development of an analog signal generator which may be phase locked to the sampler. A computer program could be written which would take into account all of the short-cuts described here and generate an efficient FFT subroutine, in some common high level language such as FORTRAN, tailored to any specific number of sample points. Also, techniques might be investigated for determining the characteristics of the receive and transmit analog filters by driving one or both of them into their nonlinear regions.

VIII-B Summary

This dissertation brought together many of the various time saving techniques, developed for performing the Fast Fourier Transform (FFT), into a coherent form and demonstrated how they may be applied to a specific problem. Some new techniques were developed where they were needed.

In a production environment it is important that the manufacturing process result in a highly reliable product at the lowest effective cost to the customer. In order to assure this reliability, tests on electronic equipment are often performed repeatedly over a period of time rather than just once. This technique provides more insite into what the final user may expect. Such tests usually require more man-hours to perform, which tends to increase the production

costs. For this reason it is important to reduce the time required to test an individual unit while still allowing the unit to be tested repeatedly. This leads to the use of automatic test equipment and the need for improved algorithms which make more efficient use of such equipment. The complex multiplication operation is the most time consuming part of the Discrete Fourier Transform (DFT) process. Therefore, this dissertation contains a derivation for the exact number of multiplication steps required for performing the DFT on any number of points. As a result of this it was shown that the order in which a composite number of points is factored may effect the number of complex multiplications required.

The conditions under which the DFT may be used to produce the actual spectral content of the test signals was explained. These conditions involve creating special test signals which do not contain and will not generate any frequency components except those present in the DFT results.

The characteristics of the signal generator required to produce these signals were defined. It was shown that an improved measurement of the quantization noise results when the table used in the signal generator contains a prime number of points. In this case 257 points was chosen since this produces an acceptable portrayal of the quantization noise and has the added advantage of an efficient Fast Fourier Transform (FFT) algorithm. The actual signal generator hardware was designed, built and functionally tested, including a computer interface through which it can be automatically controlled.

The improved algorithm which was developed for performing an FFT on a conjugate-periodic function reduces the number of complex multiplications required for a prime radix FFT by approximately twenty-five percent. This is the result of splitting the function into two halves one of which contains only real values and may take advantage of the two-at-a-time and doubling FFT techniques.

Computer controlled data input hardware was also designed and built to collect the appropriate data samples from the time multiplexed, pulse code modulated signals used in telephone communications.

Specific test signals and measurement techniques have been prescribed for measuring all of the pertinent parameters of the telephone voice channel. The FFT algorithms for 257 and 1542 points were written. It was shown that the 1542 point FFT yields the true spectrum of the test results. Although the 257 point FFT does not yield the true spectral results, it was shown that this algorithm may be used in most test situations to produce results with acceptable accuracy and reduced computation time.

For the case where it may be necessary to use some signal source other than the specially designed digital signal generator, a series of new data windows have been developed here which improve the spectral estimate derived from the FFT techniques.

These developments have direct and immediate applications in the telecommunications industry. Digital test access may be implemented in a production test environment to reduce the complexity and cost of the test systems by eliminating the need for large analog switching matrices. Since the levels in the digital transmission

systems are defined in terms of a digital reference signal, the digital signal generation and analysis techniques developed here preclude the need for periodic calibration.

Other applications involve the use of such equipment by the telephone operating companies to diagnose and isolate problems. With the current trend toward using remote computer controlled, distributed switching centers in the telephone network, the use of these techniques for remote testing of the customer's analog interface will become imperative.

Although the techniques developed here are directed toward a specific application, they can be easily extended and used in many other applications requiring FFT's. Such applications include sonar and radar data processing, antenna design and analysis, picture processing and speach analysis.

REFERENCES

1. L.R.Rabiner, J.W.Cooley, H.D.Helms, L.B.Jackson, J.F.Kaiser, C.M.Rader, R.W.Schafer, K.Steiglitz, and C.J.Weinstein, "Terminology in Digital Signal Processing," IEEE Trans. Audio Electroacoust., vol. AU-20, pp.322-337, December 1972.

2. J.W.Cooley, P.A.Lewis, and P.D.Welch, "Historical Notes on the Fast Fourier Transform," IEEE Trans. Audio Electroacoust., vol. AU-15, pp.76-79, June 1967.

3. P.D.Welch, "The Use of Fast Fourier Transform for the Estimation of Power Spectra: A Method Based on Time Averaging Over Short, Modified Periodograms," IEEE Trans. Audio Electroacoust., vol.AU-15, pp.70-73, June 1967.

4. C.M.Rader, "An Improved Algorithm for High Speed Autocorrelation with Applications to Spectral Estimation," IEEE Trans. Audio Electroacoust., vol AU-18, pp.439-441, December 1970.

5. A.Oppenheim, D.Johnson, and K.Steiglitz, "Computation of Spectra with Unequal Resolution Using the Fast Fourier Transform," Proc. IEEE, vol.59, pp.299-301, February, 1971.

6. R.C.Singleton, "An Algorithm for Computing the Mixed Radix Fast Fourier Transform," IEEE Trans. Audio Electroacoust., vol. AU-17, pp.93-103, June 1969.

7. C.M.Rader, "Discrete Fourier Transforms When the Number of Data Samples Is Prime," Proc. IEEE, vol.56, pp.1107-1108, June 1968.

8. C.J.Weinstein, "Roundoff Noise in Floating Point Fast Fourier Transform Computation," IEEE Trans. Audio Electroacoust., vol. AU-17, pp.209-215, September 1969.

9. J.Tierney, C.M.Rader, and B.Gold, "A Digital Frequency Synthesizer," IEEE Trans. Audio Electroacoust., vol. AU-19, pp.48-56, March 1971.

10. "Line Transmission," Orange Book, CCITT Sixth Plenary Assembly, Geneva 1977.

11. Digital Channel Bank Requirements and Objectives, Engineering Director - Transmission Systems, AT&TCo. 1978.

12. R.C.Singleton, "On computing the Fast Fourier Transform," Commun. ACM, vol.10, pp.647-654, October 1967.

13. B.Gold and L.R.Rabiner, Theory and Application of Digital Signal Processing, Prentice-Hall, Inc., New Jersey, 1975.

14. G.D.Bergland, "A Guided Tour of the Fast Fourier Transform," IEEE Spectrum, vol.6, pp.41-52, July 1969.

15. A.B.Carlson, Communication Systems, McGraw-Hill, New York, 1968.

16. D.V.Sarwate and M.B.Pursley, "Crosscorrelation Properties of Pseudorandom and Related Sequences," Proc. IEEE, vol.68, No.5, May 1980.

17. VT125 User Guide, Digital Equipment Corporation, Maynard, Mass.,1981.

18. PDP11 FORTRAN Language Reference Manual, Digital Equipment Corporation, Maynard, Mass.,1975.

19. IAS/RSX11 FORTRAN User's Guide, Digital Equipment Corporation, Maynard, Mass.,1976.

20. J.W.Cooley and J.W.Tukey, "An Algotithm for the Machine Calculation of Complex Fourier Series," Math. of Comput., vol.19, pp.297-301, April 1965.

21. W.M.Gentleman and G.Sande, "Fast Fourier Transforms for Fun and Profit," 1966 Fall Joint Computer Conf., AFIPS Proc., vol.29, pp.563-578, Washington, D.C.: Spartan, 1966.

22. C.Runge, Zeit. fur Math. und Physik, vol.48, p.443, 1903.

23. C.Runge, Zeit. fur Math. und Physik, vol.53, p.117, 1905.

24. G.C.Danielson and C.Lanczos, "Some Improvements in Practical Fourier Analysis and Their Applications to X-Ray Scattering form Liquids," J. Franklin Inst., vol.233, pp.365-380 and 435-452, April 1942.

25. K.Stumpff, Tafeln und Aufgaben zur Harmonischen Analyse und Periodogrammrechnung, Berlin: Julius Springer, 1939.

26. L.H.Thomas, "Using a Computer to Solve Problems in Physics," Application of Digital Computers, Boston, Mass.: Ginn, 1963.

27. P.Rudnick, "Note on the Calculation of Fourier Series," Math. of Comput., vol.20, pp.429-430, July 1966.

28. Standard Mathematical Tables, The Chemical Rubber Co., Cleveland, Ohio, 1968.